An investigation of tetraspanin proteins' role in UPEC infection

Fawzyah Albaldi

A thesis submitted in partial fulfilment of the requirements for the degree of Doctor of Philosophy

The University of Sheffield
School of bioscience

January 2022

Acknowledgments

Firstly, I would like to offer my sincerest gratitude to my supervisors Dr Lynda Partridge and Prof. Peter Monk for their guidance and continuous support throughout my PhD study, for their patience, inspiration, and immense knowledge. Their guidance helped me throughout my research and writing this thesis.

A great thanks also go to the friendly and cheerful lab members both past and present, for all the great help and support, my grateful thanks to Dr. Rahaf Issa, Dr. Luke Green, Dr. Muslim Mohesin, Lucy Urwin, Waad Aljohani for their help and real support at this project.

My sincere thanks also go to Dr Christa Walther (Light Microscope Facility, University of Sheffield) for microscopy imaging support and Susan, Kay and Julie (Flow Cytometry Unit, Medical School, University of Sheffield) for flow cytometry support.

It is an honour for me to express my deep sense of thank to Albaha University in Saudi Arabia for giving me the chance to undertake this study.

Last but not the least, special and grateful thanks to my husband Khalid Almotiri and my two beautiful and lovely daughters Ghala and Hoor for their love, patience, endurance and continuous support that kept me highly motivated throughout my PhD. From my heart, big thanks to my mother (Badriah Alfaris), my father (Obeedallah Albaldi), and I cannot forget my sisters (Ghadeer and Joud) and my brothers for their support in taking care of my kids, encouragements and their prayers. This work could not have been completed without their help and support. I would like to thank Haifa Badi for the warm heart to take care of my kids when I attended the 9th European Conference on Tetraspanins in Germany.

Abstract

Urinary tract infections (UTIs) are the most prevalent of infectious diseases and > 80% are caused by uropathogenic *E. coli* (UPEC). Infection occurs following adhesion to urothelial plaques on bladder epithelial cells, whose major protein constituent are the uroplakins (UPs). Two of the four uroplakins (UPIa and UPIb) are members of tetraspanin superfamily. The UPEC adhesin FimH is known to interact directly with UPIa.

Tetraspanins are a diverse family of transmembrane proteins that generally act as “molecular organisers” by binding different proteins and lipids to form tetraspanin enriched microdomains (TEMs). Previous work by our group has shown that TEMs are involved in the adhesion of many pathogenic bacteria to human cells. Adhesion can be blocked by tetraspanin-derived synthetic peptides, suggesting that tetraspanins may be valuable drug targets.

In this study, we investigate the role of tetraspanins in UPEC adherence to bladder epithelial cells. Human bladder cancer cell lines (T24, 5637, RT4), commonly used as *in vitro* models to investigate UPEC infection, along with primary human bladder cells, were used in this project. The aim was to establish a model for UPEC adhesion/infection with the objective of evaluating the impact of tetraspanin-derived reagents on this process. Such reagents could reduce the progression of UTI, particularly in patients with indwelling catheters.

Tetraspanin expression on the bladder cells was investigated by RTq-PCR and flow cytometry, with CD9 and CD81 generally highly expressed. Interestingly, despite these cell lines being used by other groups to investigate FimH antagonists, uroplakin proteins (UPIa, UPIb and UPIII) were poorly expressed at the cell surface, although some were present intracellularly. Attempts were made to differentiate the cell lines, to induce cell surface expression of these UPs, but these were largely unsuccessful.

Pre-treatment of bladder epithelial cells with anti-CD9 monoclonal antibody significantly decreased UPEC infection, whilst anti-CD81 had no effects. A short (15aa) synthetic peptide corresponding to the large extracellular region (EC2)

of CD9 also significantly reduced UPEC adherence. Furthermore, we demonstrated specific binding of that fluorescently tagged peptide to human cells.

CD9 is known to associate with several heparan sulphate proteoglycans (HSPGs) that have also been implicated in bacterial adhesion. Here, we demonstrated that unfractionated heparin (UFH) and heparin analogues significantly inhibited UPEC adhesion to RT4 cells, as did pre-treatment of the cells with heparinases. Pre-treatment with chondroitin sulphate (CS) and chondroitinase also significantly decreased UPEC adherence to RT4 cells. This study may shed light on a common pathogenicity mechanism involving the organisation of HSPGs by tetraspanins.

In summary, although we determined that the bladder cell lines were not suitable to investigate the role of uroplakins in UPEC adhesion, we demonstrated roles for CD9 and cell surface proteoglycans in this interaction. Agents that target these may be useful in treating/preventing UTIs.

Table of Contents

List of Tables

List of Figures

List of Equations

Declaration

The work presented in this thesis is the work of the candidate, with the following exceptions:

- The A549 cells with knockout of CD9 were produced by Dr. David J. Blake at Department of Biology, Fort Lewis College, Durango, Colorado.
- Imaging by confocal microscopy was carried out by Dr Christa Walther from the Wolfson Light Microscopy Facility, School of Bioscience at the University of Sheffield.
- Flow cytometry analysis of CD9 expression on WT and CD9 KO A549 cells was carried out by 3rd year undergraduate project student, Robert Whelan.

Some results presented in Chapter 5 have been submitted to PLOS Pathogens as "Tetraspanin CD9 organisation of heparan sulphate proteoglycans is required for staphylococcal adhesion to epithelial cells" by Luke Green, Rahaf Issa, Fawzyah Albaldi, Lucy Urwin, B Ciani, Lynda Partridge, Peter Monk. This study was conceived by all the authors. I carried out the study of fluorescent 800C peptide binding to epithelial cells.

This work was funded by Albaha University, Ministry of Education in Saudi Arabia.

List of Abbreviation

Abbreviations	Meaning
a.a.	amino acid
ANOVA	Analysis of variance
AUM	Asymmetric unit membrane
Abbreviations	Meaning
a.a.	amino acid
ADAM	A disintegrin and metalloprotease
ANOVA	Analysis of variance
AR	Androgen receptor
AUM	Asymmetric unit membrane
BPS	Bladder pain syndrome
B/B/N	BSS/BSA/NaN3
BECs	Bladder epithelial cells
CS	Chondroitin sulphate
cUTI	Complicated urinary tract infection
CR-UTIs	catheter-associated infections
CAUTIs	Urinary tract infection obtained in the community
CDC	Centres for Disease Control and Prevention
CVC	Central venous catheter
CD	Cluster of differentiation
CFU	Colony forming units
Ct	Threshold cycle
CNF1	Cytotoxic necrotizing factor 1
cryo-EM	cryo-electron microscopy
CS-B	Chondroitin sulphate B
CSPG	Chondroitin sulphate proteoglycan
CDS	Cell dissociation solution
cDNA	complementary DNA
CK20	Cytokeratin 20
CRISPR	Clustered Regularly Interspaced Short Palindromic Repeat

Cas9	CRISPR associated protein 9
CXCR1	C-X-C chemokine receptor type 1
DS	Dermatan sulphate
dH2O	Sterile distilled water
DAPI	4', 6-diamidino-2-phenylindole
DVs	TGN-derived discoidal
DMEM	Dulbecco's Modification of Eagle's Medium
DMSO	Dimethyl sulphoxide
ECM	The extracellular matrix
ER	The endoplasmic reticulum
EGF	Epidermal growth factor
EPEC	enteropathogenic E. coli
EC1	Small extracellular loop
EC2	Large extracellular loop
FVs	Fusiform vesicles
Fn	Fibronectin
FnBPs	Fibronectin-binding proteins
FSC	Forward scatter
FBS	Fetal bovine serum
FCS	Foetal calf serum
FimH	Type-1 fimbriae adhesion
FITC	Fluorescein isothiocyanate
FliC	a flagellar filament structural protein
FDA	Food and Drug Administration
FOXA1	Forkhead Box A1
GAG	The glycosaminoglycan
GPCs	The glycosylphosphoinositide-linked glypicans
gDNA	Genomic DNA
GAPDH	Glyceraldehyde 3-phosphate dehydrogenase
HSPGs	heparan sulphate proteoglycans
HlyA	Haemolysin
HS	Heparan sulphate

HA	Hyaluronic acid
HBSS	Hanks balanced salt solution
IBCs	Intracellular bacterial communities
IC	Interstitial cystitis
ICAM-1	Intercellular adhesion molecule-1
KD	Knockdown
KO	Knockout
LPS	Lipopolysaccharide
LMWH	Low molecular weight heparin
MFI	Median fluorescence intensity
MNGC	Multinucleated giant cells
MOI	Multiplicity of infection
mAbs	Monoclonal antibodies
NK	Natural killer
NHU	Normal human urothelial
NSAID	Nonsteroidal anti-inflammatory drugs
OD	Optical density
Opa	Opacity protein
PGs	Proteoglycans
PKC-b	The protein kinase C Beta
PDGF	Platelet-derived growth factor
PPARγ	Peroxisome proliferator- activated receptor gamma
PBS	Phosphate buffered saline
PFA	Paraformaldehyde
QIRs	quiescent intracellular reservoirs
RT-PCR	Real-time quantitative polymerase chain reaction
RPE	RNA precipitating elution buffer
RW1	RNA washing buffer
rUTI	Recurrence of UTIs
SRB	The sulforhodamine B
SCR	Scrambled peptide
SSC	Side scatter

SDC-1	Syndecan-1
SDCs	Syndecans
SPATES	Serine protease autotransporters of the Enterobacteriaceae
TLR4	Toll-like receptor 4
TNF- α	Tumour necrosis factor α
Tspan	Tetraspanin
TEM	Tetraspanin-enriched microdomains
TGN	trans- Golgi network
TMDs	transmembrane domains
UTIs	Urinary tract infections
UPs	Uroplakins
UPIa	Uroplakin 1a
UPIb	Uroplakin 1b
UPII	Uroplakin 2
UPIII	Uroplakin 3
UPEC	Uropathogenic Escherichia coli
UFH	Unfractionated heparin
UCs	Urothelial cells
VEGFR2	Vascular endothelial growth factor receptors
WT	Wild type
WHO	World Health Organization
ZO-1	Zonula occludens protein 1

Chapter 1: MAIN INTRODUCTION

1.1 Overview of urinary tract infection (UTI)

1.1.1 Epidemiology and the burden of UTIs

Urinary infections are the most prevalent of infectious diseases, characterized by an uncontrolled and excessive growth of uropathogenic bacteria in the urothelial umbrella cells of the bladder. About 150 million people worldwide develop UTIs each year, with high social costs (Flores-Mireles et al., 2015). According to Foxman, with about eleven million instances recorded in the United States alone each year, the yearly expenditure is estimated to be $5 billion (Foxman, 2014). UTIs are the second most prevalent infections in developed countries, resulting in an estimated 7–8 million visits to primary care physicians and over 1 million trips to the emergency department in the United States alone (Johansen *et al.*, 2011; Foxman, 2014). On the same note, the World Health Organization (WHO) reported that the cost of treating and caring for UTIs ranges between 3–5 billion US dollar each year (Klein and Hultgren, 2020). UTI-related hospitalisations are also on the rise worldwide (Simmering et al., 2017). Most women will be infected by a UTI in some point of their life, and up to 30% of those women will have recurring infections that might develop into a more severe condition, such as chronic kidney disease (Foxman, 2002).

In a survey of individuals under the age of 17, just 0.5% of children received annual treatment for UTIs (Sood et al., 2015), with the majority of those patients (89.2%) being female. In addition, the number of children being brought to emergency rooms with UTIs is on the rise. Among the possible causes are obesity in children and the possibility of developing diabetes and metabolic disorders. More often, a higher prevalence of UTIs in adolescents may be linked to increased sexual activity or the use of oral contraceptives rather than condoms (Sood et al., 2015).

1.1.2 Classifications of UTIs

UTIs can be categorised in a variety of ways, including those based on the location of the infection and the severity of the symptoms and complications. The European Association of Urology's Infection section classified the status of complicated (cUTI) or uncomplicated infection (Bonkat et al., 2018). Uncomplicated status is referred to as a minimal chance of developing cystitis, pyelonephritis, or recurrence of UTIs (rUTI). An uncomplicated UTI is one that occurs in a normal, uncatheterised patient with no known genitourinary system problems; if there is an abnormality in the genitourinary system which affects the host's defensive systems this is given a cUTI diagnosis (Lichtenberger and Hooton, 2008; Bonkat et al., 2018). Every year, around seven million women are projected to seek treatment for uncomplicated UTIs (Taur and Smith, 2007). UTIs are classified as "complicated" because of their increased risk including cystitis, pyelonephritis, recurrent infections, catheter-associated infections (CR-UTIs), UTI in male, and urosepsis. An alternative categorisation method is based on the location of the infection (community or healthcare) and the host variables associated with other concomitant conditions such as UTIs in the elderly, UTIs in diabetes, pregnancy or kidney transplant. UTIs in people with spinal cord damage is also characterised (Johansen et al., 2011; Medina and Castillo-Pino, 2019). The most prevalent bacterial infection is a urinary tract infection obtained in the community (CAUTIs) (Öztürk and Murt, 2020). UTI recurrences are defined as three or more UTIs in the same year or two or more in the past six months (Caretto et al., 2017; Terlizzi, Gribaudo and Maffei, 2017).

The ability of uropathogenic bacteria to colonise the bladder epithelium and acquire resistance to antibiotic therapy or host immune defences may be a contributing factor to recurrent UTIs (Mulvey, Schilling and Hultgren, 2001). Previous studies demonstrated that uropathogenic *E.coli* infection raises the chance of recurrence within a six-month period (Medina and Castillo-Pino, 2019).

1.1.3 Catheterization associated-UTI

Urinary catheters are the most widely used medical devices in hospitals, with up to 25% of patients undergoing catheterisation for various causes, including urinary retention, surgical operations, and protracted immobility (Haley et al., 1981; Warren, 2001; Gould et al., 2010). An indwelling urinary catheter is present in up to 13% of men and 12% of women when they are admitted to a nursing home (Mody et al., 2017). For cUTIs, catheter associated UTI (CAUTI) is the most prevalent risk factor and accounts for 40% of all nosocomial infections globally (Tambyah and Maki, 2000; Hooton et al., 2010). Secondary bloodstream infections are frequently caused by CAUTI (Tambyah and Maki, 2000; Warren, 2001; Melzer and Welch, 2013). Despite the fact that UPEC is the primary cause of UTIs, as reported by the National Healthcare Safety Network, only 23.9% of CAUTI infections are caused by UPEC, followed by *Candida spp* (17.8%), *Enterococcus spp* (13.8%), *P. aeruginosa* (10.3%), *Klebsiella spp* (10.1%), *Proteus spp* (4%), *Enterobacter spp* (3.7%), coagulase-negative staphylococci (2.4%), *S. aureus* (1.6%), and even *Bacteroides spp* (<0.1%) (Weiner et al., 2016). Recurring bacterial infections in individuals with indwelling catheters have become increasingly difficult to treat as antibiotic-resistant strains have become more common.

The most prevalent cause of bacteriuria is the formation of microbial biofilms on the urinary catheters (Stickler, 2008). As opposed to alternative materials, silicone catheters are preferred by Centres for Disease Control and Prevention (CDC), recommended because they lower the risk of encrustation in long-term catheterised patients who experience frequent obstructions (Gould et al., 2010). The development of antimicrobial/antiseptic-impregnated, silicone-based urinary catheters has been a major priority of attempts to avoid biofilm development (Ha and Cho, 2006; Singha, Locklin and Handa, 2017). Standards for the technique of implanting medical devices and managing catheters have been proposed. For example, the placement of any central venous catheter (CVC) requires the use of sterile gloves, hat, mask, sterile gown, and full-body sterile drape by trained staff in accordance with the strictest possible sterility standards (O'grady et al., 2002).

1.1.4 Route of infection and consequences of UTIs

The human gastrointestinal system is thought to be the major reservoir of UPEC. *E. coli* must first escape from the acidic environment of the stomach and upper intestine, and then penetrate the colon epithelium's viscous upper mucus layer to colonize their primary habitat in the colon (Møller *et al.*, 2003; Klein and Hultgren, 2020). The *E. coli* bacteria can live in competition with different strains and species of the complex of intestinal surface microbiota to gain its nutritional needs (Miranda *et al.*, 2004). Some *E. coli* stay in the intestinal lumen or are eventually excreted in faeces. UTIs are usually started when UPEC is successfully transmitted and colonizes the periurethral region and migrates into the bladder (Lewis, Richards and Mulvey, 2017; Mann *et al.*, 2017; Murray *et al.*, 2021). The majority of UPEC strains that have been identified enter the bladder epithelium and initiate an intracellular infection cycle. This infection cycle is a complicated process that involves epithelial adhesion, host cell invasion, and internalized growth, ultimately leading to bladder epithelial cell damage, spreading, and reinfection of neighbouring epithelial cells (Lewis, Richards and Mulvey, 2017). Lower urinary tract infections have the potential to expand to the kidneys and into the bloodstream, resulting in potentially acute infections (Flores-Mireles *et al.*, 2015; Walsh and Collyns, 2017).

UTIs are a major cause of morbidity in both genders and all ages. Frequent recurrence, pyelonephritis, renal damage in early age, premature baby delivery and drug resistance are among the possible long-term consequences of UTIs (Flores-Mireles et al., 2015). The emotional and societal burdens of recurring UTIs are intertwined. It is important to note that the societal burden covers both clinical and economic difficulties, whereas the individual's burden is tied to factors that negatively influence their quality of life (Cek et al., 2014). Symptoms like anxiety and depression have been linked to recurrent urinary tract infections. Patients are typically alarmed by the fast onset of a UTI, which can be quite painful. Due to a patient's recurring illnesses or incapacity to carry out their customary activities, they may feel guilty and have clinical depressive symptoms (Medina and Castillo-Pino, 2019). The development of UTI may result from urinary tract dysfunction and/or some genetic variants such as

polymorphisms in TLR4 and CXCR1 that are critical for innate immune defences (Köves and Wullt, 2016). Recurring UTIs are common during pregnancy and can have serious consequences for both the baby and mother, for instance, premature birth. Indeed, there are pharmacological and non-pharmacological options for treatment in this situation, which include antibiotics and alternative therapies (Schneeberger et al., 2012). Despite being less common than lower urinary tract infections, upper urinary tract infections (Czaja et al., 2007) might extend to the kidneys causing acute pyelonephritis.

1.1.5 Causative agents of UTIs

The majority of UTIs are caused by strains of uropathogenic *Escherichia coli* (UPEC), whereas the remaining cases are due to other pathogens such as *Klebsiella pneumoniae* (about 7%), *Proteus mirabilis* (about 5%), and *Pseudomonas aeruginosa*, *Enterococcus faecalis, Enterobacter cloacae, Streptococcus bovis*, and the fungus *Candida albicans* (for the remaining percentage) (Sheerin, 2011; Parish and Holliday, 2012; Palou et al., 2013; Flores-Mireles et al., 2015; Hof, 2017; Terlizzi, Gribaudo and Maffei, 2017) (Flores-Mireles et al., 2015; Klein and Hultgren, 2020). UPEC strains account for roughly 80% of uncomplicated UTIs, 95% of community-acquired infections, and half of hospital-acquired infections (Mohsen Tabasi et al., 2016). The commonest cause of cUTIs is also UPEC (Kucheria et al., 2005; Dhakal, Kulesus and Mulvey, 2008; Foxman, 2010).

1.1.6 UPEC pathogenesis

1.1.6.1 Virulence and fitness factors involved in UPEC adhesion

As discussed above, the most prevalent cause of UTIs is UPEC strains. This is due to their ability to express a wide range of virulence factors, which can be divided into two groups: virulence factors related to the surface of bacterial cells

and secreted virulence factors (Table 1.1). These virulence factors are usually encoded on specific regions on the bacterial chromosome termed “pathogenicity islands” (Hacker and Kaper, 2000). These pathogenicity islands (PAIs) are essential for identification of UPEC pathotypes since PAIs are often variable chromosomal regions (Oelschlaeger, Dobrindt and Hacker, 2002). Bacterial cell surface virulence factors include adhesive molecules (mainly fimbrial adhesins) and flagella which promote bacterial motility and attachment to host cells within the urinary tract. Type 1 fimbriae and P fimbriae are fimbrial adhesins that are involved in attachment to host cell surfaces, tissue invasion (which is critical in the pathogenesis of UPEC-caused UTIs), biofilm development, and cytokine induction (Shah et al., 2019). The most important of the filamentous adhesive molecule, type 1 fimbriae, with polymerized pilin subunits capped with lectin, is involved in attachment to mannose-containing glycoprotein receptors such as the uroplakins in the epithelial bladder cells (Ulett et al., 2013). In 1998, high resolution electron microscopy of infected mouse bladder illustrated the contribution of type 1 fimbriae to mannose-containing glycoprotein receptors in the epithelial bladder cells (Matthew A. Mulvey et al., 1998). FimH binding to its receptors enhances the formations of intracellular bacterial communities (IBCs) and mediates adhesion and invasion, indicating the importance of these fimbriae in bacterial colonization (Zhou et al., 2001; Eto et al., 2007; Dhakal, Kulesus and Mulvey, 2008). P fimbriae are necessary for UPEC colonisation in the kidneys, causing pyelonephritis (Roberts et al., 1994; Tabasi et al., 2015; M. Tabasi et al., 2016).

Flagellum are employed by UPEC strains to seek fresh nutrients and to escape from unfavourable environments including the host immune system (Lane et al., 2007). Studies have revealed that the expression of flagella in UPEC strains coincides with the bacteria ascending to the upper urinary tract, indicating that flagella play a significant role in the bacteria's transit from the bladder to the kidneys (Wright, Seed and Hultgren, 2005; Lane et al., 2007; Schwan, 2008). Flagella also have a significant role in the formation of biofilms in the urinary system at various stages of infection (Pratt and Kolter, 1998).

Bacterial cell surface virulence factors also include capsular lipopolysaccharide and outer membrane proteins. After bacterial adherence, there are various strategies of pathogenesis; avoiding the rapid flow of urine, affecting host cell signalling, enhancing the transport of bacterial proteins such as α-haemolysin and providing a good advantage for UPEC to survive inside the host cells (Mulvey, 2002). Haemolysin toxins are the most important secreted virulence factors of UPEC isolates (Bien, Sokolova and Bozko, 2012). Haemolysin (HlyA) is a pore-forming toxin that is produced by 50% of the UPEC strains (Asadi Karam, Habibi and Bouzari, 2019). It has been suggested by several studies to inhibit cytokine production in various immune cells (Konig and Konig, 1993; Bhushan et al., 2011), epithelial cells (Hilbert et al., 2012) and natural killer cells (Gur et al., 2013). HlyA has been found to interact with human natural killer (NK) cells in the bladder (Gur et al., 2013). NK cells are killed by HlyA after bacterial binding via type 1 fimbriae. It has been shown that HlyA reduces the pro-inflammatory response to UPEC by inhibiting the release of cytokine TNF- α, which is promoted by NK cells in response to infection. In addition, early in the infection, *E. coli* expressing HlyA causes a lot of exfoliation (Smith et al., 2008). Cytotoxic necrotizing factor 1 (CNF1) toxin has been found in around 30% of UPEC strains (Asadi Karam, Habibi and Bouzari, 2019), resulting in the constitutive activation of the Rho family of GTP-binding proteins, such as Cdc42, causing cytoskeleton disruption in the host cells. This toxin is also involved in UPEC binding and invasion of host cells (Lemonnier, Landraud and Lemichez, 2007; Mohsen Tabasi et al., 2016).

Several studies have revealed that there is a strong relationship between bacterial virulence factors and antibiotic resistance (Tabasi et al., 2015; Paniagua-Contreras et al., 2017; Karam, Habibi and Bouzari, 2018; Shah et al., 2019). In a prospective study of 105 patients with *E. coli* UTIs, biofilm production was observed in 62% of UPEC isolates compared to only 1% of control isolates, and was linked to greater rates of antibiotic resistance (Shah et al., 2019). A further study conducted in Iran indicated that the correlation between biofilm production and antibiotic resistance and antibiotic sensitivity is also influenced by iron receptors and hemolysin secretion (Karam, Habibi and Bouzari, 2018).

1.1.6.2 UPEC pathogenesis within the urinary tract

Whenever *E. coli* of the intestinal system reaches the urinary tract and colonises the urethra, vaginal and periurethral regions, the urinary tract infection cycle begins. UPEC mainly ascends into the bladder and adheres to the bladder epithelium through FimH-mediated mannose and other non-fimbrial adhesins (Mann et al., 2017). Internalised adherent bacteria can reach the cytoplasm and replicate rapidly, creating intracellular bacterial communities (IBCs), which serve as a source of quiescent intracellular reservoirs (QIRs) inside the urinary tract (Wright, Seed and Hultgren, 2007; Asadi et al., 2019). Bladder epithelial cells can contribute to host immune defence by activation of programmed cell death pathways that lead to exfoliation and the subsequent removal from the urinary systems with urine flow (Matthew A. Mulvey et al., 1998; McLellan and Hunstad, 2016). The remaining bacteria can evade the immune system and antimicrobial drugs by forming a biofilm in a deeper layer of the urothelium (Anderson et al., 2003; Schwartz et al., 2011). To spread into the bladders lumen or even to the kidney, some of these microorganisms are capable of breaking out of the biofilm and becoming motile bacteria (Flores-Mireles et al., 2015). Asadi Karam and co-workers suggested that the re-entry of *E. coli* strains from the gut into the urinary tract system may be the cause of recurrent UTIs (Asadi Karam, Habibi and Bouzari, 2019). Consequently, these strains are able to enter and replicate within uroepithelial cells, so providing protection from host immune defences (Mulvey, 2002).

The growth of UPEC in the nutritionally poor urinary tract is supported by multiple mechanisms. For example, iron is limited in the urinary environment, therefore bacteria utilize iron acquisition systems. These systems, called siderophores, are produced by UPEC strains and include salmochelin, aerobactin, enterobactin, and yersiniabactin, which are small- molecule iron chelators responsible for iron binding and a membrane receptor that help bacteria to absorb iron from the host (Table 1.1). Iron acquisition systems are key prerequisites for the existence and colonization by UPEC (Flores-Mireles et al., 2015). In addition, utilization of short peptides and amino acids as a

carbon source during infection is an aspect of metabolism that might be considered an essential for bacterial survival (Alteri, Smith and Mobley, 2009).

Table 1.1: Uropathogenic E. coli virulence and fitness factors that facilitate infection of the urinary system.

Different strategies are utilized by UPEC to defend against the host's immune system (Lüthje and Brauner, 2014).

Virulence factors	Examples
Adhesins	Pili Curli Afimbrial adhesins
Toxins	LPS CNF1 Haemolysin Serine protease autotransporters of the Enterobacteriaceae (SPATES)
Iron acquisition	Siderophores Haem receptors
Immune evasion	Cellulose Salmochellin O-antigen Capsule

1.1.7 Emerging therapeutics for the treatment of UTIs

Antibiotics have remained the gold standard for treating and preventing UTIs (Abou Heidar et al., 2019; Wawrysiuk et al., 2019). Treatment for UTIs has included nitrofurantoin or fosfomycin for complicated and uncomplicated UTIs, ciprofloxacin or levofloxacin for pyelonephritis (Klein and Hultgren, 2020). Nonetheless, the frequent use of antibiotics contributes to the development of antibiotic resistance, and also causes abnormalities in the natural microbiota of the vagina and the gastrointestinal tract (Wawrysiuk et al., 2019). Although nitrofurantoin continues to be effective against *E.coli*, with fewer cases of resistance than trimerthoprim (Hatton, Baumann and Fascione, 2021), nitrofurantoin has high rates of serious side effects such lung fibrosis

(Goemaere et al., 2008). Bacteria living inside the bladder cells are provided a safe harbour from antibiotics (Terlizzi, Gribaudo and Maffei, 2017). As a result, non-antibiotic preventative and alternative treatment have become increasingly important.

For the prevention and treatment of UTIs, there are now about eight main non-antibiotic options. The principal idea of the use of anti-adhesion therapy is to prevent bacterial binding to the urinary tract mucosa. Preventing UTIs with cranberry juice or pills is a common practice that is self-administered. Cranberry products have been demonstrated to mitigate the risk of UTIs in a number of studies (Jepson and Craig, 2008; Foxman et al., 2015; Singh, Gautam and Kaur, 2016). However, these results are still up for debate and may require further research due to the limited populations involved (Jepson, Williams and Craig, 2012; Takahashi et al., 2013; Liska, Kern and Maki, 2016; Maki et al., 2016; reviewed in Wawrysiuk et al., 2019).

The use of probiotics has been proposed in the urinary tract. The benefit of this treatment is the fact that the vagina can be a storage for the bacteria that cause these infections. Vaginal microbiome changes that reduce the presence of colonies of *Lactobacillus* spp. are linked to increase in the risk of urinary tract infections. The use of either oral or intravaginal probiotics to regain the natural vaginal microbiota may be a potential way to reduce antibiotic usage and antimicrobial resistance (reviewed in (Wawrysiuk et al., 2019)). Many studies have demonstrated that *Lactobacillus* therapies are safe in terms of antibiotic resistance and substantially impact the incidence of urinary tract infections (UTIs) (Stapleton et al., 2011; ter Riet et al., 2012). However, prior to proposing probiotics as an antibiotic alternative, a more thorough study is required (Gupta, Nag and Garg, 2017).

Mannosides, a class of mannose-based inhibitors and anti-adhesion agents, have been the subject of several studies in the field of urinary tract infections. These compounds can attach to the adhesin FimH at the type 1 pili tip and prevent the binding of mannosylated glycoproteins in the colon and bladder (Han et al., 2010; Klein et al., 2010; Spaulding et al., 2017; Schönemann et al., 2019). In a previous report, mannoside derivatives were shown to be able to

block UPEC adhesion and prevent bacterial invasion into the urothelium in a mouse model (Cusumano et al., 2011). The research concluded that both d-mannose and nitrofurantoin significantly decreased the chance of UTI, with the d-mannose group having a lower risk of side effects. Recent studies have summarized different classes of mannose-based treatments and their limitations (reviewed in (Hatton, Baumann and Fascione, 2021)) . For example, mannose-capped oligosaccharides which most closely reflect natural FimH ligands in structure, have the ability to act as FimH inhibitors, but their lack of oral bioavailability and difficult chemical manufacture limits their application (Hatton, Baumann and Fascione, 2021). The simplicity and smaller structure of α-d-mannopyranoside-based inhibitors make them the most acceptable class of mannoside derivatives since these compounds are easier to produce and show improved oral absorption (Hatton, Baumann and Fascione, 2021). Overall, although research suggests that d-mannose may be effective in preventing UTIs (Kranjčec, Papeš and Altarac, 2014; Hatton, Baumann and Fascione, 2021), these synthetic derivatives inhibitors need to be sufficiently tested in humans and further investigation is needed.

Active immunisation in animal studies has been found to be extremely effective in lowering the incidence and severity of UTIs. Using the type 1 pilus adhesin FimH as a vaccine has been demonstrated to significantly reduce UTI prevalence in mice infection models and non-human primates (Langermann et al., 2000). A study by Conover and colleagues in 2016 showed that immunization with FmH1s N-terminal sticky domain reduces the bacterial load 2-3 days after infection in a mouse of chronic cystitis (Conover et al., 2016). Mouse vaccination experiments using a truncated flagellin (FliC) protein from enteroaggregative *E. coli* as an adjuvant fused to FimH have shown promise for enhancing the humoral immune response (Savar et al., 2014).

The IgG and safety responses following vaccination with the FimH vaccine were evaluated in phase I clinical study, and there were no safety issues. The FDA has approved it for use as an experimental treatment (Eldridge et al., 2021). Other therapeutic agents including nonsteroidal anti-inflammatory drugs (NSAID), oestrogens, vitamins and lactoferrin were also studied (reviewed in

(Wawrysiuk et al., 2019)). Overall, in the case of UTIs, non-antibiotic approaches have not provided clear proof that these alternatives may totally substitute antibiotic use.

1.2 An overview of tetraspanins

Tetraspanins are a superfamily of membrane proteins expressed in all mammals including humans. The tetraspanins were first recognized in 1990, when a comparison of the sequences of ME491 (later named CD63) (Hotta et al., 1988), CD37, CD81 (TAPA-1) revealed strong sequence homology and a conserved structure defining a new family of transmembrane proteins (Oren et al., 1990). Since 1990, various members of this superfamily have been discovered, from a variety of species. Thirty-three known members exist in humans, found in all tissues of the body (van Spriel and Figdor, 2010; Charrin et al., 2014). Different levels of tetraspanin expression occur throughout all cell types, distributed either mainly in the plasma membrane or on intracellular vesicle membranes. Some members, such as CD9, CD63, CD82 and CD151 exhibit extensive expression in different types of human tissues (Yang et al., 2020), whereas others, like uroplakins UPIa and UPIb, are generally restricted to a specific region in the AUM of the urothelium (Xie, Zhou, S.-Y. Chan, et al., 2006), also CD37 and CD53 in lymphoid cells (Hemler, 2005). The naming of some tetraspanins refers to the 'cluster of differentiation' (CD) which classifies cell surface molecules that are recognized by specific monoclonal antibodies using a certain CD number (Table 1.2). CD9, CD37, CD53, CD63, CD81, CD82 and CD151 are the members that have been most intensively studied since the 1980s (reviewed in (Lang and Hochheimer, 2020).

Table 1.2: Expression pattern and associations of selected tetraspanins

Tetraspanin	Alternative names	Expression pattern	Known to associate with	References
TSPAN20	UPIb	Uniquely expressed on urothelium	UPII	(Hu *et al.*, 2005; Sun, 2006).

TSPAN21	UPIa	Uniquely expressed on urothelium	UPIII	(Hu *et al.*, 2005; Sun, 2006).
TSPAN24	CD151	Widely expressed on most of epithelial cells	Integrins, $\alpha 3\beta 1$, $\alpha 6\beta 1$	(Kazarov *et al.*, 2002; Hemler, 2005).
TSPAN25	CD53	Uniquely expressed on lymphoid cells.	CD2, PKC-β	(Bell *et al.*, 1992; Zuidscherwoude, V. M. E. Dunlock, *et al.*, 2017; Yang *et al.*, 2020).
TSPAN26	CD37	Uniquely expressed on lymphoid cells.	$\alpha 4\beta 1$	(van Spriel *et al.*, 2012).
TSPAN27	CD82	Widely expressed on most of the cell type	Integrins and DARC	(Bandyopadhyay *et al.*, 2006; Neumann *et al.*, 2018).
TSPAN28	CD81	Widely expressed on most of the cell type	CD19	(Shoham *et al.*, 2006; Susa *et al.*, 2021).
TSPAN29	CD9	Widely expressed on most of the cell type	EW1-2, ICAM-1 and VCAM-1	(Barreiro *et al.*, 2008; Umeda *et al.*, 2020).
TSPAN30	CD63	Widely expressed on most of the cell type	$\beta 1$ integrin and VEGFR2	(Tugues *et al.*, 2013).

1.2.1 The structural features of tetraspanins

Tetraspanins are recognized by their characteristic similarities between members of this superfamily. All tetraspanins are composed of 4 transmembrane domains, often containing polar residues in transmembrane domains 1 (Asp), 3 and 4 (Gln and Glu). Tetraspanins consist of small and large extracellular loops (EC1 and EC2), as well as a short inner loop with 2 intracellular termini (N- and C- termini) that are usually short (Figure 1.1). The first crystallographic study of an EC2 was for CD81 in 2001 (Kitadokoro et al., 2001). This region is divided into constant and variable regions. The constant region contains conserved A, B and E helices, while the variable regions differ structurally between family members and are often the site of interactions with other cell surface molecules. All tetraspanins have four conserved cysteines, including two in a distinctive, conserved CCG motif, with two disulphide bonds, which are necessary to reach a proper folding and function of the protein (DeSalle, Mares and Garcia-España, 2010). Tetraspanins can be classified based on the number of cysteines in their EC2 domain into 3 classes: C4, C6, or C8 (Seigneuret et al., 2001; DeSalle, Mares and Garcia-España, 2010) that may form two to four cysteine pairs (Huang et al., 2005). The EC1 found in tetraspanins varies in size and until recently its function has been elusive (van Deventer, Dunlock and van Spriel, 2017).

Three members of the Tspan C4 subfamily: CD9, CD53 and CD81 have been structurally reported in recent years. The first crystallization structure of a whole tetraspanin, CD81, was revealed by Zimmerman et al in 2016 (Figure 1.2) (Zimmerman, Kelly, Brian J McMillan, et al., 2016). This suggested that cholesterol is bound in a pocket formed by the transmembrane domains and when the cholesterol is unbound, the EC2 region moves away from the transmembrane domains. This suggested that this conformational change could regulate some biological functions (Zimmerman, Kelly, Brian J. McMillan, et al., 2016; Yang et al., 2020). The partial interaction of the EC2 of CD9 with

its partner protein, EW1-2, by cryo-electron microscopy (cryo-EM) has been also reported (Umeda et al., 2020). Another group has reported the cryo-EM structure of CD81 bound to its partner CD19, showing directly that CD81 can adopt an open form when bound (Figure 1.3) (Susa . et al., 2021) . More recently, in isolation and in conjunction with the Fab region of an anti-Tspan15 antibody, the crystal structure of Tspan15 EC2, a member of the TspanC8 subgroup of tetraspanins, necessary for functional association with ADAM10, has been solved (Lipper et al., 2021). These findings conclude that the Tspans adopt a more open conformation when bound to partner proteins.

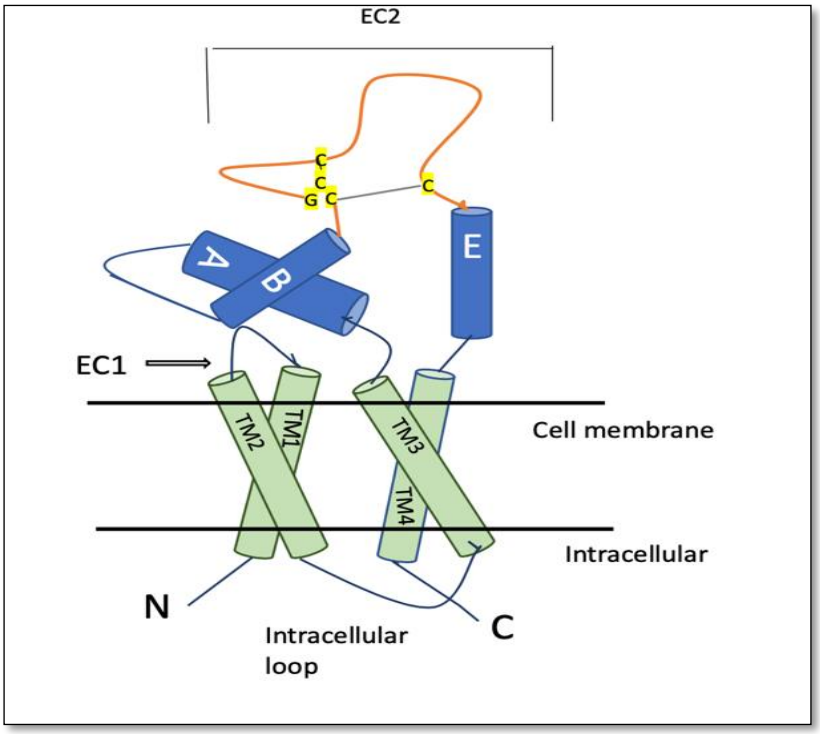

Figure 1.1: Schematic of tetraspanin structure.

The small extracellular loop, EC1, and large extracellular loop EC2 are indicated. The EC2 has two regions, variable and constant (shown in orange and blue, respectively). The variable region is thought to be the site of interaction with other transmembrane proteins, whereas A, B, and E helices in the constant region are believed to play a role in tetraspanin dimerization (Hemler, 2005). At least four cysteines are present in the EC2 forming at least two disulphide bridges. The four transmembrane domains (TM1, TM2, TM3 and TM4), an intracellular loop, a N-terminal tail and a C-terminal tail are also indicated.

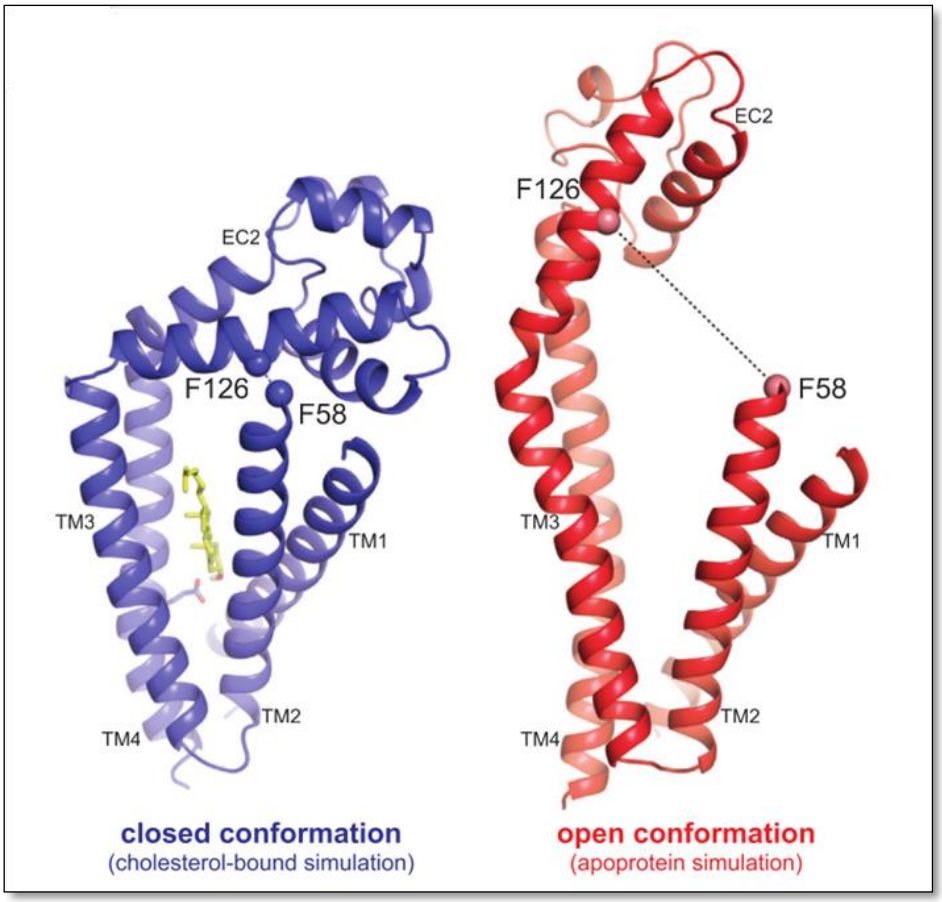

Figure 1.2: The model of human tetraspanin CD81.

This structure reveals a cholesterol binding pocket in closed conformation (blue), whereas in open conformation without bound cholesterol (red). This figure is reproduced with permission from Cell (Zimmerman, Kelly, Brian J McMillan, et al., 2016).

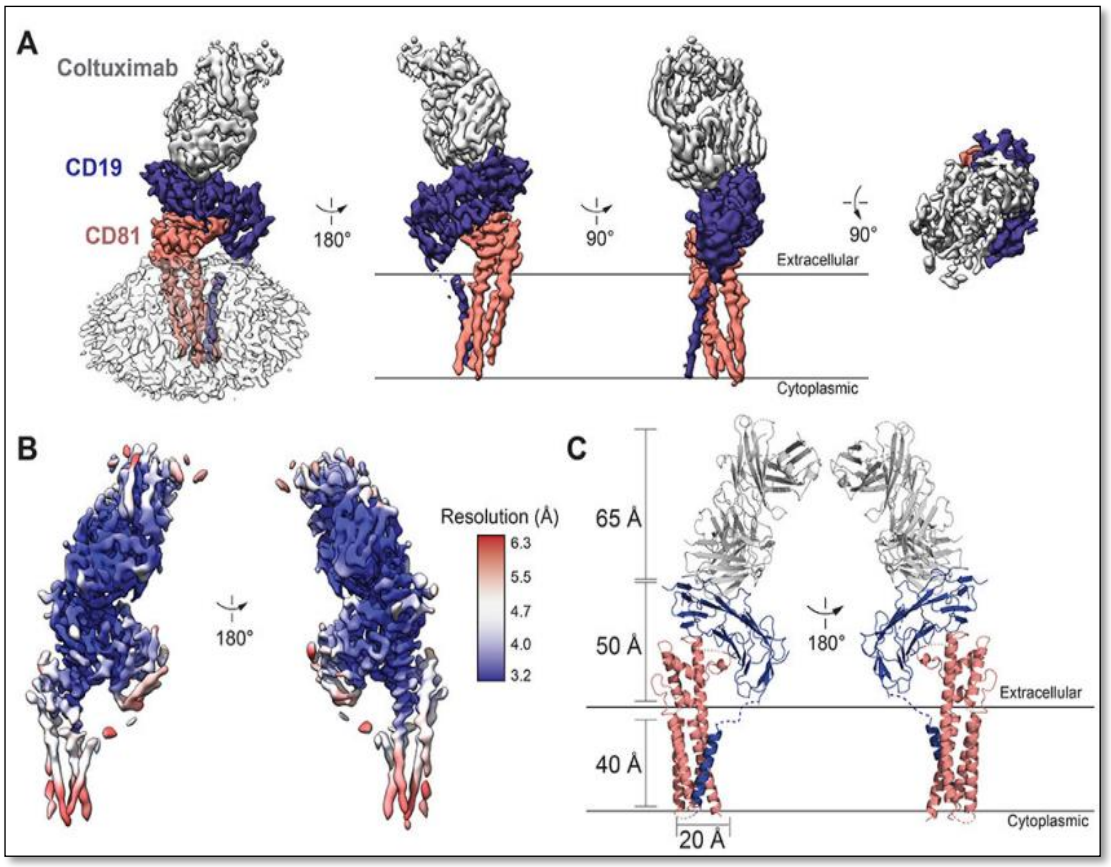

Figure 1.3: 3D reconstruction and atomic model of human CD19-CD81 complex associated to Coltuximab.

(A) Different perspectives of the CD19-CD81-Coltuximab complex cryo-EM map, coloured by subunit. In the left panel, the density associated with the detergent micelle is represented plainly in white. (B) Cryo-EM map of the CD19-CD81-Coltuximab complex, filtered locally and coloured according to local resolution, generated with cryo SPARC. (C) The structure of the complex is represented by a ribbon. CD19, CD81, and Coltuximab are coloured in the same way they are in A(Susa et al., 2021). This figure is available from the Protein Data Bank (Accession number Protein Data Bank (PDB) 7JIC).

1.2.2 The tetraspanin web

The interactions between different tetraspanins and partner proteins in the membranes of the cell, through membrane-proximal palmitoylation sites or the EC2 regions, leads to the formation of microdomains known as Tetraspanin-enriched Microdomains (TEMs) (Figure 1.4) (Hemler, 2005). Through fluorescence and immunoelectron microscopy, it has been revealed that cells contain many hundreds of TEMs, particularly containing CD9, CD63, CD81, and CD82 at the plasma membrane (Sascha et al., 2006). The composition and the size of TEMs differs from cell to cell (Barreiro et al., 2008). Tetraspanins

have been widely described in different terms such as ‘molecular organizers’ (Maecker, Todd and Levy, 1997; Umeda et al., 2020) or “master organizer” (Lang and Hochheimer, 2020), due to their ability of forming a network of multimolecular membrane microdomains, also referred to as the “tetraspanin web” (Hemler, 2003; Le Naour et al., 2006). Tetraspanins engage with one another and a wide variety of partners, many of which include proteins with immunoglobulin-like (Ig) domains. It has long been suggested that the variable region of the EC2 regulates the specificity of partner interactions such as CD53 with CD2 (Bell et al., 1992) and CD81 with CD9 (Shoham et al., 2006). More recently, a structural study has confirmed the interaction of CD81 with CD19 as described above (section 1.2.1) (Susa . et al., 2021). The crystal structure of the EC2 region of Tspan 15 has revealed the binding site with its partner ADAM10, and also showed matching with the EC2 structure from CD9, CD53 and CD81 (Lipper et al., 2021). Additionally, tetraspanins transmembrane regions have a role in partner interactions, such as CD81s TM1 supporting the evacuation of CD19 from the ER (Shoham et al., 2006). The two termini of tetraspanins are positioned on the cytosolic side, allowing for additional interaction sites such as with signalling molecules (van Deventer, Dunlock and van Spriel, 2017). For instance, the CD53 N-terminus interacts with PKC-b to control B cell signalling (Zuidscherwoude, V.-M. E. Dunlock, *et al.*, 2017). Taken together, tetraspanins’ various structural regions are essential to coordinate the interactions between them and their partners (van Deventer, Dunlock and van Spriel, 2017). However, the molecular nature of these organizations and the control of cellular responses remain largely poorly understood (Yang et al., 2020). It should be noted that the EC1-EC2 interaction is crucial for the formation of a stable open conformation since for tetraspanin–partner interactions to be successful, they must be openly conformed (Yang et al., 2020).

1.2.3 Biological processes involving tetraspanins.

In order to facilitate many cellular process, tetraspanins work in tandem with several cell membrane-bound partners and organise them on the cell membrane (van Deventer, Dunlock and van Spriel, 2017). Different

physiological and pathological processes depend on the function of tetraspanins, including regulation of cell morphology (Yang et al., 2020) cell structure and function (Yamada et al., 2008), regulating immunity (van Spriel, 2011; Yeung, Hickey and Wright, 2018), adhesion (Yanez-Mo et al., 2001; Reyes et al., 2018), transduction of signals (Termini and Gillette, 2017), viral infections (Martin et al., 2005), cell:cell fusion (Fanaei, Monk and Partridge, 2011) as well as cancer progression (Hemler, 2014; Lipper et al., 2021). However, a complete overview of tetraspanins functions is outside the scope of this thesis, but some of the most relevant functions are described below.

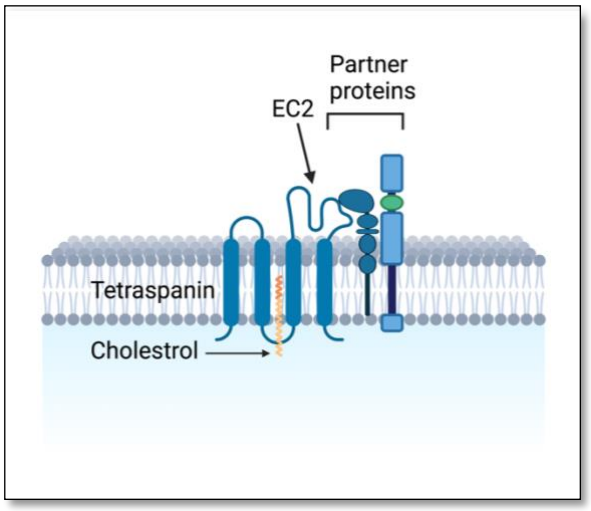

Figure 1.4: Hypothetical model of TEM.

Tetraspanin's molecular interaction with its partner proteins is mediated via both the TM and EC2 regions, however the partner proteins reliance on these regions differs. Lipid binding to the central cavity could be the molecular switch that controls the interaction of tetraspanins with partner proteins.

1.2.3.1 Roles of tetraspanins in trafficking

Tetraspanins can be found abundance on the plasma membrane as well as the membrane of intracellular vesicles and exosomes. Endocytic trafficking of many tetraspanins is possible via endocytosis, and they can either enter the cell or exit the cell in vesicles. The involvement of CD63 in the trafficking of various partner proteins to late endocytic vesicles has been extensively studied (Maaike S Pols and Klumperman, 2009). A previous study by Tugues and co-workers found that knockdown of CD63 in endothelial cells can alter the formation of

complexes between integrins and major vascular endothelial growth factor receptors, VEGFR2, resulting in poor downstream signalling (Tugues et al., 2013). Therefore, CD63 controls VEGFR2 activation and signalling in endothelial cells, and CD63 was also important for VEGFR2 internalisation upon ligand binding, suggesting that CD63 serves as a link between β1 integrin and VEGFR2 (Tugues et al., 2013). Conversely, the TspanC8 subfamily (Tspan5, Tspan10, Tspan14, Tspan15, Tspan17 and Tspan33) regulates ADAM10 metalloprotease trafficking, primarily from the endoplasmic reticulum to the plasma membrane (Dornier et al., 2012; Haining et al., 2012; Prox et al., 2012). ADAM10 expression on the surface of A549 cells is decreased by more than half after Tspan-15 is knocked out (Haining et al., 2012). TspanC8 tetraspanins also have a beneficial effect on Notch signalling since Tspan5 and Tspan14 increase the cleavage of ADAM10 (Dornier et al., 2012).

1.2.3.2 Roles for tetraspanins in cell adhesion and morphology

The ability of tetraspanins to form a significant network of multimolecular complexes, either with integrin ligands on cells or integrins that interact with extracellular matrix (ECM) components such as laminin, allows many tetraspanins to control cell migration, adhesion and maintain cell morphology. For example, tetraspanin CD151 is functionally important in regulation of several cell functions such as attachment, shape and migration; knockdown of CD151 by RNA interference can weaken integrin $\alpha 3\beta 1$ attachment with laminin 511 (Yamada et al., 2008). As a result, these cells showed aberrant membrane protrusions and reductions in the tyrosine phosphorylation of a group of kinases within the cell, namely, Src, p130Cas and paxillin. Another study has demonstrated that mutation of CD151, particularly disrupting integrin interactions (α3 and α6), are sufficient to alter cell spreading and cellular morphology (Kazarov et al., 2002).

Tetraspanin molecules are also engaged in the adhesion between neighbouring skin cells (Yanez-Mo et al., 2001). Interference of tetraspanin function, such as interaction with integrin ligand ICAM-1, using recombinant tetraspanin EC2

domains or anti-tetraspanin antibodies can reduce the interaction between leukocyte integrins and endothelial receptors during extravasation (Barreiro et al., 2008). CD9, within the context of tetraspanin- enriched microdomains (TEMs), has been reported to act as a scaffold in the regulation of adhesion molecules at the immune synapse and T lymphocyte activation (Reyes et al., 2018).

1.2.3.3 Role of tetraspanin in bacterial infection

Tetraspanins are thought to contribute to the formation of an “adhesive platform” of adhesion molecules such as ICAM-1 on endothelial cells to allow leukocyte attachment during extravasation as mentioned above (Barreiro et al., 2008). Many viruses and bacteria are able to use various partner proteins that associate with tetraspanins including integrins, heparan sulphate proteoglycans (HSPGs) and immunoglobulin superfamily members to adhere to and access host cells (Umeda et al., 2020; Green et al, manuscript submitted to PLOS Pathogens). The main principal of tetraspanin function during bacterial infection may be to facilitate the link between bacterial ligands and integrins and other TEMs surface proteins by forming clusters of adhesion molecules, similar to the adhesion platforms described above (Storm et al., 2017; Rajan et al., 2018; TerBush et al., 2018). Tetraspanins involvement in various bacterial infections has been extensively investigated by our group team. In this section, we will focus on a few bacterial pathogens that have been shown to use tetraspanins to cause infections.

1.2.3.3.1 Neisseria meningitidis

This pathogen is able to bind to host cells by its type IV pilus proteins and opacity protein (Opa). Subsequently, *Neisseria meningitidis* moves into host cells via blood vessels to cross the blood-brain barrier and cause meningitis (dos Santos Souza et al., 2020). It was determined that tetraspanins were involved in *N. meningitidis* adhesion to DETROIT 562 and HEC- 1-B human epithelial cell lines. Meningococcal adhesion to the cells was dramatically reduced after pre-treating the cells with antibodies raised against CD9, CD63

and CD151, or with recombinant proteins corresponding to the EC2s of CD9, CD63 and CD151. Anti-tetraspanin inhibition of adhesion to epithelial cells was more pronounced for *N. meningitidis* strains expressing Opa. The siRNA ablation of tetraspanins also decreased bacterial adhesion to epithelial cells. The results imply that CD151, CD63, and CD9 contribute to meningococcal adhesion to cells via particular receptor-adhesion interaction (Green et al., 2011).

1.2.3.3.2 Streptococcus pneumoniae

Infection by *Streptococcus pneumoniae* can result in pneumonia, meningitis and sepsis, which can be fatal (Ferreira-Coimbra, Sarda and Rello, 2020). Initially, infection of host cells by *S. pneumoniae* involves bacterial pili binding to glycoconjugates on the cell surface (Weiser, Ferreira and Paton, 2018). *S. pneumoniae* has a range of bacterial adhesins that are able bind to extracellular matrix proteins such as fibronectin and plasminogen (Weiser, Ferreira and Paton, 2018). After initial association with host cells, pneumococci can recruit host proteins and may induce the formation of adhesion platforms organised by tetraspanins. The role of tetraspanins in *S. pneumoniae* adherence to epithelial cells was investigated by members of our group (Green et al., 2011). Pre-treatment of epithelial cells with monoclonal antibodies specific to CD9, CD63 and CD151, or recombinant proteins corresponding to the EC2s of tetraspanins significantly reduced bacterial binding to the cells. These results suggest that tetraspanins are in involved in the adherence of *S. pneumoniae* to epithelial cells (Green et al., 2011).

1.2.3.3.3 Salmonella typhimurium

Adhesion to cells and penetration are two of the most important processes in Salmonella infection (LaRock, Chaudhary and Miller, 2015). The involvement of tetraspanins in the attachment of human macrophages and *Salmonella typhimurium* has also been addressed by our group. The roles of tetraspanins CD151 CD81, CD63, CD37, and CD9 was similarly studied using monoclonal antibodies and recombinant EC2 proteins. The EC2 proteins decreased

macrophage adherence by ~50%, while monoclonal antibodies had variable outcomes. Notably anti- CD63 antibodies appeared to inhibit *S. typhimurium* adherence to macrophages by inducing internalisation of cell surface CD63 (Hassuna et al., 2017). CD63 siRNA knockdown also significantly reduced bacterial adhesion, underscoring the critical role played in Salmonella pathogenesis by CD63 (Hassuna et al., 2017).

1.2.3.3.4 Staphylococcus aureus

Staphylococcus aureus is a common cause of skin and wound infections (Tong et al., 2015). Several adhesins expressed by *S. aureus* allow it to bind to receptors on host cells, such as surface-expressed chaperones, scavenger receptors, and fibronectin (Alva-Murillo, López-Meza and Ochoa-Zarzosa, 2014; Ventress et al., 2016). When anti-tetraspanin antibodies and recombinant EC2 proteins were used to pre-treat host cells, binding of *S. aureus* was reduced (Green et al., 2011). Short (16 a.a.) peptides derived from the CD9 EC2 domain have recently been found to inhibit *S. aureus* adhesion to epithelial cell lines and a 3D tissue-engineered model of human skin (Ventress et al., 2016).

ADAM10, a TspanC8 partner protein, has recently been demonstrated to have a role in *S. aureus* infection. TspanC8 tetraspanins promote ADAM10 trafficking from the ER to the host cell surface, as previously mentioned (Eschenbrenner et al., 2020). ADAM10, a metalloprotease, has previously been shown to be a receptor for the α-toxin generated by *S. aureus* (Winter, Zychlinsky and Bardoel, 2016). As a result of cleaving cadherins located on both endothelial and epithelial cells, ADAM10 breaks the barrier to infection, causing tissue damage and bacterial invasion (Koo et al., 2020).

1.2.3.3.5 Uropathogenic *Escherichia coli* (UPEC)

When it comes to UTIs, UPEC is one of just a very few bacteria known to interact directly with a tetraspanin (mainly UPIa) (Wu, Sun and Medina, 1996). Uroplakin-complex structures allow for the binding of FimH (a lectin with mannose-specificity) with UPIa (Tspan21), which in turn allows UPEC to adhere to epithelial cells, resulting in UTI (Zhou et al., 2001; Lewis, Richards and Mulvey, 2017). The activity of this pathogen, including its interaction with tetraspanins, will be covered in more detail in later sections of this thesis.

1.2.3.3.6 Burkholderia species

Although tetraspanins appear to be mainly involved in bacterial adhesion processes, recent work from our group suggests that they may also regulate bacterial induced host cell fusion (Elgawidi et al., 2020). Melioidosis is a serious tropical disease caused by *Burkholderia pseudomallei*, an intracellular infection. Septicaemia, pneumonia, abscesses, pyelonephritis, osteomyelitis and encephalitis can all be caused by the bacterial invasion (Wiersinga et al., 2018). A protective structure of multinucleated giant cells (MNGC) can be induced by the bacteria in order to support spreading of the bacteria between cells, contribute to the evasion of the immune system and protect against antibiotics (Kespichayawattana et al., 2000). A recent study has demonstrated that during *B. pseudomallei* infection, tetraspanins help mediate internalisation and membrane fusion (Sangsri et al., 2020). MNGC production can also be induced by *Burkholderia thailandensis*, which is only slightly pathogenic and a closely related species (Wand et al., 2011). The involvement of tetraspanins in the production of MNGCs due to *B. thailandensis* infection was examined in murine macrophage cell lines, showing that tetraspanins are involved in cell-to-cell fusion and MNGC development. CD9 or CD81 monoclonal antibodies increased the development of MNGCs. Additionally, CD9 null murine macrophages showed a considerable rise in MNGC production, but CD9 overexpressing cells showed a reduction in MNGC development on bacterial

infection. Overall these findings, indicate that CD9 and CD81 function as negative regulators inhibiting cell-to-cell fusion and as a result MNGC development (Elgawidi et al., 2020).

1.2.4 Anti-adhesion-based therapy to fight against infectious diseases

There are increasing findings that bacteria are developing a variety of defence mechanisms to counteract the effects of antibiotics. In light of the rising resistance to conventional antimicrobial medicines, it is necessary to discover new innovative strategies for fighting bacterial infections. Anti-adhesion therapy is a novel method that can directly target the host or pathogens cell surface to disrupt bacterial binding, which is an important early step in bacterial infections. Short peptides that imitate the interaction between a ligand and receptors can be employed to prevent bacteria form attaching to host cells, thus preventing pathogen penetration and limiting infection (Asadi et al., 2019). Our recent research investigating the effect of peptides derived from CD9-EC2 in *S. aureus* adherence to keratinocytes and a human tissue engineered skin model (Ventress et al., 2016) is considered promising (Karam et al., 2020). These synthetic peptides reduced *S. aureus* adherence at low (nanomolar) concentrations (Ventress et al., 2016). Peptide-based therapeutics are ideal for clinical application since they do not trigger an immune response and are quickly cleared from the body of patients (Gokhale and Satyanarayanajois, 2014). Therefore, anti-adhesion treatment with particular peptides (or antibodies, but these are more expensive) might be used initially in clinical trials in treating serious infections. In the present study, the initial idea behind this work was that agents such as tetraspanin-derived peptides might be used in patients with indwelling catheters, so that they could be introduced directly into the bladder to prevent bacteria binding. Hence, it is worthwhile to identify new biological agents that may make it feasible to treat urinary tract infections that are otherwise difficult to treat.

1.3 The unique tetraspanin network of uroplakins in bladder epithelium

As discussed previously, the bladder epithelium is the primary site of most urinary tract infections. Structurally, normal bladder is lined by a multi-layered epithelium, usually termed transitional epithelium or urothelium. The basal lamina is covered by the basal layer and the intermediate layers of cuboidal cells are lined by an apical layer of umbrella cells with a dense layer of glycosaminoglycan (GAG layer) on the surface and almost 90% covered with uroplakin proteins which are highly expressed. These umbrella cells provide a powerful boundary to the flux of particular ions (HICKS, 1975). Uroplakin proteins are integral membrane proteins, clustering together forming 16nm crystalline array plaques known as urothelial plaques or the asymmetric unit membrane (AUM) (Kachar, Liang, Lins, Ding, X.-R. Wu, et al., 1999). Four major uroplakin proteins have been identified: uroplakin Ia (27 kDa), Ib (28 kDa), II (15 kDa) and III (47 kDa) (Wu and Sun, 1993; J. H. Lin et al., 1994; Yu et al., 1994). These proteins are highly conserved within mammals. Although uroplakin II and III have only one transmembrane domain, uroplakin Ia and Ib have four transmembrane domains and belong to the tetraspanin superfamily. Both uroplakin Ia and Ib contain six highly conserved cysteines in the EC2 and share around 40% of their amino acid sequence (Yu et al., 1994; Maecker, Todd and Levy, 1997). UPIa (TSPAN 21) and UPIb (TSPAN 20) also share significant sequence homology with other members of the tetraspanin superfamily such as CD9, CD37, CD53, and CD63 (Yu et al., 1994). Importantly, UPIa and UPIb are glycoproteins with high amounts of mannose type oligosaccharides, which make them a primary target for UPEC to enter the urinary tract (Matthew A. Mulvey et al., 1998). Tetraspanin uroplakins are capable of binding to UPII and UPIII in a highly specific manner, forming UPIa/II and UPIb/IIIa, which are functionally important in many uroplakin processes (Yu et al., 1994). Visualization of urothelial plaques by cryo-EM at 6 Å–resolution has suggested that UP tetraspanins are strongly associated with the non-tetraspanin uroplakins forming rod shaped structures (Min et al., 2006b). This interaction has been considered a primary interaction because the proteins directly interact

with high stoichiometry, as confirmed by chemical crosslinking experiments (Wu, Medina and Sun, 1995). However, uroplakin gene expression has also been found in non-urothelial cell types such as in lung, prostate and corneal epithelium (Adachi, Okubo and Kinoshita, 2000; Olsburgh et al., 2003). UPIb has been found in human corneal epithelium at gene and protein level (Adachi, Okubo and Kinoshita, 2000). UPIa and UPIII were expressed at the gene level in prostate and UPIb and UPII in ocular surface epithelium (Adachi, Okubo and Kinoshita, 2000; Lee, 2011). Recently, expression of UPs was detected in other non-urothelial lineage tissues including stomach, kidney and prostate (Liao et al., 2018).

The significant functions of UPs in the urothelial cells are acting as a permeability barrier and physical stabilizer (Negrete et al., 1996; X.-R. Wu et al., 2009; Tian et al., 2015). The AUM also plays a role in development, differentiation and homeostasis of the urothelium (Carpenter et al., 2016). Previous studies have shown that UPII/III knock out in a mouse model causes renal failure and high rates of mortality (Hu et al., 2001; Kong, 2004). In addition, mutations in the UPs genes resulted in renal hypo dysplasia, a dysplasia and renal failure in humans (Jenkins et al., 2005; Schönfelder et al., 2006). Notably, the GAG layer on the urothelial luminal surface is also contributing to urothelial barrier function (more details in section 1.4.1) (Lilly and Parsons, 1990; Rozenberg et al., 2019).

1.3.1 Assembly of uroplakins and their cellular regulation

Biosynthesis of urothelial plaques is initiated in the endoplasmic reticulum (ER), with UPIa associating with UPII and UPIb with UPIII forming dimers (Figure 1.5) (Tu, Sun and Kreibich, 2002; Hu et al., 2005). In the Golgi and trans- Golgi network (TGN), a series of glycosylation and proteolytic processing of UPs occurs (Hu et al., 2005). Glycosylation at two N-glycosylation sites on the UPII pro-sequence results in the formation of complex glycans in the Golgi apparatus (J.-H. Lin et al., 1994), and the dimers associate forming heterotetramers (UPIa/UPII-UPIb/UPIII) (Hu et al., 2008). Six heterotetramers are organized in the post-Golgi compartment to form a 16-nm particle, which is

then assembled into 2D crystals and trafficked to the apical cell surface via TGN-derived discoidal (DVs) and fusiform vesicles (FVs) (Zhou et al., 2012; Wankel et al., 2016). UPIb is unique in that it can leave the ER on its own (Tu, Sun and Kreibich, 2002). UPIIIa differs from the other major uroplakins in that it has a cytoplasmic tail of 50 amino acids (Wu and Sun, 1993; Yu et al., 1994), which is involved in the transmembrane signalling (Thumbikat, Berry, Schaeffer, et al., 2009; Liao et al., 2018). The relevance of uroplakins in maintaining the urothelial permeability barrier function and the flattening and expansion of umbrella cells was established in UPII- and UPIIIa-knockout mice (Hu et al., 2001, 2002; Kong, 2004). It is unclear how uroplakin levels are regulated (Liao et al., 2019). Due to the general processes involved in trafficking from the ER to the cell surface, uroplakin cell surface expression is thought to be a hallmark of urothelial differentiation.

1.3.2 Uroplakins as markers of urothelial differentiation

Several studies on the differentiation of urothelial cells *in vitro* have examined UP expression as a marker of their success (Daher et al., 2004; Smith et al., 2006; Thumbikat, Berry, Schaeffer, et al., 2009; Gao et al., 2018). Different methods have been proposed in terms of differentiation of the urothelial cells *in vitro* as well as promoting the expression of uroplakin proteins and tight junctions. For example, growing bladder cells in a suspension forming organoids that displayed similar characteristics to highly differentiated human urothelium including expression of UPIa (Smith et al., 2006). However, some shortcomings inherent to this approach have been addressed such as a lack of vascular, the inability to control the cells and the inability to modify the cells (Sharma et al., 2021). Another approach is cultivation of the cells in a medium with 5% serum and elevated calcium, that has been previously applied to induce the expression of uroplakins in urothelium (Cross et al., 2005; Thumbikat, Berry, Zhou, et al., 2009). Sun highlighted different factors that improve the differentiated stage in cultivation of urothelial cells including: removal of different growth factors that are present in foetal calf serum, growing the cells on a collagen extracellular matrix and transplantation of the cells to an *in vivo* situation (Sun, 2006). Another study has also demonstrated that the cultivation

of human urothelial cells under cyclic hydrostatic pressure regulates UP expression (Gao et al., 2018). Although various ways of differentiated *in vitro* UTI model have been employed, these methods have not conclusive evidence that immortalised bladder cell lines could express UP at the cell surface.

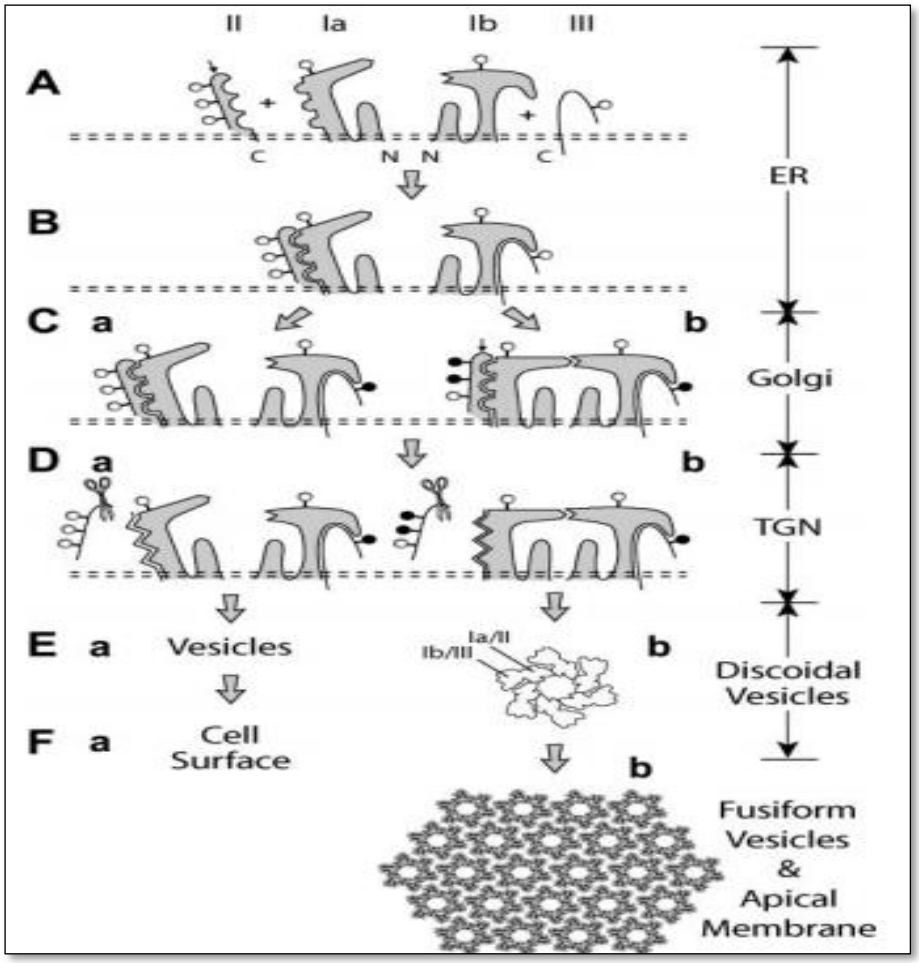

Figure 1.5: Uroplakin assembly in normal urothelium and cultured urothelial cells.

(A) and (B) depict the formation of UPIa/II and UPIb/IIIA heterodimers in the ER; (C) depicts a differentiation-dependent glycosylation phase resulting in the production of complex glycans on the UPII pro-sequence in normal urothelial umbrella cells (Cb), (Ca) shows only high-mannose glycans were found in cultured urothelial cells , which results in a variety of dimer conformations and assembly characteristics; (D) depicts the elimination of the UPII prosequence by the trans-Golgi network (TGN)- associated furin; (E) indicates that only heterotetramers in normal urothelium can assemble into 16-nm particles (Eb) and later into 2D crystals (Fb) whereas cultured cells (Ea and Fa) cannot. This figure is reproduced with permission from Molecular Biology of the Cell (Hu et al., 2005).

1.3.3 The cells used in studies of urological disease and infections

Various methods employing both cell culture and animal models such as murine and porcine have been used in studies of urological disease and infections (Bishop et al., 2007; Turner et al., 2008; Hashimoto et al., 2017). Urothelial plaques isolated from mouse, bovine and human bladder have been previously used to study the pathogenesis of urinary tract infection (Zhou et al., 2001; Xie, Zhou, S.-Y. Chan, et al., 2006). Mouse bladder is widely used as a research tool for understanding the bacterial binding to urothelium (Matthew A Mulvey et al., 1998; Bishop et al., 2007; Liu et al., 2015; Kim et al., 2018). Normal porcine urothelial cells have also been studied and shown to share similar biological properties with human urothelial cells (Turner et al., 2008; Višnjar et al., 2017). Despite the limitations of bladder epithelial cell lines (BECs) (Jerman et al., 2021), many cell lines derived from human bladder cells have been used for *in vitro* study of UTIs such as 5637 and T24 cells (Mulvey, 2002; Bower, Eto and Mulvey, 2005; Dhakal and Mulvey, 2009, 2012; Kim et al., 2018; Scharf et al., 2020). However, several development models have been investigated in recent years in order to mimic the bladder epithelium's layered architecture, for example growing 5637 cells in co-culture with bladder microvascular endothelial cells on a chip under urine flow conditions (Sharma et al., 2021). Therefore, it is worth developing an *in vitro* cell culture system that is relevant to the *in vivo* characterised model.

1.4 Glycosaminoglycans (GAGs) are involved in bacterial adhesion

Bacterial adhesins need to engage with receptors of host cell surfaces to establish appropriate adhesion and colonization (Pizarro-Cerdá and Cossart, 2006). Host receptors might also play roles in later phases of the infection process, such as invasiveness, organotropism, and host defence response interference (Wilson et al., 2002).

Microorganisms can interact with a wide range of cell surface components, which includes proteins, carbohydrates, lipids, and diverse mixtures of these. Proteoglycans (PG) serve as receptors for a wide variety of microbial pathogens (Rostand and Esko, 1997; Menozzi et al., 2002). PGs are richly found on the cell surfaces, in pericellular regions, and in the secretory vesicles of the cytoplasm (Ruoslahti, 1988; Iozzo and Schaefer, 2015). The glycosaminoglycans (GAGs) associated with PG are recognized as receptors by a diverse range of pathogens, including a variety of parasites, bacteria, and viruses (Bartlett and Park, 2010; Ivan Fernandez Vega, 2014). Infectious agents such as *Bordetella pertussis*, *Borrelia burgdorferi*, *Listeria monocytogenes*, *Neisseria gonorrhoeae* and *Streptococcus pyogenes* all have specific adhesins that can bind to glycosaminoglycans (GAGs), particularly to chains of cell surface heparan sulphate (HS) (Rostand and Esko, 1997; Menozzi et al., 2002).

In terms of both expression and composition, GAGs vary depending on the cell type and physiological conditions (Sarrazin, Lamanna and Esko, 2011). Many microbial pathogens prefer to interact with HS chains attached to the glycosylphosphoinositide-linked glypicans (GPCs) and transmembrane syndecans (SDCs) (Chen et al., 2008; Bartlett and Park, 2010). A variety of bacteria that adhere to diverse tissues such as *Helicobacter pylori*, *E. faecalis*, *N. meningitis* and *Pseudomonas aeruginosa* use HS for attachment (Ivan Fernandez Vega, 2014). Other GAGs that serve as receptors for microbes include *Borrelia burgdorferi* which utilizes HS as receptors in endothelium cells, while using chondroitin sulphate B (CS-B) and HS receptors in brain cells (Leong et al., 1998). HS and CS-B chains also play essential roles in the binding of *Chlamydia trachomatis*, *S. pyogenes* binding (Ivan Fernandez Vega, 2014). In the human pathogen *Streptococcus pyogenes*, M protein is a key surface-expressed component that facilitates binding to a variety of GAGs. Due to the high number of M proteins on the surface, strains of *S. pyogenes* with a variety of distinct M proteins bind dermatan sulphate (DS), dermatan sulphate-rich heparin, and other GAGs; strains low in the surface expressions of M protein were unable to associate with these GAGs (Frick, Schmidtchen and Sjöbring, 2003).

Some of the most prevalent respiratory tract pathogens, including *S. pneumoniae* (Tonnaer et al., 2006), *P. aeruginosa* and *Chlamydia pneumonia* (Ivan Fernandez Vega, 2014) also require GAGs, primarily HS, for attachment. The attachment of various bacterial pathogens such as *Staphylococcus aureus*, *Streptococcus pyogenes*, *Streptococcus pneumoniae* has shown to be mediated by GAG chains in the cell surface of lung and corneal cells (García et al., 2016; Rajas et al., 2017). More recently, Green et al. demonstrated that HSPGs, particularly SDC-1, is important for staphylococcal infection (Green et al, manuscript submitted to PLOS Pathogens). As an example of gram negative bacteria, UPEC can utilize type 1 fimbriae to bind fibronectin (Fn) (Sokurenko et al., 1994) . Furthermore, UPEC secreted UpaG proteins, which is a member of trimeric autotransporters family, shown to interact with laminin and Fn (Valle et al., 2008).

1.4.1 Structure and distribution of GAGs in urothelium

As discussed in section 1.3, the urothelium is the first cellular surface that is exposed to urine, and it is also the main tissue that serves as a protective barrier (Hurst and Zebrowski, 1994; Lewis, 2000; Khandelwal, Abraham and Apodaca, 2009).

Umbrella cells, which make up the most of urothelium superficial cell layer, are highly specialised. To keep the urothelial barrier intact, the luminal surface of the umbrella cell membrane is coated in GAGs, uroplakins, tight junctions, and adherence junctions (Rozenberg et al., 2019). Sulphated and non-sulphated GAGs such as hyaluronic acid (HA) and sulphated GAGs can be distinguished in the GAG layer including HS and heparan, CS, DS, and keratan sulphate. Except for HA, most GAGs form a proteoglycan when they are linked to the protein core (Lilly and Parsons, 1990; Damiano and Cicione, 2011). The negatively charged HS moiety of proteoglycans binds positively charged amino acid clusters within FnBPs (Chen et al., 2008). The proteoglycans are stacked 5 to 60 deep on the bladder surface and present in very high concentrations (Gomelsky and Dmochowski, 2012). As a result of GAGs hydrophilic nature and high negative charge, the binding of water molecules results in a bladder

surface that is well hydrated and free of adhesion. GAGs are thought to have been the first line of defence against urine solute penetration (Hauser et al., 2008) and infectious disease (Parsons, 1994; Janssen et al., 2013). Bladder pain syndrome or interstitial cystitis (BPS/IC) and other disorders may be linked to or caused by a faulty GAG layer (Parsons, Lilly and Stein, 1991). People who suffer from BPS/IC show deficient urothelial barrier components including the GAG-layer, uroplakins, and tight junctions (Slobodov et al., 2004; Hurst, Moldwin and Mulholland, 2007; Hauser et al., 2008).

About 80% to 90% of the total surface of the GAG is bound as integral membrane proteins, with HS accounting for 55% of the protein binding GAG, CS for 29%, and the rest either unidentified or dermatan sulphates (Hurst and Zebrowski, 1994). CS chains are found near to cell membranes, whereas HS chains extend into the surrounding environment (Satoh et al., 2000). The critical urothelial barrier component is CS (Hurst, Roy and Parsons, 1997; Janssen et al., 2013; Rozenberg et al., 2019). There have been several investigations examining the distribution of various GAGs in the bladder and the role they play in protecting the urothelial barrier (Hurst and Zebrowski, 1994; Janssen et al., 2013).

1.4.2 Identification of proteoglycans expressed in normal bladder and their functions

The urothelium expresses proteoglycan core proteins that include syndecan-1, perlecan, decorin, and biglycan (Slobodov et al., 2004; Hauser et al., 2008). In the normal bladder, decorin is the most common chondroitin sulphate proteoglycan (CSPG), which is a small chondroitin sulphate proteoglycan that appears to play an important role in epithelial/mesenchymal interactions throughout organ development and shape (Scholzen et al., 1994). Decorin may promote luminal cell differentiation (Hauser et al., 2008) and it is known to inhibit cancer progression (Santra et al., 1997). It has also been found that decorin expression is higher on the luminal surface of differentiated cells (Hauser et al., 2008). Decorin is also a ligand for the EGF receptor, which might control the growth of cells during remodelling and cancer progression (Iozzo et al., 1999),

despite the fact that the EGF receptor is not located on the cell layer of superficial in normal tissue with bladder (Messing et al., 1987). There are few decorin-positive cells on the umbrella cell layer, which is remarkable because decorin helps facilitate cell-cell interactions (Hurst, Moldwin and Mulholland, 2007).

The distribution within the urothelial layer suggests that it is involved in bladder physiology (Hurst, Moldwin and Mulholland, 2007). Syndecan-1, a transmembrane proteoglycan, was discovered to be limited to the basal and intermediate layers in normal controls (Hurst, Moldwin and Mulholland, 2007; Hauser et al., 2008), but was not identified as a component of the GAG layer (Hurst, Moldwin and Mulholland, 2007). Perlecan and syndecan contain heparan and chondroitin sulphate chains, and their ability to bind and sequester growth factors such as the FGF family may enable them to regulate the proliferation and differentiation of urothelial cells (Forsberg and Kjellén, 2001). Perlecan was also found on a normal bladder. Perlecan is frequently linked to the pericellular matrix and basement membrane (Iozzo, 1994).

1.5 Aims of this thesis:

Our research team has previously showed that tetraspanins have an involvement in the adherence of a range of bacterial pathogens to host cells. Specific monoclonal tetraspanin antibodies and recombinant EC2 proteins showed inhibition of the adhesion of different bacteria such as *Staphylococcus aureus*, *Neisseria lactamica*, *Escherichia coli*, and *Streptococcus pneumoniae* to epithelial cells (Green et al., 2011). Tetraspanins CD9, CD63 and CD81 were shown to be involved in macrophage infection by *Salmonella typhimurium* (Hassuna et al., 2017). Peptides derived from CD9-EC2 reduce *Staphylococcus aureus* adherence as well as *Pseudomonas aeruginosa* adherence (Alrahimi, 2017, PhD thesis, University of Sheffield; Ventress et al., 2016). As it widely known that uroplakin tetraspanins are directly involved in UPEC attachment (Zhou et al., 2001; Ulett et al., 2013), other tetraspanins might play roles in bacterial adhesion. Therefore, we speculated that applying

tetraspanin- related reagents to bladder epithelial cells could disrupt TEM at the cell surface and inhibit the bacterial binding.

The overall aim of the present project is to investigate the mechanism of UPEC adherence whereby tetraspanins or other partner proteins are involved in this infection, using an *in vitro* bladder epithelial cell model. Specific aims are:

1. To determine which tetraspanin members are present on bladder epithelial cells. This includes studying the expression of UPIa (Tspan 21), UPIb (Tspan 20), CD9 (TSPAN29), CD63 (TSPAN 30), CD81 (TSPAN 28), CD82 (TSPAN 27), and CD151 (TSPAN24), which are some of the members that had previously been shown to be important in bacterial binding.
2. To investigate the localization of uroplakins in various bladder cell lines that differ in maturity. Attempts are made to induce cell surface expression of these molecules which would be relevant to native urothelium.
3. To establish an *in vitro* cell line model that possesses some of the mature properties compared to primary bladder cells.
4. To test the effects of tetraspanin-derived reagents including specific monoclonal antibodies or peptide derived from EC2 domains on UPEC binding.
5. To determine if GAGs are involved in UPEC adhesion due to the interaction of cell surface peptidoglycans with tetraspanins as partner molecules and their role as a functional barrier.

Chapter 2: Materials and Methods

2.1 Materials

2.1.1 Reagents and buffers

Reagents and buffers were prepared according to the manufacturers' instructions or published methods, unless otherwise stated (Lausted et al., 2004; Wilson and Corlett, 2005). Sterile distilled water (dH2O) was used throughout the project unless otherwise stated. Bacteria culture media, buffers, glassware, tips and reagents were sterilised by autoclaving at 121°C for 20min. Stock solutions were sterilised by autoclaving, and antibiotics, antibodies and other heat-labile reagents were filtered using 0.2µm filter units where necessary. The tables below summarise the reagents, buffers and other materials used in this project. Buffers and reagents used in this study are listed in Table 2.1.

Table 2.1: Buffers and reagent solutions.

Buffer/reagent	Preparation
Acid /ethanol	5% acetic acid, 5% dH_2O, 90% ethanol (v/v).
Cell dissociation solution	Cell dissociation solution (CDS) was provided from Sigma (C5914) as 1X solution, 3 ml was used for a T75 flask.
Cell lysis buffer (mammalian)	1% TritonX-100 in PBS
DAPI staining solution	Vectashield Mounting Medium with DAPI (Vector Laboratories Burlingame, CA 94010).

Fix and perm kit	For fixation and permeabilisation of mammalian cells, ADG or Invitrogen (Cat. No. GAS004).
Flow cytometry and immunofluorescence microscopy blocking buffer (B/B/N)	0.1% sodium azide, 0.1% BSA in HBSS with Mg+2 and Ca+2 ions.
Freezing mixture (bacterial cells)	20% glycerol in LB medium
Freezing mixture (mammalian cells)	10% dimethyl sulphoxide (DMSO), 90% foetal calf serum (FCS)
Giemsa solution (Sigma) 0.6% w/v	10% of Giemsa solution in 1x PBS
HBSS (Hanks balanced salt solution) with divalent Mg and Ca elements	5.4mM KCl, 0.3mM Na2HPO4, 0.4mM KH2HPO4, 4.2mM NaHCO3, 1.3mM CaCl2, 0.5mM MgCl2, 0.6mM MgSO4, 137mM NaCl, 5.6mM D-glucose, 0.02% (w/v) phenol red (optional) with H2O to 1l, pH to 7.4 (purchased from Lonza)
Paraformaldehyde solution 4%	Fixation buffer was purchased from Biolegend. Diluted into 2% or 1% in HBSS.
Phosphate-buffered saline tablet	1 tablet dissolved in 200 ml dH_2O. (Sigma, 1002995618).
Propidium iodide	1:1000 dilution of propidium iodide (1mg/ml, Sigma, P4864) in PBS.
TAE 50X (1l)	57.1ml glacial acetic acid, 242.2g Tris base, and 100ml 0.5M EDTA pH 8.0.
Trypsin/EDTA solution 10X	1x solution prepared in sterile HBSS (see above): 0.25% (w/v) trypsin, 0.2% (w/v) EDTA (Sigma).

Table 2.2: Commercial kits used

Kit	Description
High-capacity cDNA reverse transcription kit.	10X RT buffer, 10X RT random primer, 25X dNTP mix (100mM), reverse transcriptase, nuclease- free H2O. (Purchased from Thermo-Fisher).
LDH cytotoxicity assay	Substrate mix, assay buffer and stop solution. (Purchased from Promega CytoTox 96 Non-radioactive cytotoxicity kit (G1780)).
RNeasy Plus Kit	Buffer RPE wash buffer, buffer RLT lysis buffer, buffer RW1 wash buffer, mini spin colum and gDNA eliminator and collection tubes. (Purchased from Qiagen).

2.1.2 Bacterial growth media

Table 2.3: Bacterial growth media

Medium	Preparation
LB (Lysogeny Broth)	10g tryptone, 5g yeast extract, 10g NaCl dissolved in 1l water. LB agar was prepared with the same recipe with an additional 15g agar.
TSA (Tryptic Soy Agar)	40g of dehydrated media (Sigma) in 1 litre of distilled water was mixed and sterilized at 121°C for 3 hr then dispensed into sterile petri dishes).
TSB (Tryptic Soy Broth)	30 g of powder (Lonza) was dissolved in 1 L of pure water then autoclaved at 121°C for 15 min.

2.1.3 Antibiotics

Table 2.4: Antibiotics with working concentrations

Antibiotic	Preparation
Gentamicin (Gibco)	Prepared to a final concentration of 150 µg/ml in media.

2.1.4 Bacterial strains

Table 2.5: Bacterial strains used

Bacterium	Description /Source
Uropathogenic *E. coli* (EC958)	A kind gift from Professor Robert Poole, Dept Molecular Biology & Biotechnology, University of Sheffield, UK.
Uropathogenic *E. coli* (J96)	This strain was obtained from ATCC.

2.1.5 Primers

NCBI Blast (www.ncbi.nlm.nih.gov/tools/primer-blas) was used to design all the primers as described by Dr Muslim Mohsin (PhD thesis, University of Sheffield, 2020), which were purchased from Thermofisher. The primers were dissolved in TE buffer at 100µM and stored at -20°C.

2.1.5.1 Tspan Primers

Table 2.6: Primer sequences used to investigate Tspan gene expression

Tspan	Human primers
Tspan-1	F CGACCAAAAAGTAGAGGGTTGC R ACAATCATGGCAGCCAGCTC
Tspan-2	F 5'AAGGGGGTAGCTATCCGACA R 5' TGGACCTGTTCGGAGCTTTC
Tspan-3	F CCTCATCTTCTGGTTTGTCATCATC

	R GGGTTGGTTCCATTGTAGGTCT
Tspan-4	F GTGGCTGTGGAGAGCTTGG R GCCACAGGAAAGAGACCAGG
Tspan-5	F GTGGGCATGGAATGAAAAAGGAG R CCAATGCACCCTGCAAATCC
Tspan-6	F TTTGCAAAGGCAAGCAAGGC R ATAACGCCAGTGATCTGCGA
Tspan-7	F TCGTCTTCTGGATCACTGGG R CCGATGAGCACATAGGGAGC
Tspan-8	F GCCCCAGGAGCTATGACAAG R AGAGATTTCTGTATCCACGGACA
Tspan-9	F TTGTTTGTCAGCAGCCAAGG R ACAGCCACAGAGCCAGAATATC
Tspan-10	F GAAGCAAAGACGAGCATCCG R GGGCTAGTCTGTGCATGGAG
Tspan-11	F CATGTGAGCAGGCCCAGAA R CCCCGACCCAGAAGAAGAAG
Tspan-12	F CCTGCTCTACGCCCTCAATC R ACTGCTTCCTCTACCCTCGT
Tspan-13	F GACACCTGTCTGGCTAGCTG R GGCCAATGCCACCAACAAAT
Tspan-14	F CAAGGTCAGCTGCTGGTACA R GACAACTCCAGCCAACCAGA
Tspan-15	F GAGCGCCCAGGATGCC R CCAATCAGCCAGAACACGGT
Tspan-16	F GAAATGACAACGGGCCACAC R AACAGCCCTTCTGGTGGATG
Tspan-17	F CTCAAACTGGTGAGAGGGGAG R ATGCCAAAGATCTGGAGGAGG
Tspan-18	F ACATCTCAACGCTGGCTCTC R GCCCCGCCCAGAAATATGAA
Tspan-19	F ACGCAGCATTTCAGGGACTG R GTCCAAGAACCAAGAAAGCTCC

Tspan-20 (UPIb)	F TCCCGAAGATGGCCAAAGAC R GCAATGCCGCAACAACCAAT
Tspan-21 (UPIa)	F CTGTTCACCAAGGGCTGCTTC R GGATGGCAAACCCAAACCAC
Tspan-22	F GGCTCTTCGAGGTGACCATT R GGCTCTCGCTCTCAGATTCC
Tspan-23	F GCCAAAAGGCTGGTGGATGA R TTGCTCTGGATCCGGTCAGC
CD151	F TGCGCCTGTACTTCATCCTG R GCTGCTGGTAGTAGGCGTAG
CD53	F TTTTACACAAATAGCCCCGGA R ATTCTTGCCCTTTTCCAGGCA
CD37	F TTCGTGTCCTTTGTGGGCTT R AAAATACAGGCCCAGGAGGC
CD82	F GGCTGCTGAAGCAGGAGAT R CAGCACTTCACCTGAGCCTG
CD81	F ACTGGGTTGGACGACACTTG R CTCCAGCCAGCTGGGAAC
CD9	F AGGTCCCGCCAGTCCC R CCGGCAAGCCAGAAGATGAA
CD63	F AGCCCTTGGAATTGCTTTTGTTT R AGACCCCTACATCACCTCGT
Tspan-31	F GAAGACGGTCCCCAATACCC R GCTCACCAGCATGTAGACCA
Tspan-32	F TCTGAGTCTGCCCTATCCACAG R CCCGCAGAGAAGGCCCATT
Tspan-33	F AGCCCGCTGGTGAAATACCT R AGGGCTGCTTCTGCATGCTT
GAPDH (human) RPL13a (Mouse)	F TGCACCACCAACTGCTTAGC R GGCATGGACTGTGGTCATGAG

2.1.5.2 Non-tetraspanin uroplakin primers

Table 2.7: Primer sequences used to investigate non- tetraspanin uroplakin gene expression

Name	Human Primers
UPII	F GCCAATGACAGGAAGTGGT R TGAGCCGAGTGACTGTGAAG
UPIII	F GGTCGACTCAGCCATTTCCA R GTCCTCCCACCCTCTGTTTG

2.1.6 Equipment and apparatus

Table 2.8: Equipment

Equipment and apparatus	Manufacturer
Bench centrifuge	Sigma (SciQuip)
Class II Microbiological Safety Cabinet	WALKER, BioMAT
BD LSRII	BD Bioscience
Incubators	BIOHIT LTE laboratory thermal equipment LTD
LT-4000 Microplate Reader	Labtech
Microscopes	Olympus Epifluorescence microscope.
	Nikon Ti Eclipse microscope.
NanoDrop lite	Thermo Scientific (6VDC-18W)
Thermocycler	G-STORM
7900HT Fast Real-Time PCR	Applied Biosystems AbiPrism sequence

2.1.7 Analysis software

Table 2.9: Software

Programme	Comment
Cell Quest Pro Flow cytometry software	Data acquisition and analysis.
Excel Microsoft	Analysis of qPCR data.
FlowJo	Analysis of flow cytometry results. Source: http://www.flowjo.com
GraphPad Prism v6	Statistical and graphical analysis. Source:http://www.graphpad.com/scientific-software/prism/

Image J	Calculation of number of nuclei per giant cell; image manipulation. Source: http://imagej.nih.gov/ij/

2.1.8 Antibodies and peptides

The primary and secondary antibodies and isotype controls used for immunofluorescence studies and infection assays are summarised in the Tables below.

2.1.8.1 Primary antibodies and isotypes

Table 2.10: Primary antibodies and isotype

Antibody (hybridoma clone)	Target	Specificity	Conc .µg/ ml	Isotype	Cat.no. or Source
Mouse anti-human CD9 (602.29)	CD9	Human	10	Mouse IgG1	In the house, Prof. Andrews Univ. of Sheffield, hybridoma grown up in house
Mouse anti-CD63 (H5C6)	CD63	Human	10	Mouse IgG1	Developmental Studies Hybridoma Bank, hybridoma grown up in house
Mouse anti-CD81 (5A6)	CD81	Human	10	Mouse IgG1	Biorad 241202
Mouse monoclonal anti-CD82 (423524)	CD82	Human	10	Mouse IgG1	R&D systems (MAB4616)

Mouse anti-CD151 (14A2)	CD151	Human	10	Mouse IgG1	Prof. Leonie Ashman University of Newcastle, Australia, hybridoma grown up in house
Mouse monoclonal control (JC1)	Isotype control		10	Mouse IgG1	Jenny Clipson-hybridoma produced in house
Mouse anti-Tspan2 (EF3)	Tspan2	Human	20	IgM	Dr.Yassin, University of Sheffield hybridoma produced in house
Mouse anti-TSPAN11 (CF9)	TSPAN11	Human	10	Mouse IgG1	Dr Arunya Jiraviriyakul, hybridoma produced in house.
Rabbit polyclonal anti-UPIa	UPIa	Human	20	Rabbit IgG	Cloud-Clone Corp (PAC588Hu01)
Rabbit polyclonal anti-UPIb	UPIb	Human	30	Rabbit IgG	Abcam (ab102961)
Rabbit monoclonal anti-UPIII	UPIII	Human	5.1	Rabbite IgG	Abcam (ab187646)
Rabbit monoclonal	Isotype control		5.1	Rabbit IgG	Abcam (ab172730)
Rabbit polyclonal	Isotype control		20	Rabbit IgG	Sigma-Aldrich

2.1.8.2 Secondary antibodies

Table 2.11: Secondary antibodies

Antibody	Target	Label	Dilution	Source
anti-mouse polyvalent Ig	Mouse immunoglobulins	FITC	1:250	Sigma-Aldrich
anti-rabbit IgG	rabbit IgG	Alexafluor 488	1:100	Biolegend

2.1.8.3 Peptides

Peptides based on various regions of the EC2 region of CD9 were synthesized using solid phase synthesis with Fmoc chemistry by Genscript, UK. We have used 800C and its stapled versions, scrambled peptides are randomly generated from the cognate CD9 sequence (Table 2.12). Tagged peptides were used to study the binding with cells and microscopy, generated with 6-FAM at the N-terminal end by Genscript, Piscataway, USA. This tag has an excitation/emission of 492/517 nm.

Table 2.12: Peptides

Peptide	Alternate name	Sequence
800 Cap	800C	DEPQRETLKAIHYALN
800 Cap I (stapled)	Peptide 1	DEPQRETLKAIHYALN*
800 Cap II (stapled)	Peptide 2	DEPQRETLKAIHYALN*
Scrambled peptide	SCR	QEALKYNRAETPLDIH

* A disulphide bond has been introduced to “staple” the peptide between the highlighted amino acids using (S)- 2-(4-pentenyl) alanine as a cross-linker. This has been shown to preserve the alpha helical structure of the peptide by circular dichroism (Dr Barbara Ciani, Dept Chemistry, personal communication). 800C is a “capped” version of the 800 (Ventress et al., 2016) with an asparagine (D) added to the N-terminus. SCR peptide is randomly synthesized from the 800C sequences. DMSO was used to dissolve the lyophilised stock of peptides at 2mM and stored at -20°C.

2.1.9 Proteoglycans and proteoglycan degrading enzymes

Multiple materials were used to study the involvement of GAGs in the adherence of UPEC to bladder cells. Some materials which are derivatives of UFH have LMW such as Dalteparin, Fondaparinux and dermatan sulphate (Table 2.13).

Table 2.13: Proteoglycans and degrading enzymes

Proteoglycans	Concentration	Source
Unfractionated heparin (UFH)	1000 Units/ml	Leo, UK
Dalteparin	25000 IU/ml	Royal Hallamshire Hospital Pharmacy, Sheffield,
Fondaparinux	10 mg/ml	Merck, Germany
Heparinase	100 U/ml	Merck, Germany
Dermatan sulphate	1 mg/ml	Iduron, UK
Heparan sulphate	1 mg/ml	Iduron, UK
Chondroitin sulphate	1 mg/ml	Iduron, UK
Chondroitinase	5 U/ml	Merck, Germany
Pixatimod	13.5 mg/ml	kindly provided by Zucero Pty, Brisbane, Australia

2.1.10 Human cell lines

Multiple types of bladder cell lines were used: RT4, 5637 and T24, as they represent the cell types commonly infected in UTIs. Normal human primary bladder epithelial cells were used as representative a mature tissue model. A549 WT and CD9KO A549 cells were used in this project as a control in an infectious study. K562 leukaemia cells used as a positive control for UPIb expression.

All bladder cells were obtained from the European Collection of Authenticated Cell Cultures (ATCC) in (Table 2.14). Bladder cells and K562 cells were grown under the same conditions at 37ºC with 5% CO2, and the media were supplemented with 10% FCS. A549 WT and CD9KO cells grown at 37ºC with 8% CO2.

E medium preparation:

E medium was made in house with 90 ml of Dulbecco's Modification of Eagle's Medium and 30 ml of F12 medium. FBS was added to reach to final concentration of 5% and elevated calcium about 1.2 mM calcium chloride (Thumbikat, Berry, Schaeffer, et al., 2009).

Table 2.14: Human cell lines

Cell line	Growth medium	Source	Comment	Reference
Human lung adenocarcinoma A549 (ECACC)	High glucose (4.5g/l) DMEM	ECACC	Used for peptide binding studies	(Donald J Giard *et al.*, 1973).
Human lung adenocarcinoma A549 KO CD9	High glucose (4.5g/l) DMEM	Dr David Blake/ Department of Biology at Fort Lewis College, Colorado, USA	Used for peptide binding studies	
Human urinary bladder papilloma RT4	McCoy's 5a medium modified	ATCC	Used for uroplakin expression and infection studies	(Rigby and Franks, 1970).
Human bladder carcinoma 5637	2mM L-glutamine, 10 mM HEPES, 1 mM sodium pyruvate, 4500 mg/L glucose, and 1500 mg/L sodium bicarbonate	ATCC	Used for uroplakin expression and infection studies	(Fogh, 1978).
Human bladder cancer T24	RPMI-1640 with L-glutamine and	ATCC	Used for tetraspanin and uroplakin	(Bubeník *et al.*, 1973).

	sodium bicarbonate		expression studies.	
Chronic myelogenous leukemia K652	RPMI 1640 +2mM glutamine + 10% foetal bovine serum (FBS).	Sigma	Used for UPIb expression studies.	
Primary bladder epithelial cells (ATCC PCS-420-010)	Epithelial Cell Basal Medium (ATCC PCS-420-032)+ Bladder Epithelial Growth Kit (ATCC PCS-420-042).	ATCC	Used for uroplakin expression and infection studies.	

2.2 Methods

2.2.1 Bacteriological techniques

2.2.1.1 Bacteria preparation

Uropathogenic *E.coli* strains J96 and EC985 were prepared as follows: An inoculum from a glycerol stock was plated on an LB agar plate overnight at 37°C. The following day, 2-3 colonies were picked and used to inoculate 30ml LB broth and then grown overnight in a shaker at 250 rpm at 37°C. The overnight culture was diluted to OD600 of 0.01 in a sterile flask and incubated at 37°C in a shaker at 250rpm until the mid-log phase was reached after 2-3 hours (OD600 ~ 0.5). The culture was then centrifuged at 5400xg for 5 minutes, the pellet washed twice by re- suspension with PBS and centrifuging again. The pellet was finally re-suspended in an appropriate volume of cell culture media for the experiment. The bacterial density was checked again (using both absorbance at OD600 and viable counts) and then used to produce the desired multiplicity of infection (MOI).

2.2.1.2 Bacterial glycerol stocks

To prepare glycerol stocks for freezing, bacteria were incubated overnight in LB broth at 37°C in a shaking incubator. 850µl bacterial culture was added to 150µl of sterile glycerol in a cryovial tube. The bacterial cells were mixed gently with the glycerol, aliquots were transferred to additional labelled cryovial tubes, and then stored at -80°C.

2.2.2 Tissue culture techniques

All experimental work in tissue culture was carried out in Class 2 laminar flow hoods (BioMAT).

2.2.2.1 Human cell harvesting

For cells grown in T75 flasks, the media was removed, and the cells were washed once with 10ml HBSS solution (without Ca and Mg ions). The cells were then treated with 3ml trypsin-EDTA or with 5ml Cell Dissociation Solution (for flow cytometry) for 10 to 20 minutes respectively at 37°C until all the cells detached from the flask surface. The cells suspension was then transferred to eppendorf tubes with 5 ml of media with 10% FBS for deactivating the trypsin. For routine subculturing, cells were split 1:3 or dispense into certain tubes at an appropriate density for assays. The cells were centrifuged at 300xg for 5 min and the cell pellets re-suspended with 10 ml medium. The cells were mixed well by pipetting up and down then transferred to fresh flasks.

2.2.2.2 Cell freezing

Cells that had reached 85-90% density were harvested using trypsin-EDTA as above and counted using a haemocytometer. The cells were centrifuged for 5min at 200xg, the supernatant was removed, and the pellet was re-suspended with freezing medium (as mentioned in Table 2.1) at $1x10^6$ to $2x10^6$ cells/ml. 1ml of cell suspension was placed in each cryovial tube and the vials were

transferred to a freezing plug above liquid nitrogen for 2-3 hr. Finally, the vials were stored in liquid nitrogen.

2.2.2.3 Cell thawing

The cryovial was removed from liquid nitrogen and was agitated under warm water until the contents were part thawed. The outside of the cryovial was dried and wiped with a 70% ethanol before opening. The cells were transferred quickly to a universal tube on ice and 9ml of cold fresh medium added. The cells were centrifuged at 200xg for 5min, the supernatant removed, and the pellet re-suspended with 10 ml complete medium and placed in a new flask.

2.2.2.4 Viability of cells

After harvesting, an aliquot of the cell suspension was transferred to a haemocytometer counting chamber. Cell viability of cells was assessed by mixing 0.5ml of 0.2% trypan blue with 0.5ml cell suspension in a tube. This was gently mixed after standing for 5min, and then loading into the haemocytometer. Dead cells were stained with the blue dye, whereas live cells did not stain.

2.2.2.5 LDH assay

The kit we used is listed in Table 2.2 and this assay was originally described in (Decker and Lohmann-Matthes, 1988). The supernatants after bacterial infection (see section 2.2.5.3) were collected and transferred to a fresh 96-well plate. The supernatants from different conditions included: uninfected cells as a positive control, cells treated with 1% triton X-100 which causes the maximum LDH release and media only as a blank. Assay reagent was added to each well with mixing up and down, the plates wrapped in foil and incubated for 30 min at room temperate. Then, stop reagent was added with mixing up and down. The absorbance of the supernatants was measured at 490 nm. The % cytotoxicity was determined used the following equation (Equation 2.1). Viable cells will release <10% of total LDH.

Equation 2.1: Percentage cytotoxicity equations to assess the cell viability

$$Percentage\ cytotoxicity = \frac{LDH\ release\ in\ treated\ cells}{Maximum\ LDH\ release} \times 100$$

2.2.3 Real-time quantitative polymerase chain reaction (RT-qPCR)

The following methods were used as described by Dr Muslim Mohsin (PhD thesis, University of Sheffield, 2020). The mRNA levels of Tspan and uroplakin proteins in bladder cells was measured using qPCR.

2.2.3.1 RNA extraction and purification

QIAGEN RNeasy Mini Kits were used to extract mRNA from 5637, RT4 and primary bladder cells grown in complete growth medium, serum free medium or E medium at different time points. The cells were grown at $9x10^5$ cells/well in 6 well plates. The cells were harvested by scraping and centrifuged at 200xg for 5min. Cells were re-suspended in 350µl of lysis buffer (from RNeasy kit) and vortexed for 30 sec. The lysate was transferred to a gDNA Eliminator spin column to remove gDNA and centrifuged for 40 sec at 9000xg. The column was discarded and the flow through used for analysis. 350µl of 70% ethanol was added and mixed gently.

The solution was transferred to RNeasy spin columns in the kit tubes, centrifuged for 15sec at 9000xg. The columns were then washed with 700µl of RNA washing buffer (RW1) and centrifuged at 9,000xg for 15sec. 500µl of RNA precipitating elution buffer (RPE) was added, the columns and tubes were centrifuged for 15 sec to remove traces of salts, 500µl of RPE was added again and the tube centrifuged at 9,000xg for 2min. Finally, 50µl of RNAse-free water was added, and the column and tubes centrifuged for 1min to elute the RNA. The total concentration of RNA was measured using a NanoDrop lite spectrophotometer.

2.2.3.2 cDNA synthesis

High-Capacity cDNA Reverse Transcription Kits were used to make complementary DNA (cDNA) for the qPCR assays (ThermoFisher). RNA samples extracted from the various sources were standardized to 75ng/µl. cDNA synthesis components were prepared as described in Table 2.15, including two negative controls: no reverse transcriptase and no RNA. Reverse transcription was performed using a thermal cycler at the settings shown in Table 2.16. The cDNA samples were used directly for qPCR.

Table 2.15: cDNA synthesis components

Materials	Volume (µl) Sample	Volume (µl) no-RT	Volume (µl) no RNA
10X RT buffer	2.0	2.0	2.0
10X RT random primer	2.0	2.0	2.0
25X dNTP mix (100mM)	0.8	0.8	0.8
Reverse transcriptase	1.0	0	1.0
Nuclease-free H_2O	4.2	5.2	14.2
RNA sample	10	10	0
Total volume	20	20	20

Table 2.16: Thermocycler steps for cDNA generation

Thermocycler steps	Step 1	Step 2	Step 3	Step 4
Temperature	25ºC	37ºC	85ºC	4ºC
Time	10min	120min	5min	Hold

2.2.3.3 Quantification of the cDNA product

The SYBR green method (Ponchel et al., 2003) was used to quantify the DNA product formed. The reactions were prepared as described in Table 2.17 using 2x qPCR Master Mix with SYBRgreen (Primer Design Precision) according to the manufacturer's instructions. Samples were loaded into a 384 well plate and centrifuged at 200xg for 2min. The plate was placed in the 7900HT AbiPrism sequence detection system and the samples amplified using the conditions shown in Table 2.18. In addition, the primer specificity was checked using melting curves as an extra step in a real-time PCR machine.

Table 2.17: 2X qPCR mastermix components

Materials	Volume (µl)
2X MasterMix with SYBR green (with ROX)	5
Forward primer	0.5
Reverse primer	0.5
Nuclease-free H_2O	3
cDNA	1
Total volume	10

Table 2.18: Parameters of qPCR reaction

qPCR reaction	1 cycle	40 cycles	
Reaction step	Enzyme activation	Denaturation	Data collection
Cycle length	10min	15sec	1min
Temperature	95°C	95°C	60°C

The threshold cycle (Ct) value was calculated as below:

Equation 2.2: Delta Ct equations to analyse qPCR results

ΔCt value (control) (ΔCtC) = average control Ct value (test gene) - average experimental Ct value (housekeeping gene).
ΔCt value experimental (ΔCtE) = average experimental Ct value (test gene) - average experimental Ct value (housekeeping gene)
Delta Delta Ct value (ΔΔCt) = ΔCtE – ΔCtC
Fold change (ΔΔCq) = 2-ΔΔCt

2.2.4 Bacterial growth in different culture conditions

2.2.4.1 Estimation of viable bacteria in bacterial culture media

The relationship between number of live bacteria and optical density (OD600) was determined using viable counts and measuring optical density at different times points (0, 2, 4, 6, 8 and 24hr). The OD600 of the growth culture was

measured and serial dilutions were plated on LB agar plates at different time points and the resulting colony-forming units (CFU) counted to determine the CFU/ml (Equation 2.3) (Pepper *et al.*, 2011). The number of bacterial cells was approximately 2×10^8 per ml at OD600 0.5 after 3 hr. This OD was used in all of the following assays to determine the Multiplicity of Infection (MOI).

Equation 2.3: Total bacteria

$$\boldsymbol{CFU\ per\ ml = average\ number\ of\ colonies} \times \left(\frac{\mathbf{1}}{\mathbf{0.01}\boldsymbol{ml}}\right) \times \boldsymbol{dilution\ factor}$$

2.2.4.2 Effect of peptides on bacterial growth

Growth curves of UPEC were performed using three different broths: LB broth as a control, LB broth containing 800C peptide and LB broth contain SCR peptide. Basically, 250 µl of 20 µM peptide was added to 25 ml of culture of (OD600 0. 05). The CFUs and OD600 were measured every hour (0, 1, 2, 4 and 6 hr) as described above.

2.2.4.3 Effect of UFH on the viability of bacteria

This was investigated as described above but using LB broth with/without UFH at 50 U/ml up until 3hr.

2.2.5 Infection assay

2.2.5.1 Host cell preparation

Bladder cell lines including RT4, 5637 and primary epithelial cells (

Table 2.14) were harvested using trypsin-EDTA as described in 2.2.2.1 and re-suspended in fresh culture medium. 3×10^4 cells per well in total volume of 100 µl was seeded in 96 well plates and cultured overnight before use in the experiment.

2.2.5.2 Optimisation of infection conditions

The adherence assay was initially based on that of (Elsinghorst, 1994), with some changes suggested by our group as described in Green et al, (manuscript submitted to PLOS Pathogens). Bacteria were prepared as described in 2.2.1.1. Different MOIs (5, 10 and 20) were initially used to infect host cells for 60 minutes. Wells contained just medium (no cells) were included as a control for each MOI. The supernatant was used for assessing the viability of the cells by LDH assay (section 2.2.2.4). The wells washed after the infection three times with 100 μl PBS. The wells were treated with 100μl 1% Triton X-100 at 37°C for 10 min, then pipette up and down several times to lyse the cells. Serial dilutions of the cell lysate in PBS were plated on LB agar for 16 hr and used to measure the number of live adherent bacteria (CFU, Equation 2.3). CFU values from wells with and without cells at each MOI were compared to determine the optimum MOI.

2.2.5.3 Infection of cultured cells

As mentioned above, this assay was developed by Dr Luke Green as seen in Green et al, (manuscript submitted to PLOS Pathogens). Bladder cells were seeded at $3x10^4$ in tissue culture 96-well plates as described in 2.2.5.1 overnight. Medium alone was placed in some wells. Next day, wells with/without cells were washed with 150 µl HBSS (+Ca/Mg) and treated for 1hr with/without 100 µl of various reagents. Wells containing no reagents treated with 100 µl free-serum medium only were referred to as untreated cells while the wells containing no cells (just incubated overnight with 100 µl of medium) were included as a background. Then, the wells were infected by adding 50 µl of medium contained a suitable MOI for 1 hr at 37°C. Then, the supernatants were harvested (often used for cytotoxicity assay (section 2.2.2.5)) and the infected cells were washed three times with 100 µl PBS. The wells were treated with 100µl 1% Triton X-100 at 37°C for 10 min, pipetting up and down several times to lyse the cells. Serial dilutions of the cell lysate in PBS were plated on LB agar for 16 hr and used to measure the number of live adherent bacteria (CFU, Equation 2.3). After subtracting the CFU values of the no-cell control from the

CFU values from that of all wells containing cells, the data was normalised to the untreated (medium alone) control and expressed as the % bacterial adhesion (relative to untreated control).

2.2.5.4 Enzymatic digestion of bladder cell GAGs

The following assay was taken from (Rajas *et al.*, 2017). BECs were seeded at an optimum density in tissue culture 96-well plates (100µl medium per well) overnight. Next day, wells with/without cells were washed with HBSS (+Ca/Mg) and incubated at 37°C for 3 hr in 100 µl of cell culture medium with/without 0.5 U/ml of heparinase I/III or chondroitinase at 250 U/ml. Then, the cells were gently washed once with 100 µl PBS and infected with 50 µl of UPEC suspension, which prepared as described in (section 2.2.1.1), for 1 hr at 37°C as. Wells without cells were used to determine backgrounds. The wells were treated with 1% TritonX-100 for 10 min. Serial dilutions of the cell lysate were prepared and used to determine the number of adherent bacteria as described previously (section 2.2.5.3).

2.2.6 Flow cytometry

Flow cytometry analysis was carried out using LSRII machines (Table 2.8) at the Flow Cytometry Facility at the Medical School, Sheffield University. These experiments were based on methods described by (Hassuna *et al.*, 2017). Mammalian cell populations were gated according to their forward scatter (FSC) and side scatter (SSC) characteristics. The data were manipulated using FlowJo software.

2.2.6.1 Assessment of cell surface protein expression

Assays using live cells were performed under cold conditions to avoid capping and internalization of antigen. The cells were harvested and washed twice with cold washing buffer (B/B/N), then re-suspended to 0.5 x 10^6 in B/B/N and dispensed in 1ml aliquots in FACS tubes (Cat No 2052-004, ELKAY). The tubes were centrifuged at 300xg for 5 minutes and the supernatant removed using a

Pasteur pipette attached to a suction pump. The pellet was re- suspended with 50 µl of primary mAbs (at 10µg ml^{-1} or manufacturer's recommendation in B/B/N) mixed by vortexing and incubated for 60 minutes on ice. The cells were then re- suspended and washed twice by adding 1ml of B/B/N and centrifuging at 300xg for 5 minutes. The cell pellet was re-suspended with 50µl of the secondary fluorescently labelled antibody and incubated for 45 minutes on ice in the dark. The cells were washed twice as described previously and then the cell pellet was re-suspended in 300µl of washing buffer on ice (if analysed on the same day) or the cells were fixed by adding 300µl of 2% paraformaldehyde (if analysed the next day).

2.2.6.2 Quantification of intracellular protein in permeabilised cells

A commercial Fix and Perm Kit™ was used (Table 2.1) to permeabilise the cells, allowing the antibodies to access intracellular antigens. Cells were harvested as described in 2.2.2.1 (0.5 – 1 x 10^6 cells per tube). The cell pellet was re-suspended with 30µl solution A (fixation reagent) and incubated for 15 minutes at room temperature (RT) then washed with 1ml PBS. Before the second wash, the cell suspension was split into two tubes (one for permeabilisation and the other not for no permeabilisation) and centrifuged 200xg for 5 minutes. The supernatant was aspirated, and the cell pellet was re-suspended by vortexing. 25µl of an appropriate concentration of primary antibody was added together with either solution B (permeabilisation reagent) or 25 µl of B/B/N (for fixed only cells) and mixed by briefly vortexing. The suspension was incubated for 30 minutes at RT. The cells then were washed twice with PBS as above, the pellet was re-suspended with 25µl of secondary labelled antibody and the cells were incubated in the dark at RT. After washing, the cells were re-suspended with 200µl of 1% PFA solution and stored at 4 °C in dark until flow analysis.

2.2.6.3 Assessment of internalized antibody into the cells

Cells were harvested using Cell Dissociation Solution and re-suspended at 0.5 x 106 cells in internalisation buffer (HBSS with Ca++ and Mg++, 0.2% BSA) in labelled FACs tubes. Cells were centrifuged at 400xg for 5 min, the appropriate concentration of primary antibody was added (50 μl diluted in internalisation buffer) for 30 min on ice. The cells were washed once by adding 1 ml of HBSS/0.2% BSA and centrifuging at 400xg for 5 min. Cell pellets were re-suspended with100μl HBSS/0.2% BSA. Controls for no internalisation (labelled 0 min) were kept on ice, while other tubes were placed in the water bath at 37°C for 1 hr. After this, any antibody internalisation was quenched by adding 2 ml ice-cold B/B/N, and also to the 0 min controls. All samples were centrifuged at 400xg for 5 min and 50 μl of appropriate dilution of a secondary FITC labelled antibody were added for 30 min on ice. The cells were fixed with 0.3 ml of 2% PFA and wrapped with a foil kept in fridge until analysis.

2.2.6.4 Assessment of fluorescent peptide binding to mammalian cells

The cells were harvested with CDS, washed once with cold wash buffer (B/B/N), then re-suspended to 0.5×10^6 in B/B/N and dispensed in 1ml aliquots in flow cytometry tubes. The tubes were centrifuged at 300xg for 5 minutes and the supernatant were removed. Fluorescent peptides (see section 2.1.8.3) at 1μM, 100 nM, 20 nM in B/B/N were added to the cells and incubated at varies temperatures (37°C or on ice) for different time periods between 5 to 30 min for optimization. The cells were fixed by adding 300μl of 2% paraformaldehyde and stored at 4 °C in dark until FACS analysis.

2.2.7 Immunofluorescence microscopy for assessing antigen expression

Microscopic analysis was carried out using two different microscopes (Table 2.8) at the Light Microscope Facility at Firth court, Sheffield University. The methods for these assays were as described by (Hassuna *et al.*, 2017).

2.2.7.1 Immunofluorescence of cells grown on chamber slides

This experiment was performed using Lab-Tek II Chamber Slides™ (8 chambers). The cells were harvested and re-suspended in culture medium at a density of 9 x 10^4. 0.5 ml of the cell suspension was placed in each chamber and cultured overnight. The slides were examined to check cell density and the cells were washed by adding and removing 0.5 ml PBS. The cells were then fixed and permeabilised by adding 0.5 ml acetone to each chamber and incubating for 5 min. The acetone was removed, and the chambers quickly washed twice with 0.5ml PBS per chamber and flicking to remove the PBS, then placing the slide in a tank containing fresh PBS and washing for 10 min. with stirring. The PBS was removed from the chambers and replaced with 100 µl of an appropriate dilution of primary mAbs (to cover the surface). The slide was incubated at room temperature in a dark and humid place for 30 min. The chambers were washed twice in PBS as before, then a third time by immersing the slide in a tank of PBS with stirring for 15 min. The PBS was removed and replaced with 100µl of an appropriate dilution of FITC- labelled secondary antibody and incubated for 30min in a dark and humid place. The chambers were washed as before and 100µl of 1-10 µg /ml of propidium iodide was added to each chamber and incubated for 3min (to stain the nuclei). The slides were washed as previously. The plastic chamber was removed according to the manufacturer's instructions and any remaining PBS was removed using a Pasteur pipette before adding a small drop of mountant (Vectashield without DAPI) to each chamber section. To seal the slide, a large coverslip and nail

varnish was used. The slide was then stored at 4°C in a dark place until examined using an Olympus Epifluorescence microscope (Table 2.8).

2.2.7.2 Immunofluorescence on cells grown on coverslips

Cells were harvested and re-suspended in medium at a density of 1 x $10^6 ml^{-1}$. 1 ml of the cell suspension was placed in the wells of a 24 well plate containing sterile glass coverslips (22mm diameter) and incubated overnight. The cells were washed by adding and removing 1ml PBS and then fixed and permeabilised by adding 1 ml acetone for 5 min. The acetone was removed, and the coverslip quickly washed three times with PBS. 200 µl of an appropriate dilution of primary mAbs was added and the plate was incubated at room temperature under humid conditions for 30 min. The plate was washed three times with PBS and 200µl of an appropriate dilution of FITC- labelled secondary antibody was added and incubated for 30min in the dark under humid conditions. The wells were washed with PBS as before previously, and the coverslips removed using thin curved ended forceps and placed on slides on which one drop of Vectashield mountant (Table 2.1) had been placed. The coverslips were placed so that the cells were facing the mountant. The coverslips were sealed using nail varnish and the slides were stored in slide folder at 4°C in the dark until examined using a Nikon Ti Eclipse microscope (Table 2.8).

To examine fluorescent peptide binding to epithelial cells by microscopy, a similar protocol was used. Briefly, the cells were harvested and re-suspended in culture medium at an optimum density and incubated overnight. After washing the cells, 0.5 ml of 200nM of tagged peptides diluted in basal cell culture media were added for 30 min at 37°C. As a background control, only medium added. Then, cells were fixed with 2% PFA for 15 min at room temperature. After the fixation the cells were washed twice with PBS, then the coverslips were placed on slides using Vectashield mounting medium with DAPI and sealed as described above. The slides were examined using a Nikon Ti Eclipse microscope (Table 2.8). Images were analysed using ImageJ. The level of fluorescence intensity was calculated using the following equation:

Equation 2.4: Total cell fluorescence

$$\textit{Total cell fluorescence} = \textit{Integrated density} - (\textit{area of selected cell or whole image} \times \textit{mean fluorescence of background})$$

2.2.8 Applied statistical analysis methods

Data were analysed using GraphPad 9 Prism software. In this study two main statistical tests were used in data analysis. Significance was established at $p < 0.05$. To compare between three groups or more (e.g. untreated control, negative controls such as isotype control or SCR peptide and the potential anti-adhesive drugs either antibody or peptide), one-way ANOVA was used to determine the significant differences between those conditions. The unpaired *t*-test was used in the case of comparison of two groups (e.g. untreated control and UFH in (Chapter 6)). Data were subjected to a normality test, and if not normal, a nonparametric method (particularly the Mann Whitney test) was selected.

Chapter 3: Expression of tetraspanin proteins on various types of bladder epithelial cells

3.1 Introduction

3.1.1 Tetraspanin protein expression

As described in section 1.2, tetraspanins are a superfamily of small transmembrane proteins that are ubiquitously expressed in mammalian cells, distributed within the cells either in the plasma membrane or on intracellular vesicle membranes. Thirty three known members exist in humans, found in all tissues of the body (van Spriel and Figdor, 2010). The quantity of tetraspanins localised to either the plasma membrane or intracellular vesicles also differs depending on specific functions (Sincock et al., 1999). Some members are named based on the original place that they were found such as uroplakins in the urothelium, while others are most commonly known by their systematic name, which has been given to all mammalian tetraspanins (Tspan1 – Tspan33) (reviewed in (Lang and Hochheimer, 2020)). With the main aim of this project being to study the role of tetraspanins in UPEC infection, it was an essential step to confirm their presence on the cell surface. Certain tetraspanins are relatively well-characterised, known to have a wide tissue distribution and have been implicated in bacterial infection (Green et al., 2011; Ventress et al., 2016; Hassuna et al., 2017). Gene and protein expression data are crucial to complete the understanding about their expression; quantitative-real time PCR, flow cytometry and immunofluorescence microscopy were used in this study. We have investigated the expression of all 33 Tspan genes. Monoclonal antibodies to CD9 (TSPAN29), CD63 (TSPAN 30), CD81 (TSPAN 28), CD82 (TSPAN 27), and CD151 (TSPAN24), are readily commercially available or had been produced in our laboratory (Table 2.10). Moreover, the expression of uroplakin tetraspanins is covered in a separate chapter (chapter 4).

3.1.2 Cell line models

Several human bladder cancer cell lines derived from various tumour grades and primary bladder epithelial cells were used in this study. We have assessed all tetraspanin gene expression in the selected cell lines then screened for the expression of certain tetraspanin proteins on the cell surface. The urothelial cells used in this study have been previously ranked based on their differentiated phenotype and the different grades of tumour from which they were derived. From poorly to well differentiated cells, the bladder cancer cell lines are ranked: T24, 5637, RT4 cells, based on differences in gene expression and morphological characteristics (Liu et al., 2014). T24 is a cell line originally established from grade III poorly differentiated bladder carcinoma (Bubeník et al., 1973). This cell line has been used as an *in vitro* model of invasive urothelial carcinoma cells in many studies (Imani et al., 2015; Yu et al., 2016). Another well-known human bladder carcinoma cell line, 5637, which is derived from grade II carcinoma, was also used. Several studies have represented 5637 as a moderately differentiated model (Laaksovirta et al., 1999; Brassesco et al., 2013; Yoshida et al., 2015). Importantly, this cell line is well-studied in terms of use as an infection system (Bishop et al., 2007). The human urinary bladder papilloma RT4 (grade I), referred to as a well-differentiated cell line in several studies, was also used. This cell line is a non-invasive model that has been widely reported as naturally similar to the normal bladder epithelium (Theodorescu *et al.*, 1990; Redwood *et al.*, 1992; Fujiyama *et al.*, 2001; Kabaso *et al.*, 2011; Liu *et al.*, 2014). Although T24 and RT4 are originally from the same basic cell type (Kabaso et al., 2011), they showed differences in biophysical properties (Liu et al., 2014). As an additional mature model, primary bladder epithelial cells have been used in this thesis and the expression of tetraspanin proteins CD9 and CD81 on these cells was examined. However, these different types of cells have extensively been used as an *in vitro* model in several UTI studies (Martinez, 2000; Schilling et al., 2001; Bishop et al., 2007; Dhakal and Mulvey, 2009; Song et al., 2009; De Llano et al., 2015).

The objectives of the work described in this chapter were mainly to assess the cell surface expression of certain tetraspanins on bladder epithelial cells

(BECs), to study gene expression of all tetraspanins in selected cell lines and to appraise any differences in tetraspanin levels between the different types of bladder carcinoma cells.

3.2 Results

3.2.1 Expression of tetraspanin genes by different types of bladder cell lines

The gene expression in T24 and 5637 bladder cell lines have been studied (Figure 3.1). We found that in general there was a similar pattern of gene expression between these cell lines. Most Tspan genes such as Tspan 1, Tspan2, Tspan3, Tspan4, Tspan5, Tspan 11, Tspan 12, Tspan 15, Tspan17, Tspan 19, CD151 (Tspan 24), Tspan 25, CD82 (Tspan 27), CD9 (Tspan 29), Tspan 31 are expressed at relatively the same level in both cell lines (Figure 3.1). In contrast, expression of Tspan8 and Tspan23 genes in T24 cells is low compared to the level in 5637 cells. Although there is relatively low abundance of uroplakin Tspan (Tspan 20 and Tspan 21) mRNA in these cells compared to other mature cells (detailed in the following chapter (Chapter 4)), 5637 seems to be expressing higher levels of these genes than T24 cells.

3.2.2 Expression of tetraspanin proteins by different types of bladder cell lines

The expression of Tspan proteins were studied in T24, 5637, RT4 and primary bladder cells. The flow cytometry data for these different cells is summarised as MFI (median fluorescence intensity) values in Figure 3.2 and shows a variable level of protein expression of Tspan between these cells. In the following sections, the expression of Tspan at protein level and the correlation with gene level (where appropriate) is described in more detail for each bladder cell type.

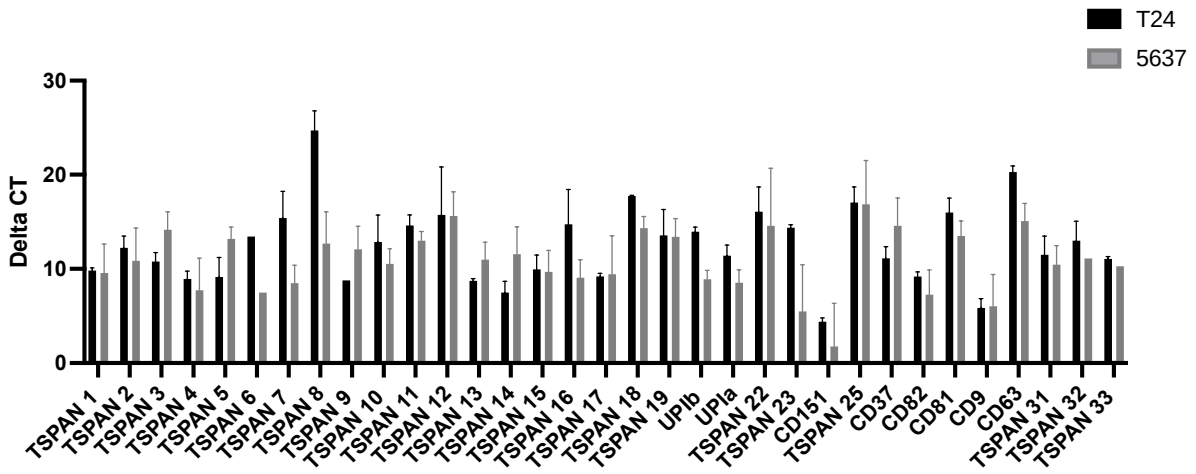

Figure 3.1: Tspan gene expression at the mRNA level in bladder cell lines.

Expression levels in bladder cells T24 and 5637 relatives to the housekeeping gene GAPDH were determined using suitable TSPAN primers as described in (section 2.2.3). ΔCt levels are depicted on the Y axis, where low values correspond to high gene expression and vice versa. The data represent the means, while error bars describe standard error means. n=3 experiments in performed in triplicates.

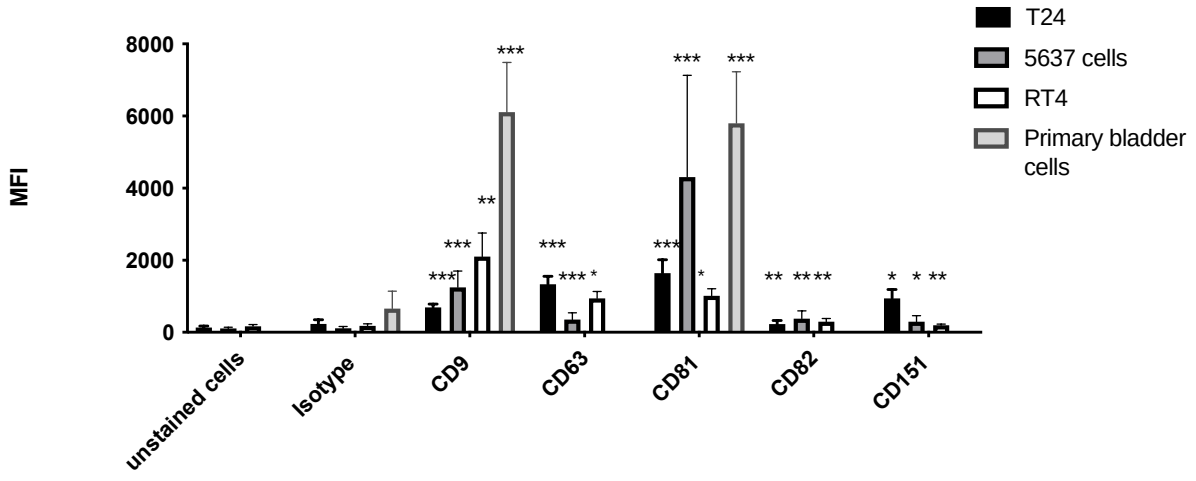

Figure 3.2: Expression level of tetraspanin in bladder cell lines by flow cytometry.

The graph illustrates MFI (median fluorescence intensity) of tetraspanin expression in different cell lines: T24, 5637 and RT4 cells and primary bladder cells. The data describe means, while error bars describe standard error means. n=3 independent experiments, performed in duplicate. Tetraspanin expression relative to the isotype control was analysed by unpaired t-test, where * $p<0.05$; ** $p<0.01$; *** $p<0.001$ significant; ns is non- significant.

3.2.2.1 Tetraspanin expression in the T24 cell line

The quantitative expression of tetraspanins in the human bladder cancer cells, T24, was estimated by real-time qPCR, flow cytometry and immunofluorescence microscopy. Representative data of gene expression level is displayed in (Figure 3.1). In general, expression for all tetraspanin genes was detected compared to the housekeeping gene but with different abundance. CD151 (Tspan 24) mRNA was richly expressed compared with other tetraspanin genes. Expression of CD9 (Tspan 29) was relatively high, while some Tspan genes were expressed in low abundance such as Tspan 8.

Flow cytometry was used to study the expression level on the cell surface (section 2.2.6.1). The healthy cell populations were gated depending on FSC and SSC parameters (Figure 3.3). A relatively low expression of CD81 mRNA was observed compared to CD9 and CD151 (Figure 3.1); this is not correlated with the flow cytometry data where high expression of CD81 was found on the cell membrane (Figure 3.2 & Figure 3.3). Although expression of the CD82 gene was detected by RT-PCR (Figure 3.1), the cell surface expression was very low for this protein (Figure 3.2 & Figure 3.3). High expression of CD9 was also observed (Figure 3.2 & Figure 3.3), correlating with gene expression result. CD9 expression was also studied by immunofluorescence microscopy (Figure 3.4). A large amount of green fluorescence distributed across the plasma membrane was observed, consistent with flow cytometry results.

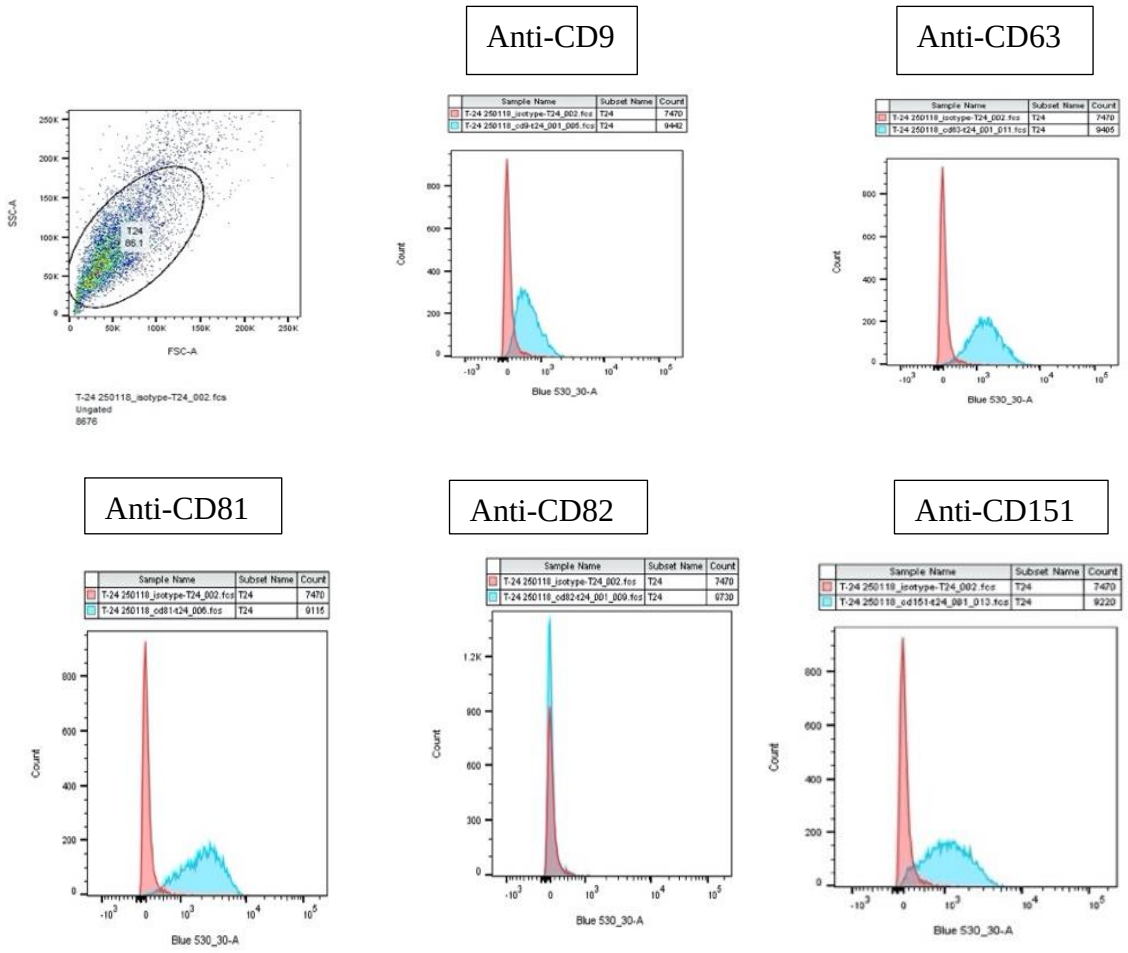

Figure 3.3: Analysis of tetraspanin expression in T24 cells by flow cytometry.

The primary monoclonal antibodies were used with appropriate isotype controls and FITC-conjugated anti-mouse IgG as a secondary antibody. The dot plot shows T24 cells gated according to forward scatter (FSC) and side scatter (SSC), the histogram plots show the MFI overlap of isotype (red) and anti-tetraspanin (blue) treated cells.

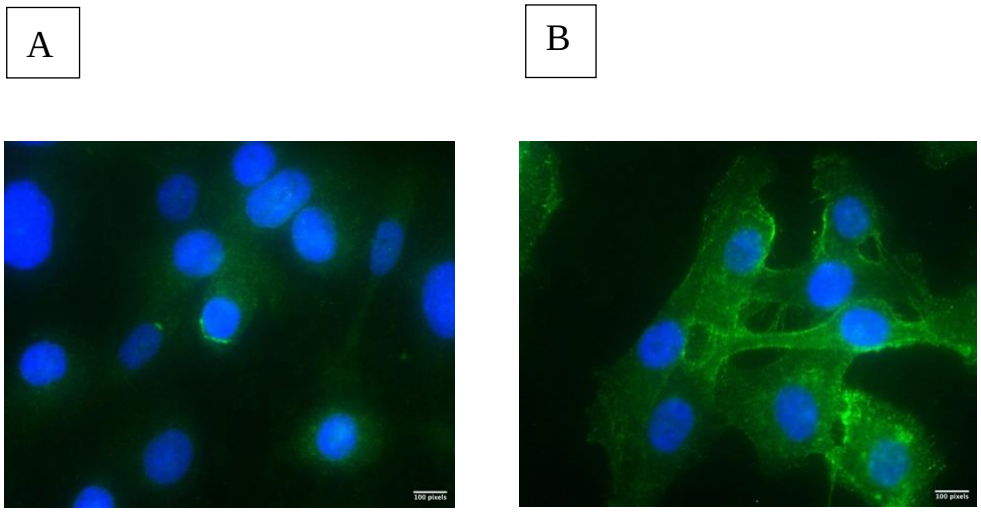

Figure 3.4: Microscopic visualisation of CD9 expression in T24 cells by immunofluorescence microscopy.

Cells were cultured on chamber slides and fixed and permeabilised as described in section 2.2.7.1, then stained with primary monoclonal antibody anti CD9 or isotype control antibody followed by FITC-conjugated anti- mouse IgG. (A) Isotype control treatment. (B) Anti-CD9 antibody treatment. These images were obtained using the 100X objective, scale bar = 100 pixels, DAPI shown in blue, FITC shown in green.

3.2.2.2 Tetraspanin expression in the 5637-cell line

Screening of tetraspanin expression in human bladder cancer cell line 5637 was performed at both gene and protein level as described previously. CD9 (Tspan 29) and CD151 (Tspan 24) mRNA were present at high abundance, and expression of other tetraspanin genes were detected compared to the reference gene (Figure 3.1). Flow cytometric data showed that there is high expression of tetraspanins CD81 and CD9 proteins on the cell surface (Figure 3.2 & Figure 3.5). The median fluorescence intensity data illustrated significantly increased levels of fluorescence on CD81 (up to 4000 MFI value) and CD9 (approximate 2000) compared to their isotype control (about 100) (Figure 3.2). Although CD151 (Tspan 24) and CD82 (Tspan 27) genes were expressed in high abundance (Figure 3.1), low expression of these tetraspanins was observed by flow cytometry at about 295 and 380 MFI value, respectively (Figure 3.2 & Figure 3.5). The expression level of the CD63 (Tspan 30) gene was at moderate abundance (Figure 3.1), while low expression has seen at the cell surface compared to their isotype control (Figure 3.2 & Figure 3.5); this may reflect the

fact that this protein is mainly intracellular in most cells. Visualisation of tetraspanin expression in 5637 cells is demonstrated in (Figure 3.6). This data was consistent with the flow cytometry result, with heavy staining with CD81 antibody in comparison with the isotype control. Cells treated with CD9 antibody also stained relatively well compared to isotype control.

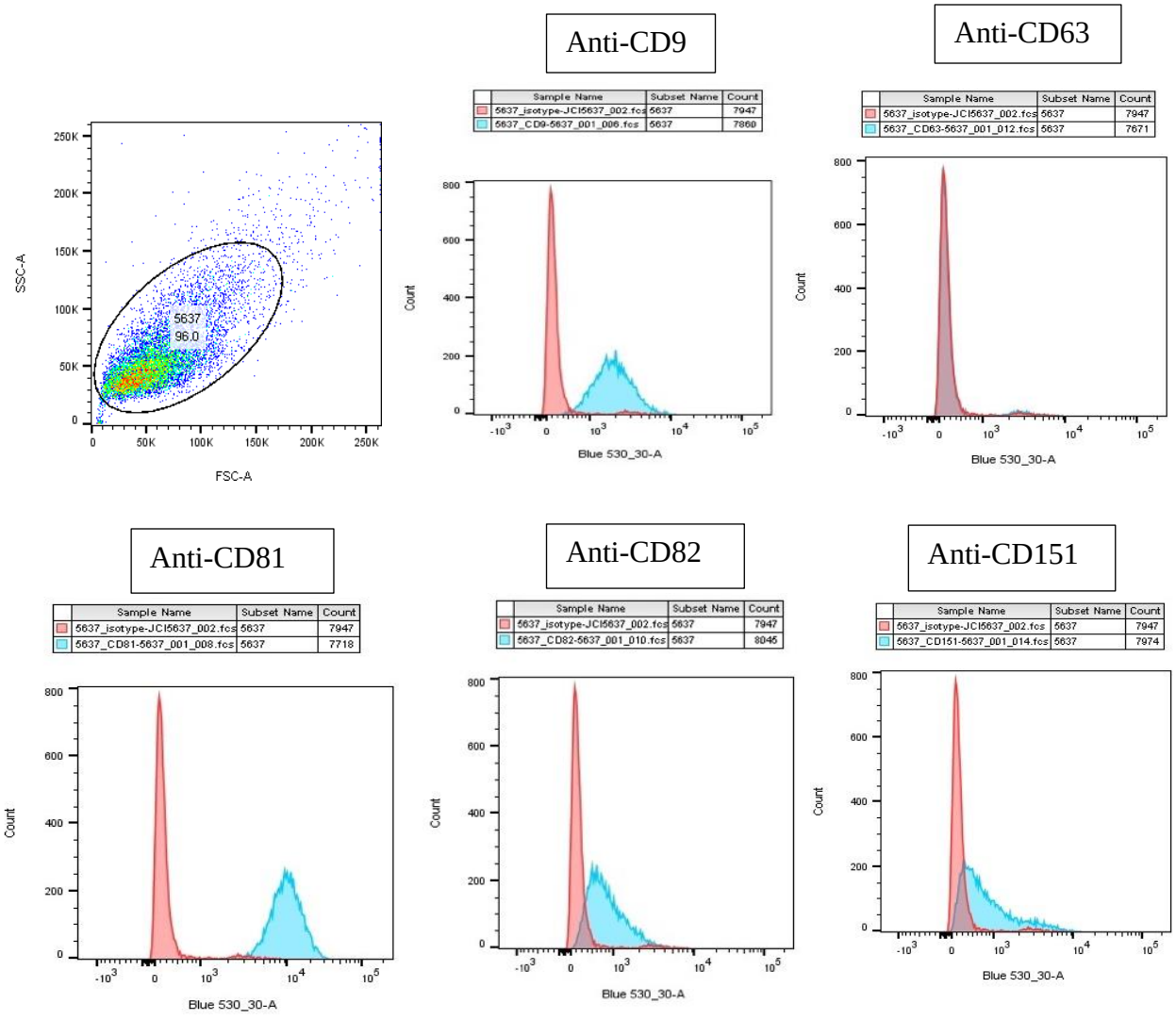

Figure 3.5: Analysis of tetraspanin expression in 5637 cells by flow cytometry.

The primary monoclonal antibodies were used with appropriate isotype controls and FITC-conjugated anti-mouse IgG as a secondary antibody. The dot plot shows 5637 cells gated according to forward scatter (FSC) and side scatter (SSC), the histogram plots show the MFI overlap of isotype (red) and anti-tetraspanin (blue) treated cells.

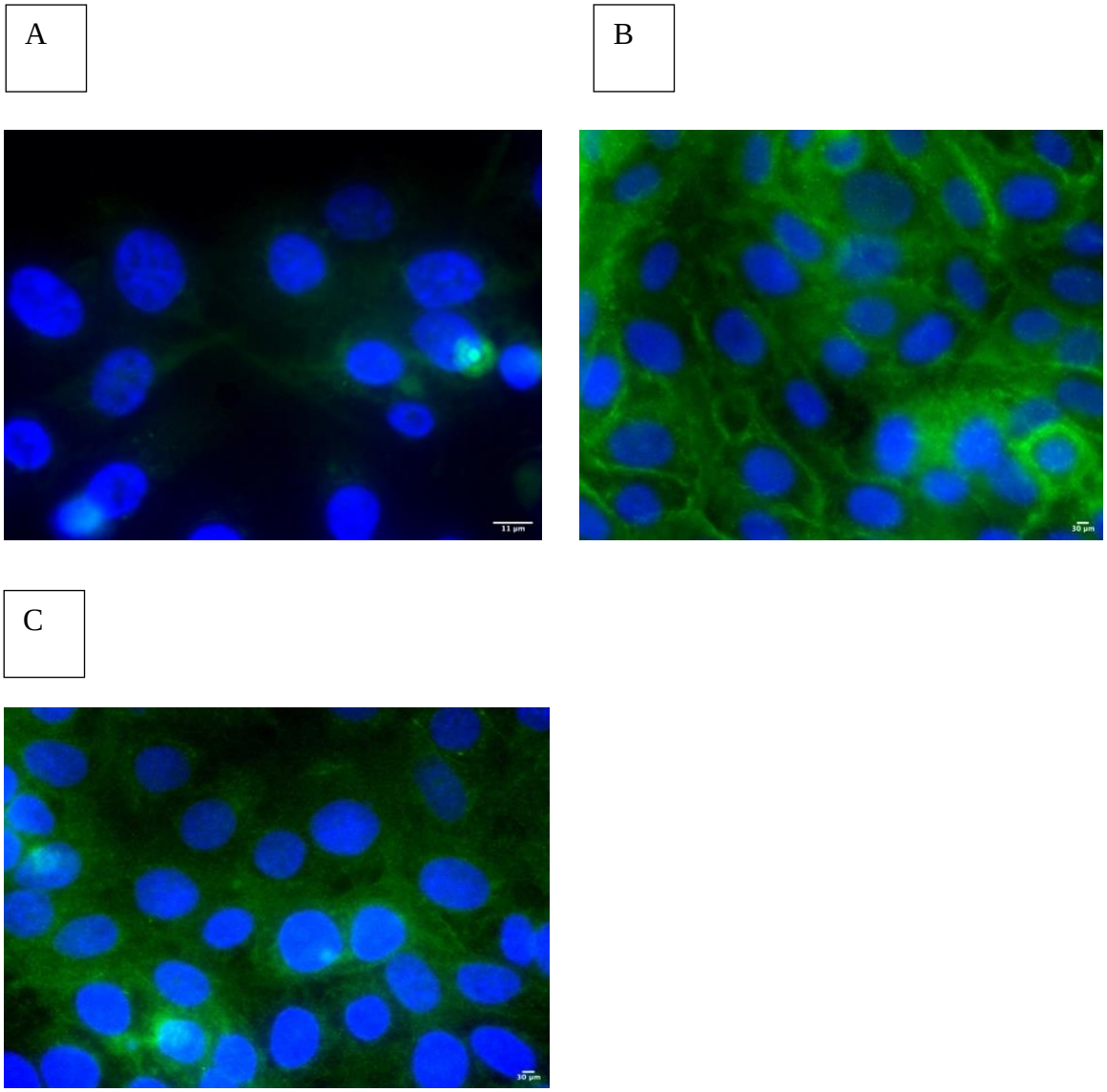

Figure 3.6: Microscopic visualisation of CD9 and CD81 expression in 5637 cells by immunofluorescence microscopy.

Cells were cultured on chamber slides and fixed and permeabilised as described in section 2.2.7.1, then stained with primary monoclonal antibody anti CD9/CD81 or isotype control antibody followed by FITC-conjugated anti- mouse IgG. (A) Isotype control treatment. (B) Anti-CD81 antibody treatment. (C) Anti-CD9 antibody treatment. These images were obtained using the 100X objective. scale bar = 11 µm in (A) 30 µm in (B&C), DAPI shown in blue, FITC shown in green.

3.2.2.3 Tetraspanin expressions in RT4 cell line

Gene expression of tetraspanins in this cell line was not studied due to time constraints, and as the previous sections show, we did not find a correlation between gene and protein expression. Therefore, cell surface Tspan expression on the human urinary bladder papilloma cell line RT4 was directly studied by using flow cytometry. Representative data for a healthy population of RT4 cells and their tetraspanin expression is displayed in (Figure 3.7). Expression of CD81 (about 1000 MFI) and CD63 (945 MFI) was significantly increased from the isotype control treated cells (below 200 MFI), while no significant differences were observed between the isotype control treated cells and anti-CD151 (around 190 MFI) and anti-CD82 treated cells (below 300 MFI) (Figure 3.2 & Figure 3.7). This suggests that CD151 and CD82 could be absent in this cell line or could be located intracellularly. The expression level of CD9 was very significantly high compared to isotype control (Figure 3.2 & Figure 3.7). Apparently, CD9 expression on RT4 cells was higher than on the other cell lines, T24 and 5637 (Figure 3.2).

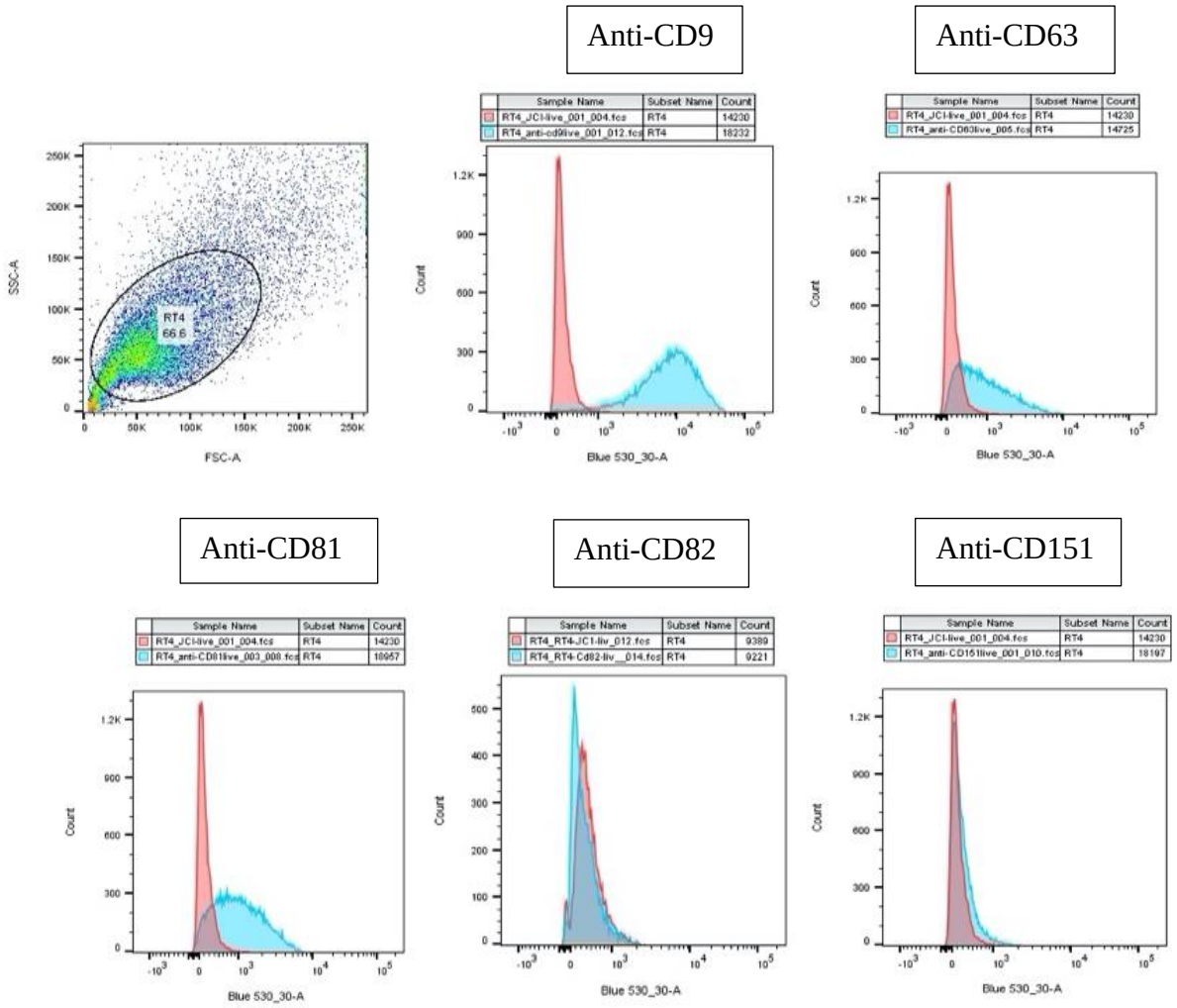

Figure 3.7: Analysis of tetraspanin expression in RT4 cells by flow cytometry.

The primary monoclonal antibodies were used with appropriate isotype controls and FITC-conjugated anti-mouse IgG as a secondary antibody. The dot plot shows RT4 cells gated according to forward scatter (FSC) and side scatter (SSC), the histogram plots show the MFI overlap of isotype (red) and anti-tetraspanin (blue) treated cells.

3.2.2.4 Tetraspanin expressions in primary bladder cells

Primary bladder epithelial cells were used in this study as an example of mature bladder cells. Due to the high cost of these cells and their relatively low number, we studied the cell surface expression of only two tetraspanin proteins, CD9 and CD81, as they are known to be involved in many cellular functions, including infection. As described in chapter 4, cell surface expression was of interest here, therefore only live cells were gated using propidium iodide staining to exclude dead cells (displayed in Figure 4.5). It is noticeable that the

expression level of CD9 and CD81 was significantly above the isotype control, with both at very high levels on the surface of these cells (Figure 3.2 & Figure 3.8).

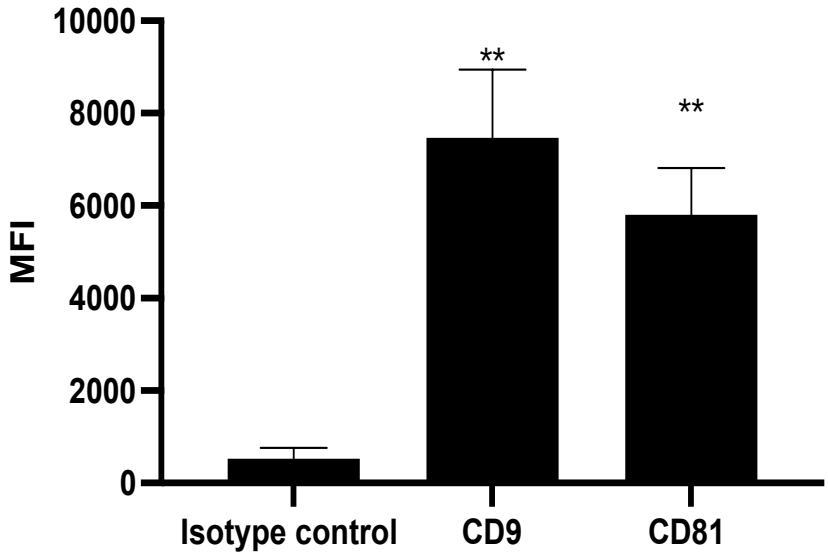

Figure 3.8: Analysis of tetraspanin expression in primary bladder cells by flow cytometry.

The primary monoclonal antibodies were used with appropriate isotype controls and FITC-conjugated anti-mouse IgG as a secondary antibody. The graph represents the level of CD9 and CD81 expression in primary bladder cells. The data describe means, while error bars describe standard errors means. n=3 independent experiments, performed in duplicate. Tetraspanin expression relative to the isotype control was analysed by unpaired t-test, where * significant at $P<0.05$; ** significant at $P<0.01$; ns is non- significant.

3.2.3 Comparison of protein and gene expression of Tspan between the bladder cell types

In general, there were greater differences between the bladder cell types in terms of Tspan protein expression on the surface than was evident from gene expression data (Figure 3.1 & Figure 3.2). There was high expression of CD9 (Tspan 29) in RT4 and in primary cells, whereas CD151 was absent from RT4 cells but present on T24 and 5637 cells. CD81 was in high abundance in primary cells and 5637 and also present at lower levels on RT4 and T24. CD82 was expressed on the cell surface of 5637 while absent from RT4 and T24 cells. Expression of CD63 in 5637 was lower than in RT4 and T24 cells.

The correlation between mRNA and protein level is discordant in some cases. For example, there was low expression of CD63 mRNA in T24, while expression of CD63 at cell surface was evident. Also, good expression of CD151 mRNA was found in 5637 cells but low abundance of CD151 at the cell surface. The expression of CD81 gene in T24 and 5637 appears low, whereas high expression of this molecule was found at the cell surface. In contrast, we found that CD9 gene expression highly correlated with protein levels in both tested cell lines (5637 and T24).

3.3 Discussion

In this chapter we studied the expression of tetraspanins using RT-qPCR, flow cytometry and in some cases immunofluorence microscopy. The main aim of using RT-qPCR was to assess the relative abundance of Tspan gene expression compared to reference gene (GAPDH). Here, all 33 Tspans had detectable mRNA in different quantities in two separate cell lines, 5637 and T24. These cell lines have a common pattern of Tspan gene expression (Figure 3.1). CD9 mRNA was expressed in these cells, whilst the genes encoding CD63 (Tspan 27) had a relatively low level of expression in both cell lines. Although the Tspan 8 gene is overexpressed in various types of poorly differentiated human carcinoma cells (Kanetaka et al., 2001; Zöller, 2006, 2009), here the T24 cell line showed low expression of this gene. However, bladder cells isolated from high grade carcinomas are genetically unstable due to variations in the tumours (Simon *et al.*, 2002; Hoque *et al.*, 2003). Notably, CD151 gene expression was high in bladder cancer cells that showed positive CD151 expression by flow cytometry. Similar observations were made for CD9 expression with most immunofluorescence results showing a good agreement with RT-qPCR assays.

We found that the bladder epithelial cell lines possess different levels of tetraspanin on the plasma membrane. From poorly differentiated cells (T24) to primary bladder cells were tested and differences were identified between tetraspanin expression levels. Varied levels of the generally widely expressed CD9, CD81, CD63, CD151 and CD82 proteins were observed on the cell membrane using flow cytometry (Figure 3.2). The results were supported by immunofluorescence images for CD9 in T24 and 5637 cells and CD81 in 5637 cells. We demonstrated significant increases in the median fluorescence intensity of CD9, CD81 on all tested cell lines compared to their isotype control, indicating that a large number of these tetraspanin molecules are present in those cells. As was demonstrated in the T24 cell line, a large amount of CD9 was distributed across the plasma membrane compared to the isotype control cells. Strong CD9 staining was seen across the cytoplasm and cell membrane as well as at cell-cell junctions where cells were adjacent (Figure 3.4). The level

of CD9 expression appeared higher in more mature cell lines such as RT4 and the primary bladder cells (Figure 3.2). Tetraspanin CD82 (also named KAI1) (Zhang et al., 2010) was not detectable above the isotype control in RT4 and T24 cells, whilst it was present in low abundance in 5637 cells (Figure 3.2). This is in contrast to a previous study that showed that CD82 had normal expression in T24 compared to normal bladder cells by Western blot and reduced levels of CD9 and CD81 proteins (White, Lamb and Barrett, 1998). This is possibly due to the fact that CD82 is frequently associated with intracellular vesicles (Zhang et al., 2010), so might not be detected on the surface of live cells. A study on the metastatic suppressor role for CD82 in different types of carcinomas has shown that CD9 and CD81 showed high expression in most human tumour-derived cell lines with low expression of CD82, suggesting that CD82 has significant prognostic value in metastasis (White, Lamb and Barrett, 1998).

It is widely known that the CD81 molecule tends to be expressed on the cell membrane and that it is involved in many cellular functions (Vences-Catalán et al., 2017). It was therefore beneficial to study the expression of this tetraspanin on the bladder cell lines using flow cytometry to detect the expression on the cell surface independently and confirm the result by immunofluorescence microscopy. Cell surface expression of CD81 in primary bladder epithelial cells and 5637 cells was higher than that in the other tested bladder cancer cells (Figure 3.2). We provide images confirming the data observed with flow cytometry and demonstrating the cell surface localisation of CD81 in 5637 cells. As shown in Figure 3.6, CD81 and CD9 showed similar localisation pattern across the plasma membrane and at cell-cell junctions in 5637 cells, with less fluorescence of CD9 compared to CD81. However, similar patterns of CD81 expression were observed on low-grade bladder cells RT4 and high-grade T24 with good expression on all cell lines. Previous studies have shown that expression of CD81 is associated with the invasive activity of bladder cells, as it has been shown that RT4 cells expressed more CD81 than T24 cells using western blotting (Lee et al., 2015; Park et al., 2019). This suggests that RT4 could retain some of this protein inside the cells. However, due to good expression of CD81 in all bladder cells, it is worth studying the role of this protein in UPEC infections. CD63 was also found on the cell surface in two cell

lines: RT4 and T24 cells and low surface expression was observed in 5637; this could be because CD63 is known to be quickly recycled from and to plasma membrane during the fusion of the endocytic vesicles (Maaike S. Pols and Klumperman, 2009). The expression of CD151 appears to vary considerably, as whilst in the high-grade tumour cells the expression was high, it was decreased in the lower grade cancer cells, 5637, then not present in the low grade RT4 cells. Our observations agree with previous studies showing that CD151 expression correlates with the stage of carcinogenesis and cancer cell proliferations (Hemler, 2014). High levels of CD151 expression are seen in different types of human tumour cells including prostate (Ang et al., 2004) , lung (Tokuhara et al., 2001), colon (Hashida et al., 2003) and skin and is linked with advanced tumour stage and poor prognosis (Zeng et al., 2017).

As previously mentioned, tetraspanin proteins are ubiquitously expressed in all human cell types and can be found on the plasma membrane or within intracellular organelles (Hemler, 2005; Charrin et al., 2009). This study suggests that the pattern of tetraspanin expression could be seen to depend on the specific cell type and the level of maturity. Several groups have demonstrated the physical formation of integrins-tetraspanin complexes including α1β1 and α3β1 linked to CD9 in different epithelial cells types, which suggests that the interaction is involved in cell adhesion and migration (Reyes et al., 2018). Also, a previous study has shown that α3β1integrins are involved in UPEC adherence to BECs suggesting a possible role of tetraspanins in FimH adhesion (Eto et al., 2007). It will be important to investigate the function of tetraspanins in urothelial cells particularly in UPEC infection. Therefore, in chapter five we will discuss the effect of tetraspanin- derived reagent in the bacterial adherence to bladder cells. However, the next chapter discusses the expression of uroplakin expression on bladder cell lines.

Chapter 4: Studying uroplakin expression in human bladder cells

4.1 Introduction

4.1.1 The regulation of uroplakins and their expression in the urinary tract

As described in Chapter 1, in bladder urothelium, four major integral uroplakin proteins, UPIa, UPIb, UPII, and UPIII are interacting together in two specific pairs forming unique plaques. UPIa and UPIb have four transmembrane domains (TMDs), share about 40% similar sequence of their amino acids, and are classified as members of the tetraspanin superfamily (Yu et al., 1994; Hemler, 2001). The other two uroplakins UPII and UPIII have only one transmembrane domain (Wu and Sun, 1993; J. H. Lin et al., 1994). UPIa and UPIb join with UPII and UPIII, respectively, forming specific heterodimers in the endoplasmic reticulum (ER) (Tu et al.,2002; Hu et al., 2005, 2008). Uroplakin pairs Ia/II and Ib/III become stabilized and mature after the cleavage of the prosequence of UPII by trans-Golgi network associated furin (Hu et al., 2005). They form 16 nm particle two-dimensional crystals known as urothelial plaques or asymmetric unit membrane (AUM) in post- Golgi compartments (Pavelka et al., 2011). Later in maturation they are delivered to the apical cell surface by fusiform vesicles (FVs) (Hudoklin et al., 2012).

As a result, the apical surface of the urothelium is entirely covered with AUM. The urothelium enables the urinary bladder to keep the urine in its original position during storage. To perform this function, the urothelium should ideally have four properties. First, it has a low epithelial surface area-to-urine volume ratio, which limits the available surface area for passive transport between the lumen and the blood. Second, the apical membrane and tight junctions have very low passive permeability to ions and non-ions. Third, the urothelium possesses a hormonally regulated sodium absorption mechanism, thus active

sodium reabsorption neutralizes passive sodium transport from blood to urine. Finally, most molecules found in the urine or blood have no effect on the apical membrane's permeability properties or the tight junctions of the urothelium (Lewis, 2000). Due to the distinct uroplakins structure showed by cryo-EM, it has been suggested that the interaction between the uroplakin proteins and some lipid molecules in the urothelial plaques contributes to permeability barrier function between urine and cellular contents , especially when the bladder is enlarged with urine (Hu et al., 2002; Min et al., 2003, 2006a). UPIII-Knockout mice have a deficiency in barrier function due to shrinkage of urothelial plaques (Hu et al., 2001).

At present, there is little information about the regulation and expression of uroplakins in the bladder epithelial cell lines (BECs). Several studies seem to have assumed that the cell lines express at least some uroplakins at the cell surface such as UP1a (Scharenberg et al., 2011; Kurimura et al., 2012). However, more investigation is needed. The aims of the present study were to assess the expression of selected uroplakins in certain human bladder cells and study the correlation between the differentiation stage of these cells and UP expression. For the work detailed below, we studied a variety of human bladder cell lines, which are commonly used for *in vitro* models of bladder infection (Martinez, 2000; Mulvey, Schilling and Hultgren, 2001; Schilling et al., 2001; Bishop et al., 2007; Dhakal and Mulvey, 2009; Song et al., 2009), reflective of the various tumour grades (Laaksovirta et al., 1999). RT4 cells derive from well differentiated (grade1) human urinary bladder papilloma (Lobban et al., 1998; Kabaso et al., 2011). 5637 derive from moderately differentiated (grade 2) human bladder carcinoma, and T24 derive from poorly differentiated (grade 3) human bladder carcinoma (Lobban et al., 1998; Liu et al., 2014; Yoshida et al., 2015; Yu et al., 2016). Another model system used here is primary bladder cells. Initially, 5637 and T24 were used for UPIa and UPIb expression studies as they have been extensively used as a model of UPEC infections, then we moved onto investigating RT4 and primary cells.

4.1.2 Attempts to differentiate urothelial cancer cell lines

Although uroplakins are a major differentiation marker, others are also important including cytokeratin 20 (CK20) and the tight junction protein and ZO-1 (Southgate, 1999; Olsburgh et al., 2003; Turner et al., 2008). Interestingly, the CK20 sub-apical network seems to regulate UPs movement to the apical surface (Hudoklin et al., 2012). Various studies have shown that different factors can induce urothelial differentiation including mechanical stimuli, cyclic hydrostatic pressure and complementary serum-dependent medium (Sun, 2006; Cattan et al., 2011; Gao et al., 2018). There are extensive studies on the establishment of models where urothelial cell differentiation is regulated using human, mouse or porcine tissue (Apodaca, 2004; Veranič, Romih and Jezernik, 2004; Romih et al., 2005; Turner et al., 2008; Thumbikat, Berry, Schaeffer, et al., 2009; Gao et al., 2018). However, few studies have used urothelial cancer cell lines as a model to develop the differentiation stage.

The next part of this chapter was to try to induce bladder epithelial cells to express UPs at the apical surface, making them more equivalent to native urothelium and providing a useful tool for clinical research. This would allow us to study the effectiveness of UPIa as a potential target to inhibit and treat urinary tract infection.

4.2 Results

4.2.1 Quantitation of uroplakin gene expression

RT-PCR was performed to detect the mRNA expression of UPIa, UPIb, UPII, and UPIII (2.2.3). As mentioned above, 5637 and T24 cells have been first used in this study. We did not detect expression of the uroplakin genes in T24 cells compared to the housekeeping gene, whereas 5637 cells possessed slight amounts of UPIa and UPIII mRNA (

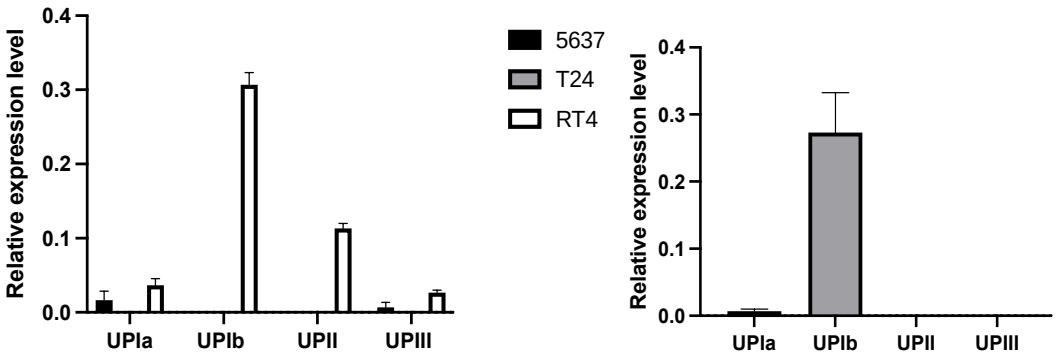

Figure 4.1-A). This could indicate that these cells were not mature enough. Therefore, we started work with RT4 and then eventually primary bladder cells. All uroplakin genes are expressed in RT4 cells, with especially high expression of the UPIb gene (

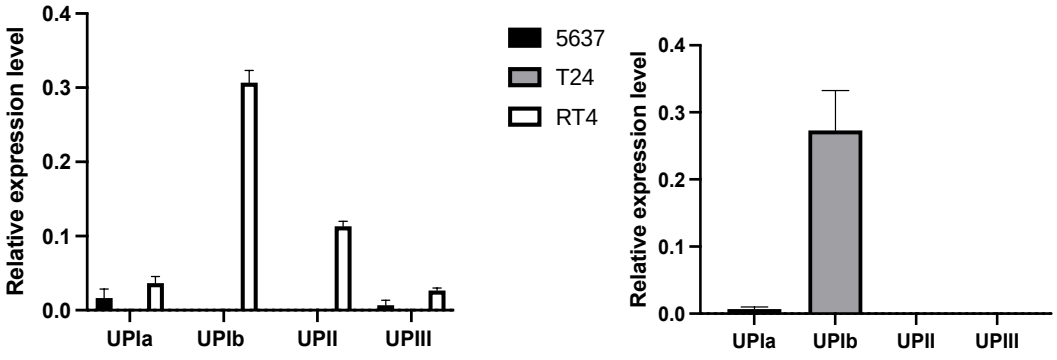

Figure 4.1-A). Notably, primary cells, which were presumed to correspond to a mature bladder tissue type, also show high expression of UPIb, but low levels of UPIa mRNA and non-detectable expression of the other uroplakin genes (

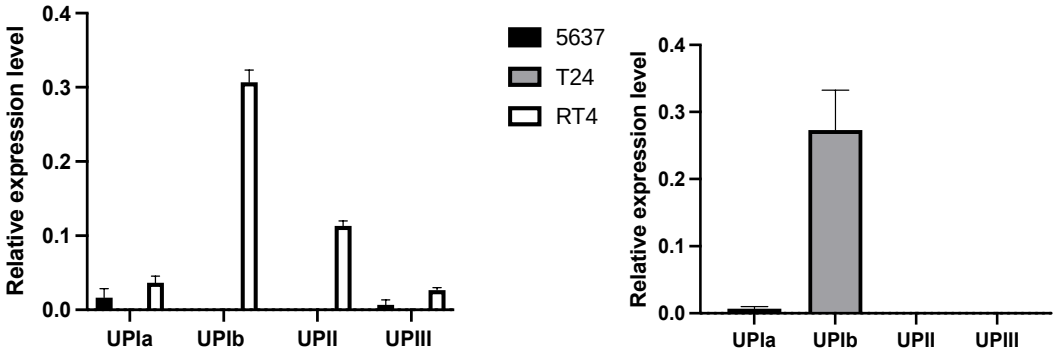

Figure 4.1-B).

A

B

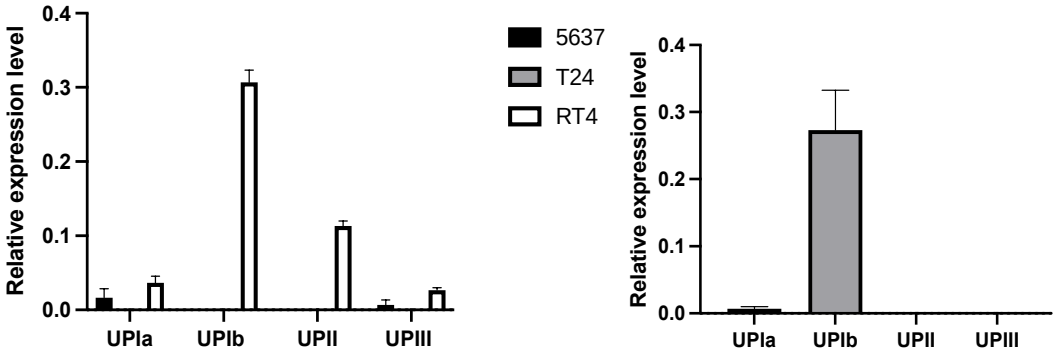

Figure 4.1: Uroplakin gene expression at the mRNA level in various types of human bladder cells.

(A) The means of uroplakin gene expression relative to the housekeeping gene (GAPDH) in three different bladder cell lines: 5637, T24 and RT4. (B) The means of relative uroplakin gene expression in primary bladder cells. The normalized fold change was calculated using the delta Ct method with GAPDH as the control gene. The data represent the means, while error bars describe standard error means. n=3 independent experiments, performed in triplicate.

4.2.2 Tetraspanin uroplakin expression on the cell surface

Flow cytometry was used to determine whether UPIa and UPIb are expressed on the bladder epithelial cells, as described (in section 2.2.6.1). Propidium iodide stain was used to detect any dead cells then the cell population was gated to exclude these. Since there are no available monoclonal antibodies against UPIa and UPIb, rabbit polyclonal antibodies were used as stated in section (Table 2.10). Titration of these antibodies was carried out with the appropriate concentration of isotype control in order to take account of any non-specific binding. Anti- UPIa was consequently used at 20 µg/ml with the same concentration of rabbit polyclonal isotype control. Anti-UPIb was used at 30 µg/ml (the optimal concentration recommended by the manufacturer).

RT4 cells showed undetectable expression of UPIa as no positive cells were determined (Figure 4.2-A & C). Low expression of UPIa was seen in other urothelial cells (Figure 4.2-A). UPIb was slightly expressed in primary bladder

cells compared to very low levels in 5637 and RT4 cells (Figure 4.2-A & B). Cell surface expression of the tetraspanin CD9 was used as a positive control in these experiments and gave MFI values above 2000 in RT4 and primary bladder cells, and nearly 1000 in T24 and 5637 cells, as discussed in chapter 3 (Figure 3.2), with 90-100% of BECs expressing CD9 at cell surface. UPIb protein appears to be present on the cell surface at very low levels in most cell types with about 15 % positivity (Figure 4.2 & Figure 4.3), while UPIa shows no expression at the cell surface of RT4 cells and very low levels in others (Figure 4.2). Overall, the expression levels of the tetraspanin uroplakins on the cell membrane are very low compared to the CD9 positive control. However, in the study of gene expression described above, UPIb was relatively expressed in RT4, and primary bladder cells compared to other cell lines. This suggested that uroplakin proteins could potentially be retained inside the cells and therefore a permeabilization assay was needed to investigate the localisation of these proteins.

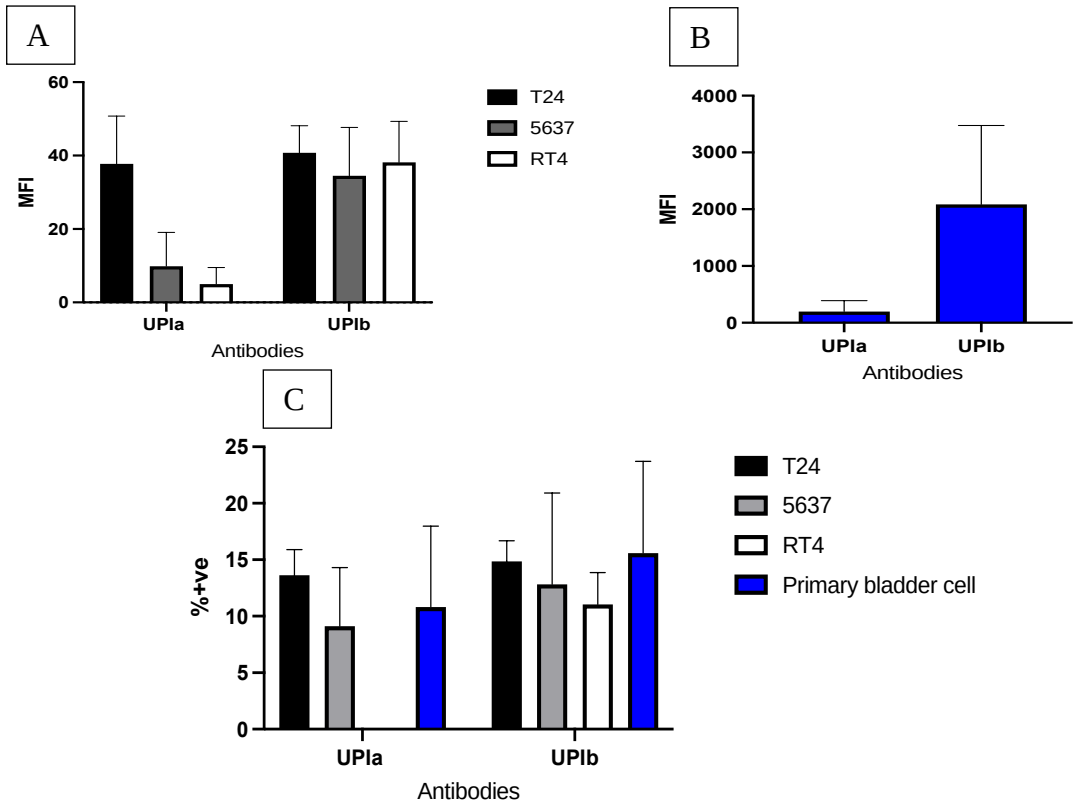

Figure 4.2: Cell surface expression of uroplakins on four different types of human bladder epithelial cells determined by flow cytometry.

The levels of UPIa and UPIb expression were measured as the MFI (median fluorescence intensity) of staining with the antibodies after subtracting the MFI of the appropriate isotype control. The primary polyclonal antibodies anti-UPIa and anti-UPIb were used with rabbit polyclonal antibody as an isotype control. The secondary antibody was an Alexa fluor 488-conjugated anti-rabbit IgG. (A) The expression level of tetraspanin uroplakins in BECs while (B) in primary bladder cells. (C) The percentage of positive cells in all four cell types. The data represent the means, while error bars describe standard error means. n=3 independent experiments, performed in duplicates.

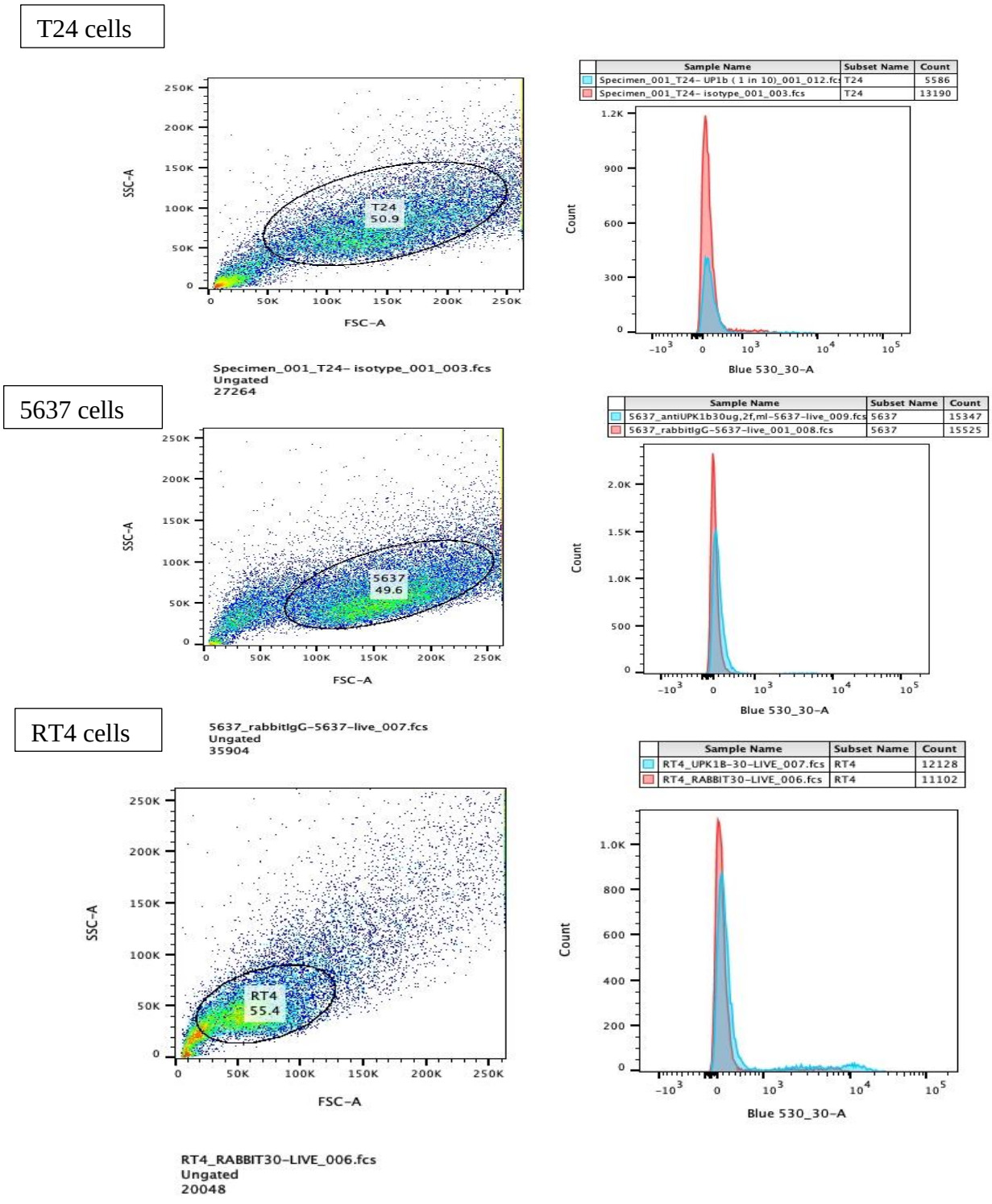

Figure 4.3: Flow cytometric data of cell surface expression of UPIb in bladder epithelial cells.

The dot plot (left side) showing the gated population of bladder cells according to forward scatter (FSC) and side scatter (SSC). The histogram plots (right side) show the fluorescence intensity overlap of isotype (red) and anti-uroplakins (blue) stained cells.

4.2.3 Non tetraspanin uroplakin (UPIII) surface expression in urothelial cells

UPIII is one of the four major uroplakins that has only one TMD. The presence of UPIII on the surface of urothelial cell lines has not to our knowledge been investigated. This study used only the mature RT4 cell line and primary bladder cells. As shown in Figure 4.4, the median fluorescence intensity of UPIII in both cell lines is still low, less than 30, compared to the CD9 positive control (Figure 3.2). The determination of the positive cell population, based on comparison with the isotype control, gives less than 2% positive cells (Figure 4.4-B). More detail, the profile scatter of primary bladder cells showing the expression of UPs at cell surface, is shown in Figure 4.5, indicating slight expression of only UPIb at the cell surface. Although these cells are described as well-differentiated, UPIII was not detected upon the cell surface. As for the other uroplakins, it was considered worth investigating whether UPIII is intracellular in these types of cells.

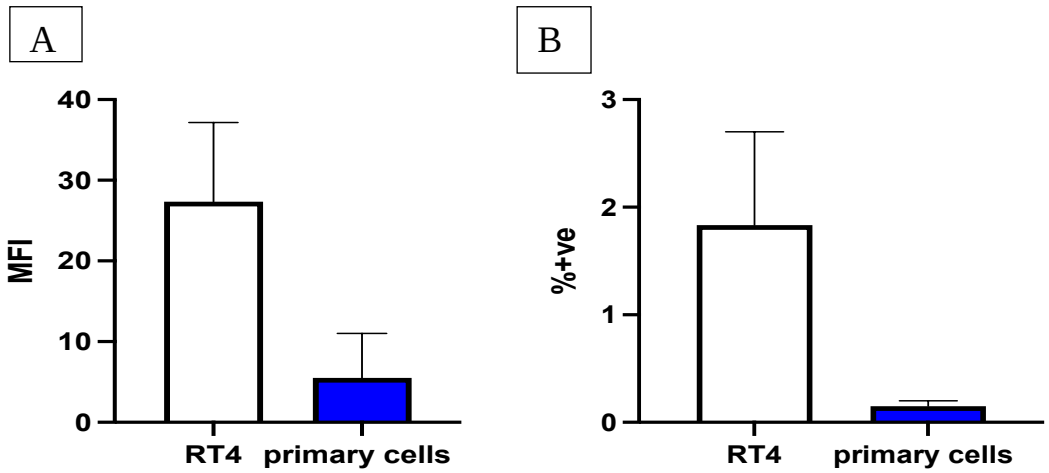

Figure 4.4: Cell surface expression of UPIII on human bladder cells by flow cytometry.

The levels of UPIII expression were measured as the MFI of staining with the antibodies after subtracting the MFI of the appropriate isotype control. The primary antibody was rabbit monoclonal anti-UPIII (described by the manufacturers as suitable for flow cytometry) at 1/130 dilution compared to rabbit monoclonal IgG isotype control. The secondary antibody was an Alexa fluor 488- conjugated anti-rabbit IgG. (A) The expression level of UPIII in RT4 and primary bladder cells. (B) The percentage of positive cells in cells. The data represent the means, while error bars describe standard error means. n=3 independent experiments, performed in duplicates.

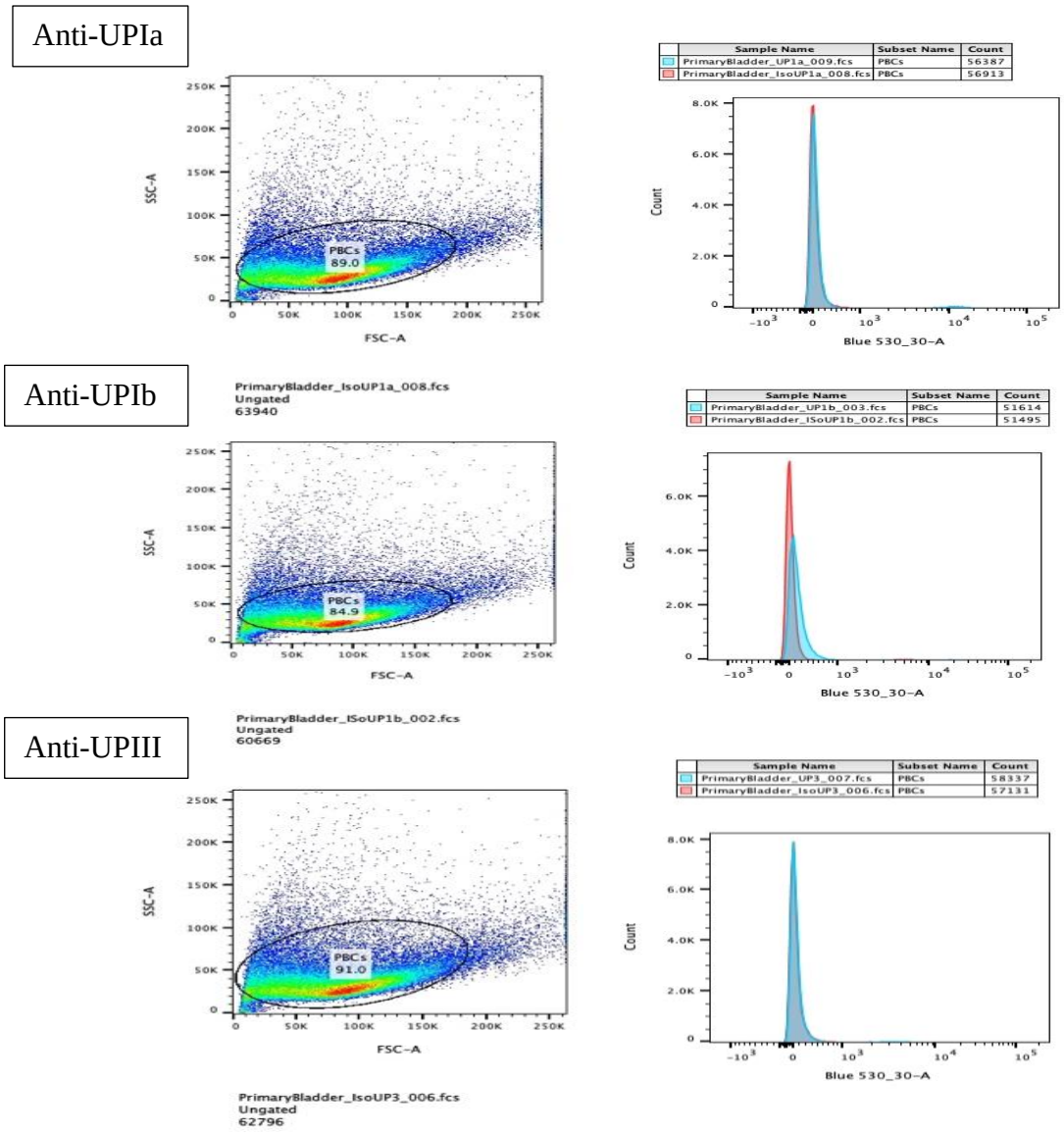

Figure 4.5: Flow cytometric data of primary bladder cells.

The dot plot (left side) shows primary cells gated according to forward scatter (FSC) and side scatter (SSC). The histogram plots (right side) show the fluorescence intensity overlap of isotype (red) and anti-uroplakins (blue) stained cells.

4.2.4 Intracellular staining assay

Permeabilising the cell with certain agents allows the antibody to enter the cells and bind to intracellular antigen. The uroplakins studied in this section were UPIa, UPIb and UPIII from the cell lines only.

4.2.4.1 Existence of UPIa in bladder epithelial cells

Cells were permeabilised and labelled with anti-UPIa as stated in section 2.2.6.2, followed by an Alexa Fluor-488 labelled anti-rabbit secondary antibody. Rabbit polyclonal IgG was used as an isotype control.

All bladder cell lines have a good expression level of UPIa inside the cells. Due to the high backgrounds observed with the isotype control in these experiments, the difference in fluorescence intensity between the test antibody and control was analysed using a t-test to show if the differences were statistically significant. The median fluorescence intensity values (about 400-700) were high compared to the values for cell surface expression (less than 40) (Figure 4.2 & Figure 4.6). Looking at the percentage of positive cells relative to the isotype control, between 35-70% of the cells are expressing UPIa (Figure 4.6-B). Unexpectedly, T24, which showed low UPIa gene expression, has 70% positive cells. In contrast, UPIa gene was detected in 5637 but less number of positive cells (about 40%) were observed. RT4 showed a high expression of UPIa protein, and this is correlated gene expression data (

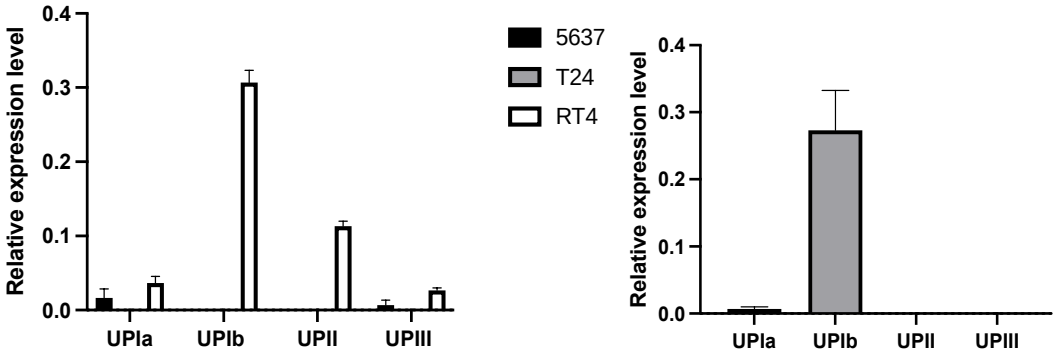

Figure 4.1).

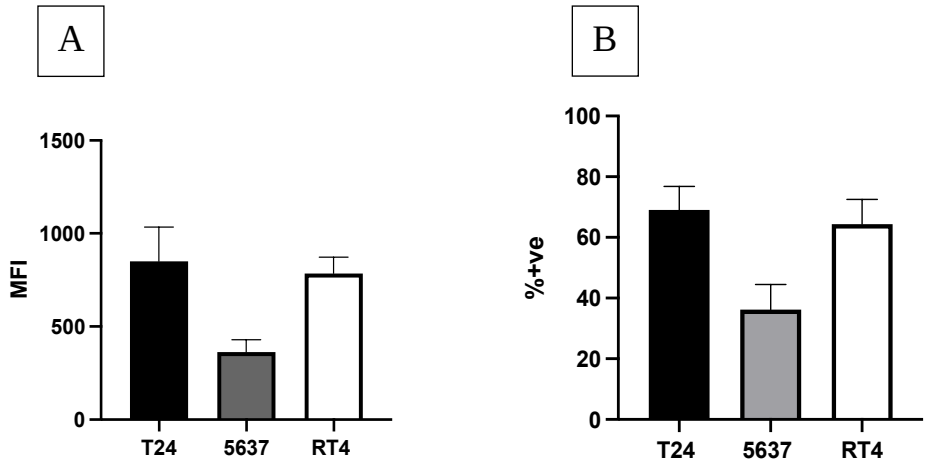

Figure 4.6: Intracellular expression level of UPIa in BECs.

The levels of UPIa expression were measured as the MFI (median fluorescence intensity) of staining with the antibodies after subtracting the MFI of the isotype control. The primary polyclonal antibodies anti-UPIa was used with rabbit polyclonal antibody as an isotype control. The secondary antibody was an Alexa fluor 488-conjugated anti-rabbit IgG. (A) The expression level of UPIa in permeabilised BECs. (B) The percentage of positive cells. The data represent the means, while error bars describe standard error means. n=3 independent experiments, performed in duplicates.

4.2.4.2 The presence of tetraspanin UPIb in bladder epithelial cells

The expression of UPIb in permeabilised cells relative to the isotype control was assessed as described in the previous section. A positive control cell line was included in this study as suggested in the datasheet provided by the manufacturer (Abcam), to check that the antibody was working. K562 cells (chronic myelogenous leukemia) are known to express UPIb, so these cells were used in comparison with the bladder cells (Baglo et al., 2014). As seen in (Figure 4.7-A), the expression level of UPIb was high in K562, with about 100% of the cells expressing this protein (Figure 4.7-B.). Notably, we did not detect any UPIb on the surface of K562 cells (data not shown), indicating that this protein is only found in the cytoplasm.

Also here, the difference in MFI between the antibody and isotype control was studied using t-test analysis due to high backgrounds. As shown in (Figure 4.7), UPIb expression in T24 and 5637 was lower compared to the K562 control cells, with only 15 to 20% of cells positive (Figure 4.7 & Figure 4.8); also the MFI was low (Figure 4.7) and not statistically different from the isotype control. This suggests that UPIb is not present in T24 and 5637. The percentage of positive RT4 cells is about 60% for permeabilised cells (Figure 4.7 & Figure 4.8), suggesting that UPIb is present inside RT4 in good abundance. This result correlated with the study of gene expression described above, where UPIb was relatively well expressed in RT4 cells compared to other cell lines (

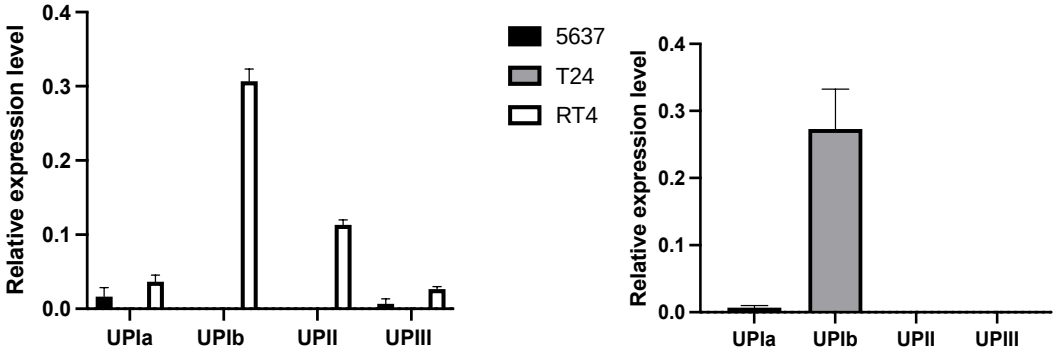

Figure 4.1).

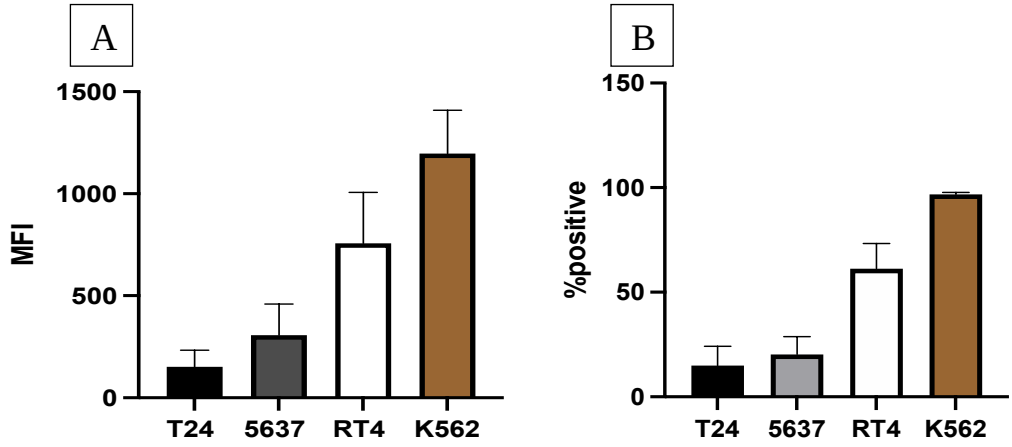

Figure 4.7: Intracellular expression level of UPIb in BECs and K562 leukaemia cells.

The levels of UPIb expression were measured as the MFI (median fluorescence intensity) of the test antibodies after subtracting the MFI of the isotype controls. The primary polyclonal antibodies anti-UPIb was used with rabbit polyclonal antibody as an isotype control. The secondary antibody was an Alexa fluor 488-conjugated anti-rabbit IgG. (A) The expression level of UPIb in permeabilised BECs and K562. (B) The percentage of positive cells. The data represent the means, while error bars describe standard error means. n=3 independent experiments, performed in duplicates.

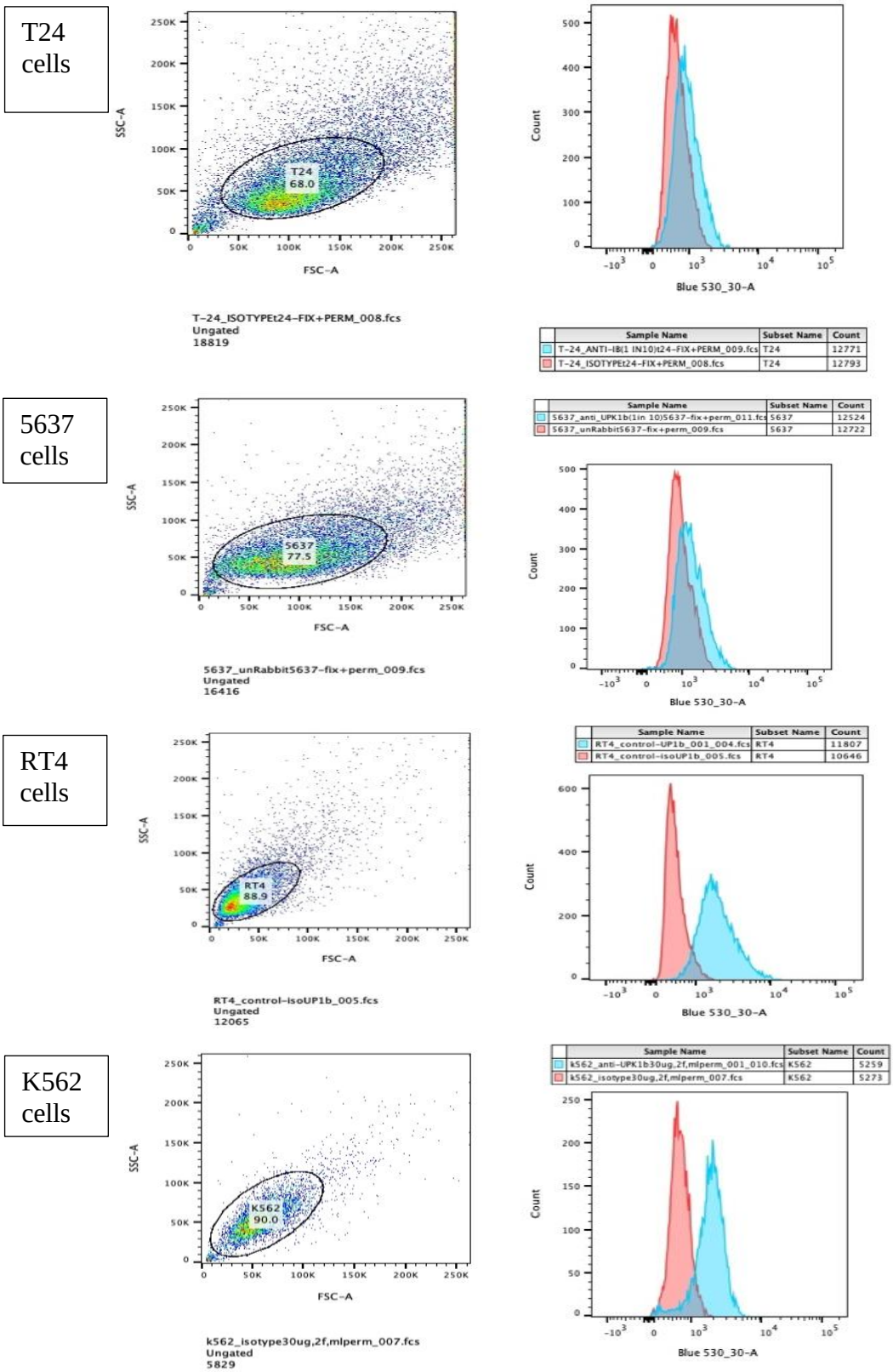

Figure 4.8: Flow cytometry data of the expression of UPIb in permeabilised bladder cells.

The dot plot (left side) shows primary cells gated according to forward scatter (FSC) and side scatter (SSC). The histogram plots (right side) show the fluorescence intensity overlap of isotype (red) and anti-uroplakins (blue) stained cells.

4.2.4.3 Non tetraspanin UPIII localisation in 5637 and RT4 cells

In this study only relatively well differentiated cells (5637 and RT4) were used because these cells showed some relative level of UPIII gene expression (

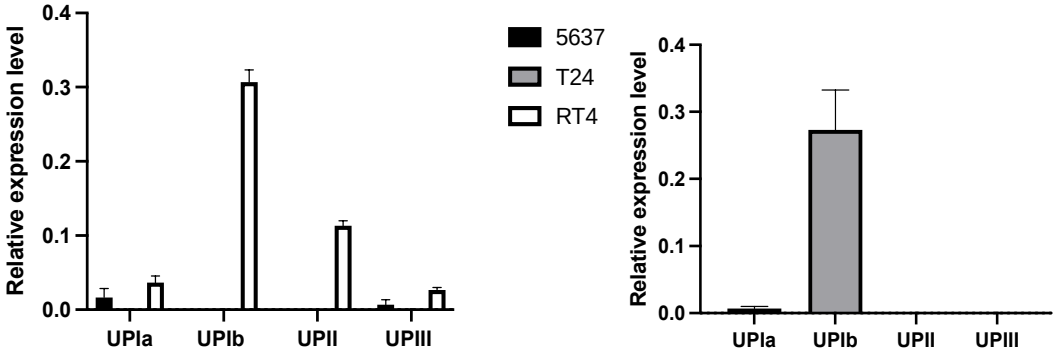

Figure 4.1). Based on the flow cytometry data, we could conclude that UPIII was well expressed inside these cells (Figure 4.9). In both cell lines, about 80% of the cells express UPIII intracellularly (Figure 4.9-B).

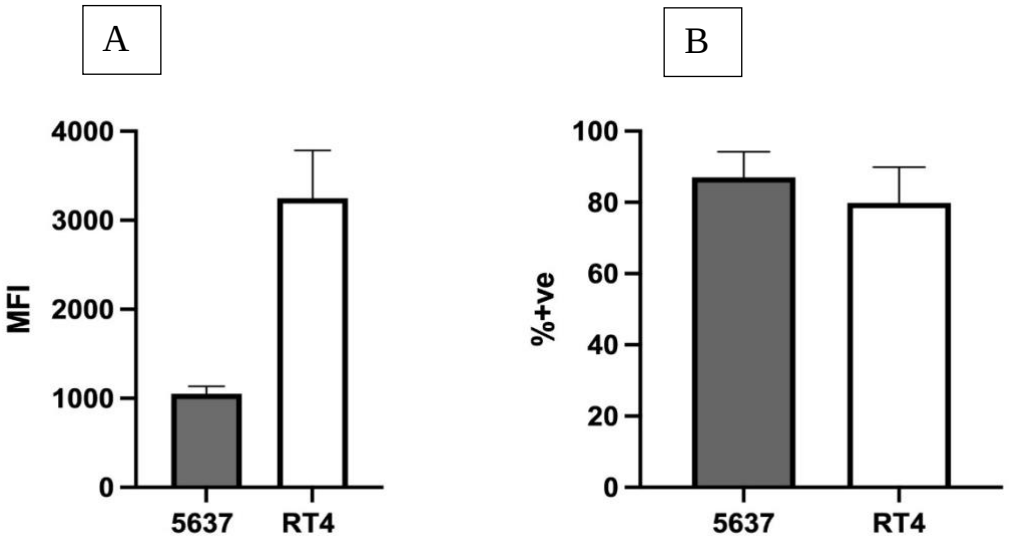

Figure 4.9: Intracellular expression level of UPIII in BECs.

The levels of UPIII expression were measured as the MFI of the test antibodies after subtracting the MFI of the isotype control. The primary rabbit monoclonal anti-UPIII at 1/130 dilution compared to rabbit monoclonal IgG isotype control. The secondary antibody was an Alexa fluor 488- conjugated anti-rabbit IgG. (A) The expression level of UPIII in permeabilised RT4 and 5637 cells. (B) The percentage of positive cells in cells. The data represent the means, while error bars describe standard error means. n=3 independent experiments, performed in duplicates.

4.2.5 Localization of uroplakins in the bladder urothelial cells by immunofluorescence microscopy

Indirect immunofluorescence microscopy was used to visualise the uroplakin proteins. Staining of the cells seeded on chamber slides was carried as described in 2.2.7.1. Visualisation of uroplakin expression was studied in comparison with the positive control staining of CD9 shown in chapter 3.

Representative images of uroplakin staining in T24 cells is displayed in Figure 4.10. Although there are similar amounts of green fluorescence between the cells labelled with uroplakin antibodies and their isotype control, there is relative higher intensity of UPIa in or over the nucleus of the cells compared to the negative control (Figure 4.10-A & B), indicating a low-level expression of UPIa inside T24 cells. The similar pattern of staining for both anti-UPIb alongside and the isotype control indicates little expression of UPIb in these cells (Figure 4.10-C & D), consistent with the flow cytometry data described above. In addition, background staining appeared in each image particularly at concentration of 30 µg/ml of rabbit polyclonal antibodies, thus due to non-specific binding of IgG antibodies.

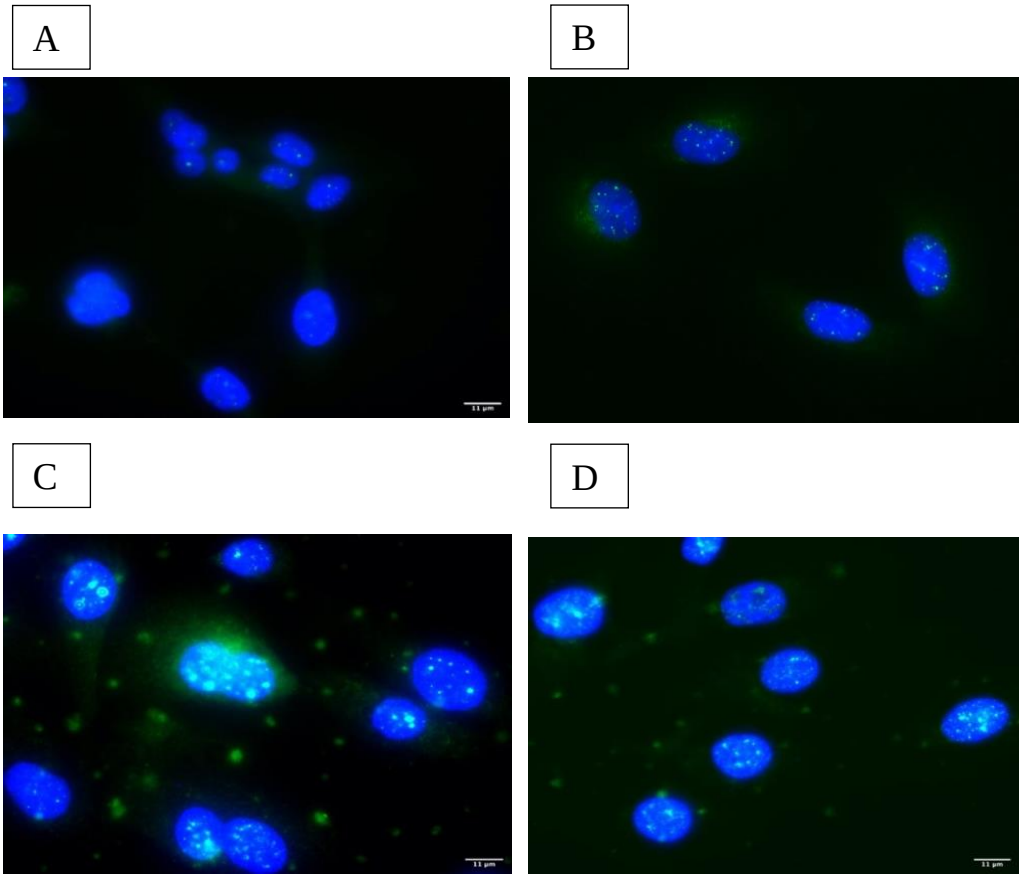

Figure 4.10: Microscopic visualisation of UPs expression in T24 cells.

Cells were cultured on chamber slides and then fixed and permeabilised before incubating with primary polyclonal antibody (anti-UPIa and anti-UPIb) and rabbit isotype control for 30 minutes. Alexa fluor 488- conjugated secondary antibody was used to visualise the expression by fluorescence microscopy. (A) Isotype control for UPIa, (B) anti-UPIa, (C) Isotype control for UPIb, (D) anti- UPIb. Nuclei were stained with DAPI. These images were obtained using the 100X objective. The scale bar corresponds to 11 µm.

The presence of UPs in 5637 cells was observed and the staining was consistent with data obtained by flow cytometry (Figure 4.11). There is relatively higher fluorescence of UPIa with granular staining compared with the isotype control (Figure 4.11-A & B). UPIb staining appears in or over the nucleus at a higher level compared with isotype control (Figure 4.11-C & D).

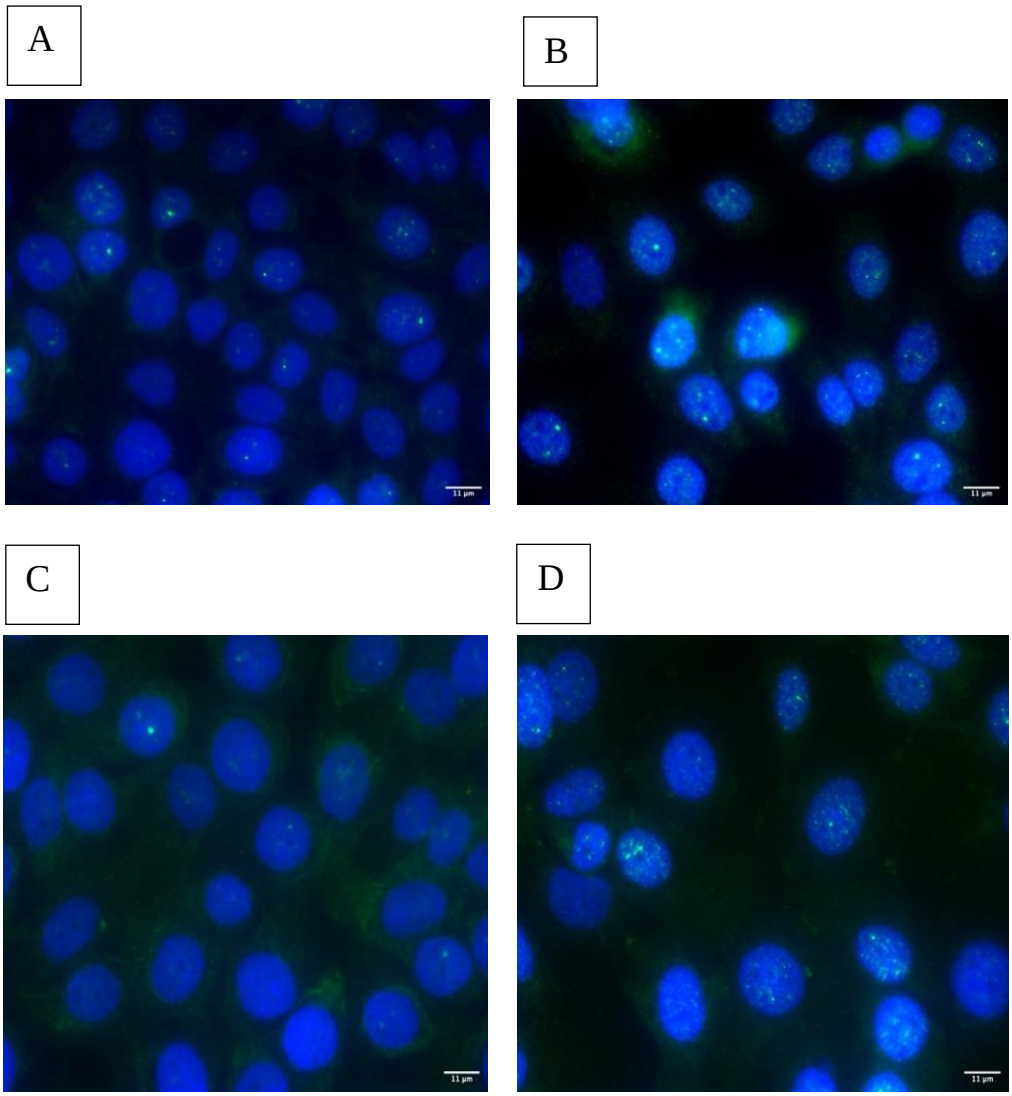

Figure 4.11: Microscopic visualisation of UPs expression in 5637 cells.

Cells were cultured on chamber slides and then fixed and permeabilised before incubated with primary polyclonal antibody (anti-UPIa and anti-UPIb) and rabbit isotype control for 30 minutes. Alexa fluor 488- conjugated secondary antibody was used to visualise the expression by fluorescence microscopy. (A) Isotype control for UPIa, (B) anti-UPIa, (C) Isotype control for UPIb, (D) anti- UPIb. Nuclei were stained with DAPI. These images were obtained using the 100X objective. The scale bar corresponds to 11 µm.

The relative amount of green fluorescence displayed inside the cells reflects the level of UP expression in urinary bladder papilloma cell line RT4 cells. As shown in (Figure 4.12), the level of fluorescence displayed in Figure 4.12-A & B, demonstrated little expression of UPIa in RT4 cells compared with the isotype control. However, the images in Figure 4.12-C & D showed relatively strong intracellular staining for UPIb compared to the isotype control. As shown in (Figure 4.12-E & F) UPIII protein was located at low levels in or over the nuclei, suggesting that RT4 retained the uroplakin inside the cells.

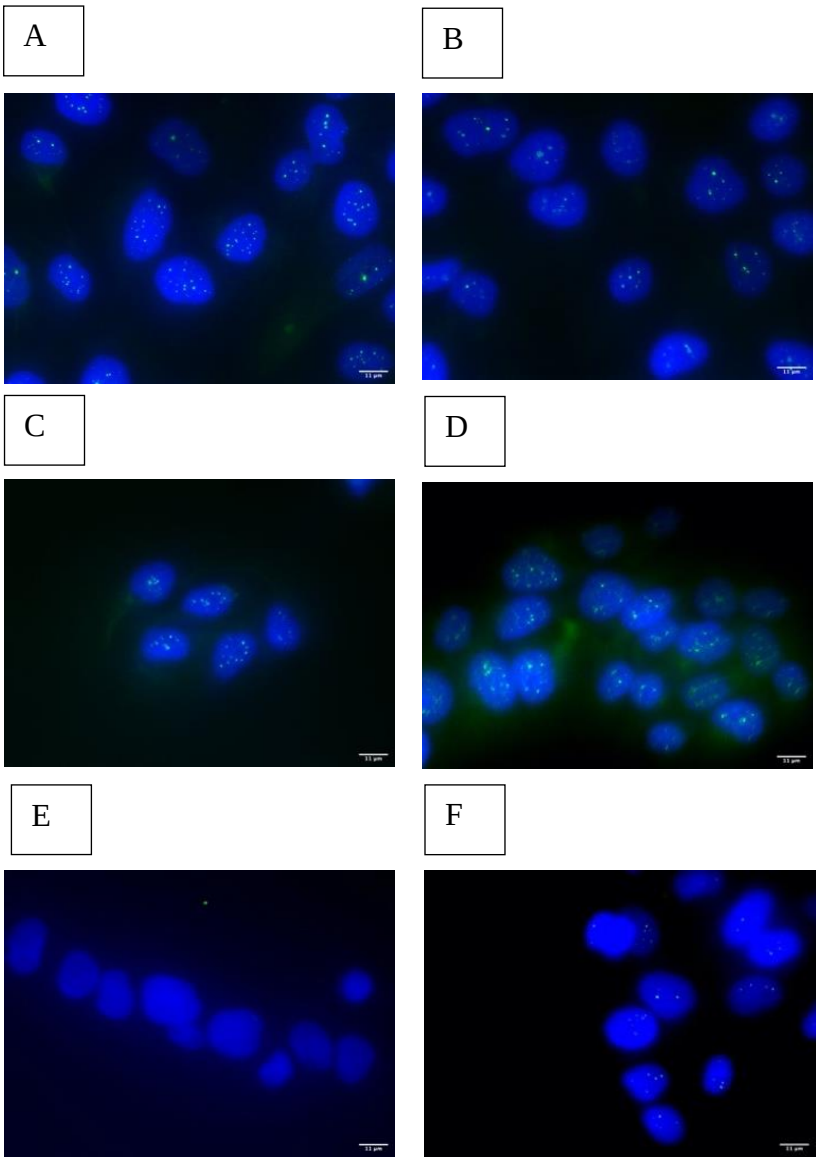

Figure 4.12: Microscopic visualisation of UPs expression in RT4 cells.

Cells were cultured on chamber slides and then fixed and permeabilised before incubated with primary polyclonal antibody (anti-UPIa and anti-UPIb) and rabbit isotype control for 30 minutes. Alexa fluor 488- conjugated secondary antibody was used to visualise the expression by fluorescence microscopy. (A) Isotype control for UPIa, (B) anti-UPIa, (C) Isotype control for UPIb, (D) anti- UPIb, (E) Isotype control for UPIII, (F) anti-UPIII. Nuclei were stained with DAPI. These images were obtained using the 100X objective. The scale bar corresponds to 11 µm.

4.2.6 Culturing urothelial cells in different conditions promotes uroplakin expression

Data obtained from permeabilised cells indicated that the uroplakins were retained inside the bladder cell lines. In an effort to promote cell surface expression, attempts were made to differentiate the cells, using previously published protocols.

4.2.6.1 Role of calcium dependent medium in urothelial differentiation

BECs were cultured in medium with low-serum and additional calcium (Thumbikat, Berry, Schaeffer, et al., 2009). As descried in chapter 2, E medium is a 3:1 mix of Dulbecco's modified Eagle medium and Ham's F-12 medium containing 5% FBS and elevated calcium. 5637 and RT4 cells were cultured in complete growth medium as a control condition. These cells were maintained under the two conditions for up to 8 days. The major uroplakins UPIa, UPIb, UPII and UPIII were selected as differentiation markers. After 2, 4, and 8 days, transcripts of these genes were analysed by RT-PCR. Once the best conditions had been determined based on the relative gene expression in test compared to control conditions, the protein level was measured by flow cytometry or alternatively confocal microscope. Although the urinary bladder papilloma cell line RT4 is referred to as terminally differentiated in different studies (Fujiyama *et al.*, 2001), it was also tested here.

From quantitative RT-PCR analysis, we found that on culturing RT4 cells in E medium, most UPs genes appeared to be induced and relatively high expression was observed compared to control conditions after 4 days, with that of UPIa statistically significant (Figure 4.13). In contrast, the UPIb gene was significantly upregulated after 2 days in E medium (Figure 4.13). Hence, investigating the expression of UPIa under this condition was initially a priority to determine the localization of this molecules. After 4 days UPIa, UPIb and UPIII were examined by flow cytometry in non-permeabilized RT4. We observed slightly higher expression of UPIa and UPIII at the cell surface

compared to the control condition, but it was not a significant difference (Figure 4.14). UPIb showed less expression on E medium after 4 days and this is correlated with the gene expression result regardless of the low percentage of positive cells in both conditions (Figure 4.14). Assays with permeabilized RT4 cells showed relatively similar patterns of expression of UPIb and UPIII under both conditions (Figure 4.15). UPIa is slightly more expressed in E medium with about 70 % of the cells positive (Figure 4.15-B). However, E medium did not seem to promote the differentiation of RT4 cells in terms of cell surface protein expression.

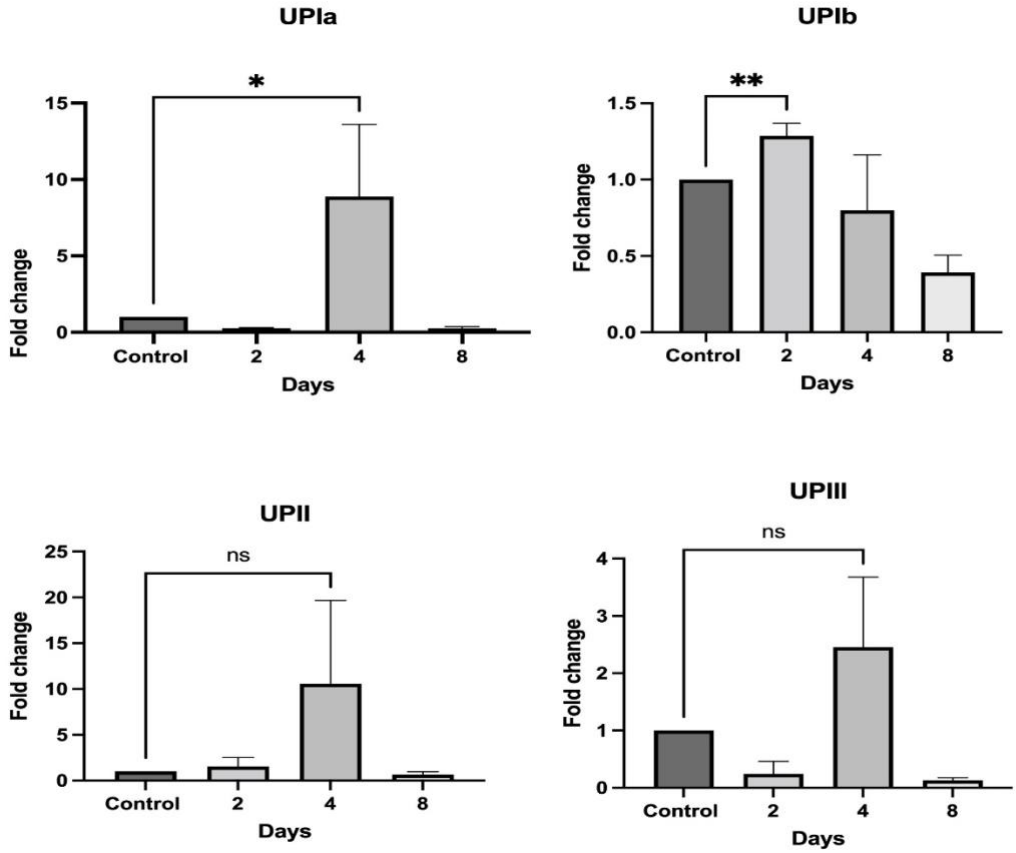

Figure 4.13: Expression of the four major uroplakin genes in RT4 cells cultured in E medium over time.

RT4 were cultured in E medium for 2,4 or 8 days and then assessed for UPIa, UPIb, UPII and UPIII mRNA expression by quantitative RT-PCR. Expression of these markers in control and E medium was calculated using delta Ct value method, values reflect fold change relative to cells maintained in completed growth medium withing days. The data represent the means, while error bars describe standard error means. $n \geq 3$ independent experiments, performed in triplicates. Data were analysed by unpaired *t*-test, where ** = $p \leq 0.01$, * = $p \leq 0.05$.

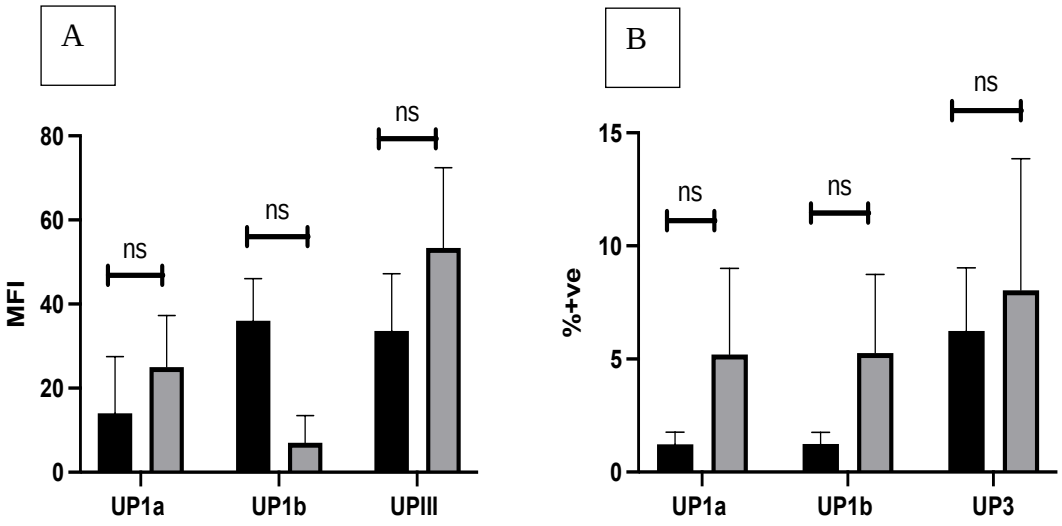

Figure 4.14: Comparison of cell surface expression of uroplakins in complete growth medium and E medium in RT4 cells.

The expression level of UPs and the suitable isotype control under two conditions at day 4 are shown as MFI obtained with the antibodies after subtracting the appropriate isotype control. (A) The expression level of UPs in RT4. (B) The percentage of positive cells. Black bars reflect control (cells in completed growth medium), whereas grey bars are treated cells (cells in E medium). The data represent the means, while error bars describe standard error means. n=3 independent experiments, performed in replicate. Data were analysed by *t*-test, where ns is non- significant.

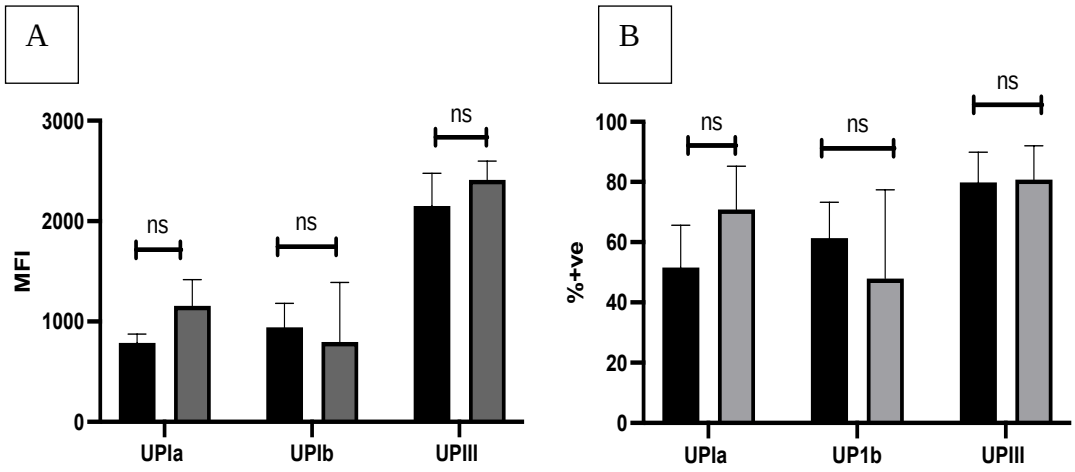

Figure 4.15: Comparison of expression level of uroplakins in permeabilized RT4 maintained in complete growth medium and E medium.

The expression level of UPs and the suitable isotype control under two conditions at day 4 are shown as MFI obtained with the antibodies after subtracting the appropriate isotype control. (A) The expression level of UPs in permeabilized RT4. (B) The percentage of positive cells. Black bars reflect control (cells in completed growth medium), whereas grey bars are treated cells (cells in E medium). The data represent the means, while error bars describe standard error means. n=3 independent experiments, performed in replicates. Data were analysed by *t*-test, where ns is non- significant.

A similar approach was used with the cell line 5637, which is referred to as moderately differentiated (Yoshida et al., 2015), and showed expression of UPIa intracellularly under normal conditions (Figure 4.6). In this study, we found that 5637 exhibited higher UPII mRNA expression after culturing in E medium for 4 days (Figure 4.16). Although there was higher level of UPIa, UPIb and UPIII mRNA expression compared to the control after 2 days, these differences were not statically significant (Figure 4.16). However, due to the lack of correlation we noticed between gene expression and protein level in some cases, we also studied the expression of UPIa protein at the cell surface first and then inside the cells after 2 days. We did not find any difference in expression at the cell surface (Figure 4.17), whilst in permeabilized cells, UPIa was increased in E medium (Figure 4.18). The percentage of positive cells was about 55% in E medium in comparison with only 18% positive cells in control conditions (Figure 4.18-B). Looking at the median fluorescence intensity, cells maintained in E medium were 4 times higher than in control conditions (Figure 4.18-A). This data suggest that E medium could induce the expression of UPIa intracellularly.

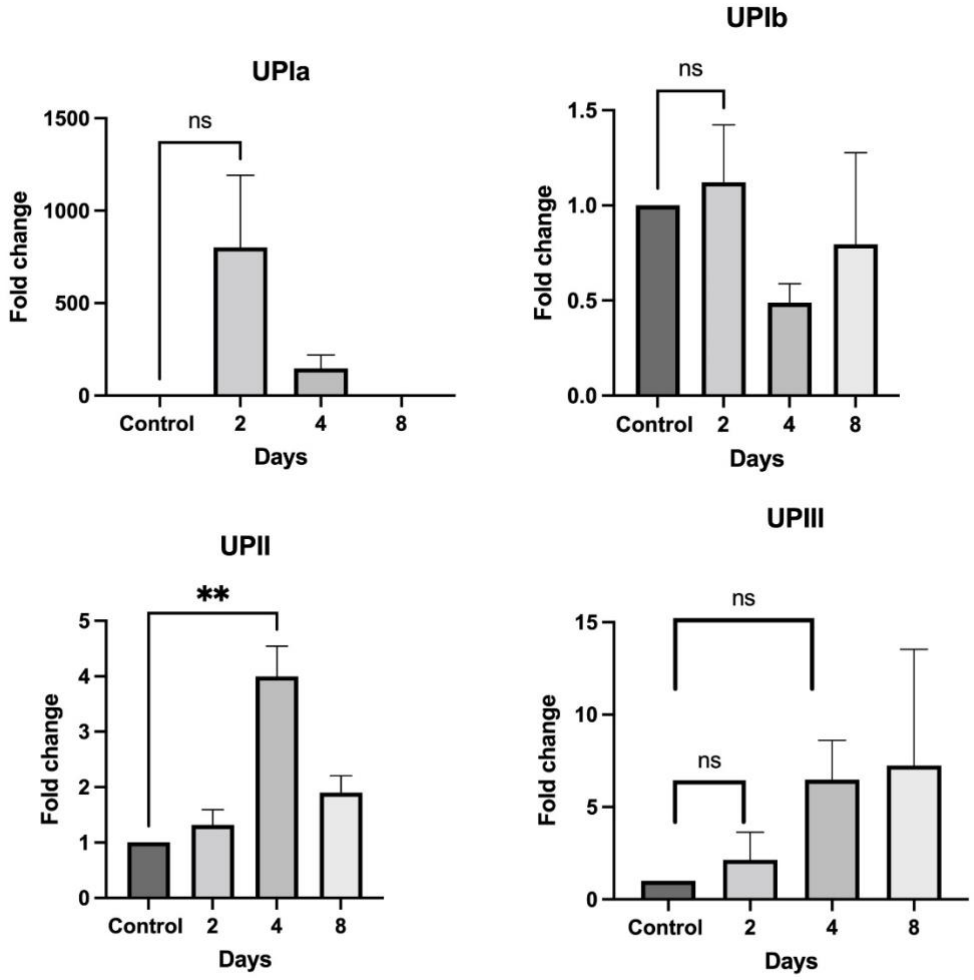

Figure 4.16: Expression of the four major uroplakin genes in 5637 cells cultured in E medium over time.

5637 were cultured in E medium for 2,4 or 8 days and then assessed for UPIa, UPIb, UPII and UPIII mRNA expression by quantitative RT-PCR. Expression of these markers in control and E medium was calculated using delta Ct value method, values reflect fold change relative to cells maintained in completed growth medium within days. The data represent the means, while error bars describe standard error means. n=3 independent experiments, performed in triplicates. Data were analysed by unpaired t-test, where ** = $p \leq 0.01$, * = $p \leq 0.05$.

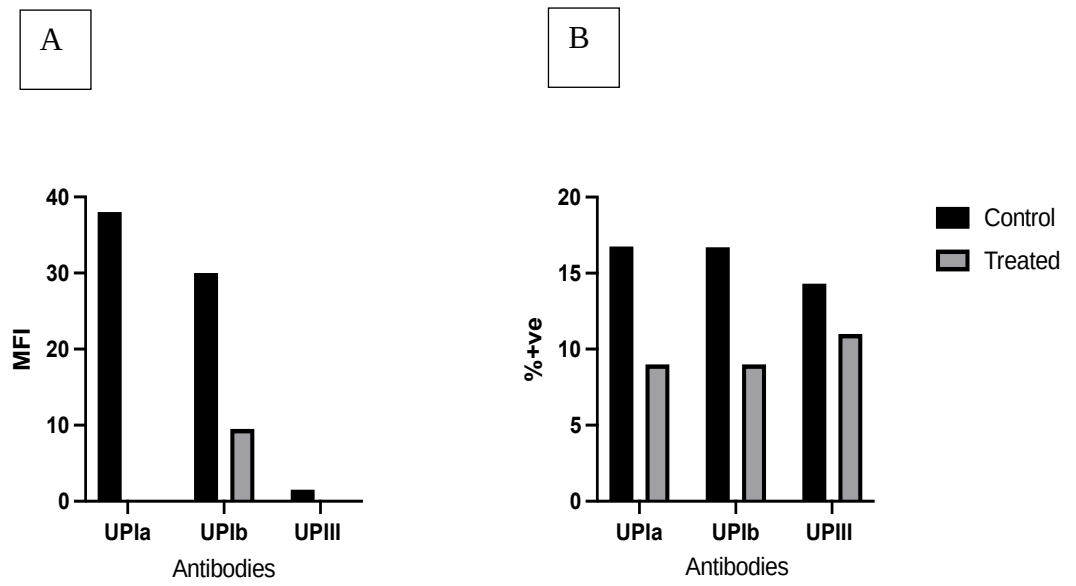

Figure 4.17: Comparison of cell surface expression of uroplakins in complete growth medium and E medium in 5637 cells.

The expression level of UPs and the suitable isotype control under two conditions at day 2 are shown as MFI obtained with the antibodies after subtracting the appropriate isotype control. (A) The expression level of UPs in 5637. (B) The percentage of positive cells. Black bars reflect control (cells in completed growth medium), whereas grey bars are treated cells (cells in E medium). The data represent the means of three technical repeats, this experiment was done once.

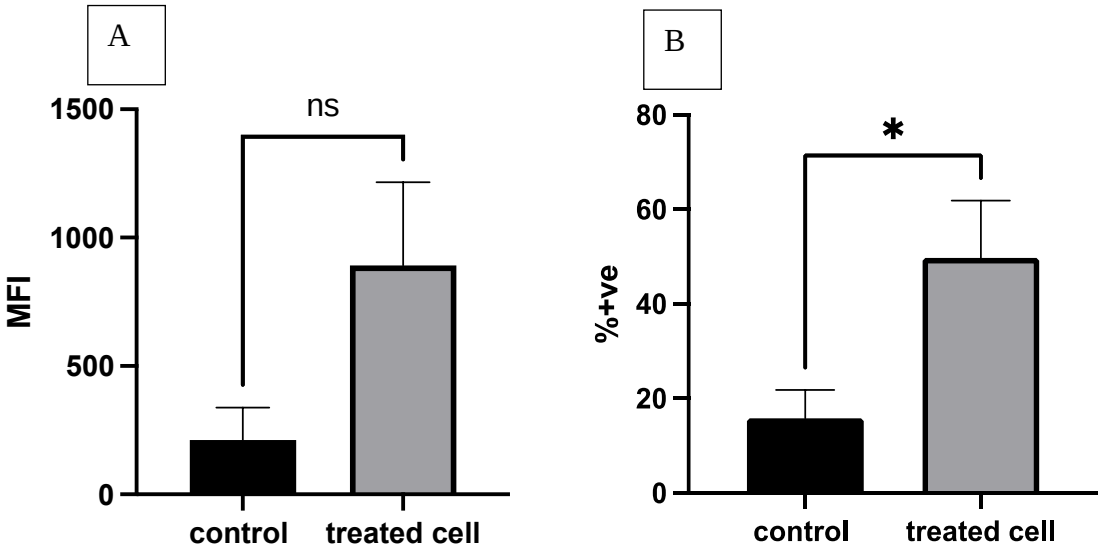

Figure 4.18: Comparison of expression level of UPIa in permeabilized 5637 maintained in complete growth medium and E medium.

The expression level of UPs and the suitable isotype control under two conditions at day 2 are shown as MFI obtained with the antibodies after subtracting the appropriate isotype control. (A) The expression level of UPs in permeabilized 5637. (B) The percentage of positive cells. Black bars reflect control (cells in completed growth medium), whereas grey bars are treated cells (cells in E medium). The data represent the means, while error bars describe standard error means. n=5 in duplicate. n=5 independent experiments performed in duplicate. Data were analysed by *t*-test, where ns is non- significant, * significant at $P<0.05$.

4.2.6.2 The impact of serum-free culture in urothelial differentiation

Differentiation of urothelial cancer cells was also attempted in a medium that lacks foetal bovine serum by studying the expression of UPs (Sun, 2006). RT4 and 5637 cells, or cells in complete medium as a control, were maintained under the two conditions for up to 8 days. After 2, 4, and 8 days, mRNA was extracted for gene expression measurement using RT-PCR as described previously.

In RT4 cells, UPIa and UPIb appear to be induced after 4 days of maintaining the cells in serum-free medium, with UPIa mRNA highly significantly upregulated (Figure 4.19). RT4 cells maintained in the medium with absence of serum for 4 days were then used to study protein expression. Notably, about 90% of the cells appeared dead after trypsinization to harvest the cells and this was confirmed by staining the cells with propidium iodide using flow cytometry. Confocal microscopy was consequently used as an alternative method for assessing protein expression (section 2.2.7.2). Images from confocal microscopy show that there is stronger UPIa in serum free conditions than in complete growth condition (Figure 4.20-A). This was confirmed by measuring total cell fluorescence (Equation 2.4 in section 2.2.7.2) (Figure 4.20-B). In conclusion, as shown in (Figure 4.20), UPIa after induction was apparently located inside the cells not at the cell surface.

In 5637 cells, each gene was significantly upregulated on certain days. For instance, UPIa was shown to be highly expressed after 8 days, while UPII after 2 days and UPIII after 4 days (Figure 4.21). Due to the time constraints, protein expression was not studied in these cells. It could be addressed for future work.

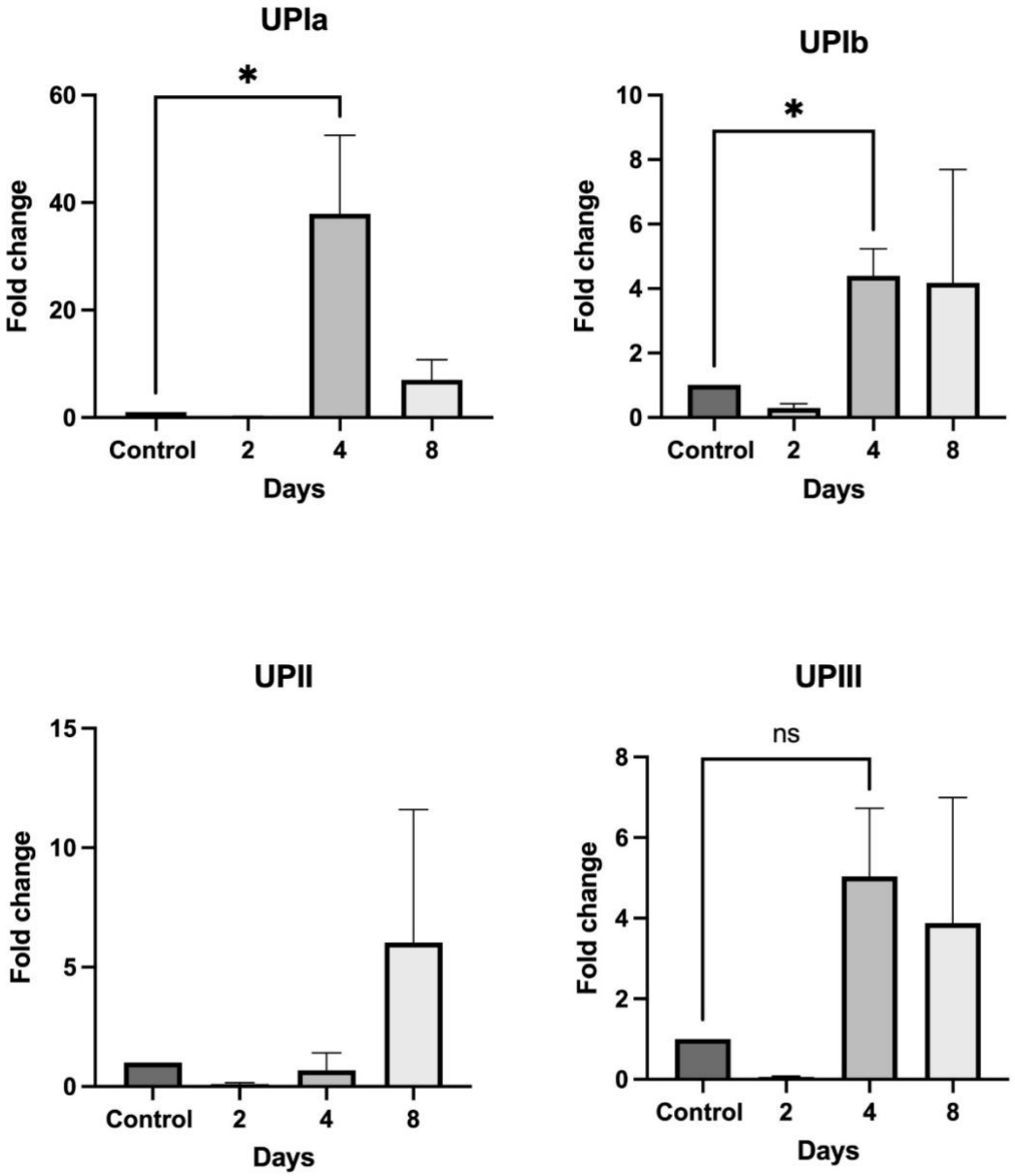

Figure 4.19: Expression of the four major uroplakin genes in RT4 cells cultured in serum free medium over time.

RT4 were cultured in medium without FCS for 2,4 or 8 days and then assessed for UPIa, UPIb, UPII and UPIII mRNA expression by quantitative RT PCR. Expression of these markers in control and E medium was calculated using delta Ct value method, values reflect fold change relative to cells maintained in completed growth medium withing days. The data represent the means, while error bars describe standard error means.. n=3 independent experiments, performed in triplicates. Data were analysed by unpaired *t*-test, where ns is non- significant, * = $p \leq 0.05$.

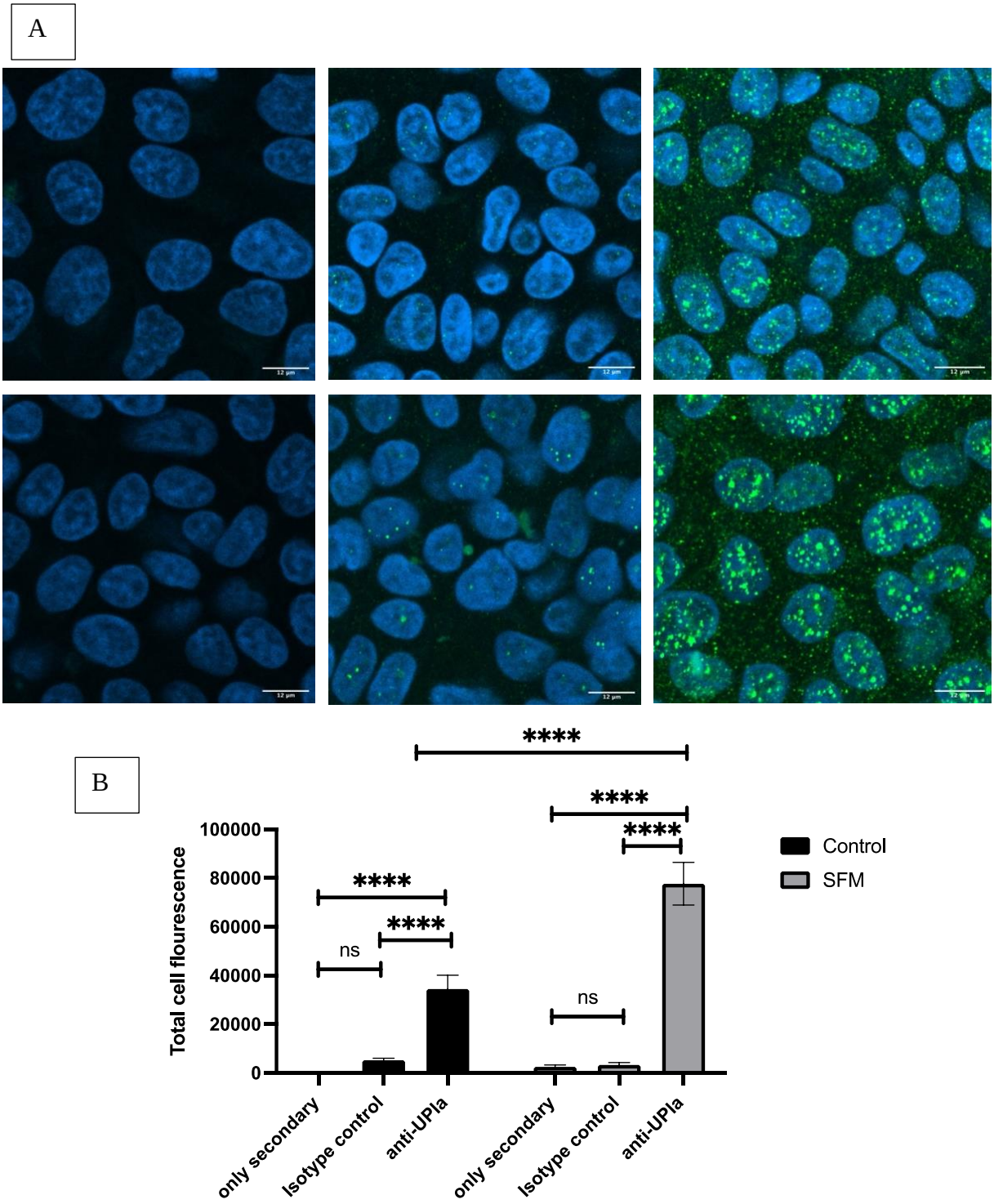

Figure 4.20: UPIa fluorescence in RT4 grown in serum free medium (SFM) after 4 days.

RT4 cells were seeded onto sterile coverslips and maintained in serum free medium for 4 days alongside cells in complete growth medium as a control (section 2.2.7.2). Primary polyclonal antibody anti-UPIa and rabbit isotype control were used with Alexafluor-488 conjugated secondary antibody to visualise uroplakin expression by confocal microscopy. The upper panel of images show control cells whilst the lower panel shows RT4 cells grown in SFM. Nuclei were stained with DAPI. These images were obtained using the 100X objective. The graph shows the total cell fluorescence calculated using ImageJ software. The data represent the means, while error bars describe standard error means. Each dot represents a cell from one slide. Data were analysed by one- way ANOVA, where ** = $p \leq 0.01$, * = $p \leq 0.05$.

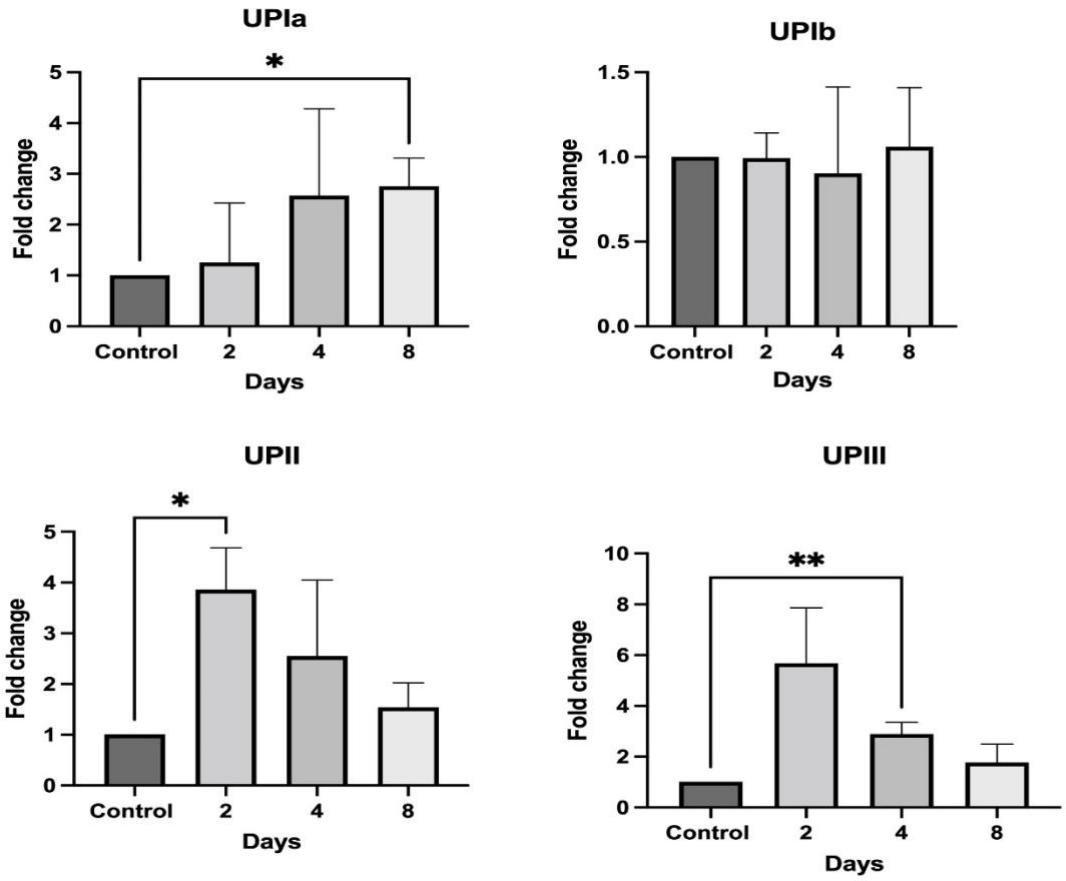

Figure 4.21: Expression of the four major uroplakin genes in 5637 cells cultured in serum free medium over time.

5637 were cultured in medium without FCS for 2,4 or 8 days and then assessed for UPIa, UPIb, UPII and UPIII mRNA expression by quantitative RT PCR. Expression of these markers in control and E medium was calculated using delta Ct value method, values reflect fold change relative to cells maintained in completed growth medium withing days. The data represent the means, while error bars describe standard error means. n =3 independent experiments, performed in triplicates. Data were analysed by unpaired *t*-test, where ** = $p \leq 0.01$, * = $p \leq 0.05$.

4.3 Discussion

Using qPCR, we observed the relative expression levels of uroplakin genes from three separate urothelial cancer cells and primary bladder cells (section 4.2.1). RT4, which is derived from a grade 1 TCC and described as a well differentiated cell line, expressed all four UPs genes at the mRNA level. Consistent with previous studies in RT4 cells, UPIb and UPII showed high mRNA expression levels, while UPIa and UPIII were expressed in lower abundance (Lobban et al., 1998; DeGraff et al., 2012). In contrast, there was a

lack of detectable expression of those genes in T24, derived from a poorly differentiated grade III bladder carcinoma. The moderately differentiated 5637 cell line showed relatively low expression of UPIa and UPIII genes. There was obvious expression of the UPIb gene in primary bladder cells, while lower expression of UPIa gene was evident. This result is consistent with a report by another group (Varley et al., 2004) in that primary urothelial cells weakly expressed UPIa mRNA in post-confluent culture, whereas expression of the UPIb gene was upregulated; in contrast UPII and UPIII gene expression were not detected. Several studies have shown that the expression of UPIb is not restricted to urothelial cells as it has been detected in human corneal epithelium as well as in respiratory epithelium (Adachi, Okubo and Kinoshita, 2000; Olsburgh et al., 2003). Also, A549 human lung carcinoma cells showed good expression of tetraspanin uroplakins UPIa and UPIb at the mRNA level (Mohsin, 2019, PhD thesis, University of Sheffield). In a previous study on the expression of UPIb in human corneas, UPIb was also shown to be present by Western blotting and in the membrane of corneal epithelial cells by immunofluorescence microscopy (Adachi, Okubo and Kinoshita, 2000).

The expression of these uroplakin proteins upon the cell surface of the bladder cells was not as we initially expected, however. Previous studies have used T24 and 5637 cells to study FimH antagonists. For example, a number of groups have previously used T24 cells (Meiland et al., 2004) and 5637 cells (Wellens et al., 2008; Scharenberg et al., 2011; Kurimura et al., 2012) to study the effects of FimH antagonists, presumed to interfere with FimH interaction with UP1a, on UPEC adhesion. Scharenberg and co-workers showed good expression of UPIa protein by Western blotting in 5637 cells, but did not study the localisation of UPIa in these cells (Scharenberg et al., 2011).

By staining non-permeabilized cells with anti-UP antibodies then quantifying the intensity of fluorescence by flow cytometry, we found that there was very little expression of UPIa and UPIb on the cell surface of T24, 5637, and RT4 cells (Figure 4.2 & Figure 4.3), while some cell surface expression of UPIb among other UPs on primary bladder cells was observed (Figure 4.2 & Figure 4.5). It should be noted that UPIb was presented in low abundance on the surface of

cells that are expected to have the most differentiated phenotype, RT4 and primary cells. The possible explanation might be the ability of UPIb to transport to the plasma membrane alone (Tu, Sun and Kreibich, 2002).

However, assays using permeabilised cells showed varied levels of intracellular UPIa, UPIb and UPIII protein expression between these cell lines. We observed that poorly differentiated T24 cells contained UPIa protein while UPIb was not expressed (Figure 4.6, Figure 4.7 and Figure 4.8). A similar pattern of expression was observed in 5637 cells, with good expression of UPIa, but no expression of UPIb inside the cells (Figure 4.6, Figure 4.7 and Figure 4.8). In more mature RT4 cells, all uroplakins are expressed intracellularly, but at different levels. The human chronic myelogenous leukaemia cell line K562 provided a good positive control for UPIb expression (Andersson, Nilsson and Gahmberg, 1979). In the present study, K562 showed high expression of UPIb with 100% positive cells; in comparison with these 5637 and RT4 had a significant expression of this intracellular protein, with approximately 60% positive cells (Figure 4.7).

The present study shows some correlation between the gene expression level and the corresponding protein level, with high mRNA expression of UPIb in RT4 cells and correspondingly relatively high levels of intracellular protein, but little on the cell membrane. Also, 5637 cells show expression of UPIa and UPIII genes then conversion into proteins that is retained within the cells. UPIb mRNA was apparently expressed in primary bladder cells and little protein was detected at the cell surface (Figure 4.5). By contrast, the correlation between the gene expression and protein level in T24 cells is not as good, since there appeared to be very low mRNA expression of UPIa but at least some UPIa protein was detected in permeabilized cells.

Immunofluorescence microscopy confirms the data seen by the flow cytometry and demonstrates that uroplakins are mostly associated with intracellular vesicular compartments. However, for T24 only UPIa appeared to be expressed with specific staining compared with the isotype control. For 5637 cells, looking particularly at the nuclear area, the quantity of fluorescence was high in the cells stained with the antibodies compared to the isotype control, suggesting

that 5637 might contain some uroplakins at intermediate levels. The urinary bladder papilloma cell line RT4 had obvious UPIb expression and relatively good expression of UPIII. The staining obtained with anti-UPIa and with rabbit polyclonal isotype control in RT4 cells was also studied by confocal microscopy which confirmed that the protein is present in/over the nucleus and in cytoplasmic vesicles. As the uroplakin proteins are not being transported to the cell surface, it is possible that this staining corresponds to proteins being retained in the ER.

Overall, these results indicate that the tumour differentiation stage of bladder cancer cells is related to UPs expression level. We observed that a well differentiated cell line, RT4, expresses UPIa, UPIb and UPIII while there was no expression of UPIb in the poorly differentiated cell line T24. Further studies have demonstrated the role of FOXA1 expression, one of the urothelial differentiation markers, in the expression of UPs in different tumour grades of bladder cancer cells. The results showed that reduction of FOXA1 expression in well differentiated grade 1 papillary tumour RT4 cells resulted in increased UPs expression and increased cell proliferation, while in poorly differentiated tumour grade 3 T24 cells the overexpression of FOXA1 affects the growth and invasion of the cells (DeGraff et al., 2012).

A major technical issue in this study was the high background staining observed with the rabbit polyclonal isotype control, which showed high fluorescence intensity in both flow cytometry and immunofluorescence microscopy. We gated the positive cells based on the isotype control values to try to account for nonspecific binding. Previous studies have used 10% goat serum before incubating the cells with rabbit polyclonal anti-UPII but it is difficult to judge how successful this is as they do not use isotype control (Gao et al., 2018). We attempted to pre-treat the cells with 10% rabbit serum in order to reduce the high backgrounds, but this had no effect.

The only study showing UPs expression at the cell surface of human urothelial cells (PD07i) using immunofluorescence microscope was by Thumbikat and his group (Thumbikat, Berry, Zhou, et al., 2009). Although 5637 were used in same study as a positive control for uroplakin expression, there was no mention of

the precise location of those proteins (Thumbikat, Berry, Zhou, et al., 2009). PD07i cells are immortalized human urothelial cells derived from primary bladder culture, and have not been as extensively used as the 5637 and T24 cell lines (Chen, Mudge and Klumpp, 2006).

In this study, we have demonstrated those cells that are widely used as an *in vitro* cell model for urinary tract infections, do not actually express UPIa on the cell surface, presumably because they are not assembled into AUM. Notably, Mulvey and his groups have extensively utilized 5637 cells for understanding the mechanisms of the uptake of pathogens and their immune response; however the UPs expression is unclear in these studies (Martinez, 2000; Mulvey, Schilling and Hultgren, 2001; Schilling et al., 2001; Dhakal and Mulvey, 2009). Indeed, work presented in the following chapters of this thesis provides additional evidence that UPEC can use an alternative receptor to UPIa during *in vitro* infection. Despite the limitations of using cell culture models of UTI including the absence of uroplakin quaternary structure, there are many notable advantages such as the abundance of the cells, ease of use and an affordable system. The cell culture model system can be used to test the validity of potential therapeutic drugs, but must take into account various limitations (Barber et al., 2016).

In the next part of this chapter, we invested some efforts to induce the differentiation of bladder epithelial cell lines and try to promote the expression of UP on the cell surface. We present data showing that urothelial cell lines in vitro could be influenced by different culture conditions to undergo changes consistent with differentiation. Several cytokeratins and uroplakin protein expression, particularly CK20 and UPII have been extensively used for evaluating urothelial differentiation state in other studies (DeGraff et al., 2012; Hoffmann et al., 2016; Gao et al., 2018; Yoshida et al., 2018). Here, expression of all four UPs were selected as major differentiation markers at the gene level. Expression of UPII at the protein level was not studied due to the difficulty of obtaining suitable antibodies. Two culture approaches were used: cells adapted to serum-free medium and medium containing 5% serum and 2mM final concentration of supplemented calcium. In general, although there were no

terminal differentiation features observed in these two approaches, both models were shown to promote uroplakin expression.

In E medium, expression of UPs was elevated slightly in long term culture of RT4 cells (96 hr). UPIa gene expression was more abundant in E medium conditions compared with control cultures, but there was only a slight increase of UPIa protein. Although gene expression of UPIII was upregulated after 4 days, the difference was not significant. Correspondingly, inconsistent expression of UPIII proteins was noticed at the cell surface (Figure 4.14). In 5637 cells there were non-significant increases in the expression of UPIa, UPIb and UPIII genes when cultured in E medium after a shorter time period (48 hr). The UPII gene was significantly upregulated after 4 days, but protein expression was not investigated.

Live cells were tested using flow cytometry to check the expression on the cell surface. We found only slight differences in UPs expression levels between those conditions. Looking at permeabilised cells, there was a significant level of UPIa expression in 5637 cells cultured in the E medium (Figure 4.18), suggesting that this medium could enhance differentiation state but to a limited extent. These observations are consistent with previous findings in a different human urothelial cell line (PD07i) maintained in E medium for 6 days, where the cells were shown to express more UPIa and UPIb proteins in comparison with their negative control (Thumbikat, Berry, Schaeffer, et al., 2009). Another previous study using a similar approach, medium with serum and elevated calcium for culturing normal human urothelial (NHU) cells, found that these conditions provided good stratified urothelial cells, but UP expression was not investigated (Cross et al., 2005). This lack of stable expression of uroplakin proteins at the apical surface could potentially be because they are not assembled together forming AUM. It has previously been shown by studying the expression of tight junction proteins that physiological calcium has profound effects upon stratification of human urothelial cells irrespective of differentiation (Rickard et al., 2008). The stratification phenotype is not necessarily related to differentiation stage (Southgate et al., 1994). In this study we have

demonstrated that the level of calcium in culture conditions could also affect urothelial differentiation.

The main idea of using serum-free medium is that the absence of some transcription factors such as EGF, PDGF and also retinoic acid, contributes to suppressing cell growth and subsequently stimulating differentiation (Sun, 2006). This was also observed in our study, as no increase in cell density occurred during the culture period. We observed that uroplakin gene expression was induced under this condition. This might be associated with the degree of activation of PPARγ, which is related to the absence of the EGFR signalling pathway (Varley et al., 2004). However, uroplakin gene expression particularly UPIa and UPIb was preferentially induced in RT4 cells within a similar period of time in E medium (96 hr). It was difficult to measure the protein expression under these conditions using flow cytometry due to the high percentage of dead cells after harvesting. Therefore, confocal microscopy was used as to determine the localization of UPIa. We observed that UPIa distribution appears as intensely stained vesicles in/over the nucleus and in the cytoplasm in serum-free conditions, with a significant increase in fluorescence intensity of UPIa staining in the serum-free system. Despite success in inducing increased expression of UPIa, it was difficult to stimulate the protein to be delivered into the cell surface. In 5637 cells, the uroplakin genes showed varied expression over time. As previously stated, UPIa was significantly upregulated after 8 days in serum-free medium while UPIII was upregulated after 4 days. We could not look at the protein level due to the time constraints. Ultimately, the protein could localised inside the cells. A previous study has shown that EGF promotes 5637 proliferation through modulation of the androgen receptor (AR) (Izumi et al., 2012). Therefore, it was predictable that serum-free culture (in the absence of some growth factors) could induce 5637 differentiations.

Some of these cell lines have previously been cultivated as organoid cultures. These organoids exhibited increased expression of differentiation hallmarks (E-cadherin, Cingulin, CK20 and UPIa) in comparison with monolayers cultures (Smith et al., 2006). Although 3D organoids technology is a powerful tool for urological study, it has a several limitations that need to be considered (Wang,

Gao and Chen, 2017). In addition, there has been little reported to date on the use of some advanced based- in vitro models such as 3D tissue architecture for studying UTI (Horsley et al., 2018; Murray et al., 2021).

Similar investigations showed undetectable UPs expression of PD07i cells cultured in serum-free condition using western blotting (Thumbikat, Berry, Schaeffer, et al., 2009). Other studies have used porcine bladder urothelium, which shares similar biological properties with human urothelium. It was shown that growing porcine urothelial cells in serum-free medium negatively affected the functional barrier properties, whereas greater resistance was apparent when the cells grown in serum/calcium supplemented cultures (Turner et al., 2008). However, additional research is needed to understand the kinetics of growth and differentiation of bladder cancer cells. In the agreement with previous studies, we have shown that the culture environment plays a role in the promoting UPs expression (Turner et al., 2008; Thumbikat, Berry, Schaeffer, et al., 2009; Cattan et al., 2011; Gao et al., 2018).

This study has demonstrated that BECs including primary cells which are referred as a normal epithelial cells (Kabaso et al., 2011) may be considered poorly differentiated cells, due to absence of cell surface uroplakins. It is possible, however, to promote uroplakin expression by using different culture conditions, hence enhancing the differentiation stage, but it is difficult to achieve delivery to the apical surface. This finding suggests that growing urothelial cells in 3D structures allowing integrated multilayers of cells are crucial for maturation. It would be valuable to generate a method that can improve the differentiation stage of urothelial cells in a similar way to the native urothelium, which be used as a novel model to study physiological and pathological purposes.

Chapter 5: The effect of tetraspanins on UPEC adhesion

5.1 Introduction

As described in Chapter 1 several bacterial pathogens cause UTIs, but uropathogenic *Escherichia coli* (UPEC) strains are broadly considered to be the primary causative agents (Flores-Mireles et al., 2015). As mentioned earlier, UPEC have several virulence properties and the most critical traits are the presence of filamentous adhesive molecules, type 1 fimbriae (Mulvey, 2002). However, type 1-fimbriated *E. coli* can recognize multiple receptors on the bladder umbrella cells, either members of the tetraspanin proteins, or alternative molecules associated with tetraspanins.

5.1.1 UPEC and direct association with tetraspanins

Tetraspanin have been linked directly with a few bacterial pathogens such as uropathogenic *E. coli* and *Listeria monocytogenes* (Xie, Zhou, S. Y. Chan, et al., 2006; Tham et al., 2010). The type 1-fimbriated *E. coli* can bind to mannose-containing glycoprotein receptors, including uroplakin 1a (UPIa) (Ulett et al., 2013). As stated earlier, UPIa and UPIb associate with UPII and UPIII respectively, forming 16nm crystalline array plaques known as urothelial plaques or asymmetric unit membrane (AUM) (Kachar, Liang, Lins, Ding, X. R. Wu, et al., 1999). In 1996, Wu and colleagues used a gel overlay assay to show that bands corresponding to UP1a and UP1b bound FimH (Wu, Sun and Medina, 1996). A few years later, high resolution electron microscopy of infected mouse bladder illustrated the contribution of type 1 fimbriae to mannose-containing glycoprotein receptors in the epithelial bladder cells (Matthew A. Mulvey et al., 1998). Zou and co-workers reported that mouse UPIa and UPIb are differently glycosylated, and although these tetraspanin uroplakins share similar amino acid sequence, only UPIa serves as the urothelial receptor for uropathogenic *E. coli* (Zhou et al., 2001). Importantly,

glycosylation in UPs may change during different pathological conditions such as cancer and UTI (Kątnik-Prastowska, Lis and Matejuk, 2014).

5.1.2 UPEC and indirect association with tetraspanins

It is widely known that tetraspanins associate with other partner proteins on the cell surface. In bladder infection, it has been shown that β1 and α3 integrin molecules, which are commonly associated with tetraspanins (Hemler, 2003), are involved in bacterial invasion along with other host factors that can play a role in regulating endocytosis and cytoskeletal actin reorganization within the bladder urothelium (Eto et al., 2007). It was shown that FimH appears to bind to N-linked oligosaccharides on β1 and α3 integrins and specific antibodies to these integrins also inhibited FimH-mediated invasion in bladder cells (Eto et al., 2007). Disruption of lipid rafts in mouse bladder abolishes UPEC invasion, indicating that type 1-fimbriae invade through caveolae and lipid rafts which are strongly associated with UPIa (Duncan et al., 2004). The pattern recognition receptor Toll-like receptor 4 (TLR4), which is commonly present in the umbrella cells of urothelium in a complex with a number of tetraspanins particularly UPIa (Liu et al., 2015), is also a direct receptor for *E.coli* FimH adhesin, and is involved in activation of the immune response (Ashkar et al., 2008). In addition to those receptors, FimH adhesin can bind with various proteins including the integrin CD11b/CD18, GPI-linked CD48, nonspecific cross-reacting antigen-50, glycoprotein 2, members of carcinoembryonic antigen family, Type I and IV collagens, fibronectin and laminin (reviewed in Mulvey 2016).

5.1.3 Tetraspanins as anti-adhesion therapies

As previously mentioned, tetraspanins are membrane proteins found in mammalian tissue and 33 tetraspanins have been identified in humans. It is widely known that tetraspanins associate with other molecules on the cell membrane to form tetraspanin enriched microdomains (TEM). TEM have been implicated in many biological functions such as cell adhesion, membrane trafficking and fusion (Hemler, 2005; Berditchevski and Odintsova, 2007). However, the role of tetraspanins in bacterial infection is becoming more

obvious since various bacterial pathogens utilise tetraspanins to invade host cells (reviewed in Karam et al., 2020). Previous studies from our group have shown that TEM are involved in the adherence of a range of bacterial pathogens to host cells including *Salmonella typhimurium*, *Neisseria meningitidies, Streptococcus pneumonia*, *Staphylococcus aureus* and *Pseudomonas aeruginosa* (Green et al., 2011; Ventress et al., 2016; Hassuna et al., 2017). In this chapter, we employed cultured human BECs to study UPEC adhesion. Since CD9 is richly expressed on BECs as shown in Chapter 3, it was of interest to study its role in bacterial adhesion. As in previous studies (Green et al., 2011; Ventress et al., 2016), we hypothesised that tetraspanin-derived reagents (either antibody against CD9 or peptide derived from EC2:CD9) can disrupt the adhesion platform for bacteria. This may result in the disorganisation of potential bacterial receptor proteins such as integrins or lipid rafts that affect the bacterial interactions subsequently prohibiting infections. Therefore, we aim to study the effect of tetraspanin proteins in the adhesion of UPEC to human bladder cells. The cell lines that are extensively used in this part were RT4 (urinary bladder papilloma cell line; tumour grade1), which shows a relatively similar properties with primary bladder cells (Chapter 4). We also used another well-established bladder cell line, 5637 which is widely used as an in vitro infection model system by Mulvey's group (Mulvey, 2002; Bower, Eto and Mulvey, 2005; Dhakal and Mulvey, 2009, 2012). Also, primary bladder cells were used to study the effect of CD9 EC2-derived peptide 800C peptides on bacterial adhesion.

5.1.3.1 Tetraspanin-based peptides.

Multiple synthetic peptides are available in our laboratory (section 2.1.8.3). These peptides are derived from the primary sequence of the EC2 domain of CD9 (Figure 5.1) and their effects on *S.aureus* adhesion to human keratinocyte (HaCaT) cells has been previously described (Ventress et al., 2016). Three short segments (8001, 810 and 800) were synthesised from the EC2 region (Figure 5.1). Previous findings from our group have studied their ability to inhibit pathogenic bacteria adhesion; this has led to the current investigation. In this study, we have tested 800C and a "stapled" version of this peptide (Table 2.12).

The peptides are described in 2.1.8.3) where staples were added into the original version of 800C to favour alpha-helical structures (Dr Barbara Ciani, Dept Chemistry, University of Sheffield, personal communication). Peptide 800C was constructed by adding an aspartic acid residue (D) to the N-terminus of the original 800 peptide to form a stabilising “cap” and is also present in peptides 1 and 2. A scrambled peptide (SCR) containing the same amino acids in a different order was used as a negative control. Furthermore, fluorescently labelled versions of peptides 800C and 800SCR were used in order to see the interaction between the peptides and bladder cells.

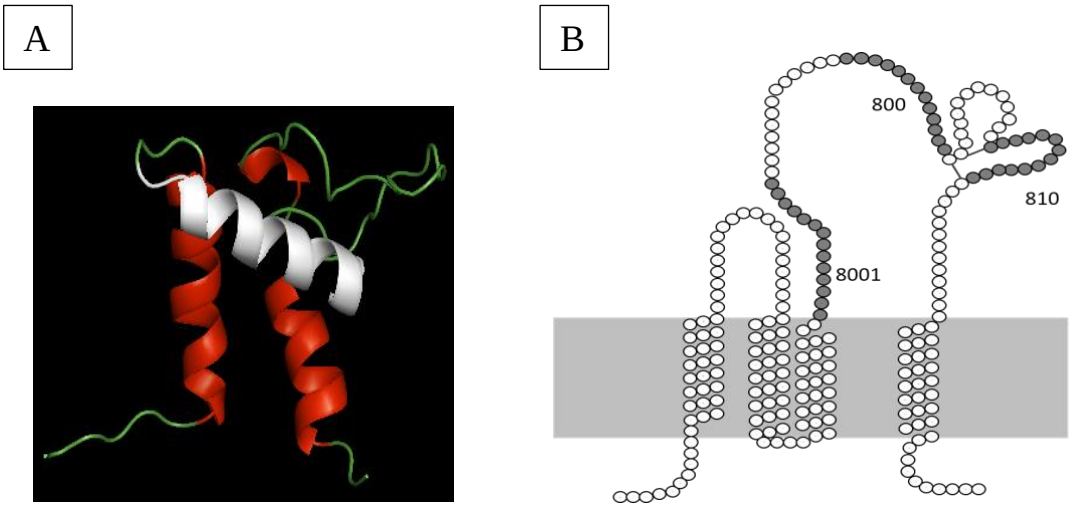

Figure 5.1: The position of CD9-based peptides in the EC2 domain of CD9.

(A) A model of EC2 of CD9 with the peptide corresponding to the 800 shown in white. (B) A schematic of tetraspanin structure representing the different segments of EC2 that were used to generate the synthetic peptides described previously (Ventress et al., 2016).

5.1.3.2 Anti-tetraspanin antibodies

The effect of monoclonal antibodies raised against CD9 (hybridoma clone 602.29), CD81 (hybridoma clone 1.3.3.22)- and the IgG1 isotype control (JC1) on bacterial adhesion were tested (section 2.1.8.1). We studied the effect of the antibodies before we tested the peptides on the bacterial adhesion as in the past it was shown that antibodies to tetraspanins inhibited adhesion. Previous

study from our group has shown that recombinant EC2 protein inhibited adhesion and knock down of CD9 and CD63 expression also inhibited adhesion (Green et al., 2011). Moreover, CD63 knock down inhibited *S.typhimurium* adhesion (Hassuna et al., 2017).

5.2 Results

5.2.1 Preparation before infection and selected cell models in this study

Two strains of UPEC were utilized that are known to express Type 1 fimbriae: J96 from (ATCC) and a multidrug-resistant UPEC, EC958 kindly provided by Professor Robert Poole, Dept. Molecular Biology & Biotechnology, University of Sheffield. Initially, growth curves were obtained for these strains to identify the mid-log phase that would be used for infection. As stated in Chapter 2, growth curves were obtained by growing the UPEC strains in appropriate medium and measuring both optical density (OD600) and viable bacterial counts (colony forming unit (CFU)) through different time periods (0- 8 hours). The mid-log phase chosen from the average to use for the J96 infection assay was OD600 ~0.5-0.6, time ~ 3 hours, CFU~ 2 x108) and for the EC958 strain, OD600 ~0.5-0.6, time ~2 hours and CFU~ 6.5-7 x107). Different MOI and infection times were investigated to establish those that were most suitable. To optimise the MOI and infection time, the various bladder cell lines were infected at different MOIs (10, 20, and 50) and for different infection times (1 and 2 hours). In the initial experiments, the optimum MOIs were determined based on the quantity of viable bladder cells after bacterial infection by using the LDH assay. We found that high MOIs and longer infection times caused a lower percentage of viable host cells and high numbers of bacteria that made counting difficult, whilst at shorter time points, host cells remained viable. Therefore, the most suitable MOI was chosen at MOI 10 for 1 hr infection in all selected cell lines. For further confirmation of the MOI used, the number of CFU was measured separately for each separate experiment (optimisation data not shown).

5.2.2 Effect of anti-tetraspanin antibodies on uropathogenic E. coli adherence to urothelial cells

5.2.2.1 Effect of anti-CD9 antibody on selected cell lines

As mentioned above, we hypothesized that CD9 tetraspanin may be involved in UPEC adhesion to host bladder cells. To check this, we have investigated the effect of pre-incubating the human bladder cells with specific monoclonal antibody before infection with UPEC.

5.2.2.1.1 Determining the optimum dose for anti-CD9 antibody in bladder cells.

A dose response curve was produced for the effects of the anti-CD9 on UPEC adhesion to RT4 cells. As shown in **Error! Reference source not found.**, a significant inhibition was seen at 20 µg/ml. This corresponds to a concentration of the antibody that gives saturating binding to CD9 by flow cytometry. The decreasing binding at high concentration of antibody (100 µg/ml) is typical of a prozone effect. Across all concentrations, pre-treatment of the RT4 cells with the IgG1 isotype control gave no significant reduction in bacterial adhesion. This data confirmed that 20 µg/ml is the optimum concentration of 602.29 anti-CD9 antibody to use in subsequent experiments.

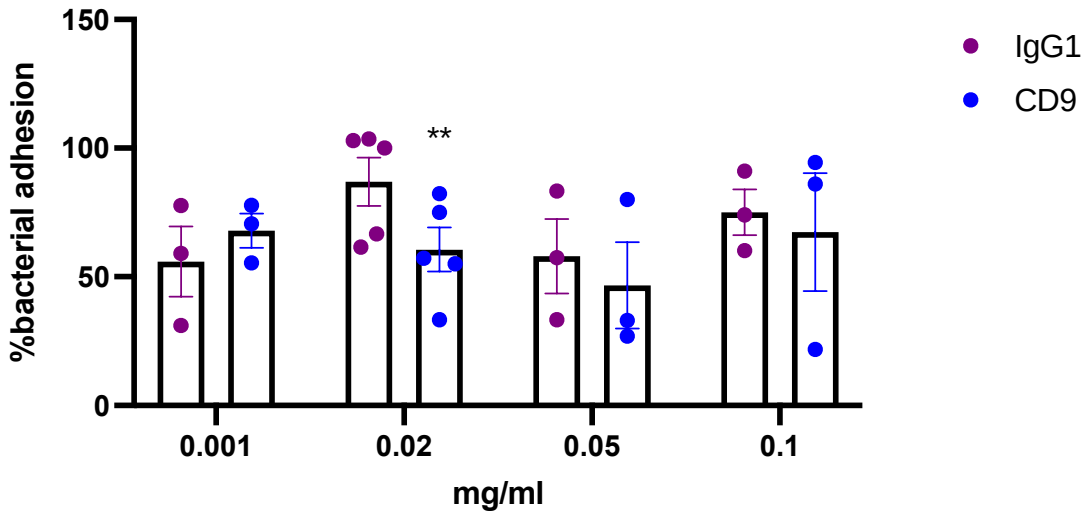

Figure 5.2: Dose response curve of anti-CD9 pre-treatment effect on UPEC adherence to human bladder cells.

Adherent RT4 cells in 96 well plates were pre-treated with 602.29 (anti-CD9) or an IgG1 isotype control over a range of concentrations (1, 20,50, 100 µg/ml) for 1 hr. The cells were infected with UPEC (EC958 strain) for 1 hr at an MOI of 10. Cells were then washed three times with PBS, lysed with 1% Triton X-100 and bacteria plated on LB agar plates to determine cfu (section 2.2.5.3). The data represent the means, while error bars describe standard error means. n ≥3 independent experiments, performed in four replicates. Data were analysed by one-way ANOVA against untreated control, where ** = $p < 0.01$ and * = $p < 0.05$.

5.2.2.1.2 Effect of anti-CD9 antibody treatment upon UPEC adherence to RT4 cells

RT4 was used in this present study. Cells were pre-treated with 20 µg/ml of antibody and then infected with one of two different strains of UPEC. As shown in **Error! Reference source not found.**, a significant reduction in bacterial adherence was observed on pre-treatment of host cells with anti-CD9 compared with the untreated controls, with ~ 40% reduction of J96 adherence and 50% reduction with the multidrug-resistant pathogen EC958. No significant reduction of bacterial binding was seen in the isotype control treatment.

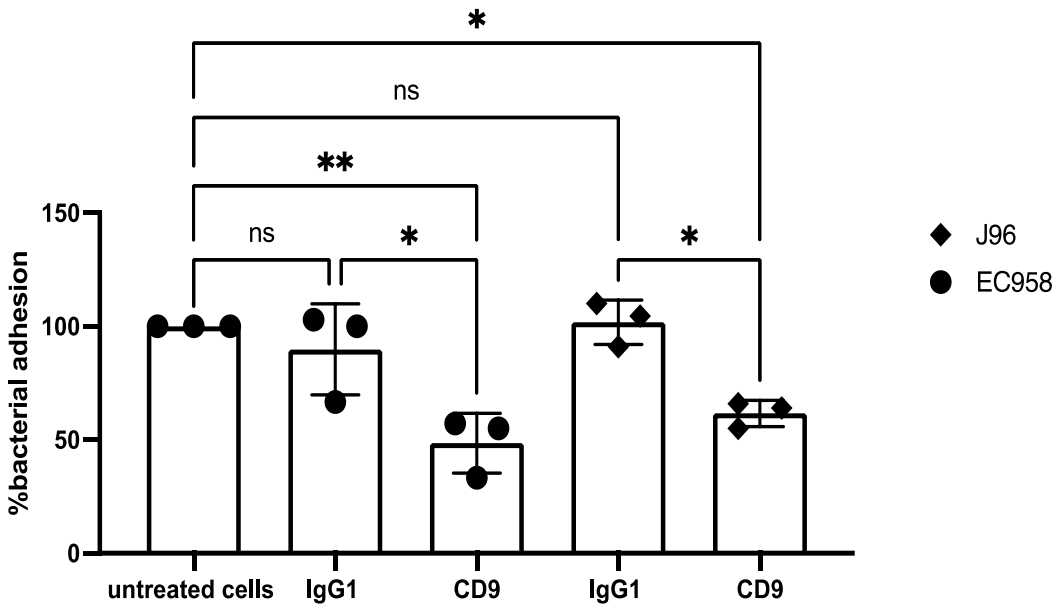

Figure 5.3: Effect of anti-CD9 on the adherence of UPEC strains to RT4 cells.

RT4 cells were pre-treated with anti-CD9 (602.29) or IgG1 isotype control (20 µg/ml), infected with bacteria for 1 hr and then the number of cell-associated bacteria determined as described in (**Error! Reference source not found.**). The data represent the means, while error bars describe standard error means. n=3 independent experiments, performed in four replicates. Data were analysed by one- way ANOVA, where ** = $p < 0.01$ and * = $p < 0.05$.

5.2.2.1.3 Effect of anti-CD9 antibody treatment upon UPEC adherence to 5637 cells

5637 was used as another an in vitro model of bladder infection in this study, using the J96 UPEC strain. Treatment of 5637 cells with anti-CD9 caused significant inhibition of bacterial binding in of about 60% (**Error! Reference source not found.**). There is a slight effect of isotype control treatment in with about 30% reduction of bacterial binding, but it is non-significant.

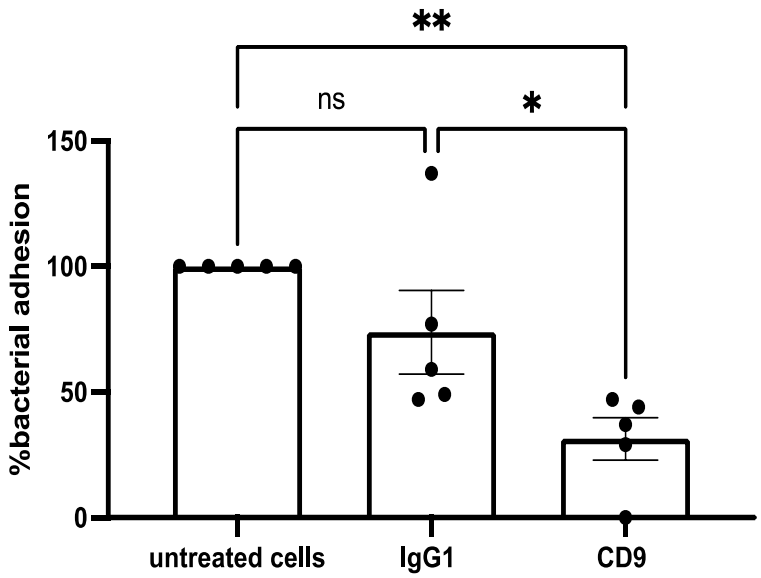

Figure 5.4: Effect of anti-CD9 on the adherence of J96 to 5637 cells.

5637 cells were pre-treated with anti-CD9 (602.29) or IgG1 isotype control (20 µg/ml), infected with J96 for 1 hour and then the number of cell-associated bacteria determined as described in (**Error! Reference source not found.**). The data represent the means, while error bars describe standard error means. n=5 independent experiments, performed in four replicates. Data were analysed by one- way ANOVA, where ** = $p < 0.01$ and * = $p < 0.05$.

5.2.2.1.4 Effect of anti-CD9 antibody treatment upon UPEC adherence to primary bladder cells

As previously discussed, primary bladder cells were used in this study as they might more closely represent bladder cells *in vivo* compared with bladder cancer cell lines (section 2.1.10). Primary bladder cells were pre-treated with 20 µg/ml antibody before infection with UPEC (strain J96) as described above. As shown in **Error! Reference source not found.**, a significant reduction in bacterial adherence (of ~ 60%) was observed on pre-treatment of host cells with anti-CD9 compared with the untreated controls. A non-significant reduction in adhesion of ~ 40% with isotype control treatment was observed.

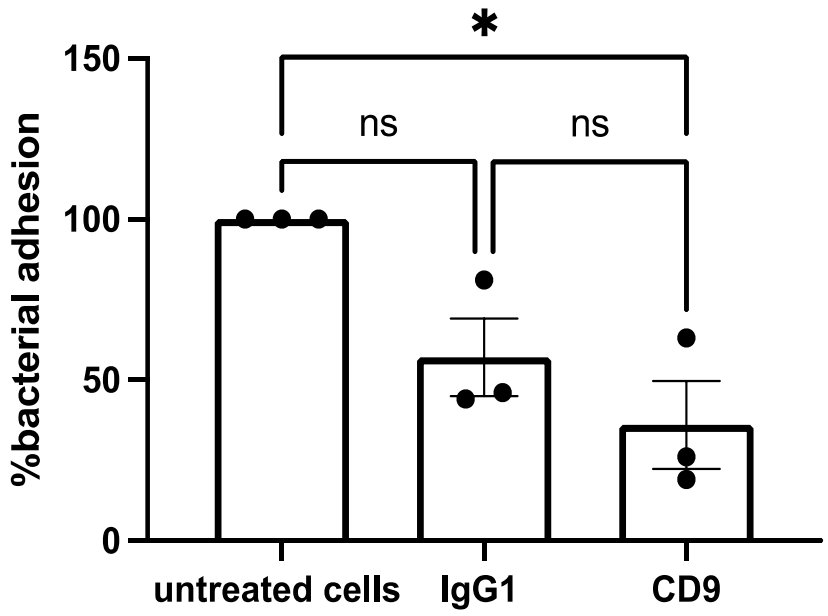

Figure 5.5: Effect of anti-CD9 on the adherence of J96 to primary bladder cells.

Human primary bladder cells were pre-treated with anti-CD9 (602.29) or IgG1 isotype control (20 µg/ml), infected with J96 for 1 hour and then the number of cell-associated bacteria determined as described in (**Error! Reference source not found.**). The data represent the means, while error bars describe standard error means. n=3 independent experiments, performed in four replicates. Data were analysed by one- way ANOVA, where ** = $p < 0.01$ and * = $p < 0.05$.

5.2.2.2 Effect of anti-CD81 antibody treatment upon UPEC adherence to BECs

Since there is a high level of cell surface expression of CD81 in BECs (especially on 5637 cells (Figure 3.2)), and it has previously been shown that some pathogens require CD81 to access epithelial cells (Tham et al., 2010), it was considered worth studying the effect of anti-CD81 on UPEC adherence to BECs. Therefore, we investigated the role of anti-CD81 in the adherence of J96 strain to both 5637 and RT4 cells as described above. The result indicates that CD81 does not seem to be involved in UPEC adhesion to either type of bladder cells since there was no significant reduction in the percentage of bacterial binding with anti-CD81 pre-treatment compared with controls (**Error! Reference source not found.**).

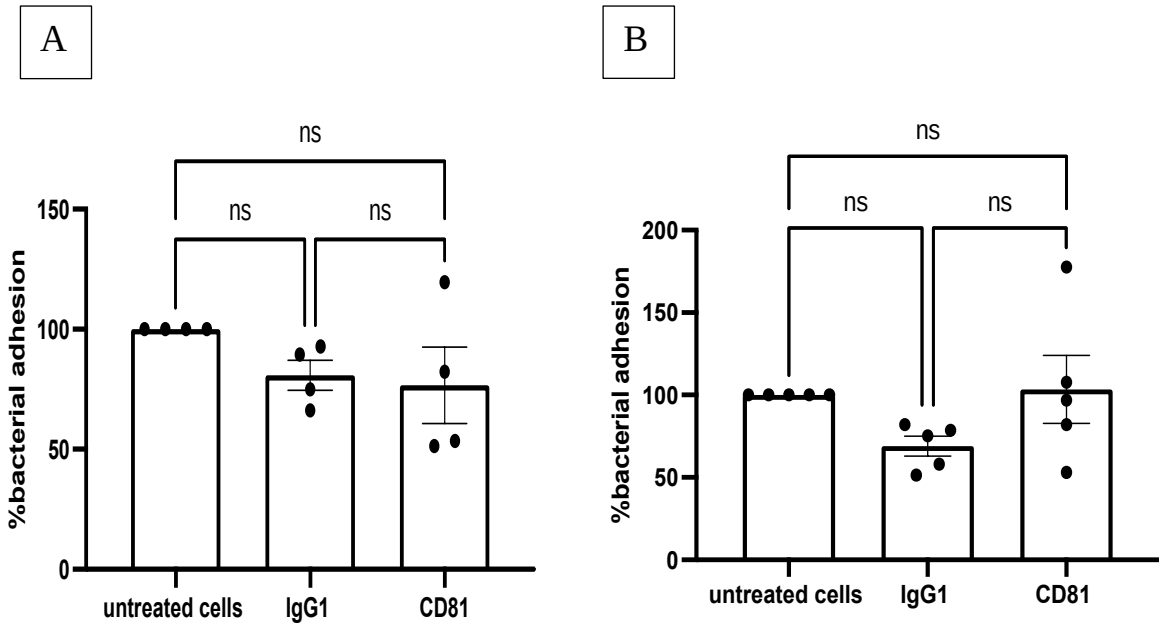

Figure 5.6: Effect of anti-CD81 on the adherence of J96 to BECs.

Cells were pre-treated with anti-CD81 or IgG1 isotype control (20 µg/ml), infected with J96 for 1 hour and then the number of cell-associated bacteria determined as described in (**Error! Reference source not found.**). (A) shows the percentage of adherence to RT4 cells while (B) shows the percentage of binding to 5637 cells. The data represent the means, while error bars describe standard error means. n ≥4 independent experiments, performed in four replicates. Data were analysed by one- way ANOVA, where ** = $p < 0.01$ and * = $p < 0.05$.

5.2.3 Investigation of internalization of anti-CD9 antibody in bladder cells

The ability of certain antibodies to induce internalization of their target antigens and associated molecules on the cell surface might possibly be one explanation for the effect of anti-CD9 on UPEC adhesion. To investigate this, the potential of anti-CD9 to induce internalization of CD9 in RT4 cells was studied using flow cytometry. The internalization assay was carried at as described in (section 2.2.6.3). Briefly, RT4 cells were incubated with unlabelled anti-CD9 at the same concentration as used in the infection assay and the level of anti-CD9 remaining on the cell surface was compared for cells that had been incubated on ice (control) or at 37°C for 1 hr, using FITC-labelled secondary antibody. As shown in (**Error! Reference source not found.**), there was no decrease in the level of anti-CD9 detected on the cell surface for cells that had been incubated at 37°C, compared with the control cells incubated on ice. A slight increase in MFI

in (1 hr) samples compared with the control of MFI (0 min) was found (**Error! Reference source not found.**). This may be due to the fact that the antibody binding becomes more saturated after a long duration. This indicates that anti-CD9 does not induce internalization of CD9 during the time (1hr) of the infection assay, so this is not the explanation for the decrease in bacterial adhesion observed on pre-treatment of bladder cells with this antibody.

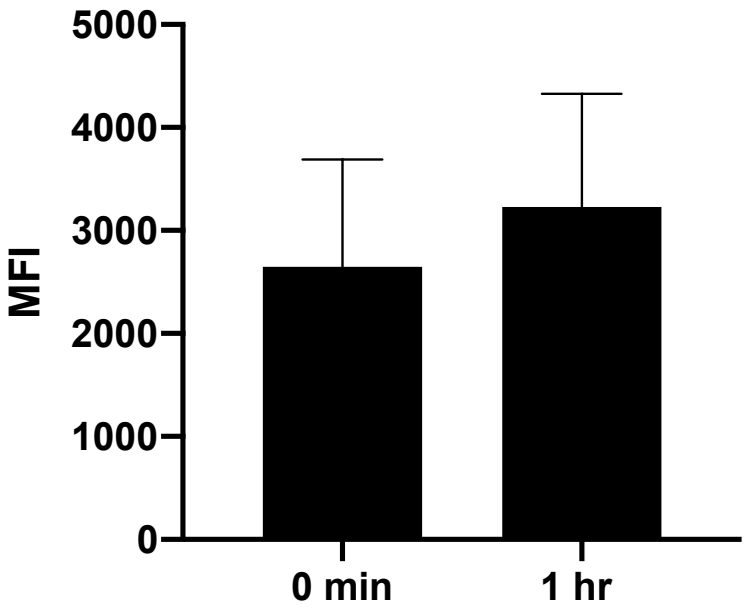

Figure 5.7: Internalization assay using anti-CD9 antibody on RT4 cells.

RT4 cells were first incubated with primary anti-CD9 (602.29) for 30 min on ice. Then, the cells were washed with cold HBSS + 0.2%BSA and incubated for 1 hr at 37°C. Control cells were kept on ice, and a labelled secondary anti-mouse IgG antibody was added for 30 min on ice. Flow cytometry was used to detect how much anti-CD9 remained on the cell surface. The expression level was measured and expressed as median fluorescence intensity (MFI) values. The data represent the means, while error bars describe standard error means. n=4 independent experiments, performed in replicates.

5.2.4 Effect of CD9-EC2 peptides on both bacterial growth and adherence to BECs

As shown in Figure 5.1, peptides corresponding to different segments of the large extracellular domain (EC2) of CD9 were characterized in our laboratory. In this study, we tested 800C particularly and its scrambled version as

described in (section 2.2.5.3). The effects of these peptides on the adherence of UPEC to bladder cells was investigated.

5.2.4.1 Effect of CD9-EC2 peptides on bacterial growth

As mentioned earlier, CD9 is multifunctional molecule. Therefore, it was important to test if there is any toxicity of peptide treatment on bacterial growth. In this study, we have utilized 800-cap and scrambled peptide (SCR) to check if they might be affecting the growth of UPEC. A growth curve of J96 strain was performed under three different conditions: bacteria grown on LB broth as a control condition, LB with 200 nM final concentration of 800C, and LB with 200 nM of SCR peptide (section 2.2.4.2). As shown in **Error! Reference source not found.**, no big change in the growth curve was observed between peptide or scrambled control treatment and normal control condition. This assay indicates that the peptide treatment had no effect on bacterial growth.

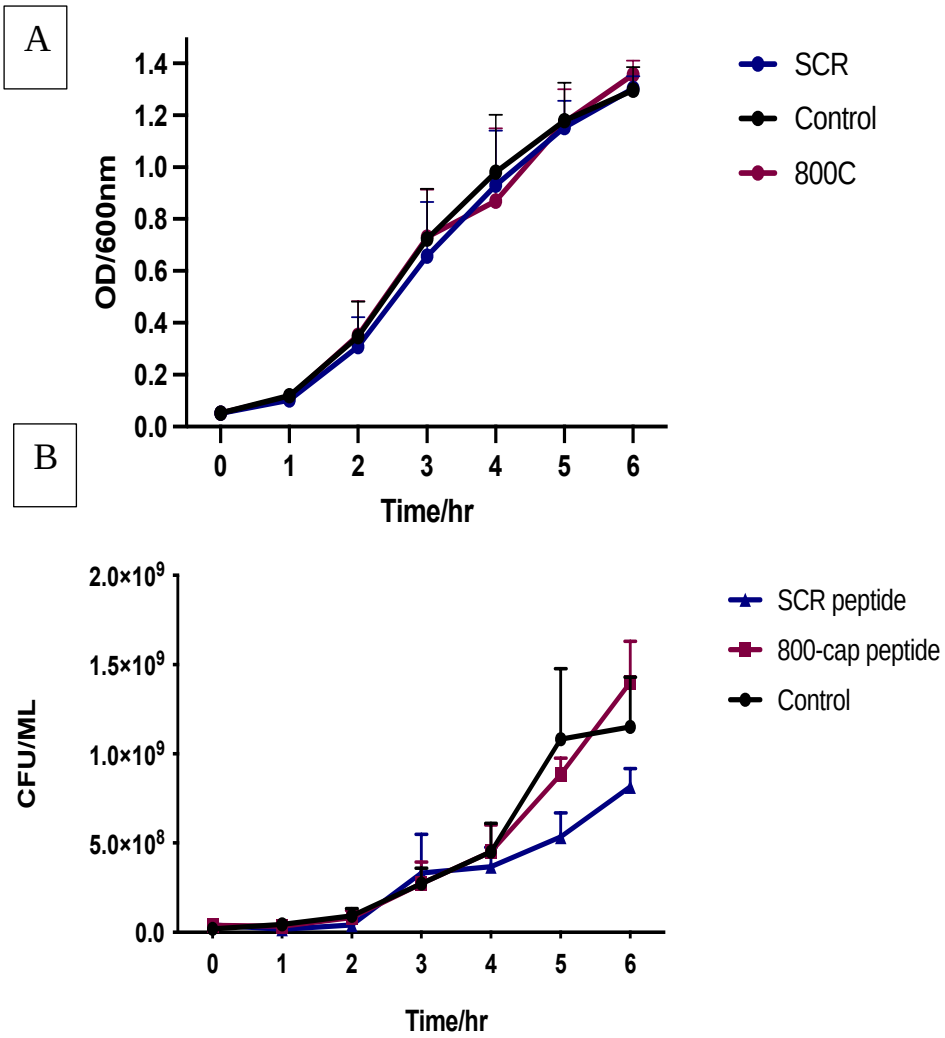

Figure 5.8: Growth of J96 in the presence of CD9 peptides.

J96 bacteria were grown in LB broth alone (control) or in the presence of 200nM final concentration of 800C or SCR. (A) Bacterial growth was assessed by measuring the OD of the culture at 600nm and by (B) CFU counting at times indicated as described in (2.2.4.2). The data represent the means, while error bars describe standard error means. n=3 independent experiments.

5.2.4.2 Effect of CD9-EC2 peptides on human bladder cell viability

Measurement of lactate dehydrogenase (LDH) release is commonly used to assess cell viability and determine the level of cytotoxicity (Decker and Lohmann-Matthes, 1988). This assay was performed as described in (section 2.2.2.5). In this study, RT4 cells were pre-treated with/without CD9-EC2 peptides and infected with J96 at MOI 10. After the infection the supernatants were collected and used for the LDH assay to determine the cytotoxicity level. As shown in **Error! Reference source not found.**, none of the treatments with peptides gave cytotoxicity values above 10% and were similar to untreated controls, indicating that the tetraspanin-derived peptides do not affect bladder epithelial cell viability.

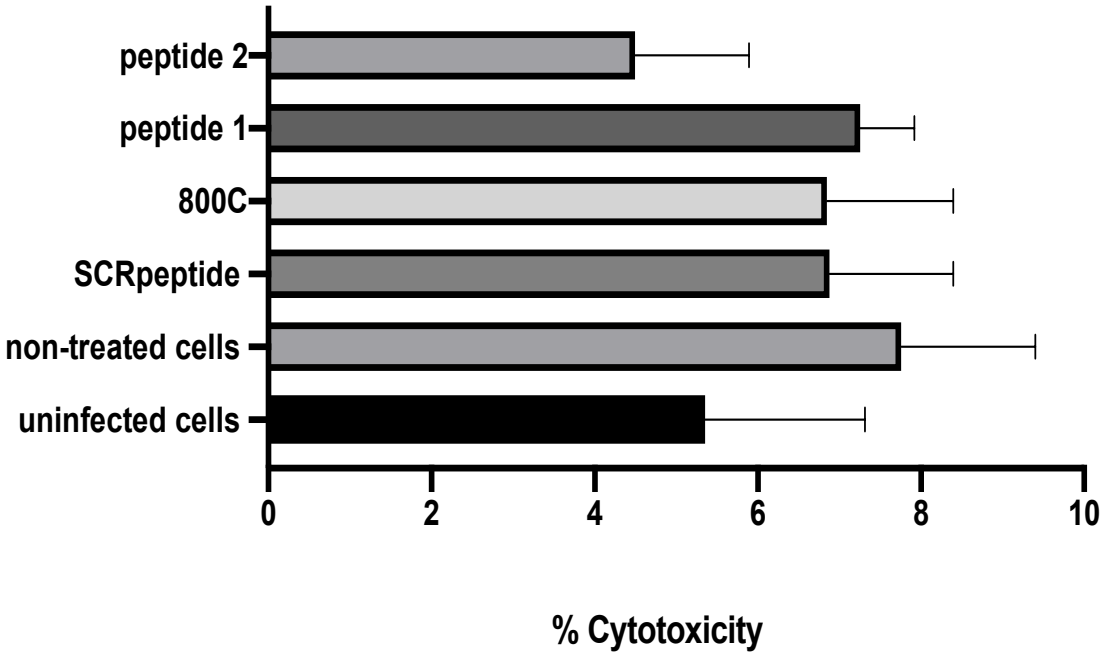

Figure 5.9: Effect of CD9-EC2 peptides on RT4 cell viability during the infection assay.

Cell monolayers were pre-treated with 20nM CD9-EC2 peptides, scrambled peptide or buffer (non-treated control) for 1hr then infected with J96 at MOI 10 for 1hr. LDH release into the supernatant was then measured and used to determine % cytotoxicity. The data represent the means, while error bars describe standard error means. n ≥3 independent experiments, performed in triplicates.

5.2.4.3 Effect of CD9-EC2 peptides on bacterial adhesion to RT4 cells

In initial experiments, we tested the effects of pre-treatment of RT4 cells with different versions of 800C at various concentrations ranging from 0.2 nM to 200nM on bacterial adhesion. The results suggested that the most specific effects were in the 10 to 50 nM range and so this was examined in more detail (**Error! Reference source not found.**). It was determined that the 800C peptide at 20nM had the greatest effect on bacterial binding, with a maximum 40% reduction (**Error! Reference source not found.**), whereas the scrambled peptide control had little effect at this concentration. After this we decided to test this concentration of 800C peptide (or scrambled control) on UPEC adhesion. As shown in **Error! Reference source not found.**, pre-treatment of RT4 cells with 20nM of 800C peptide had a significant reduction of adherence

of the J96 strain of 40% compared to non-treated cells, whilst giving 40% maximum reduction of EC958 adhesion.

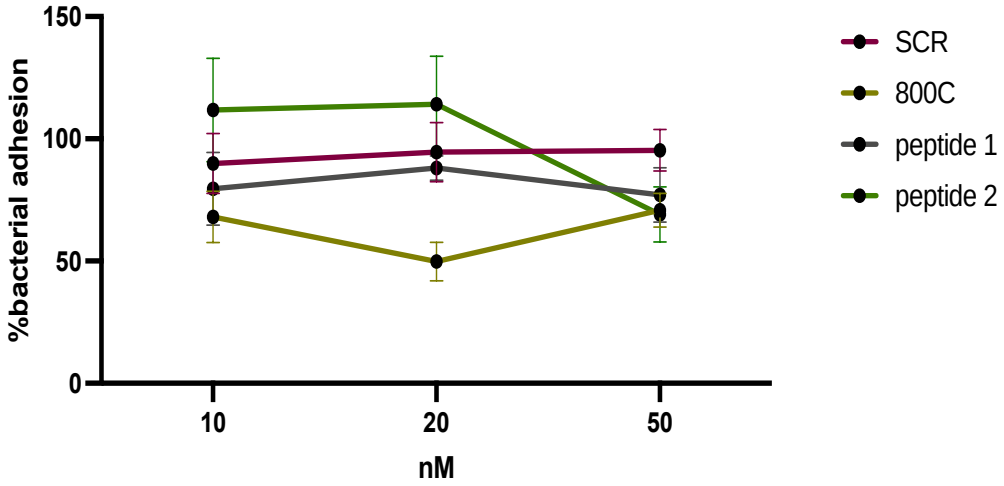

Figure 5.10: Dose response curve of CD9-EC2 peptides pre-treatment effect on UPEC adherence to human bladder cells.

Adherent RT4 cells in 96 well plates were pre-treated with CD9-derived synthetic peptides or a scrambled control peptide over a range of concentrations (10, 20 and 50 nM) for 1 hr. The cells were infected with UPEC (J96 strain) for 1 hr at an MOI of 10. Cells were then washed three times with PBS, lysed with 1% Triton X-100 and bacteria plated on LB agar plates to determine cfu (section 2.2.5.3). The data represent the means, while error bars describe standard error means. n ≥5 independent experiments, performed in four replicates.

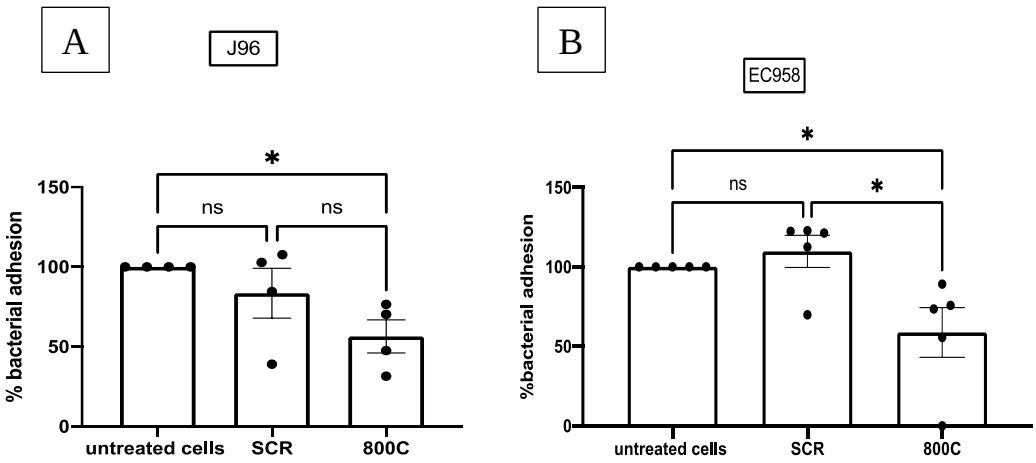

Figure 5.11: Effect of 800C peptide on the adherence of UPEC strains to RT4 cells.

RT4 cells were pre-treated with 20 nM 800C or SCR control peptide, infected with bacteria for 1 hr and then the number of cell-associated bacteria determined as described in (**Error! Reference source not found.**). Values are expressed as the number of bacteria in pre-treated cells/the number of bacteria in untreated cells x 100%. (A) shows the percentage of J96 strain adhesion while (B) representative the percentage of EC958 strain adhesion. The data represent the means, while error bars describe standard error means. n ≥4 independent experiments, performed in four replicates. Data were analysed by one- way ANOVA, where ** = $p < 0.01$ and * = $p < 0.05$.

5.2.4.4 Effect of 800C peptides on bacterial adhesion to 5637 cells

The effects of pre-treatment of 5637 cells with 800C at 20 nM on bacterial adhesion (UPEC J96) have also been tested. Similar to the effect on RT4 cells, a significant reduction in the bacterial binding (~ 50%) with cells treated with 800C compared to untreated cells was observed (**Error! Reference source not found.**). No significant reduction of bacterial binding was seen in the control peptide treatment (**Error! Reference source not found.**).

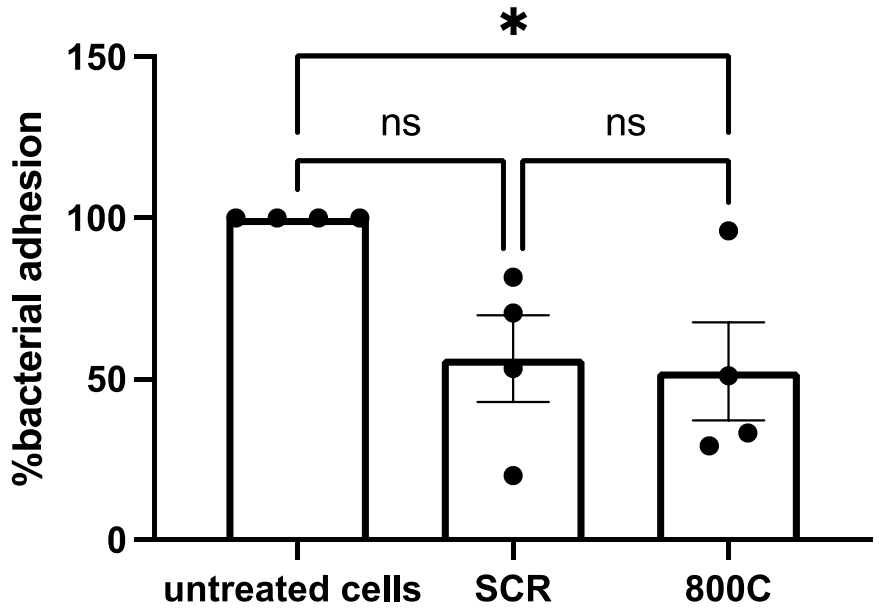

Figure 5.12: Effect of 800C peptide on the adherence of J96 strain to 5637 cells.

5637 cells were pre-incubated with 20nM 800C or SCR control peptide, infected with bacteria for 1 hr and then the number of cell-associated bacteria determined as described in (**Error! Reference source not found.**). Values are expressed as the number of bacteria in pre-treated cells/the number of bacteria in untreated cells x 100%. The data represent the means, while error bars describe standard error means. n=4 independent experiments, performed in four replicates. Data were analysed by one- way ANOVA, where ** = $p < 0.01$ and * = $p < 0.05$.

5.2.4.5 Effect of 800C on primary bladder cells

The effect of 800C peptide on bacterial adhesion (UPEC J96) was also tested on the primary bladder cells. As shown in **Error! Reference source not found.**, although a reduction in bacterial adherence was observed on pre-treatment of host cells with 800C with an average of ~ 40% inhibition (similar to the cell lines), this was not statistically significant compared with the untreated controls.

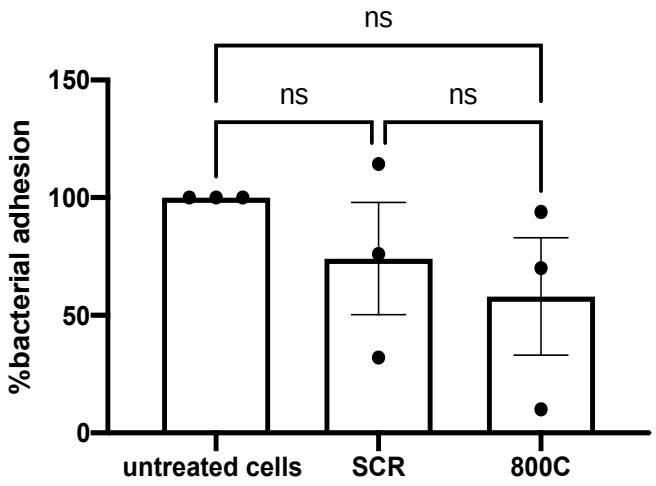

Figure 5.13: Effect of 800C on the adherence of J96 to primary bladder cells.

Human primary bladder cells were pre-treated with 20nM 800C or SCR control peptide, infected with bacteria for 1 hr and then the number of cell-associated bacteria determined as described in (Figure 5.2). Values are expressed as the number of bacteria in pre-treated cells/the number of bacteria in untreated cells x 100%. The data represent the means, while error bars describe standard error means. n =3 independent experiments, performed in triplicates. Data were analysed by one- way ANOVA, where ** = $p < 0.01$ and * = $p < 0.05$.

5.2.5 Interaction of fluorescently labelled peptides with epithelial cell lines

From the data presented in sections (5.2.4.3 and 5.2.4.4), it appeared that peptide 800C inhibited UPEC adhesion to RT4 and 5637 cells when compared to non-peptide treated controls. However, there was no statically significant difference between the 800C-treated and SCR control- treated cells. To investigate this further, the interaction of fluorescently labelled peptides with RT4 cells and a wild type of human lung epithelial cell line, A549, and A549 cells where the CD9 gene had been knocked out using CRISPR Cas9 was investigated (Don J Giard et al., 1973) (Table 2.14). Studies on the expression of CD9 on A549 WT and CD9 KO cells were carried out in our lab by a 3rd year project student, Robert Whelan (**Error! Reference source not found.**). Despite the reported knock-out, there is a slight expression of CD9 in the A549 KO cells, so it is probably better to consider it as knocked down for CD9 rather than knocked out in these cells.

Initially, we attempted to use flow cytometry under various different conditions as described in (section 2.2.6.4) to investigate binding of fluorescent peptide. However, possibly due to the low affinity of peptide binding, we could not find any specific interaction between the peptides and the cells (data not shown). An obvious specific binding of labelled peptide to primary keratinocytes had previously been observed by immunofluorescence microscopy by Ventress (Ventress et al., 2016). Therefore, we decided to use a confocal microscopy. To do this, cells were grown overnight on coverslips at the optimum cell density, then treated with peptides for 30 minutes. Then, the cells were fixed using 2% paraformaldehyde and analysed by confocal microscopy (section 2.2.7.2). Peptides were observed interacting with the cells (**Error! Reference source not found.**), but it was difficult to assess any differences in the signal between 800C and SCR peptides by eye. We therefore measured the total cell fluorescence using the Image J program (). These data indicate that WT A549 and RT4 cells, which expressed high levels of CD9, interact better with fluorescently labelled 800C compared with 800SCR, whilst A549 CD9KO cells show lower fluorescence intensity and a similar pattern of binding between

800C and 800SCR. This supports our hypothesis that peptide derived from EC2:CD9 binds to endogenous CD9 on the cells.

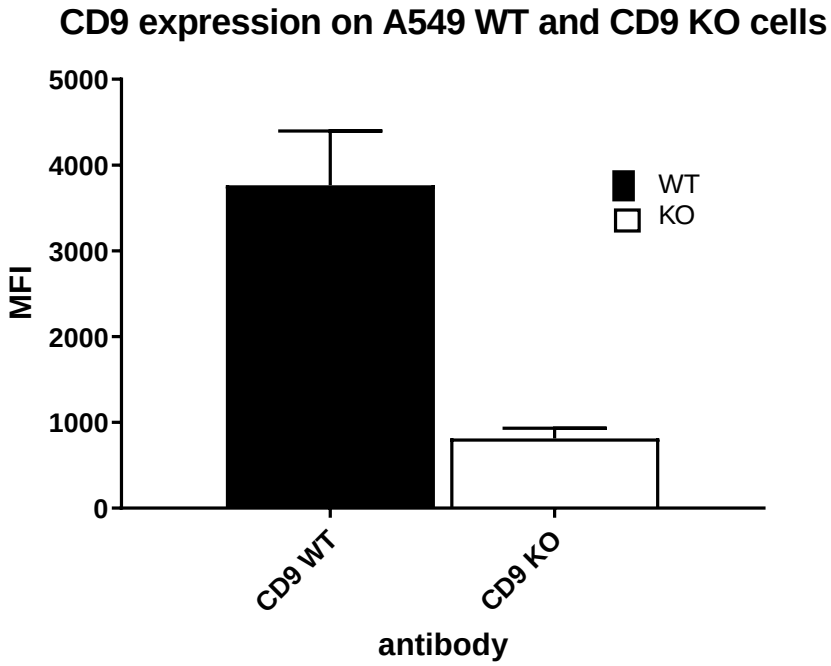

Figure 5.14: Cell surface expression of CD9 on A549 WT and CD9KO by flow cytometry.

The levels of CD9 expression are represented as the MFI (median fluorescence intensity) obtained with the anti-CD9 antibody (602.29) s after subtracting the MFI obtained with the appropriate isotype control (IgG1). The secondary antibody was a FITC-conjugated anti-mouse IgG. The data represent the means, while error bars describe standard error means. n=8 independent experiments, performed in replicate. This work was carried out by a 3rd year project student working in the laboratory.

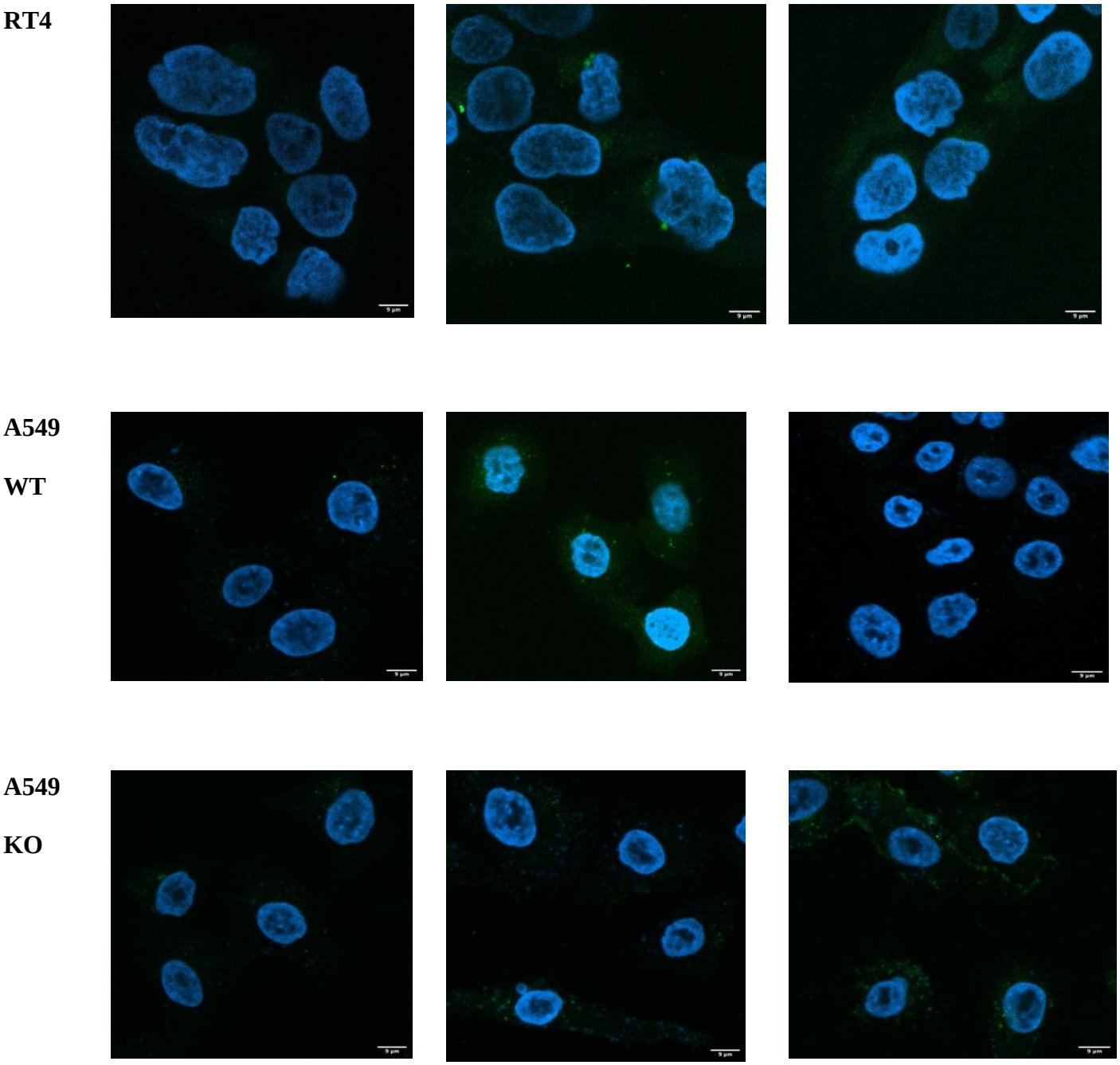

Figure 5.15: Binding of fluorescent peptides 800C and 800SCR with the cell surface of epithelial cell lines.

Representative images showing the binding of peptides to RT4, A549 WT and A549 CD9 KO. Cells were seeded onto glass coverslips and grown overnight, then treated with 800C peptide or SCR peptide conjugated with a 6-FAM tag or media only control for 30 minutes. The cells were then fixed in paraformaldehyde and stained with DAPI before imaging by confocal microscopy (section 2.2.7.2). Images were taken using the 100x objective, scale bar = 9µm. DAPI shown in blue, FITC shown in green.

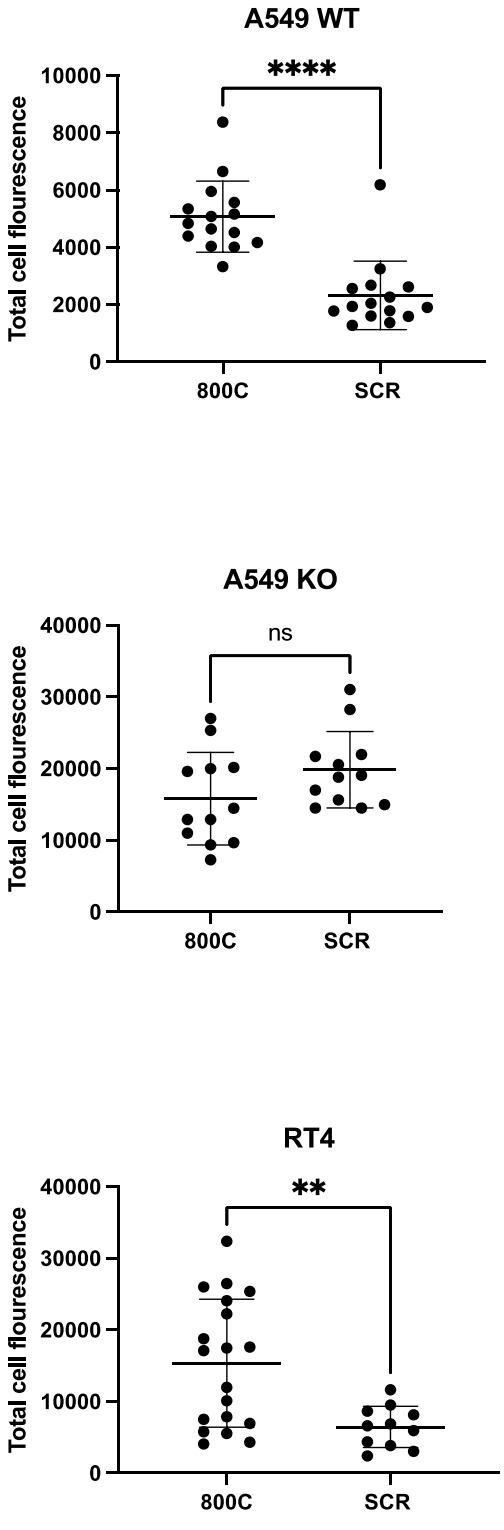

Figure 5.16: Cell fluorescence intensity analysis of different cell lines, comparing staining with 6-FAM tagged 800C and SCR control.

The total cell fluorescence was calculated by using the following formula: integrated density-(area of selected cell X mean fluorescence of background). Data represents each cell from one slide per cell line. The data represent the means, while error bars describe standard error means. Data was analysed by t-test comparing 800C to SCR control. ** $p \leq 0.01$, * $p \leq 0.05$ and ns is non- significant.

5.3 Discussion

In this Chapter it has been shown that CD9-based reagents reduce the adherence of uropathogenic *E.coli* to human bladder cell lines and primary bladder cells. This anti-adhesive activity was not seen when cells were pre-treated with anti-CD81 (**Error! Reference source not found.**), suggesting that CD9 has a specific involvement in bacterial adhesion. CD9 is known to be involved in organizing other cell surface molecules that act as bacterial receptors (Green et al., 2011). It has also been deduced that the synthetic CD9 peptides are acting on host cells, not with bacteria, since no effect of 20 nM peptide treatment was observed against J96 strain UPEC growth or viability over 8 hours (**Error! Reference source not found.**). The initial work here was to establish a bladder cell model to investigate the role of tetraspanins in UPEC infection. In this study, different cell lines including human bladder cell lines (5637 and RT4) and human primary bladder cells were infected with UPEC strains. The conditions for the infection assay were optimized by selecting a suitable multiplicity of infection (MOI) and the time of infection.

Pre-treatment with anti-CD9 antibody has previously proven effective in inhibiting adhesion of various types of bacteria by about 50 % on different cell types (Green et al., 2011; Fawwaz Ali, PhD thesis, University of Sheffield 2016). Here, whilst anti-CD9 antibody caused inhibition of bladder infection, whereas no effect was seen with anti-CD81 treatment, despite the bladder cells expressing good levels of tetraspanin CD81 (Figure 3.7). Interestingly, no effect with CD81 EC2 recombinant protein was observed on bacterial adhesion (Luke Green PhD thesis, University of Sheffield, 2010).

Despite a previous finding by our group that anti-CD81 antibodies inhibited *S.typhimurium* adhesion to human macrophages (Hassuna et al., 2017), the present study showed no effect with anti-CD81 in UPEC adherence. Previous reports have shown that the bacterial effector EspH stimulates CD81 clustering at enteropathogenic *E. coli* (EPEC) infection sites in HeLa and Caco-2 cells at the early stage of infection. This disorganization leads to inhibition of the phosphorylation of Erk which helps to facilitate the bacterial survival in the

infected gut (Ramachandran et al., 2018). This study showed CD81 molecules are not involved in EPEC adhesion and colonization (Ramachandran et al., 2018), similar to the observations in this study.

The impaired effect of anti-CD9 at high concentrations observed might be due to a prozone or “hook” effect, seen in immunoassays where the concentration of antibody is too high (**Error! Reference source not found.**) (Miller and Levinson, 1996). It was useful to examine dose/response effects to determine the best concentration of anti-CD9 that gave significant reductions in UPEC adherence. However, blockade of tetraspanin CD9 reduced the adherence of UPEC, with maximum inhibition on average of 50% in various type of infected bladder cells. It appears that the effect on adhesion is not due to internalisation of CD9 by anti-CD9 mAb since CD9 remained on the cell surface after treatment with antibody for up to 1hr at 37°C without affecting the cell viability (**Error! Reference source not found.**). These results are consistent with previous investigations carried out in our laboratory where antibodies targeting tetraspanins were capable of significantly reducing bacterial adherence (Green et al., 2011).

CD9-internalization by mAb was evaluated, as mentioned, and as expected CD9 remained at the cell surface for up to 1hr after treatment with antibody at 37°C. Previous work has shown that CD9 molecules exist predominantly at the cell surface, with low abundance in intracellular vesicles (Fernvik *et al.*, 1995; Miyado *et al.*, 2000). CD9 has been shown to internalize more slowly in cancer cell lines stimulated with PMA than Tspan8 (Rana et al., 2011). Previous data from our group also showed little internalization of CD9 on RBL2H3 cells after antibody crosslinking (Higginbottom et al, unpublished data). This is presumably due to the absence of specific internalization motifs in CD9, which are present in some tetraspanins such as CD63 (Berditchevski and Odintsova, 2007).

Short synthetic CD9-derived peptides have been designed to mimic regions of the human CD9 EC2 domain (Ventress et al., 2016). In this study, peptides 1 and 2 which are different versions of 800 peptide supplied with peptide stabilisers to encourage the chains to form alpha- helical structure were used

(section 2.1.8.32). These stapled peptides alongside a capped version of the original version of the 800 peptide were tested for their ability to inhibit UPEC adherence to bladder epithelial cells. Although, all different versions of 800 peptide reduced the bacterial adhesion to some extent, a significant achievement of reduction was observed with 800C peptide at a concentration of 20nM (**Error! Reference source not found.**). This peptide at this certain concentration was therefore used in subsequent studies. Notably, we found a non-significant reduction with the SCR peptide, suggesting that the 800C CD9-EC2 peptide interacts specifically with the cells. The 800C peptide gives 50% reduction of UPEC adhesion on all cell lines, similar to the effect seen with anti-CD9 antibodies and also similar to the effect of peptide on *S.aureus* adhesion to keratinocytes as well as to A549 lung cells (Ventress et al., 2016; Green et al., manuscript submitted to PLOS pathogens).

Although peptide 800C gave significantly reduced adhesion of UPEC compared to untreated controls, there was no significant difference between this and SCR control. To investigate the specificity of the peptides further, the binding of fluorescent versions of 800C and the scrambled control to cells expressing different levels of CD9 was examined. We have shown that the activity of these peptides correlates with CD9 expression. A549 WT cells, which express high levels of CD9 (**Error! Reference source not found.**) were shown to interact with 800C significantly compared to the SCR peptide (**Error! Reference source not found.**). Pre-treatment of A549 WT cells with 800C has proven effective in inhibiting adhesion of *S. aureus*, whilst this peptide has no effect on adhesion of bacteria to A549 CD9KO (Green et al., manuscript submitted to PLOS Pathogens). By contrast, for A549 cells where the CD9 gene had been knocked out, there was no difference in binding of 800C and SCR peptides. RT4 cells, which also express high levels of CD9 (Figure 3.7), also showed significant interaction of 800C compared with SCR control (Figure 5.15).

Also, using super resolution microscopy, it has been shown by our group that fluorescently labelled clusters of endogenous cell surface CD9 on epithelial cells are disrupted in the presence of peptide (Dr Rahaf Issa, unpublished data).

Thus, this would support our hypothesis that CD9 peptides bind specifically to endogenous CD9 and cause a disruption at the epithelial cell surface.

The correlation between CD9 expression and the efficiency of peptide treatment has previously been shown. Skin fibroblasts with low CD9 expression showed no effect of CD9-derived peptides on bacterial adhesion, whilst primary keratinocytes and the HaCaT cell line, which had high levels of CD9, showed 50-60% reduction of *S.aureus* adhesion on peptide treatment (Ventress et al., 2016). In the present study, CD9 is richly expressed across bladder cells, and it has been shown that CD9 reagents (anti-CD9 antibodies or peptides based on the EC2 domain of the tetraspanin CD9) can reduce the binding of various strains of UPEC to host cells. A possible scenario would be that those reagents may interact with host CD9 on the cell surface leading to disruption of the tetraspanin web structures and consequently disorganizing the adhesion platforms required by UPEC. There is supportive evidence of CD9-based peptides interacting with host cell membranes from confocal microscopy in this study. Furthermore, fluorescently-tagged 800 peptide interacts with primary keratinocytes while 800SCR was not shown to bind to the cell membrane (Ventress et al., 2016).

The use of primary cells is a more representative model of the human infection than immortalised cell lines. Despite the low expression of UPs at the cell surface, cell surface CD9 exists in high abundance on these cells (Figure 3.8 & Figure 4.5). Within the 33 tetraspanin members, only the FimH/UPIa complex has been identified as a direct bacterial interaction, but this bacterial receptor is absent *in vitro*, suggesting that bacteria are able to recognize alternative proteins present in TEM adhesion platforms. This findings in this Chapter indicate that CD9 is potentially important in organizing other molecules that are interacting directly with UPEC. To conclude, it has been shown that by blocking CD9, UPEC adhesion can be inhibited by up to 50-60%, suggesting that the CD9 tetraspanin is involved in bacterial infection.

Overall, this chapter has shown that CD9-derived reagents either antibody or synthetic peptides have some potential to increase the efficiency of reducing bacterial adhesion. Although high expression of CD81 found on the bladder

cells, CD81 does not show any anti-adhesive activity against UPEC adhesion. Using the LDH assay, tetraspanin-derived peptides do not affect bladder cells viability or bacterial growth. It has also been shown that anti-CD9 antibody stays at the cell surface and so CD9 molecules do not leave the cell membrane during the treatment time. Subsequently, this study suggests that tetraspanin-based reagents may provide a potential for anti-adhesion-based therapy to fight against bacterial infections.

Chapter 6: The effect of HSPGs in UPEC adhesion

6.1 Introduction: Proteoglycans and glycosaminoglycans in the urinary tract

As mentioned in Chapter 1, the bladder luminal surface is covered by a dense layer of glycosaminoglycans (GAGs), UP proteins, tight junctions, and adherence molecules in polarized distribution. Functionally, it provides a strong barrier protecting the bladder form urine solutes and pathogens (Khandelwal, Abraham and Apodaca, 2009). GAGs are known to interact with a core protein, forming a proteoglycan (Lilly and Parsons, 1990; Damiano and Cicione, 2011). Most of the total surface of GAG in human bladder is bound to integral membrane proteins, approximately half of the protein-bound GAG being heparan sulphate, 29% being CS, and the remainder either not identified or dermatan sulphates (Hurst and Zebrowski, 1994). The GAG-layer in normal bladder has a high density on the surface (Hurst, 1994; Slobodov et al., 2004), which mainly act as first line of defence against penetration of urinary toxic substance such as ammonia, urea and potassium into bladder muscle as well as bacterial adherence (Parsons, 1994; Damiano and Cicione, 2011). Work in the past demonstrated that bacterial adhesion may be increased as a result of damage to the GAG layer in bladder epithelium (Parsons, 1997). Previous studies have been shown an increased in *E. coli* binding to rabbit bladder up to 100-fold after GAG layer removal and heparin treatment were able to prevent bacterial binding to these deficient bladders (Parsons, Greenspan and Mulholland, 1975; Fritz et al., 1981; Parsons, 1997). Another study by Ruggieri et al in a rabbit model found that the adhesion of numerous common bacterial uropathogens, including *Escherichia coli, Klebsiella ozonae*, *Proteus mirabilis*, and *Streptococcus faecalis*, but not *Pseudomonas aeruginosa* ,was reduced when mucin-deficient rabbit bladders were exposed to heparin (Ruggieri, Hanno and Levin, 1984). Indeed, GAG replacement therapy with intravenous

instillations of hyaluronic acid and proteoglycans such chondroitin sulphate or heparin has been found to be a successful treatment option (Madersbacher, Ophoven and Kerrebroeck, 2013; Cicione et al., 2014; Dutta and Lane, 2018; Goddard and Janssen, 2018). Therefore, several exogenous GAG products that contain CS, hyaluronic acid, and heparin are being investigated in a wide range of urinary diseases such as IC and rUTIs. Although much evidence showed the efficiency of GAG-replenishment in the treatment of UTIs, this proposed therapy is not conclusive due to their small scale, lack of controls and non-randomised design (Cicione et al., 2014; Dutta and Lane, 2018; Goddard and Janssen, 2018; Negus, Phillips and Hindley, 2020). More prospective randomised trails are required, and *in vitro* model can be used to assess these anti-adhesive therapeutic agents.

As previously mentioned, tetraspanins are known to interact with various proteins at the cell surface, forming tetraspanin-enriched microdomains (TEMs). These proteins could be integrins, heparan sulphates proteoglycans (HSPGs) and immunoglobulin superfamily members (Umeda et al., 2020), which are considered to be important for bacterial adherence. We have demonstrated that CD9 expression is important for heparin inhibition of *S. aureus* adhesion to lung A549 cells (Green et al, manuscript submitted to PLOS Pathogens). We also have demonstrated that CD9 is involved in bacterial adherence to bladder cells as described in Chapter five. Therefore, it was valuable to investigate the role of GAGs, mainly HS/heparin and CS/DS on UPEC binding to the applied in vitro model in this project.

6.2 Result

6.2.1 Involvement of heparin and heparan sulphate (HP/HS) in UPEC adherence.

Bladder cells were treated with unfractionated heparin (UFH) and then infected with UPEC as described (section 2.2.5.3). Bladder cells RT4, 5637 and primary bladder cells infected with the multidrug resistant pathogen EC985 strain were used in this study. Unfractionated heparin (UFH) was tested as a commercial form of heparin (Table 2.13). Different concentrations were initially tested from 5-100 U/ml in RT4 cells (Figure 6.1-A). A maximum inhibition of UPEC (EC985 strain) adherence to RT4 cells of about 80% at a concentration of 50 U/ml was observed, indicating that this inhibitory impact of UFH was biphasic since it was less effective at higher concentrations. Similar results were observed in primary bladder cells and 5637 cells, with about 80% reduction of bacterial adherence at similar effective dose (50 U/ml) (Figure 6.1-B).

Dalteparin and Fondaparinux, which are low molecular weight heparin analogues (Table 2.13) were also tested on RT4 cells. Reductions in UPEC adherence to RT4 cells of about 40% were observed when cells were pre-treated with these molecules (Figure 6.2-A). Heparan sulphate (HS) and dermatan sulphates (DS) were also used to pre-treat RT4 cells, resulting in a significant decrease in UPEC adherence of about 40% at 100 µg/ml (Figure 6.2-A).

Reduction of UPEC adherence by heparin analogues and LMWH suggests that HSPGs are involved in UPEC adherence. To further investigate this, adherence of UPEC to bladder cells was measured after digestion of HS from the cell surface using heparinase (section 2.2.5.4). Treatment with a mixture of 0.5 U/ml heparinase I/II caused a significant reduction of UPEC adherence to bladder cells with about 30% compared to untreated cells (Figure 6.2-B). PG545 (pixatimod), which has known anti- heparanase activity and is a HS mimetic (Dredge et al., 2018), was also tested in a range between 10-100 µg/ml (Figure 6.3-A). We noticed disruption of the cell monolayer and the cells did not look healthy after treatment with 20 to 100 µg/ml PG545. Therefore, measurement

of LDH in each experiment was important to check cell viability (Figure 6.3-B). We found that PG545 at 50 µg/ml gives a significant reduction of UPEC binding of about 70%, with a slightly varied but insignificant effect on cell viability (Figure 6.3). Overall, the results obtained indicate that HS chains play a crucial role in mediating UPEC adherence.

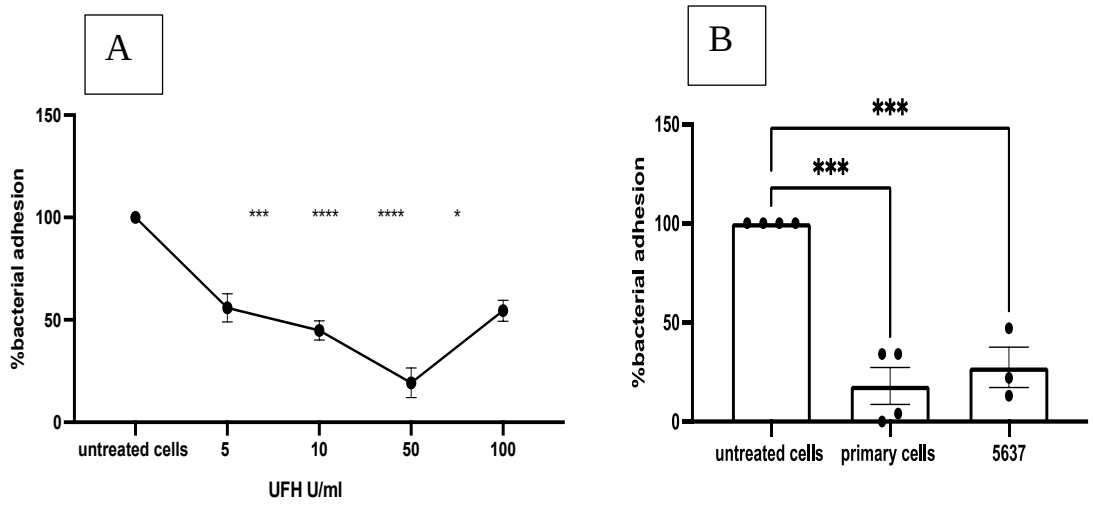

Figure 6.1: Effect of UFH on the adherence of UPEC strain to bladder cells.

Adherent bladder cells in 96 well plates were pre-treated with UFH for 1 hr then infected with UPEC (EC958 strain) for 1 hr (MOI 10). Cells were washed three times with PBS, lysed with 1% Triton X-100 and bacteria plated on LB agar plates to determine cfu (section 2.2.5.3). (A) dose: response curve of the effect of UFH pre-treatment on EC958 adherence to RT4 cells. (B) Effect of UFH on the adherence of EC958 to primary bladder and 5637 cells. The data represent the means, while error bars describe standard error means. n ≥3 independent experiments, performed in four replicates Data was analysed by *t*-test against untreated cells where ** $p \leq 0.01$, * $p \leq 0.05$ and ns is non- significant.

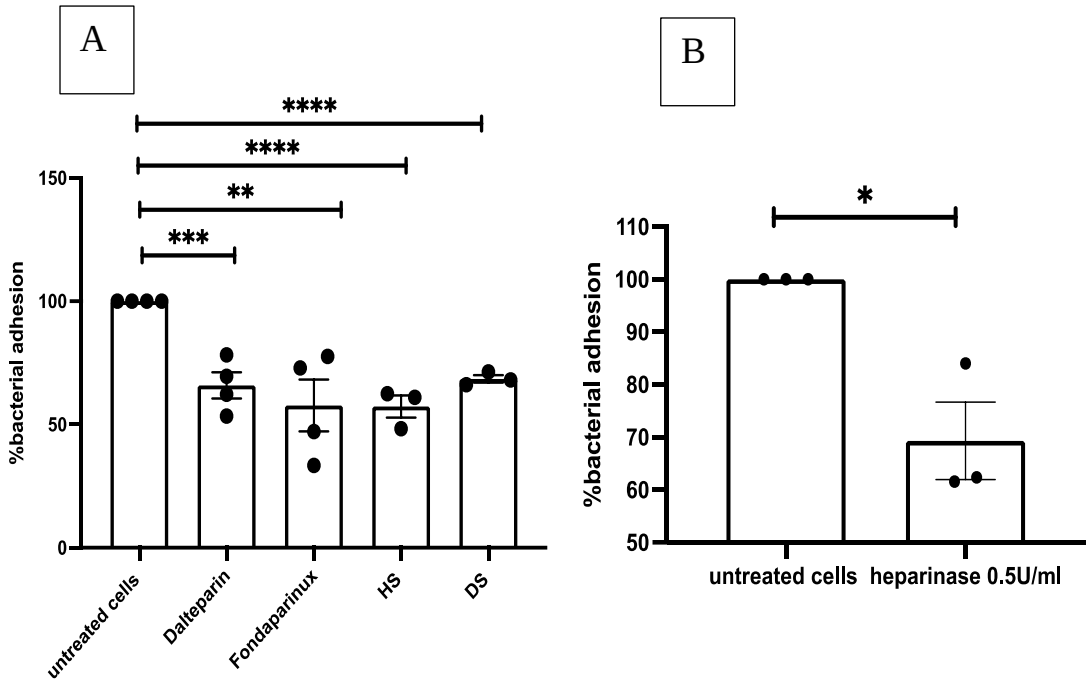

Figure 6.2: Effect of on HSPG analogues on the adherence of UPEC to RT4 cells.

RT4 cells were pre-treated with LMWH Dalteparin (200 U/ml) or Fondaparinux (10 µg/ml) as well as HS or DS (100 µg/ml), then infected with EC958 for 1 hr. The bacterial adherence was calculated as described previously (section 2.2.5.3). (B) RT4 were pre-treated with 0.5 U/ml of a mixture of heparinase I/III for 3 hr, followed by a quick wash then infected with EC958 for 1 hr as described previously (section 2.2.5.4). The data represent the means, while error bars describe standard error means. n ≥3 independent experiments, performed in four replicates. Data was analysed by *t*-test against untreated cells where ** $p \leq 0.01$, * $p \leq 0.05$ and ns is non-significant.

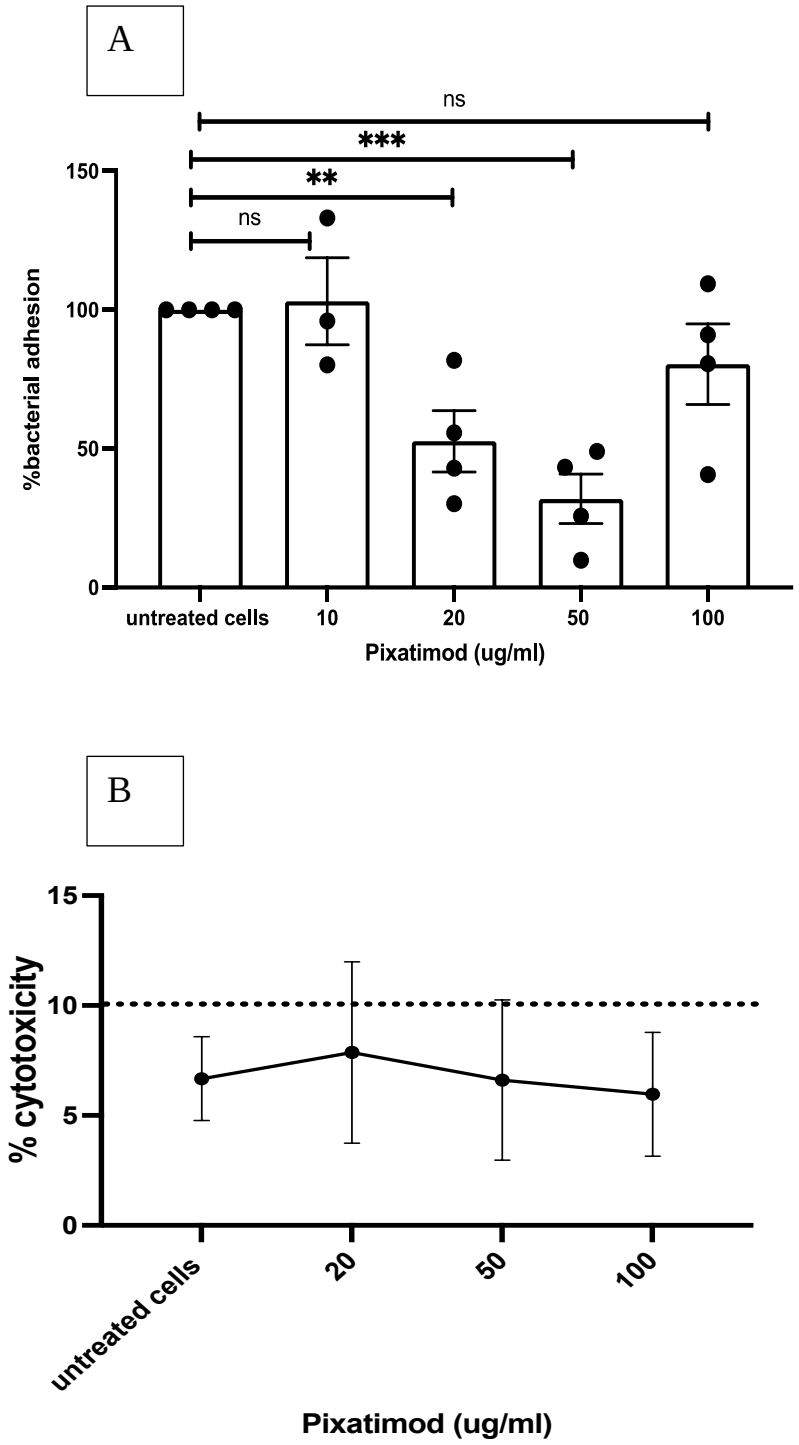

Figure 6.3: Effect of pixatimod (PG545) on the adherence of UPEC to RT4 cells.

Adherent RT4 cells were pre-treated with pixatimod over a range of concentrations then infected with EC958 strain for 1 hr. The bacterial adherence was calculated as described previously (section 2.2.5.3). (B) Effect of different concentrations of pixatimod on RT4 viability. Briefly, cell monolayers were pre-treated with pixatimod or buffer (non-treated control) for 1hr. LDH release into the supernatant was then measured and used to determine % cytotoxicity as described (section 2.2.2.5). The data represent the means, while error bars describe standard error means. n ≥3 independent experiments, performed in triplicates. Data was analysed by t-test against untreated cells where ** $p \leq 0.01$, * $p \leq 0.05$ and ns is non-significant.

6.2.2 Chondroitin sulphates as an effective treatment in reducing UPEC adherence.

To study the role of chondroitin sulphates (CS), another major class of GAGs, in UPEC adherence two types of assays were performed: by applying commercial CS-A on bladder cells as described in 2.2.5.3) or by removing CS chain from the cell surface using chondroitinase (section 2.2.5.4). Initially, different concentrations of CS-A were tested to determine the effective dose in a range between 50-500 µg/ml (Figure 6.4-A). As shown in Figure 6.4-A, pre-treatment of RT4 cells with 100 µg/ml of CS-A caused a significant decrease in the binding of UPEC to the cells of about 60%. Furthermore, a significant reduction, around 35%, of UPEC adhesion was observed when using 0.25 U/ml of chondroitinase (Figure 6.4-B). Together, these results indicate an important role for chondroitin sulphates in the binding between UPEC and bladder cells.

6.2.3 Effect of UFH on bacterial growth

For further understanding the mechanisms of heparin on urothelial cells, we investigated whether heparin affects the pathogen growth/viability. Therefore, we tested bacterial growth in the absence and presence of heparin as described (section 2.2.4.3). We found that bacterial growth was similar in media contained 50 U/ml of heparin compared to control conditions (LB broth alone) (Figure 6.5-A). Also, there was no big difference in the viable bacteria counts between these two conditions (Figure 6.5-B). This indicates that the effects of heparin on bacterial adhesion is not due to any deleterious effects on the bacteria themselves.

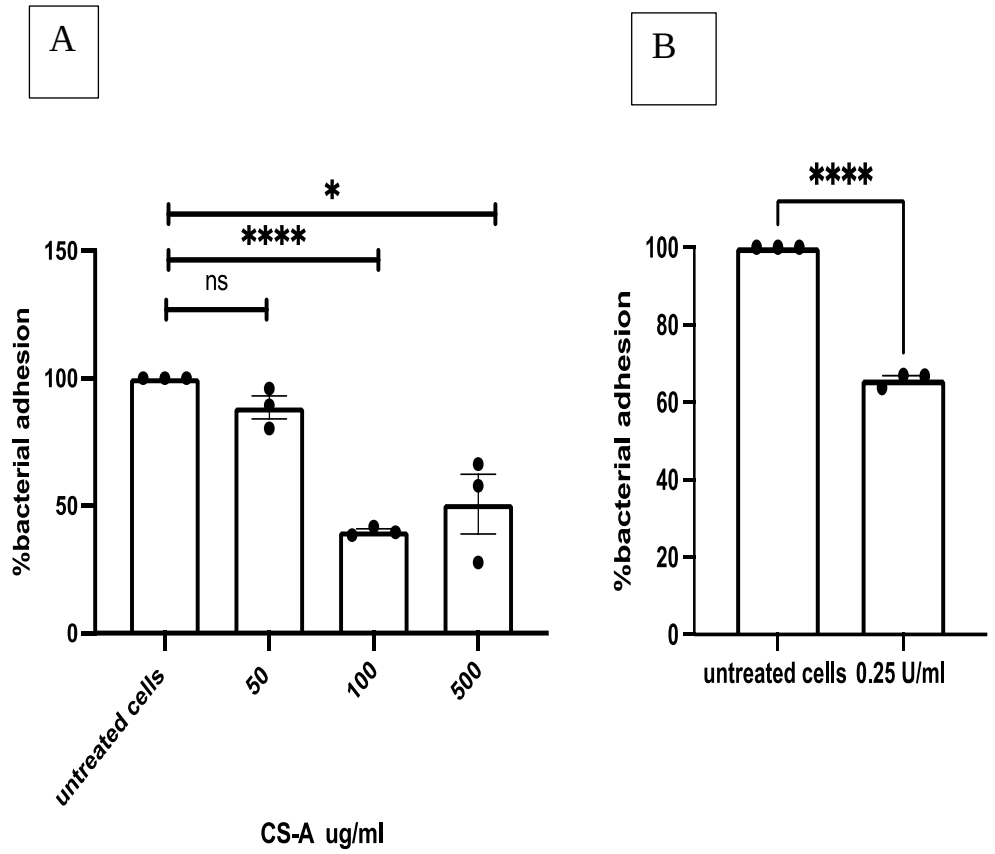

Figure 6.4: Effect of chondroitin sulphate (CS-A) on the adherence of UPEC to RT4 cells.

(A) Adherent RT4 cells were pre-treated with CS-A over a range of concentrations then infected with EC958 for 1 hr. The bacterial adherence was calculated as described (section 2.2.5.3). (B) RT4 were pre-treated with 0.25 U/ml of chondroitinase for 3 hr, followed by a quick wash then infected with EC958 for 1 hr as described (section 2.2.5.4). The data represent the means, while error bars describe standard error means. n=3 independent experiments, performed in triplicates. Data was analysed by *t*-test against untreated cells where ** $p \leq 0.01$, * $p \leq 0.05$ and ns is non-significant.

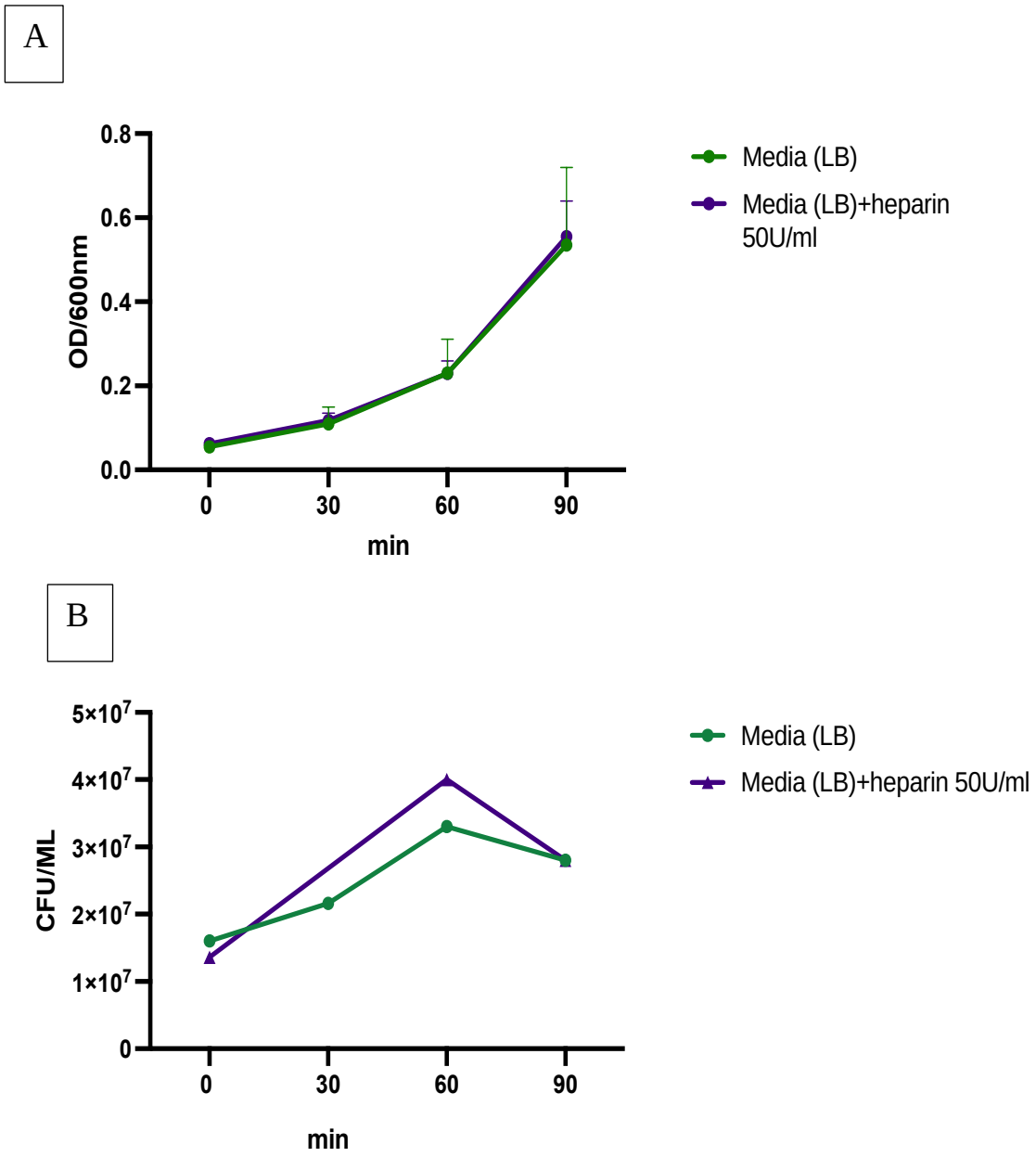

Figure 6.5: Growth of UPEC pathogen in the presence of UFH.

EC958 bacteria were grown in LB broth alone (control) or in the presence of 50 U/ml final concentration of UFH. (A) Bacterial growth was assessed by measuring the OD of the culture at 600nm and by (B) CFU counting at times indicated as described in (section 2.2.4.3). Bacterial growth was assessed by measuring the OD of the culture at 600nm and by CFU counting at times indicated as described in (section 2.2.4.3). The data represent the means, while error bars describe standard error means. n=3 independent experiments.

6.3 Discussion

From the previous chapter, CD9 was demonstrated to be involved in UPEC adherence. CD9 has been shown to be associated with a number of HSPGs including syndecans (Jones, Bishop and Watt, 1996). Our group has shown previously that treatment of WT A549 cells with unfractionated heparin (UFH) or LMWH significantly reduced *S.aureus* adherence to these cells. In contrast, no effect of UFH and LMWH was observed in A549 cells where the CD9 gene had been knocked out, suggesting that CD9 is important for the heparin activity. In addition, treatment of WT A549 cells with a combination of UFH and the CD9 synthetic peptide 800C had shown no further additional effects on *S.aureus* adhesion, suggesting they are affecting the same mechanism (Green et al., manuscript submitted to PLOS Pathogens). Therefore, it was considered worth investigating the role of HSPG in UPEC adherence.

Exogenous GAG products such as hyaluronic acid and chondroitin sulphate have been used clinically to try to replace the bladder cells GAG layer, where this has become deficient. The trials, however, were relatively small and not well-controlled and the mechanism of action was not investigated (Cicione et al., 2014; Goddard and Janssen, 2018; Negus, Phillips and Hindley, 2020). Therefore, it would be worth studying the effects of GAGs in bacterial adherence and the mechanism of action in a tissue rather than giving GAGs to patients and evaluating the results based on placebo studies (Damiano and Cicione, 2011; Negus, Phillips and Hindley, 2020). In this study, we have demonstrated that UFH and heparin analogues including, LMWH and heparan sulphate had a significant inhibition of UPEC adhesion to bladder cells, as did pre-treatment of the cells with heparinase. UFH inhibited 80% of UPEC adherence to bladder cells (Figure 6.1), whereas the CD9 synthetic peptide 800C was slightly less effective with a maximum 40% reduction of EC985 adhesion (**Error! Reference source not found.**), indicating that heparin is more active than CD9 peptide 800C for UPEC adhesion. We also demonstrated that HS, which is known to bind to PGs in the luminal layer of the urothelium (Hurst, 1994), reduced UPEC adherence to a similar extent as CD9 peptide 800C (Figure 6.2). Interestingly, our group recently observed that UFH inhibited

the binding of recombinant S1S2 SARS-cov-2 spike protein to RT4 cells by about 80% (Partridge, Green and Monk, 2020).

More recently, a significant reduction of staphylococcal adherence to keratinocytes, corneal and intestinal epithelial cells was observed with UFH, varying between 50-70% inhibition (Green et al., manuscript submitted to PLOS Pathogens). LMWH and heparan sulphate (HS) showed a significant inhibition of UPEC adhesion, but with lower efficacy than UFH (Figure 6.1 & Figure 6.2), suggesting that UFH could be used as an anti-adhesive therapeutic for UTI patients. Heparin is already used in catheter lock solutions as an anticoagulant (Gray, Hogwood and Mulloy, 2012), therefore further considerations are required for a role in treating bladder infection.

Pixatimod PG545, an HS-mimetic used at the clinical stage with significant anti-cancer and anti-inflammatory properties (Hammond and Dredge, 2020), also had a significant anti-adhesive activity against UPEC at concentrations from 20 to 50 µg/ml (Figure 6.3-A). Investigation of pixatimod cytotoxicity for RT4 cells using LDH assay revealed that although the cells underwent a morphology change, they remained viable (Figure 6.3-B). In retrospect, it may have been better to use another assay such as the sulforhodamine B (SRB) assay (Skehan et al., 1990), which gives an indication of cell number, as the cells may have been coming off the plate. Pixatimod has also been reported by our group to inhibit staphylococcal adherence (Green et al., manuscript submitted to PLOS Pathogens). Pixatimod has also been shown to have antiviral effect against viruses that utilise HS as receptors, including SARS-COV-2, HSV-2, HIV, RSV, and Dengue Fever (Said et al., 2010, 2016; Lundin et al., 2012; Modhiran et al., 2019; Guimond et al., 2021).

This study indicates that HSPGs may be directly utilised by UPEC strains or in co-operation with other partner proteins such as integrins. Although previous reports have demonstrated that α3β1 integrins were functionally the main receptors for Type 1 fimbriae within bladder cells, it has been suggested that other receptors could be involved (Eto et al., 2007). Various pathogens utilise HSPGs to gain the entry into the host cells: *Helicobacter pylori*, *Streptococcus pyogenes*, *Neisseria* sp., *Yersinia* sp., *Staphylococcus* sp. (Duensing, Wing and

Van Putten, 1999; Ivan Fernandez Vega, 2014). In addition, different strains of *E.coli* ,such as EXEC and ETEC, have been extensively studied in the past, which showed the binding to HSPGs, including fibronectin and vitronectin, but UPEC strains were not well-studied (Fröman et al., 1984; Chhatwal et al., 1987; FARis et al., 1988; Fleckenstein, Holland and Hasty, 2002).

Pre-treatment with chondroitin sulphate (CS) resulted in a significant decrease in bacterial adherence to bladder cells by 60% (Figure 6.4). Furthermore, a significant reduction was observed when cells were treated with chondroitinase ABC (by 35%), confirming that CS is involved in bacterial adhesion (Figure 6.4). Similar results have been previously found by Rajas and his colleagues, where treatment with either chondroitinase ABC or heparinases I/III were able to reduce the adherence of *S. aureus* by 30% in A549 cells (Rajas et al., 2017). Although treatment with CS is commonly used for UTI patients, the mechanisms of action of this molecule has not been well-studied. The main idea for the application of CS, mostly used in a combination with HA, is to restore the GAGs-layer in order to recover any damage and improve the barrier function of urothelium (Damiano et al., 2011; De Vita and Giordano, 2012; Madersbacher, Ophoven and Kerrebroeck, 2013); subsequently, this could decrease bacterial binding (Rozenberg et al., 2019). A previous study showed that inhibition of *Enterohemorrhagic E coli* (EHEC) O157:H7 binding to human colonic epithelial cells is specific to heparin and HS since CS had no effect (Gu, Wang, Y. L. Guo, et al., 2008). Also, heparinase treatment showed no effect in this study, suggesting that HS could interact with β1 integrins; heparin and HS blocked bacterial adhesion to immobilised, purified integrins (Gu, Wang, Y.-L. Guo, et al., 2008). This present study indicates that GAGs are specifically involved in UPEC adherence since heparinase had a significant reduction of UPEC adhesion.

Although DS is present at slightly lower abundance than HS and CS in the GAGs-layer (Hurst and Zebrowski, 1994), it seems that DS also play a role in UEPC adherence. As shown in (Figure 6.2), UPEC adherence to RT4 cells was significantly reduced when pre-incubated with dermatan sulphate (DS), suggesting that GAGs associated with bladder include HS, CS, and DS is

involved in UPEC adherence. We also have demonstrated in this chapter that unfractionated heparin does not affect the growth or viability of the pathogen, indicating that heparin is specifically working on host cells. In summary, whilst previous studies have not identified GAGs a being potentially important in UPEC adhesion, this study demonstrated the critical important of GAGs present in bladder cells (mainly HS, CS and DS) for UPEC adherence. These results are promising, highlighting the potential of heparins as anti-adhesive therapeutics for pathogens in urinary infections.

Chapter 7: Final Discussion

7.1 General discussion

UTIs are a severe public health problem that affect over 150 million people worldwide each year (Motse et al., 2019). Uropathogenic *Escherichia coli* (UPEC) is responsible for 80–90% of UTIs. Antibiotics are frequently used to treat these infections (Abou Heidar et al., 2019). As a result, UPEC strains are becoming more resistant to antibiotics, and in some cases have become multidrug-resistant bacteria (MDR), and this is similar to the global rise in antibiotic resistance that has been documented (Dehbanipour et al., 2016; Lee, Lee and Choe, 2018; Karam, Habibi and Bouzari, 2019; Kot, 2019; Signing et al., 2020; Arsene et al., 2021; Guimond et al., 2021). It is therefore becoming important to search for alternatives such as anti-adhesive therapeutics that prevent the initial attachment stages of bacterial infections. Work from our group indicates that TEM is implicated in the adhesion of a wide range of bacteria, including *Staphylococcus aureus*, *Neisseria meningitidis*, *Salmonella enterica*, *Streptococcus pneumoniae, Burkholderia thailandensis* and *Pseudomonas aeruginosa.* More recently, HSPGs have been shown to be involved in CD9-mediated staphylococcal adherence (Green et al, manuscript submitted to PLOS Pathogens).

The ability of UPEC to attach and invade a wide range of bladder cell lines has commonly been studied (Mulvey, 2002; Bower, Eto and Mulvey, 2005; Dhakal and Mulvey, 2009, 2012; Kim et al., 2018; Scharf et al., 2020), so it was considered worthwhile to investigate the involvement of TEM in the infection process in this project. In the present study, different cell lines and primary bladder cells, representing human bladder epithelial cells, were used to investigate the effect of two potential anti-adhesive therapeutic, CD9-derived reagents and GAG products, on UPEC infection.

In the first stage of this project, the surface expression of the most commonly expressed tetraspanins (including CD9) and UPIa and UP1b was investigated since these molecules were considered candidate bacterial receptors either in co-operation with other partner proteins or independently.

In Chapters 3 & 4, CD9 and CD81 were shown to be extensively present at the cell surface, while studies with permeabilized and non-permeabilized cells showed only intracellular localization of uroplakin proteins. We also found that the gene expression of tetraspanins was not strongly correlated with expression at the protein level. This led us to attempts to develop a model that could differentiate the bladder cell lines. Two approaches have been used in this study using UP expression as a specific correlate of terminal urothelial differentiation. Previous investigations reported that E medium promoted epithelial differentiation, by looking at the expression of UPs at the gene and protein level (Thumbikat, Berry, Schaeffer, et al., 2009). We observed that this culture medium induced only a significant increase in gene expression of the UPs, mainly UPIa. Meanwhile, UPIa was the only uroplakin that showed a slight increase in expression at the protein level at both cells, but it should be noted that the expression of UPIa remained intracellular. This result was different from the previous study where E medium was shown to induce all UP proteins (Thumbikat, Berry, Schaeffer, et al., 2009); however this expression was detected by using immunoblotting, which did not give information about the localization of the protein. Also, the previous study did not report any statistical analysis of differences between the two conditions. Another approach was to culture the BECs in medium in the absence of growth factors in order to suppress proliferation and stimulate differentiation (Sun, 2006). Although this condition successfully induced UPIa expression at gene and protein level, particularly in RT4 cells, this protein remained intracellular. Taken together, these data demonstrated that terminal differentiation features are difficult to achieve in cell lines despite some conditions promoting increased UP mRNA expression.

Many groups have used bladder cell lines for research on UPEC infections, including studies aimed at investigating FimH antagonists that might interfere

with adherence to UP1a (Scharenberg et al., 2011; Kurimura et al., 2012). However, as far as we are aware, the absence of UP1a on the surface of undifferentiated bladder epithelial cell lines has not been reported. From our finding, it appears that such cell lines are not really suitable for investigating UPEC adhesion that relies on surface UP1a expression. Furthermore, our work indicates that UPEC can use alternative mechanisms to adhere to human bladder epithelial cells. This led us to investigate the role of other tetraspanins in UPEC adhesion.

The overall results in Chapter 5 show a significant reduction of UPEC adhesion after treating the bladder epithelial cell models with anti-CD9 prior to UPEC infection (**Error! Reference source not found.**& **Error! Reference source not found.** & **Error! Reference source not found.**). This is consistent with previous studies as it has been found that anti-CD9 antibody inhibited adhesion of a wide range of bacteria including *E.coli* to human epithelial cell lines (Green et al., 2011). However, there were no effects with anti-CD81, despite CD81 being expressed at high levels on BECs (Figure 3.2) and reports of the involvement of this antigen in infection by other types of bacteria (Hassuna et al., 2017). This indicates that CD81 has no role in UPEC adhesion to bladder cells.

We also showed that a peptide based on the EC2 domain of CD9 reduced the adherence of UPEC strains to bladder cells, and that the efficacy of this peptide correlates approximately with the presence of CD9 on host cells. Confocal microscopy and fluorescence imaging support the idea that this peptide is associating with the native membrane CD9 in RT4 and A549 cells, since no significant interaction was seen on CD9KO A549 cells. This indicates that this peptides adhesion activity is specific to CD9 and could potentially be acting by disrupting the organization of CD9-containing adhesion platforms that bacteria use to stick to the cell membrane. Our findings add to others that CD9 is involved in bacterial adherence to host cells. Short CD9 EC2-derived peptides have shown to be able to significantly reduce staphylococcal adherence to keratinocytes and in an ex vivo human skin infection model (Ventress et al., 2016). The maximum reduction in bacterial adhesion by the CD9-EC2 peptide

is roughly 60% across all bacteria tested and various epithelial cells derived from lung, corneal, intestinal, skin and bladder cells (Ventress et al., 2016; Green et al., manuscript submitted to PLOS pathogens). The lack of complete inhibition would support the idea that bacteria can also utilize non-tetraspanin adhesion mechanisms to adhere to cells (Green et al., manuscript submitted to PLOS pathogens). Similar effects have previously been observed with anti-tetraspanin antibodies (Cozens, 2015, PhD thesis, University of Sheffield). Further research is required to determine the dynamics of action of the peptide and whether it interacts specifically with the EC2 domain region of CD9 or randomly interferes with TEM organization.

In chapter 6, we identified a critical role of HSPGs which are richly present in bladder epithelial cells for UPEC adherence. HSPGs have also recently been shown to be important in the adhesion of *S. aureus* to human cells, since heparin and heparin analogues inhibit this interaction. It should be noted that CD9 is critical for heparin activity since in the absence of CD9 no effect of UFH was observed (Green et al., manuscript submitted to PLOS pathogens). We found that UFH and heparin analogues such as LMWH, and heparan sulphate and also pre-treatment of cells with heparinise I/III, significantly inhibited UPEC adhesion. UFH inhibited 80% of UPEC adherence to bladder cells, while staphylococcal adherence showed a maximum reduction of around 70% in intestinal epithelial cells (Green et al., manuscript submitted to PLOS pathogens). We also demonstrated that CS is involved in UPEC adhesion, in contrast to a previous study that CS showed no effect of *E.coli* binding to colonic epithelial cells (Gu, Wang, Y. L. Guo, et al., 2008). The present study confirmed the role of CS as well as DS in the UPEC adherence. Multiple bacteria and viruses which are known to invade the urogenital tract have been shown to utilize cell surface HS (Aquino and Park, 2016). Our study adds a significant input to the increasing body of evidence that suggests that heparin could be used as an anti-adhesive therapeutic for UTIs. Hence, we could propose that UPEC use GAG to access BECs and further investigation is needed in order to develop new and effective antimicrobials.

In summary, the rising cost of antibiotic resistance, as well as its health consequences, has generated interest in using non-antibiotic strategies for preventing UTIs. Anti-adherence compounds are novel approaches in the treatment of this infection. In this study, tetraspanin-based reagents show some promise in terms of infection control practices. Furthermore, heparin showed a direct inhibition of UPEC adherence. Heparin (UFH) has a number of advantages, including low toxicity, inexpensive, and simple to use, as well as the fact that bacteria have yet to develop resistance to them.

7.2 Limitation

There are several limitations to this study, mainly due to the Covid-19 pandemic, and also limited funding and time. A major issue we found was that no monoclonal UPIa and UPIb antibodies are available. Therefore, rabbit polyclonal antibodies were used, but the rabbit isotype control gave high backgrounds in flow cytometry making it difficult to investigate the UPs expression. To tackle this, the t-test values were always calculated to compare values obtained between the isotype control and the anti-UP antibody to detect the expression.

Moreover, tetraspanin gene expression of RT4 cells could not be studied due to closure of the Core Genomic Facility in the University of Sheffield during the pandemic. We also had planned to look at the biofilm formation in BECs, and then to treat the cells with potential anti-adhesion agents to evaluate their efficiency in UPEC infection under flow condition using the Bioflux machine. This system is available in Sheffield Collaboratorium for Antimicrobial Resistance and Biofilms (SCARAB), which has recently been established in Chemical and Biological Engineering, University of Sheffield. Unfortunately, the Department was closed, and visitors could not access this building during the lockdown.

The initial idea behind this work was that tetraspanin-based peptide derived from UPIa might be used as a potential target and treat UTI. However, bladder cancer cells have many limitations including mainly lack of UPs expression at the cell surface (as demonstrated in the present study), and possible genetic

drift as a result of long-term culture. We could not therefore test the role of UPIa in the UPEC adherence. Hence, several differentiation approaches have been proposed in this study. It would be good to try growing the cells in organoid culture, but this model required optimisation, and there was not enough time to go through this process. This was not in the main objectives of this project, but it would be useful to be consider it for future works.

Another issue was that when the cells were grown in serum free medium (for attempts to differentiate them), they died immediately after trypsinisation, making it difficult to carry out flow cytometry experiments. Therefore, I tended to use confocal microscopy which was more expensive. Finally, *in vivo* studies were not included in the present work, but it would be interesting to fully understand the role of different molecules such as heparin, CD9 and UPIa in UPEC infection in an animal model. This might be addressed for future work.

7.3 Future direction

Ultimately, it is strongly advisable to use a more mature model such as a mouse model of UTI for this type of project. Although this in vitro study should be considered as a first step, it would be worth validating the anti-adhesive activity of these therapeutic agents in an in vivo model and to verify the physiological relevance to the in vitro studies.

Also, more efforts in the differentiation study of bladder cells are needed, such as the advanced model published more recently that involves growing BECs on a chip (Sharma et al., 2021). This model could provide a valuable tool for further understanding of how UPEC access the cells and how efficient the treatments described in this thesis are at removing them. Although the differentiation approaches applied here did not show promising results, it would be worth investigating the expression of other non-UPs marker such as CK20. This could again be considered for future work. Another point is that HSPG was shown to be involved in the UPEC adherence and HSPGs including syndecans are known to be associated with CD9 (Jones, Bishop and Watt, 1996). It would be worth testing the involvement of syndecans such as SDC-1 and SDC-4 in UPEC adherence by using antibody blockade. This could be addressed for next future

work. Finally, we can advise that it would be useful to study the effect of CD9 peptide as well as heparin on bladder infection under flow conditions as discussed above.

Bibliography

Abou Heidar, N. F. *et al.* (2019) 'Management of urinary tract infection in women: A practical approach for everyday practice', *Urology annals*. Wolters Kluwer--Medknow Publications, 11(4), p. 339.

Adachi, W., Okubo, K. and Kinoshita, S., 2000. Human uroplakin Ib in ocular surface epithelium. *Investigative ophthalmology & visual science*, *41*(10), pp.2900-2905.

Alteri, C. J., Smith, S. N. and Mobley, H. L. T. (2009) 'Fitness of Escherichia coli during urinary tract infection requires gluconeogenesis and the TCA cycle', *PLoS pathogens*, 5(5), p. e1000448.

Alva-Murillo, N., López-Meza, J. E. and Ochoa-Zarzosa, A. (2014) 'Nonprofessional phagocytic cell receptors involved in Staphylococcus aureus internalization', *BioMed research international*, 2014.

Anderson, G. G. *et al.* (2003) 'Intracellular bacterial biofilm-like pods in urinary tract infections', *Science*, United States, 301(5629), pp. 105–107. doi: 10.1126/science.1084550.

Andersson, L. C., Nilsson, K. and Gahmberg, C. G. (1979) 'K562—A human erythroleukemic cell line', *International Journal of Cancer*. John Wiley & Sons, Ltd, 23(2), pp. 143–147. doi: 10.1002/ijc.2910230202.

Ang, J. *et al.* (2004) 'CD151 protein expression predicts the clinical outcome of low-grade primary prostate cancer better than histologic grading: A new prognostic indicator?', *Cancer Epidemiology Biomarkers and Prevention*, 13(11), pp. 1717–1721.

Apodaca, G. (2004) 'The uroepithelium: Not just a passive barrier', *Traffic*, 5(3), pp. 117–128. doi: 10.1046/j.1600-0854.2003.00156.x.

Aquino, R. S. and Park, P. W. (2016) 'Glycosaminoglycans and infection', *Frontiers in bioscience (Landmark edition)*. NIH Public Access, 21, p. 1260.

Arsene, M. M. J. *et al.* (2021) 'Antagonistic effects of raffia sap with probiotics against pathogenic microorganisms', *Foods and Raw materials*, 9(1), pp. 24–31.

Asadi, A. *et al.* (2019) 'A review on anti-adhesion therapies of bacterial diseases', *Infection*. Springer, 47(1), pp. 13–23.

Asadi Karam, M. R., Habibi, M. and Bouzari, S. (2019) 'Urinary tract infection:

Pathogenicity, antibiotic resistance and development of effective vaccines against Uropathogenic Escherichia coli', *Molecular Immunology*, 108, pp. 56–67. doi: 10.1016/j.molimm.2019.02.007.

Ashkar, A. A. *et al.* (2008) 'FimH adhesin of type 1 fimbriae is a potent inducer of innate antimicrobial responses which requires TLR4 and type 1 interferon signalling', *PLoS Pathogens*, 4(12). doi: 10.1371/journal.ppat.1000233.

Baglo, Y. *et al.* (2014) 'Enhanced efficacy of bleomycin in bladder cancer cells by photochemical internalization', *BioMed Research International*, 2014. doi: 10.1155/2014/921296.

Bandyopadhyay, S. *et al.* (2006) 'Interaction of KAI1 on tumor cells with DARC on vascular endothelium leads to metastasis suppression.', *Nature medicine*, 12(8), pp. 933–938. doi: 10.1038/nm1444.

Barber, A. E. *et al.* (2016) 'Strengths and Limitations of Model Systems for the Study of Urinary Tract Infections and Related Pathologies', *Microbiology and Molecular Biology Reviews*, 80(2), pp. 351–367. doi: 10.1128/mmbr.00067-15.

Barreiro, O. *et al.* (2008) 'Endothelial adhesion receptors are recruited to adherent leukocytes by inclusion in preformed tetraspanin nanoplatforms.', *The Journal of cell biology*, 183(3), pp. 527–542. doi: 10.1083/jcb.200805076.

Bartlett, A. H. and Park, P. W. (2010) 'Proteoglycans in host-pathogen interactions: Molecular mechanisms and therapeutic implications', *Expert Reviews in Molecular Medicine*,12, pp. 1–25. doi: 10.1017/S1462399409001367.

Bell, G. M. *et al.* (1992) 'The OX-44 molecule couples to signaling pathways and is associated with CD2 on rat T lymphocytes and a natural killer cell line.', *The Journal of experimental medicine*, 175(2), pp. 527–536. doi: 10.1084/jem.175.2.527.

Berditchevski, F. and Odintsova, E. (2007) 'Tetraspanins as regulators of protein trafficking', *Traffic*, 8(2), pp. 89–96. doi: 10.1111/j.1600-0854.2006.00515.x.

Bhushan, S. *et al.* (2011) 'Uropathogenic E. coli induce different immune response in testicular and peritoneal macrophages: Implications for testicular immune privilege', *PLoS ONE*, 6(12), pp. 1–15. doi: 10.1371/journal.pone.0028452.

Bien, J., Sokolova, O. and Bozko, P. (2012) 'Role of uropathogenic escherichia coli virulence factors in development of urinary tract infection and kidney damage', *International Journal of Nephrology*, 2012. doi: 10.1155/2012/681473.

Bishop, B. L. *et al.* (2007) 'Cyclic AMP-regulated exocytosis of Escherichia coli from infected bladder epithelial cells', *Nature Medicine*, 13(5), pp. 625–

630. doi: 10.1038/nm1572.

Bonkat, G. *et al.* (2018) 'Urological infections', *Arnhem: European Association of Urology*.

Bower, J. M., Eto, D. S. and Mulvey, M. A. (2005) 'Covert operations of uropathogenic Escherichia coli within the Urinary Tract', *Traffic*, 6(1), pp. 18–31. doi: 10.1111/j.1600-0854.2004.00251.x.

Brassesco, M. S. *et al.* (2013) 'In vitro targeting of Polo-like kinase 1 in bladder carcinoma: Comparative effects of four potent inhibitors', *Cancer Biology and Therapy*, 14(7), pp. 648–657. doi: 10.4161/cbt.25087.

Bubeník, J. *et al.* (1973) 'Established cell line of urinary bladder carcinoma (T24) containing tumour-specific antigen', *International Journal of Cancer*, 11(3), pp. 765–773. doi: 10.1002/ijc.2910110327.

Caretto, M. *et al.* (2017) 'Preventing urinary tract infections after menopause without antibiotics', *Maturitas*, 99, pp. 43–46. doi: https://doi.org/10.1016/j.maturitas.2017.02.004.

Carpenter, A. R. *et al.* (2016) 'Uroplakin 1b is critical in urinary tract development and urothelial differentiation and homeostasis', *Kidney International*, 89(3), pp. 612–624. doi: https://doi.org/10.1016/j.kint.2015.11.017.

Cattan, V. *et al.* (2011) 'Mechanical stimuli-induced urothelial differentiation in a human tissue-engineered tubular genitourinary graft', *European Urology*, 60(6), pp. 1291–1298. doi: 10.1016/j.eururo.2011.05.051.

Charrin, S. *et al.* (2009) 'Lateral organization of membrane proteins: Tetraspanins spin their web', *Biochemical Journal*, 420(2), pp. 133–154. doi: 10.1042/BJ20082422.

Charrin, S. *et al.* (2014) 'Tetraspanins at a glance', *Journal of Cell Science*, 127(17), pp. 3641–3648. doi: 10.1242/jcs.154906.

Chen, M. C., Mudge, C. S. and Klumpp, D. J. (2006) 'Urothelial lesion formation is mediated by TNFR1 during neurogenic cystitis', *American Journal of Physiology - Renal Physiology*, 291(4), pp. 741–749. doi: 10.1152/ajprenal.00081.2006.

Chen, Y. *et al.* (2008) 'Microbial subversion of heparan sulfate proteoglycans', *Molecules and Cells*, 26(5), pp. 415–426.

Chhatwal, G. S. *et al.* (1987) 'Specific binding of the human S protein (vitronectin) to streptococci, Staphylococcus aureus, and Escherichia coli', *Infection and immunity*, 55(8), pp. 1878–1883.

Cicione, A. *et al.* (2014) 'Intravesical treatment with highly-concentrated hyaluronic acid and chondroitin sulphate in patients with recurrent urinary tract infections: Results from a multicentre survey', *Journal of the Canadian*

Urological Association, 8(9-10), pp. E721–E727. doi: 10.5489/cuaj.1989.

Conover, M. S. *et al.* (2016) 'Inflammation-induced adhesin-receptor interaction provides a fitness advantage to uropathogenic E. coli during chronic infection', *Cell host & microbe*, 20(4), pp. 482–492.

Cross, W. R. *et al.* (2005) 'A biomimetic tissue from cultured normal human urothelial cells: Analysis of physiological function', *American Journal of Physiology - Renal Physiology*, 289(2 58-2), pp. 459–468. doi: 10.1152/ajprenal.00040.2005.

Cusumano, C. K. *et al.* (2011) 'Treatment and prevention of urinary tract infection with orally active FimH inhibitors', *Science translational medicine*. American Association for the Advancement of Science, 3(109), pp. 109ra115-109ra115.

Daher, A. *et al.* (2004) 'Growth, differentiation and senescence of normal human urothelium in an organ-like culture', *European Urology*, 45(6), pp. 799–805. doi: 10.1016/j.eururo.2004.01.002.

Damiano, R. *et al.* (2011) 'Prevention of recurrent urinary tract infections by intravesical administration of hyaluronic acid and chondroitin sulphate: A placebo-controlled randomised trial', *European Urology*. European Association of Urology, 59(4), pp. 645–651. doi: 10.1016/j.eururo.2010.12.039.

Damiano, R. and Cicione, A. (2011) 'The role of sodium hyaluronate and sodium chondroitin sulphate in the management of bladder disease', *Therapeutic Advances in Urology*, 3(5), pp. 223–232. doi: 10.1177/1756287211418723.

Decker, T. and Lohmann-Matthes, M. L. (1988) 'A quick and simple method for the quantitation of lactate dehydrogenase release in measurements of cellular cytotoxicity and tumor necrosis factor (TNF) activity.', *Journal of immunological methods*, 115(1), pp. 61–69. doi: 10.1016/0022-1759(88)90310-9.

DeGraff, D. J. *et al.* (2012) 'Loss of the urothelial differentiation marker FOXA1 is associated with high grade, late stage bladder cancer and increased tumor proliferation', *PLoS ONE*, 7(5). doi: 10.1371/journal.pone.0036669.

Dehbanipour, R. *et al.* (2016) 'High prevalence of multidrug-resistance uropathogenic Escherichia coli strains, Isfahan, Iran', *Journal of natural science, biology, and medicine*. Wolters Kluwer--Medknow Publications, 7(1), p. 22.

DeSalle, R., Mares, R. and Garcia-España, A. (2010) 'Evolution of cysteine

patterns in the large extracellular loop of tetraspanins from animals, fungi, plants and single-celled eukaryotes.', *Molecular phylogenetics and evolution*. United States, 56(1), pp. 486–491. doi: 10.1016/j.ympev.2010.02.015.

van Deventer, S. J., Dunlock, V.-M. E. and van Spriel, A. B. (2017) 'Molecular interactions shaping the tetraspanin web.', *Biochemical Society transactions*, 45(3), pp. 741–750. doi: 10.1042/BST20160284.

Dhakal, B. K., Kulesus, R. R. and Mulvey, M. A. (2008) 'Mechanisms and consequences of bladder cell invasion by uropathogenic Escherichia coli', *European Journal of Clinical Investigation*, 38(s2), pp. 2–11. doi: https://doi.org/10.1111/j.1365-2362.2008.01986.x.

Dhakal, B. K. and Mulvey, M. A. (2009) 'Uropathogenic escherichia coli invades host cells via an HDAC6-modulated microtubule-dependent pathway', *Journal of Biological Chemistry*, 284(1), pp. 446–454. doi: 10.1074/jbc.M805010200.

Dhakal, B. K. and Mulvey, M. A. (2012) 'The UPEC pore-forming toxin α-hemolysin triggers proteolysis of host proteins to disrupt cell adhesion, inflammatory, and survival pathways', *Cell Host and Microbe*, 11(1), pp. 58–69. doi: 10.1016/j.chom.2011.12.003.

Dornier, E. *et al.* (2012) 'Tspanc8 tetraspanins regulate ADAM10/Kuzbanian trafficking and promote Notch activation in flies and mammals', *Journal of Cell Biology*, 199(3), pp. 481–496. doi: 10.1083/jcb.201201133.

Dredge, K. *et al.* (2018) 'A Phase I study of the novel immunomodulatory agent PG545 (pixatimod) in subjects with advanced solid tumours.', *British journal of cancer*, 118(8), pp. 1035–1041. doi: 10.1038/s41416-018-0006-0.

Duensing, T. D., Wing, J. S. and Van Putten, J. P. M. (1999) 'Sulfated polysaccharide-directed recruitment of mammalian host proteins: A novel strategy in microbial pathogenesis', *Infection and Immunity*, 67(9), pp. 4463–4468. doi: 10.1128/iai.67.9.4463-4468.1999.

Duncan, M. J. *et al.* (2004) 'Bacterial Penetration of Bladder Epithelium through Lipid Rafts', *Journal of Biological Chemistry*, 279(18), pp. 18944–18951. doi: 10.1074/jbc.M400769200.

Dutta, S. and Lane, F. (2018) 'Intravesical instillations for the treatment of refractory recurrent urinary tract infections', *Therapeutic Advances in Urology*, 10(5), pp. 157–163. doi: 10.1177/1756287218757655.

Eldridge, G. R. *et al.* (2021) 'Safety and immunogenicity of an adjuvanted Escherichia coli adhesin vaccine in healthy women with and without histories of recurrent urinary tract infections: results from a first-in-human phase 1 study', *Human Vaccines and Immunotherapeutics*, 17(5), pp. 1262–1270. doi: 10.1080/21645515.2020.1834807.

Elgawidi, A. *et al.* (2020) 'A role for tetraspanin proteins in regulating fusion induced by Burkholderia thailandensis', *Medical Microbiology and*

Immunology, 209(4), pp. 473–487. doi: 10.1007/s00430-020-00670-6.

Elsinghorst, E. A. (1994) 'Measurement of invasion by gentamicin resistance', in *Methods in enzymology*. (Vol. 236, pp. 405-420). Academic Press.

Eschenbrenner, E. *et al.* (2020) 'TspanC8 tetraspanins differentially regulate ADAM10 endocytosis and half-life', *Life science alliance*. Life Science Alliance, 3(1).

Eto, D. S. *et al.* (2007) 'Integrin-mediated host cell invasion by type 1-piliated uropathogenic Escherichia coli', *PLoS Pathogens*, 3(7), pp. 0949–0961. doi: 10.1371/journal.ppat.0030100.

Fanaei, M., Monk, P. N. and Partridge, L. J. (2011) 'The role of tetraspanins in fusion', *Biochemical Society Transactions*, 39(2), pp. 524–528.

FARis, A. *et al.* (1988) 'Adhesion of Enterotoxigenic (ETEC) and Bovine Mastitis Escherichia coli Strains to Rat Embryonic Fibroblasts Role of Amino-Terminal Domain of Fibronectin in Bacterial Adhesion', *Microbiology and immunology*, 32(1), pp. 1–13.

Fernvik *et al.* (1995) 'Intracellular and surface distribution of CD9 in human eosinophils', *APMIS*. John Wiley & Sons, Ltd, 103(7-8), pp. 699–706. doi: https://doi.org/10.1111/j.1699-0463.1995.tb01426.x.

Ferreira-Coimbra, J., Sarda, C. and Rello, J. (2020) 'Burden of community-acquired pneumonia and unmet clinical needs', *Advances in therapy*, 37(4), pp. 1302–1318.

Fleckenstein, J. M., Holland, J. T. and Hasty, D. L. (2002) 'Interaction of an outer membrane protein of enterotoxigenic Escherichia coli with cell surface heparan sulfate proteoglycans', *Infection and Immunity*, 70(3), pp. 1530–1537. doi: 10.1128/IAI.70.3.1530-1537.2002.

Flores-Mireles, A. L. *et al.* (2015) 'Urinary tract infections: epidemiology, mechanisms of infection and treatment options', *Nature reviews. Microbiology*. 2015/04/08, 13(5), pp. 269–284. doi: 10.1038/nrmicro3432.

Fogh, J. (1978) 'Cultivation, characterization, and identification of human tumor cells with emphasis on kidney, testis, and bladder tumors', *National Cancer Institute monograph*, (49), p. 5—9. Available at: http://europepmc.org/abstract/MED/571047.

Forsberg, E. and Kjellén, L. (2001) 'Heparan sulfate: lessons from knockout mice', *The Journal of clinical investigation*. Am Soc Clin Investig, 108(2), pp. 175–180.

Foxman, B. (2002) 'Epidemiology of urinary tract infections: incidence, morbidity, and economic costs', *The American Journal of Medicine*, 113(1, Supplement 1), pp. 5–13. doi: https://doi.org/10.1016/S0002-9343(02)01054-9.

Foxman, B. (2010) ‘The epidemiology of urinary tract infection’, *Nature Reviews Urology*, 7(12), pp. 653–660. doi: 10.1038/nrurol.2010.190.

Foxman, B. (2014) ‘Urinary tract infection syndromes: occurrence, recurrence, bacteriology, risk factors, and disease burden.’, *Infectious disease clinics of North America*. United States, 28(1), pp. 1–13. doi: 10.1016/j.idc.2013.09.003.

Foxman, B. *et al.* (2015) ‘Cranberry juice capsules and urinary tract infection after surgery: results of a randomized trial’, *American journal of obstetrics and gynecology*, 213(2), pp. 194-e1.

Frick, I. M., Schmidtchen, A. and Sjöbring, U. (2003) ‘Interactions between M proteins of Streptococcus pyogenes and glycosaminoglycans promote bacterial adhesion to host cells’, *European Journal of Biochemistry*, 270(10), pp. 2303–2311. doi: 10.1046/j.1432-1033.2003.03600.x.

Fritz, W. *et al.* (1981) ‘UROLOGY HEPARIN - ADSORPTION EXAMINATION PROPERTIES * OF ITS ANTIBACTERILiL’, XVIII(3), pp. 273–276.

Fröman, G. *et al.* (1984) ‘Binding of Escherichia coli to fibronectin. A mechanism of tissue adherence.’, *Journal of Biological Chemistry*, 259(23), pp. 14899–14905.

Fujiyama, C. *et al.* (2001) ‘Human bladder cancer invasion model using rat bladder in vitro and its use to test mechanisms and therapeutic inhibitors of invasion.’, *British journal of cancer*, 84(4), pp. 558–564. doi: 10.1054/bjoc.2000.1641.

Gao, X. *et al.* (2018) ‘Cyclic hydrostatic pressure promotes uroplakin expression in human urothelial cells through activation of ERK1/2 signaling’, *Biochemical and Biophysical Research Communications*, 503(4), pp. 2499–2503. doi: 10.1016/j.bbrc.2018.07.006.

García, B. *et al.* (2016) ‘Different use of cell surface glycosaminoglycans as adherence receptors to corneal cells by gram positive and gram negative pathogens’, *Frontiers in Cellular and Infection Microbiology*, 6(NOV), pp. 1–12. doi: 10.3389/fcimb.2016.00173.

Giard, Donald J *et al.* (1973) ‘In Vitro Cultivation of Human Tumors: Establishment of Cell Lines Derived From a Series of Solid Tumors2’, *JNCI: Journal of the National Cancer Institute*, 51(5), pp. 1417–1423. doi: 10.1093/jnci/51.5.1417.

Giard, Don J *et al.* (1973) ‘In Vitro Cultivation of Human Tumorsfile:///C:/Users/LarsLanghanki/Downloads/1471-2164-8-171.pdf : Establishment of Cell Lines Derived From’, 51(5), pp. 1417–1423. Available at: http://citeseerx.ist.psu.edu/viewdoc/download;jsessionid=CDDE28DCC656DB33D0B5999FA72D7063?doi=10.1.1.878.55&rep=rep1&type=pdf.

Goddard, J. C. and Janssen, D. A. W. (2018) ‘Intravesical hyaluronic acid and chondroitin sulfate for recurrent urinary tract infections: systematic review and

meta-analysis', *International Urogynecology Journal*. International Urogynecology Journal, 29(7), pp. 933–942. doi: 10.1007/s00192-017-3508-z.

Goemaere, N. N. T. *et al.* (2008) 'Nitrofurantoin-induced pulmonary fibrosis: a case report', *Journal of medical case reports*. BioMed Central, 2(1), pp. 1–5.

Gokhale, A. S. and Satyanarayanajois, S. (2014) 'Peptides and peptidomimetics as immunomodulators', *Immunotherapy*. Future Medicine, 6(6), pp. 755–774.

Gomelsky, A. and Dmochowski, R. R. (2012) 'GAG Layer Replenishment Therapy for Recurrent Infectious Bladder Dysfunction', *Current Bladder Dysfunction Reports*, 7(2), pp. 113–119. doi: 10.1007/s11884-012-0121-3.

Gould, C. V *et al.* (2010) 'Guideline for prevention of catheter-associated urinary tract infections 2009', *Infection Control & Hospital Epidemiology*, 31(4), pp. 319–326.

Gray, E., Hogwood, J. and Mulloy, B. (2012) 'The anticoagulant and antithrombotic mechanisms of heparin.', *Handbook of experimental pharmacology*. Germany, (207), pp. 43–61. doi: 10.1007/978-3-642-23056-1_3.

Green, L. R. *et al.* (2011) 'Cooperative role for tetraspanins in adhesin-mediated attachment of bacterial species to human epithelial cells', *Infection and Immunity*, 79(6), pp. 2241–2249. doi: 10.1128/IAI.01354-10.

Gu, L., Wang, H., Guo, Y. L., *et al.* (2008) 'Heparin blocks the adhesion of E. coli O157:H7 to human colonic epithelial cells', *Biochemical and Biophysical Research Communications*, 369(4), pp. 1061–1064. doi: 10.1016/j.bbrc.2008.02.160.

Gu, L., Wang, H., Guo, Y.-L., *et al.* (2008) 'Heparin blocks the adhesion of E. coli O157:H7 to human colonic epithelial cells', *Biochemical and Biophysical Research Communications*, 369(4), pp. 1061–1064. doi: https://doi.org/10.1016/j.bbrc.2008.02.160.

Guimond, S. E. *et al.* (2021) 'Synthetic Heparan Sulfate Mimetic Pixatimod (PG545) Potently Inhibits SARS-CoV-2 By Disrupting The Spike-ACE2 interaction', *bioRxiv*, p. 2020.06.24.169334. doi: 10.1101/2020.06.24.169334.

Gupta, V., Nag, D. and Garg, P. (2017) 'Recurrent urinary tract infections in women: how promising is the use of probiotics?', *Indian journal of medical microbiology*, 35(3), pp. 347–354.

Gur, C. *et al.* (2013) 'Natural Killer Cell-Mediated Host Defense against Uropathogenic E. coli Is Counteracted by Bacterial HemolysinA-Dependent Killing of NK Cells', *Cell Host & Microbe*, 14(6), pp. 664–674. doi: https://doi.org/10.1016/j.chom.2013.11.004.

Ha, U.-S. and Cho, Y.-H. (2006) 'Catheter-associated urinary tract infections: new aspects of novel urinary catheters', *International journal of antimicrobial*

agents, 28(6), pp. 485–490.

Hacker, J. and Kaper, J. B. (2000) 'Pathogenicity islands and the evolution of microbes', *Annual Reviews in Microbiology*, 54(1), pp. 641–679.

Haining, E. J. *et al.* (2012) 'The TspanC8 subgroup of tetraspanins interacts with a disintegrin and metalloprotease 10 (ADAM10) and regulates its maturation and cell surface expression', *Journal of Biological Chemistry*, 287(47), pp. 39753–39765. doi: 10.1074/jbc.M112.416503.

Haley, R. W. *et al.* (1981) 'Nosocomial infections in US hospitals, 1975–1976: estimated frequency by selected characteristics of patients', *The American journal of medicine*, 70(4), pp. 947–959.

Hammond, E. and Dredge, K. (2020) 'Heparanase Inhibition by Pixatimod (PG545): Basic Aspects and Future Perspectives', in *Heparanase*, pp. 539–565.

Han, Z. *et al.* (2010) 'Structure-based drug design and optimization of mannoside bacterial FimH antagonists', *Journal of medicinal chemistry*, 53(12), pp. 4779–4792.

Hashida, H. *et al.* (2003) 'Clinical significance of transmembrane 4 superfamily in colon cancer', *British Journal of Cancer*, 89(1), pp. 158–167. doi: 10.1038/sj.bjc.6601015.

Hashimoto, J. *et al.* (2017) ' Surfactant Protein A Inhibits Growth and Adherence of Uropathogenic Escherichia coli To Protect the Bladder from Infection ', *The Journal of Immunology*, 198(7), pp. 2898–2905. doi: 10.4049/jimmunol.1502626.

Hassuna, N. A. *et al.* (2017) 'A role for the tetraspanin proteins in Salmonella infection of human macrophages', *Journal of Infection*, 75(2), pp. 115–124. doi: 10.1016/j.jinf.2017.06.003.

Hatton, N. E., Baumann, C. G. and Fascione, M. A. (2021) 'Developments in Mannose-Based Treatments for Uropathogenic Escherichia coli-Induced Urinary Tract Infections', *ChemBioChem*, 22(4), pp. 613–629. doi: 10.1002/cbic.202000406.

Hauser, P. J. *et al.* (2008) 'Abnormal expression of differentiation related proteins and proteoglycan core proteins in the urothelium of patients with interstitial cystitis', *The Journal of urology*, 179(2), pp. 764–769.

Hemler, M. E. (2001) 'Specific tetraspanin functions', *Journal of Cell Biology*, 155(7), pp. 1103–1107. doi: 10.1083/jcb.200108061.

Hemler, M. E. (2003) 'Tetraspanin Proteins Mediate Cellular Penetration, Invasion, and Fusion Events and Define a Novel Type of Membrane Microdomain', *Annual Review of Cell and Developmental Biology*, 19, pp. 397–422. doi: 10.1146/annurev.cellbio.19.111301.153609.

Hemler, M. E. (2005) ‘Tetraspanin functions and associated microdomains’, *Nature Reviews Molecular Cell Biology*, 6(10), pp. 801–811. doi: 10.1038/nrm1736.

Hemler, M. E. (2014) ‘Tetraspanin proteins promote multiple cancer stages’, *Nature Reviews Cancer*. Nature Publishing Group, 14(1), pp. 49–60. doi: 10.1038/nrc3640.

HICKS, R. M. (1975) ‘The mammalian urinary bladderan accommodating organ’, *Biological Reviews*, 50(2), pp. 215–246.

Hilbert, D. W. *et al.* (2012) ‘Clinical Escherichia coli isolates utilize alpha-hemolysin to inhibit in vitro epithelial cytokine production’, *Microbes and Infection*, 14(7), pp. 628–638. doi: https://doi.org/10.1016/j.micinf.2012.01.010.

Hof, H. (2017) ‘Candidurie! Was nun?’, *Der Urologe*, 56(2), pp. 172–179.

Hoffmann, M. J. *et al.* (2016) ‘The new immortalized uroepithelial cell line HBLAK contains defined genetic aberrations typical of early stage urothelial tumors’, *Bladder Cancer*, 2(4), pp. 449–463. doi: 10.3233/BLC-160065.

Hooton, T. M. *et al.* (2010) ‘Diagnosis, prevention, and treatment of catheter-associated urinary tract infection in adults: 2009 International Clinical Practice Guidelines from the Infectious Diseases Society of America’, *Clinical infectious diseases*, 50(5), pp. 625–663.

Hoque, M. O. *et al.* (2003) ‘Genome-wide genetic characterization of bladder cancer: a comparison of high-density single-nucleotide polymorphism arrays and PCR-based microsatellite analysis.’, *Cancer research*, 63(9), pp. 2216–2222.

Horsley, H. *et al.* (2018) ‘A urine-dependent human urothelial organoid offers a potential alternative to rodent models of infection’, *Scientific Reports*, 8(1), pp. 1–14. doi: 10.1038/s41598-018-19690-7.

Hotta, H. *et al.* (1988) ‘Molecular cloning and characterization of an antigen associated with early stages of melanoma tumor progression.’, *Cancer research*, 48(11), pp. 2955–2962.

Hu, C.-C. A. *et al.* (2005) ‘Assembly of urothelial plaques: tetraspanin function in membrane protein trafficking’, *Molecular biology of the cell*, 16(9), pp. 3937–3950.

Hu, C. A. *et al.* (2008) ‘Assembly of a membrane receptor complex : roles of the uroplakin II prosequence in regulating uroplakin bacterial receptor oligomerization’, 203, pp. 195–203. doi: 10.1042/BJ20080550.

Hu, P. *et al.* (2001) ‘Ablation of uroplakin III gene results in small urothelial plaques, urothelial leakage, and vesicoureteral reflux.’, *Urology*, 57(6 Suppl

1), p. 117. doi: 10.1016/s0090-4295(01)01062-7.

Hu, P. *et al.* (2002) 'Role of membrane proteins in permeability barrier function: Uroplakin ablation elevates urothelial permeability', *American Journal of Physiology - Renal Physiology*, 283(6 52-6), pp. 1200–1207. doi: 10.1152/ajprenal.00043.2002.

Huang, S. *et al.* (2005) 'The phylogenetic analysis of tetraspanins projects the evolution of cell-cell interactions from unicellular to multicellular organisms.', *Genomics*, 86(6), pp. 674–684. doi: 10.1016/j.ygeno.2005.08.004.

Hudoklin, S. *et al.* (2012) 'Electron tomography of fusiform vesicles and their organization in urothelial cells', *PLoS ONE*, 7(3), pp. 1–8. doi: 10.1371/journal.pone.0032935.

Hurst, R. E. (1994) 'Structure, function, and pathology of proteoglycans and glycosaminoglycans in the urinary tract', *World Journal of Urology*, 12(1), pp. 3–10. doi: 10.1007/BF00182044.

Hurst, R. E., Moldwin, R. M. and Mulholland, S. G. (2007) 'Bladder Defense Molecules, Urothelial Differentiation, Urinary Biomarkers, and Interstitial Cystitis', *Urology*, 69(4 SUPPL.). doi: 10.1016/j.urology.2006.03.083.

Hurst, R. E., Roy, J. B. and Parsons, C. L. (1997) 'The role of glycosaminoglycans in normal bladder physiology and the pathophysiology of interstitial cystitis', *Interstitial Cystitis*. Lippincott-Raven Philadelphia, pp. 93–100.

Hurst, R. E. and Zebrowski, R. (1994) 'Identification of Proteoglycans Present at High Density on Bovine and Human Bladder Luminal Surface', *The Journal of Urology*, 152(5, Part 1), pp. 1641–1645. doi: https://doi.org/10.1016/S0022-5347(17)32495-3.

Imani, R. *et al.* (2015) 'Combined cytotoxic effect of UV-irradiation and TiO2 microbeads in normal urothelial cells, low-grade and high-grade urothelial cancer cells', *Photochemical and Photobiological Sciences*, 14(3), pp. 583–590. doi: 10.1039/c4pp00272e.

Iozzo, R. V. and Schaefer, L. (2015) 'Proteoglycan form and function: A comprehensive nomenclature of proteoglycans', *Matrix Biology*, 42, pp. 11–55. doi: 10.1016/j.matbio.2015.02.003.

Iozzo, R. V (1994) 'Perlecan: a gem of a proteoglycan', *Matrix Biology*, 14(3), pp. 203–208.

Iozzo, R. V *et al.* (1999) 'Decorin is a biological ligand for the epidermal growth factor receptor', *Journal of Biological Chemistry*, 274(8), pp. 4489–4492.

Ivan Fernandez Vega, B. G. (2014) 'The Role of Heparan Sulfate Proteoglycans in Bacterial Infections', *Journal of Medical Microbiology & Diagnosis*, 03(04). doi: 10.4172/2161-0703.1000157.

Izumi, K. *et al.* (2012) 'Epidermal growth factor induces bladder cancer cell proliferation through activation of the androgen receptor', *International Journal of Oncology*, 41(5), pp. 1587–1592. doi: 10.3892/ijo.2012.1593.

Janssen, D. A. W. *et al.* (2013) 'The distribution and function of chondroitin sulfate and other sulfated glycosaminoglycans in the human bladder and their contribution to the protective bladder barrier', *Journal of Urology*. Elsevier Inc., 189(1), pp. 336–342. doi: 10.1016/j.juro.2012.09.022.

Jenkins, D. *et al.* (2005) 'De novo Uroplakin IIIa heterozygous mutations cause human renal adysplasia leading to severe kidney failure', *Journal of the American Society of Nephrology*, 16(7), pp. 2141–2149.

Jepson, R. G. and Craig, J. C. (2008) 'Cranberries for preventing urinary tract infections', in Jepson, R. G. (ed.) *Cochrane Database of Systematic Reviews*. doi: 10.1002/14651858.CD001321.pub4.

Jepson, R. G., Williams, G. and Craig, J. C. (2012) 'Cranberries for preventing urinary tract infections', *Cochrane database of systematic reviews,* (10).

Jerman, U. D. *et al.* (2021) 'Attachment of cancer urothelial cells to the bladder epithelium occurs on uroplakin-negative cells and is mediated by desmosomal and not by classical cadherins', *International Journal of Molecular Sciences*, 22(11). doi: 10.3390/ijms22115565.

Johansen, T. E. B. *et al.* (2011) 'Critical review of current definitions of urinary tract infections and proposal of an EAU/ESIU classification system', *International Journal of Antimicrobial Agents*, 38(SUPPL.), pp. 64–70. doi: 10.1016/j.ijantimicag.2011.09.009.

Jones, P. H., Bishop, L. A. and Watt, F. M. (1996) 'Functional significance of CD9 association with β1 integrins in human epidermal keratinocytes', *Cell Communication and Adhesion*, 4(4–5), pp. 297–305. doi: 10.3109/15419069609010773.

Kabaso, D. *et al.* (2011) 'Temperature and cholera toxin B are factors that influence formation of membrane nanotubes in RT4 and T24 urothelial cancer cell lines.', *International journal of nanomedicine*, 6, pp. 495–509. doi: 10.2147/ijn.s16982.

Kachar, B., Liang, F., Lins, U., Ding, M., Wu, X.-R., *et al.* (1999) 'Three-dimensional analysis of the 16 nm urothelial plaque particle: luminal surface exposure, preferential head-to-head interaction, and hinge formation', *Journal of molecular biology*, 285(2), pp. 595–608.

Kachar, B., Liang, F., Lins, U., Ding, M., Wu, X. R., *et al.* (1999) 'Three-dimensional analysis of the 16 nm urothelial plaque particle: Luminal surface exposure, preferential head-to-head interaction, and hinge formation', *Journal of Molecular Biology*, 285(2), pp. 595–608. doi: 10.1006/jmbi.1998.2304.

Kanetaka, K. *et al.* (2001) 'Overexpression of tetraspanin CO-029 in hepatocellular carcinoma', *Journal of Hepatology*, 35(5), pp. 637–642. doi:

10.1016/S0168-8278(01)00183-0.

Karam, J. *et al.* (2020) 'The roles of tetraspanins in bacterial infections', *Cellular Microbiology*, 22(12). doi: 10.1111/cmi.13260.

Karam, M., Habibi, M. and Bouzari, S. (2018) 'Osong Public Health and Research Perspectives Relationships between Virulence Factors and Antimicrobial Resistance among Escherichia coli Isolated from Urinary Tract', 9(5), pp. 217–224.

Karam, M. R. A., Habibi, M. and Bouzari, S. (2019) 'Urinary tract infection: Pathogenicity, antibiotic resistance and development of effective vaccines against Uropathogenic Escherichia coli', *Molecular immunology*, 108, pp. 56–67.

Kątnik-Prastowska, I., Lis, J. and Matejuk, A. (2014) 'Glycosylation of uroplakins. Implications for bladder physiopathology', *Glycoconjugate Journal*, 31(9), pp. 623–636. doi: 10.1007/s10719-014-9564-4.

Kazarov, A. R. *et al.* (2002) 'An extracellular site on tetraspanin CD151 determines α3 and α6 integrin-dependent cellular morphology', *Journal of Cell Biology*, 158(7), pp. 1299–1309. doi: 10.1083/jcb.200204056.

Kespichayawattana, W. *et al.* (2000) 'Burkholderia pseudomallei induces cell fusion and actin-associated membrane protrusion: a possible mechanism for cell-to-cell spreading', *Infection and immunity*. Am Soc Microbiol, 68(9), pp. 5377–5384.

Khandelwal, P., Abraham, S. N. and Apodaca, G. (2009) 'Cell biology and physiology of the uroepithelium', *American Journal of Physiology - Renal Physiology*, 297(6). doi: 10.1152/ajprenal.00327.2009.

Kim, W. J. *et al.* (2018) 'Uropathogenic Escherichia coli invades bladder epithelial cells by activating kinase networks in host cells', *Journal of Biological Chemistry*, 293(42), pp. 16518–16527. doi: 10.1074/jbc.RA118.003499.

Kitadokoro, K. *et al.* (2001) 'CD81 extracellular domain 3D structure: insight into the tetraspanin superfamily structural motifs', *The EMBO journal*. Oxford University Press, 20(1–2), pp. 12–18. doi: 10.1093/emboj/20.1.12.

Klein, R. D. and Hultgren, S. J. (2020) 'Urinary tract infections: microbial pathogenesis, host–pathogen interactions and new treatment strategies', *Nature Reviews Microbiology*, 18(4), pp. 211–226. doi: 10.1038/s41579-020-0324-0.

Klein, T. *et al.* (2010) 'FimH antagonists for the oral treatment of urinary tract infections: from design and synthesis to in vitro and in vivo evaluation', *Journal of medicinal chemistry*. ACS Publications, 53(24), pp. 8627–8641.

Kong, X. T. (2004) 'Deng FM, Hu P, Liang FX, Zhou G, Auerbach AB, Genieser N, Nelson PK, Robbins ES, Shapiro E, Kachar B, Sun TT', *Roles of*

uroplakins in plaque formation, umbrella cell enlargement, and urinary tract diseases. J Cell Biol, 167, pp. 1195–1204.

Konig, B. and Konig, W. (1993) 'Induction and suppression of cytokine release (tumour necrosis factor-α; interleukin-6, interleukin-1β) by Escherichia coli pathogenicity factors (adhesions, α-haemolysin)', *Immunology*. 78(4), p.526. Mikrobiol./Immunol., AG Infektabwehrmechanismen, Ruhr-Universitat, Universitatsstrasse 150, 4630 Bochum, Germany, 78(4), pp. 526–533. Available at: https://www.scopus.com/inward/record.uri?eid=2-s2.0-0027399079&partnerID=40&md5=64188f3d18cfdb2f463d3a266bb528e1.

Koo, C. Z. *et al.* (2020) 'The tetraspanin Tspan15 is an essential subunit of an ADAM10 scissor complex', *Journal of Biological Chemistry*. ASBMB, 295(36), pp. 12822–12839.

Kot, B. (2019) 'Antibiotic resistance among uropathogenic Escherichia coli', *Polish journal of microbiology*. The Polish Society of Microbiologists, 68(4), p. 403.

Kranjčec, B., Papeš, D. and Altarac, S. (2014) 'D-mannose powder for prophylaxis of recurrent urinary tract infections in women: a randomized clinical trial', *World journal of urology*, 32(1), pp. 79–84.

Kucheria, R. *et al.* (2005) 'Urinary tract infections: New insights into a common problem', *Postgraduate Medical Journal*, 81(952), pp. 83–86. doi: 10.1136/pgmj.2004.023036.

Kurimura, Y. *et al.* (2012) 'Surfactant protein D inhibits adherence of uropathogenic Escherichia coli to the bladder epithelial cells and the bacterium-induced cytotoxicity: A possible function in urinary tract', *Journal of Biological Chemistry*, 287(47), pp. 39578–39588. doi: 10.1074/jbc.M112.380287.

Laaksovirta, S. *et al.* (1999) 'The cytostatic effect of 9-cis-retinoic acid, tretinoin, and isotretinoin on three different human bladder cancer cell lines in vitro', *Urological Research*, 27(1), pp. 17–22. doi: 10.1007/s002400050084.

Lane, M. C. *et al.* (2007) 'Expression of flagella is coincident with uropathogenic Escherichia coli ascension to the upper urinary tract', *Proceedings of the National Academy of Sciences*, 104(42), pp. 16669 LP – 16674. doi: 10.1073/pnas.0607898104.

Lang, T. and Hochheimer, N. (2020) 'Tetraspanins', *Current Biology*, 30(5), pp. R204–R206. doi: 10.1016/j.cub.2020.01.007.

Langermann, S. *et al.* (2000) 'Vaccination with fimh adhesin protects cynomolgus monkeys from colonization and infection by uropathogenic Eschevichia coli', *The Journal of infectious diseases*, 181(2), pp. 774–778.

LaRock, D. L., Chaudhary, A. and Miller, S. I. (2015) 'Salmonellae interactions with host processes', *Nature Reviews Microbiology*. Nature Publishing Group, 13(4), pp. 191–205.

Lausted, C. *et al.* (2004) 'POSaM: a fast, flexible, open-source, inkjet oligonucleotide synthesizer and microarrayer', *Genome Biology*, 5(8), p. R58. doi: 10.1186/gb-2004-5-8-r58.

Lee, D. S., Lee, S.-J. and Choe, H.-S. (2018) 'Community-acquired urinary tract infection by Escherichia coli in the era of antibiotic resistance', *BioMed research international*, 2018.

Lee, G. (2011) 'Uroplakins in the lower urinary tract', *International Neurourology Journal*, 15(1), pp. 4–12. doi: 10.5213/inj.2011.15.1.4.

Lee, M. S. *et al.* (2015) 'Prognostic significance of CREB-binding protein and CD81 expression in primary high grade non-muscle invasive bladder cancer: Identification of novel biomarkers for bladder cancer using antibody microarray', *PLoS ONE*, 10(4), pp. 1–15. doi: 10.1371/journal.pone.0125405.

Lemonnier, M., Landraud, L. and Lemichez, E. (2007) 'Rho GTPase-activating bacterial toxins: from bacterial virulence regulation to eukaryotic cell biology', *FEMS Microbiology Reviews*, 31(5), pp. 515–534. doi: 10.1111/j.1574-6976.2007.00078.x.

Leong, J. M. *et al.* (1998) 'Different classes of proteoglycans contribute to the attachment of Borrelia burgdorferi to cultured endothelial and brain cells', *Infection and Immunity*, 66(3), pp. 994–999. doi: 10.1128/iai.66.3.994-999.1998.

Lewis, A. J., Richards, A. C. and Mulvey, M. A. (2017) 'Invasion of host cells and tissues by uropathogenic bacteria', *Urinary Tract Infections: Molecular Pathogenesis and Clinical Management*, pp. 359–381.

Lewis, S. A. (2000) 'Everything you wanted to know about the bladder epithelium but were afraid to ask', *American Journal of Physiology-Renal Physiology*, 278(6), pp. F867–F874.

Liao, Y. *et al.* (2018) 'Uroplakins play conserved roles in egg fertilization and acquired additional urothelial functions during mammalian divergence', *Molecular biology of the cell*. Am Soc Cell Biol, 29(26), pp. 3128–3143.

Liao, Y. *et al.* (2019) 'Mitochondrial lipid droplet formation as a detoxification mechanism to sequester and degrade excessive urothelial membranes', *Molecular Biology of the Cell*, 30(24), pp. 2969–2984. doi: 10.1091/mbc.E19-05-0284.

Lichtenberger, P. and Hooton, T. M. (2008) 'Complicated urinary tract infections', *Current infectious disease reports*, 10(6), pp. 499–504.

Lilly, J. D. and Parsons, C. L. (1990) 'Bladder surface glycosaminoglycans is a human epithelial permeability barrier.', *Surgery, gynecology & obstetrics*, 171(6), pp. 493–496.

Lin, J.-H. *et al.* (1994) 'Precursor sequence, processing, and urothelium-specific expression of a major 15-kDa protein subunit of asymmetric unit

membrane.', *Journal of Biological Chemistry*, 269(3), pp. 1775–1784.

Lin, J. H. *et al.* (1994) 'Precursor sequence, processing, and urothelium-specific expression of a major 15-kDa protein subunit of asymmetric unit membrane', *Journal of Biological Chemistry*, 269(3), pp. 1775–1784.

Lipper, C. H. *et al.* (2021) 'Crystal structure of the Tspan15 LEL domain reveals a conserved ADAM10 binding site', *Structure*, pp. 1–9. doi: 10.1016/j.str.2021.10.007.

Liska, D. J., Kern, H. J. and Maki, K. C. (2016) 'Cranberries and urinary tract infections: how can the same evidence lead to conflicting advice?', *Advances in Nutrition*, 7(3), pp. 498–506.

Liu, H. *et al.* (2014) 'Biophysical Characterization of Bladder Cancer Cells with Different Metastatic Potential', *Cell Biochemistry and Biophysics*, 68(2), pp. 241–246. doi: 10.1007/s12013-013-9702-9.

Liu, Y. *et al.* (2015) 'Dual ligand/receptor interactions activate urothelial defenses against uropathogenic E. coli', *Scientific Reports*. Nature Publishing Group, 5, pp. 1–18. doi: 10.1038/srep16234.

De Llano, D. G. *et al.* (2015) 'Anti-adhesive activity of cranberry phenolic compounds and their microbial-derived metabolites against uropathogenic escherichia coli in bladder epithelial cell cultures', *International Journal of Molecular Sciences*, 16(6), pp. 12119–12130. doi: 10.3390/ijms160612119.

Lobban, E. D. *et al.* (1998) 'Uroplakin gene expression by normal and neoplastic human urothelium', *American Journal of Pathology*. American Society for Investigative Pathology, 153(6), pp. 1957–1967. doi: 10.1016/S0002-9440(10)65709-4.

Lundin, A. *et al.* (2012) 'Potent anti-respiratory syncytial virus activity of a cholestanol-sulfated tetrasaccharide conjugate', *Antiviral research,* 93(1), pp. 101–109.

Madersbacher, H., Ophoven, A. van and Kerrebroeck, P. E. V. A. van (2013) 'GAG Layer Replenishment Therapy for Chronic Forms of Cystitis With Intravesical Glycosaminoglycans—A Review Helmut', *Neurourology and Urodynamics*, 32(1), pp. 9–18. doi: 10.1002/nau.

Maecker, H. T., Todd, S. C. and Levy, S. (1997) 'The tetraspanin superfamily: molecular facilitators.', *FASEB journal : official publication of the Federation of American Societies for Experimental Biology*, 11(6), pp. 428–442.

Maki, K. C. *et al.* (2016) 'Consumption of a cranberry juice beverage lowered the number of clinical urinary tract infection episodes in women with a recent history of urinary tract infection', *The American journal of clinical nutrition*, 103(6), pp. 1434–1442.

Mann, R. *et al.* (2017) 'Metabolic adaptations of Uropathogenic E. coli in the urinary tract', *Frontiers in Cellular and Infection Microbiology*,7,p.241.

Martin, F. *et al.* (2005) ‘Tetraspanins in viral infections: a fundamental role in viral biology?’, *Journal of virology*. Am Soc Microbiol, 79(17), pp. 10839–10851.

Martinez, J. J. (2000) ‘Type 1 pilus-mediated bacterial invasion of bladder epithelial cells’, *The EMBO Journal*, 19(12), pp. 2803–2812. doi: 10.1093/emboj/19.12.2803.

McLellan, L. K. and Hunstad, D. A. (2016) ‘Urinary Tract Infection: Pathogenesis and Outlook’, *Trends in Molecular Medicine*, 22(11), pp. 946–957. doi: https://doi.org/10.1016/j.molmed.2016.09.003.

Medina, M. and Castillo-Pino, E. (2019) ‘An introduction to the epidemiology and burden of urinary tract infections’, *Therapeutic Advances in Urology*, 11, pp. 3–7. doi: 10.1177/1756287219832172.

Meiland, R. *et al.* (2004) ‘Fimch antiserum inhibits the adherence of Escherichia coli to cells collected by voided urine specimens of diabetic women.’, *The Journal of urology*, 171(4), pp. 1589–1593. doi: 10.1097/01.ju.0000118402.01034.fb.

Melzer, M. and Welch, C. (2013) ‘Outcomes in UK patients with hospital-acquired bacteraemia and the risk of catheter-associated urinary tract infections’, *Postgraduate medical journal*. The Fellowship of Postgraduate Medicine, 89(1052), pp. 329–334.

Menozzi, F. D. *et al.* (2002) ‘Enhanced bacterial virulence through exploitation of host glycosaminoglycans’, *Molecular Microbiology*, 43(6), pp. 1379–1386. doi: 10.1046/j.1365-2958.2002.02841.x.

Messing, E. *et al.* (1987) ‘Epidermal Growth Factor—Interactions with Normal and Malignant Urothelium: In Vivo and in Situ Studies’, *Journal of Urology*. WoltersKluwer, 138(5), pp. 1329–1335. doi: 10.1016/S0022-5347(17)43593-2.

Miller, J. J. and Levinson, S. S. (1996) ‘Interferences in immunoassays’, pp. 165–190.

Min, G. *et al.* (2003) ‘Structural basis of urothelial permeability barrier function as revealed by Cryo-EM studies of the 16 nm uroplakin particle’, *Journal of Cell Science*, 116(20), pp. 4087–4094. doi: 10.1242/jcs.00811.

Min, G. *et al.* (2006a) ‘Structural basis for tetraspanin functions as revealed by the cryo-EM structure of uroplakin complexes at 6-A resolution.’, *The Journal of cell biology*, 173(6), pp. 975–983. doi: 10.1083/jcb.200602086.

Min, G. *et al.* (2006b) ‘Structural basis for tetraspanin functions as revealed by the cryo-EM structure of uroplakin complexes at 6-A resolution’, *The Journal of cell biology*, 173(6), pp. 975–983.

Miranda, R. L. *et al.* (2004) ‘Glycolytic and gluconeogenic growth of Escherichia coli O157: H7 (EDL933) and E. coli K-12 (MG1655) in the mouse intestine’, *Infection and immunity*. Am Soc Microbiol, 72(3), pp. 1666–1676.

Miyado, K. *et al.* (2000) ‘Requirement of CD9 on the Egg Plasma Membrane for Fertilization’, *Science*, 287(5451), pp. 321 LP – 324. doi: 10.1126/science.287.5451.321.

Modhiran, N. *et al.* (2019) ‘Dual targeting of dengue virus virions and NS1 protein with the heparan sulfate mimic PG545’, *Antiviral research*, 168, pp. 121–127.

Mody, L. *et al.* (2017) ‘A national implementation project to prevent catheter-associated urinary tract infection in nursing home residents’, *JAMA internal medicine*. American Medical Association, 177(8), pp. 1154–1162.

Møller, A. K. *et al.* (2003) ‘An Escherichia coli MG1655 lipopolysaccharide deep-rough core mutant grows and survives in mouse cecal mucus but fails to colonize the mouse large intestine’, *Infection and immunity*. Am Soc Microbiol, 71(4), pp. 2142–2152.

Motse, D. F. K. *et al.* (2019) ‘Etiologic Profile and Sensitivity Pattern of Germs Responsible for Urinary Tract Infection Among Under-five Children in Douala, Cameroon: A Hospital-Based Study’, *Avicenna Journal of Clinical Microbiology and Infection*, 6(2), pp. 49–56.

Mulvey, Matthew A. *et al.* (1998) ‘Induction and evasion of host defenses by type 1-piliated uropathogenic Escherichia coli’, *Science*, 282(5393), pp. 1494–1497. doi: 10.1126/science.282.5393.1494.

Mulvey, Matthew A *et al.* (1998) ‘Induction and evasion of host defenses by type 1-piliated uropathogenic Escherichia coli’, *Science*. American Association for the Advancement of Science, 282(5393), pp. 1494–1497.

Mulvey, M. A. (2002) ‘Adhesion and entry of uropathogenic Escherichia coli.’, *Cellular microbiology*, 4(5), pp. 257–271. doi: 10.1046/j.1462-5822.2002.00193.x.

Mulvey, M. A., Schilling, J. D. and Hultgren, S. J. (2001) ‘Establishment of a persistent Escherichia coli reservoir during the acute phase of a bladder infection’, *Infection and Immunity*, 69(7), pp. 4572–4579. doi: 10.1128/IAI.69.7.4572-4579.2001.

Murray, B. O. *et al.* (2021) ‘Recurrent Urinary Tract Infection: A Mystery in Search of Better Model Systems’, *Frontiers in Cellular and Infection Microbiology*, 11(May), pp. 1–29. doi: 10.3389/fcimb.2021.691210.

Le Naour, F. *et al.* (2006) ‘Profiling of the Tetraspanin Web of Human Colon

Cancer Cells * ', *Molecular & Cellular Proteomics*m, 5(5), pp. 845–857. doi: 10.1074/mcp.M500330-MCP200.

Negrete, H. O. *et al.* (1996) 'Permeability properties of the intact mammalian bladder epithelium', *American Journal of Physiology-Renal Physiology*, 271(4), pp. F886–F894.

Negus, M., Phillips, C. and Hindley, R. (2020) 'Recurrent urinary tract infections: a critical review of the currently available treatment options', *The Obstetrician & Gynaecologist*, 22(2), pp. 115–121. doi: 10.1111/tog.12644.

Neumann, E. *et al.* (2018) 'Tetraspanin CD82 affects migration, attachment and invasion of rheumatoid arthritis synovial fibroblasts', *Annals of the Rheumatic Diseases*, 77(11), pp. 1619–1626. doi: 10.1136/annrheumdis-2018-212954.

O'grady, N. P. *et al.* (2002) 'Guidelines for the prevention of intravascular catheter–related infections', *Clinical infectious diseases*, 35(11), pp. 1281–1307.

Oelschlaeger, T. A., Dobrindt, U. and Hacker, J. (2002) 'Pathogenicity islands of uropathogenic E. coli and the evolution of virulence', *International journal of antimicrobial agents*, 19(6), pp. 517–521.

Olsburgh, J. *et al.* (2003) 'Uroplakin gene expression in normal human tissues and locally advanced bladder cancer', *Journal of Pathology*, 199(1), pp. 41–49. doi: 10.1002/path.1252.

Oren, R. *et al.* (1990) 'TAPA-1, the target of an antiproliferative antibody, defines a new family of transmembrane proteins.', *Molecular and cellular biology*, 10(8), pp. 4007–4015. doi: 10.1128/mcb.10.8.4007-4015.1990.

Öztürk, R. and Murt, A. (2020) 'Epidemiology of urological infections: a global burden', *World Journal of Urology*, 38(11), pp. 2669–2679. doi: 10.1007/s00345-019-03071-4.

Palou, J. *et al.* (2013) 'Randomized comparative study for the assessment of a new therapeutic schedule of fosfomycin trometamol in postmenopausal women with uncomplicated lower urinary tract infection', *Actas Urológicas Españolas (English Edition)*, 37(3), pp. 147–155.

Paniagua-Contreras, G. L. *et al.* (2017) 'Virulence factors, antibiotic resistance phenotypes and O-serogroups of Escherichia coli strains isolated from community-acquired urinary tract infection patients in Mexico', *Journal of Microbiology, Immunology and Infection*, 50(4), pp. 478–485.

Parish, A. and Holliday, K. (2012) 'Long-term care acquired urinary tract infections' antibiotic resistance patterns and empiric therapy: a pilot study', *Geriatric Nursing*, 33(6), pp. 473–478.

Park, H. S. *et al.* (2019) 'Suppression of CD81 promotes bladder cancer cell invasion through increased matrix metalloproteinase expression via

extracellular signal-regulated kinase phosphorylation', *Investigative and Clinical Urology*, 60(5), pp. 396–404. doi: 10.4111/icu.2019.60.5.396.

Parsons, C. L. (1994) 'A model for the function of glycosaminoglycans in the urinary tract', *World Journal of Urology*, 12(1), pp. 38–42. doi: 10.1007/BF00182049.

Parsons, C. L. (1997) 'Epithelial coating techniques in the treatment of interstitial cystitis', *Urology*, 49(5), pp. 100–104.

Parsons, C. L., Greenspan, C. and Mulholland, S. G. (1975) 'The primary antibacterial defense mechanism of the bladder.', *Investigative urology*, 13(1), pp. 72–78.

Parsons, C. L., Lilly, J. D. and Stein, P. (1991) 'Epithelial dysfunction in nonbacterial cystitis (interstitial cystitis)', *The Journal of urology*, 145(4), pp. 732-735.

Öztürk, R. and Murt, A., 2020. Epidemiology of urological infections: a global burden. *World journal of urology*, *38*(11), pp.2669-2679.

Partridge, L. J., Green, L. R. and Monk, P. N. (2020) 'Unfractionated heparin potently inhibits the binding of SARS-CoV-2 spike protein to a human cell line', *bioRxiv*, p. 2020.05.21.107870. doi: 10.1101/2020.05.21.107870.

Pavelka, M. *et al.* (2011) 'Urothelial Plaque Formation in Post-Golgi Compartments', 6(8), pp. 2–10. doi: 10.1371/journal.pone.0023636.

Pepper, I. L. *et al.* (2011) *Environmental microbiology*. Academic press.

Pizarro-Cerdá, J. and Cossart, P. (2006) 'Bacterial adhesion and entry into host cells', *Cell*, 124(4), pp. 715–727. doi: 10.1016/j.cell.2006.02.012.

Pols, Maaike S and Klumperman, J. (2009) 'Trafficking and function of the tetraspanin CD63', *Experimental cell research*, 315(9), pp. 1584–1592.

Pols, Maaike S. and Klumperman, J. (2009) 'Trafficking and function of the tetraspanin CD63', *Experimental Cell Research*, 315(9), pp. 1584–1592. doi: 10.1016/j.yexcr.2008.09.020.

Ponchel, F. *et al.* (2003) 'Real-time PCR based on SYBR-Green I fluorescence : An alternative to the TaqMan assay for a relative quantification of gene rearrangements , gene amplifications and micro gene deletions TCR-alpha', 13, pp. 1–13.

Pratt, L. A. and Kolter, R. (1998) 'Genetic analysis of Escherichia coli biofilm formation: Roles of flagella, motility, chemotaxis and type I pili', *Molecular Microbiology*, 30(2), pp. 285–293. doi: 10.1046/j.1365-2958.1998.01061.x.

Prox, J. *et al.* (2012) 'Tetraspanin15 regulates cellular trafficking and activity of the ectodomain sheddase ADAM10', *Cellular and Molecular Life Sciences*,

69(17), pp. 2919–2932.

Rajan, A. *et al.* (2018) ‘Enteric Species F Human Adenoviruses use Laminin-Binding Integrins as Co-Receptors for Infection of Ht-29 Cells’, *Scientific Reports*, 8(1), p. 10019. doi: 10.1038/s41598-018-28255-7.

Rajas, O. *et al.* (2017) ‘Glycosaminoglycans are involved in bacterial adherence to lung cells’, *BMC Infectious Diseases*. BMC Infectious Diseases, 17(1), pp. 1–14. doi: 10.1186/s12879-017-2418-5.

Ramachandran, R. P. *et al.* (2018) ‘EspH Suppresses Erk by Spatial Segregation from CD81 Tetraspanin Microdomains’, *Infection and Immunity*. Edited by V. B. Young, 86(10), pp. e00303-18. doi: 10.1128/IAI.00303-18.

Rana, S. *et al.* (2011) ‘Activation-induced internalization differs for the tetraspanins CD9 and Tspan8: Impact on tumor cell motility’, *International Journal of Biochemistry and Cell Biology*, 43(1), pp. 106–119. doi: 10.1016/j.biocel.2010.10.002.

Redwood, S. M. *et al.* (1992) ‘Abrogation of the invasion of human bladder tumor cells by using protease inhibitor(s)’, *Cancer*, 69(5), pp. 1212–1219. doi: 10.1002/cncr.2820690524.

Reyes, R. *et al.* (2018) ‘Tetraspanin CD9: A key regulator of cell adhesion in the immune system’, *Frontiers in Immunology*, 9(APR), pp. 1–9. doi: 10.3389/fimmu.2018.00863.

Rickard, A. *et al.* (2008) ‘Characterization of tight junction proteins in cultured human urothelial cells’, *In Vitro Cellular and Developmental Biology - Animal*, 44(7), pp. 261–267. doi: 10.1007/s11626-008-9116-y.

ter Riet, G. *et al.* (2012) ‘Lactobacilli vs antibiotics to prevent urinary tract infections: a randomized, double-blind, noninferiority trial in postmenopausal women’, *Archives of internal medicine*. American Medical Association, 172(9), pp. 704–712.

Rigby, C. C. and Franks, L. M. (1970) ‘A human tissue culture cell line from a transitional cell tumour of the urinary bladder: Growth, chromosome pattern and ultrastructure’, *British Journal of Cancer*, 24(4), pp. 746–754. doi: 10.1038/bjc.1970.89.

Roberts, J. A. *et al.* (1994) ‘The Gal(α1-4)Gal-specific tip adhesin of Escherichia coli P-fimbriae is needed for pyelonephritis to occur in the normal urinary tract’, *Proceedings of the National Academy of Sciences*, 91(25), pp. 11889–11893. doi: 10.1073/pnas.91.25.11889.

Romih, R. *et al.* (2005) ‘Differentiation of epithelial cells in the urinary tract’, *Cell and Tissue Research*, 320(2), pp. 259–268. doi: 10.1007/s00441-004-1005-4.

Rostand, K. S. and Esko, J. D. (1997) 'Microbial adherence to and invasion through proteoglycans', *Infection and Immunity*, 65(1), pp. 1–8. doi: 10.1128/iai.65.1.1-8.1997.

Rozenberg, B. B. *et al.* (2019) 'Improving the barrier function of damaged cultured urothelium using chondroitin sulfate', *Neurourology and Urodynamics*, 39(2), pp. 558–564. doi: 10.1002/nau.24240.

Ruggieri, M. R., Hanno, P. M. and Levin, R. M. (1984) 'The effects of heparin on the adherence of five species of urinary tract pathogens to urinary bladder mucosa', *Urological Research*, 12(4), pp. 199–203. doi: 10.1007/BF00256803.

Ruoslahti, E. (1988) 'STRUCTURE AND BIOLOGY Erkki Ruoslahti', *Cell Differentiation*.

Said, J. *et al.* (2010) 'Lipophile-conjugated sulfated oligosaccharides as novel microbicides against HIV-1', *Antiviral research*, 86(3), pp. 286–295.

Said, J. S. *et al.* (2016) 'The cholestanol-conjugated sulfated oligosaccharide PG545 disrupts the lipid envelope of herpes simplex virus particles', *Antimicrobial agents and chemotherapy*. Am Soc Microbiol, 60(2), pp. 1049–1057.

Sangsri, T. *et al.* (2020) 'Tetraspanins are involved in Burkholderia pseudomallei-induced cell-to-cell fusion of phagocytic and non-phagocytic cells', *Scientific Reports*, 10(1), p. 17972. doi: 10.1038/s41598-020-74737-y.

dos Santos Souza, I. *et al.* (2020) 'Meningococcal disease: A paradigm of type-IV pilus dependent pathogenesis', *Cellular microbiology*, 22(4), p. e13185.

Santra, M. *et al.* (1997) 'Ectopic expression of decorin protein core causes a generalized growth suppression in neoplastic cells of various histogenetic origin and requires endogenous p21, an inhibitor of cyclin-dependent kinases.', *The Journal of clinical investigation*, 100(1), pp. 149–157.

Sarrazin, S., Lamanna, W. C. and Esko, J. D. (2011) 'Heparan sulfate proteoglycans', *Cold Spring Harbor Perspectives in Biology*, 3(7), pp. 1–33. doi: 10.1101/cshperspect.a004952.

Sascha, N. *et al.* (2006) 'Mapping of tetraspanin-enriched microdomains that can function as gateways for HIV-1 ', *Journal of Cell Biology*, 173(5), pp. 795–807. doi: 10.1083/jcb.200508165.

Satoh, A. *et al.* (2000) 'New role of glycosaminoglycans on the plasma membrane proposed by their interaction with phosphatidylcholine.', *FEBS letters*, 477(3), pp. 249–252. doi: 10.1016/s0014-5793(00)01746-4.

Savar, N. S. *et al.* (2014) 'In silico and in vivo studies of truncated forms of flagellin (FliC) of enteroaggregative Escherichia coli fused to FimH from uropathogenic Escherichia coli as a vaccine candidate against urinary tract infections', *Journal of biotechnology*, 175, pp. 31–37.

Scharenberg, M. *et al.* (2011) ‘A flow cytometry-based assay for screening FimH antagonists’, *Assay and Drug Development Technologies*, 9(5), pp. 455–464. doi: 10.1089/adt.2010.0357.

Scharf, B. *et al.* (2020) ‘Antiadhesive natural products against uropathogenic E. coli: What can we learn from cranberry extract?’, *Journal of Ethnopharmacology*, 257, p. 112889. doi: 10.1016/j.jep.2020.112889.

Schilling, J. D. *et al.* (2001) ‘ Bacterial Invasion Augments Epithelial Cytokine Responses to Escherichia coli Through a Lipopolysaccharide-Dependent Mechanism ’, *The Journal of Immunology*, 166(2), pp. 1148–1155. doi: 10.4049/jimmunol.166.2.1148.

Scholzen, T. *et al.* (1994) ‘The murine decorin. Complete cDNA cloning, genomic organization, chromosomal assignment, and expression during organogenesis and tissue differentiation.’, *Journal of Biological Chemistry*, 269(45), pp. 28270–28281. doi: 10.1016/S0021-9258(18)46924-4.

Schönemann, W. *et al.* (2019) ‘Improvement of aglycone π-stacking yields nanomolar to sub-nanomolar FimH antagonists’, *ChemMedChem*, 14(7), pp. 749–757.

Schönfelder, E.-M. *et al.* (2006) ‘Mutations in Uroplakin IIIA Are a Rare Cause of Renal Hypodysplasia in Humans’, *American Journal of Kidney Diseases*, 47(6), pp. 1004–1012. doi: https://doi.org/10.1053/j.ajkd.2006.02.177.

Schwan, W. R. (2008) ‘Flagella allow uropathogenic Escherichia coli ascension into murine kidneys’, *International Journal of Medical Microbiology*, 298(5), pp. 441–447. doi: https://doi.org/10.1016/j.ijmm.2007.05.009.

Schwartz, D. J. *et al.* (2011) ‘Population dynamics and niche distribution of uropathogenic Escherichia coli during acute and chronic urinary tract infection’, *Infection and Immunity*, 79(10), pp. 4250–4259. doi: 10.1128/IAI.05339-11.

Seigneuret, M. *et al.* (2001) ‘Structure of the tetraspanin main extracellular domain. A partially conserved fold with a structurally variable domain insertion.’, *The Journal of biological chemistry*, 276(43), pp. 40055–40064. doi: 10.1074/jbc.M105557200.

Shah, C. *et al.* (2019) ‘Virulence factors of uropathogenic Escherichia coli (UPEC) and correlation with antimicrobial resistance’, *BMC Microbiology*. BMC Microbiology, 19(1), pp. 1–6. doi: 10.1186/s12866-019-1587-3.

Sharma, K. *et al.* (2021) ‘Dynamic persistence of intracellular bacterial communities of uropathogenic escherichia coli in a human bladder-chip model of urinary tract infections’, *eLife*, 10, pp. 1–30. doi: 10.7554/eLife.66481.

Sheerin, N. S. (2011) ‘Urinary tract infection’, *Medicine*, 39(7), pp. 384–389.

Shoham, T. *et al.* (2006) 'Building of the tetraspanin web: distinct structural domains of CD81 function in different cellular compartments.', *Molecular and cellular biology*, 26(4), pp. 1373–1385. doi: 10.1128/MCB.26.4.1373-1385.2006.

Signing, A. T. *et al.* (2020) 'Antibiotic Resistance Profile of Uropathogenic Bacteria in Diabetic Patients at the Bafoussam Regional Hospital, West Cameroon Region', *Cureus*. Cureus Inc., 12(7).

Simmering, J. E. *et al.* (2017) 'The Increase in Hospitalizations for Urinary Tract Infections and the Associated Costs in the United States, 1998–2011', *Open Forum Infectious Diseases*, 4(1), pp. 1–7. doi: 10.1093/ofid/ofw281.

Simon, R. *et al.* (2002) 'Ampli ® cation pattern of 12q13-q15 genes (MDM2 , CDK4 , GLI) in urinary bladder cancer', *Oncogene*, 21, pp. 2476–2483. doi: 10.1038/sj/onc/1205304.

Sincock, P. M. *et al.* (1999) 'PETA-3/CD151, a member of the transmembrane 4 superfamily, is localised to the plasma membrane and endocytic system of endothelial cells, associates with multiple integrins and modulates cell function', *Journal of Cell Science*, 112(6), pp. 833–844.

Singh, I., Gautam, L. K. and Kaur, I. R. (2016) 'Effect of oral cranberry extract (standardized proanthocyanidin-A) in patients with recurrent UTI by pathogenic E. coli: a randomized placebo-controlled clinical research study', *International Urology and Nephrology*, 48(9), pp. 1379–1386. doi: 10.1007/s11255-016-1342-8.

Singha, P., Locklin, J. and Handa, H. (2017) 'A review of the recent advances in antimicrobial coatings for urinary catheters', *Acta biomaterialia*, 50, pp. 20–40.

Skehan, P. *et al.* (1990) 'New colorimetric cytotoxicity assay for anticancer-drug screening.', *Journal of the National Cancer Institute*, 82(13), pp. 1107–1112. doi: 10.1093/jnci/82.13.1107.

Slobodov, G. *et al.* (2004) 'Abnormal expression of molecular markers for bladder impermeability and differentiation in the urothelium of patients with interstitial cystitis', *Journal of Urology*, 171(4), pp. 1554–1558. doi: 10.1097/01.ju.0000118938.09119.a5.

Smith, Y. C. *et al.* (2006) 'Novel three-dimensional organoid model for evaluation of the interaction of uropathogenic Escherichia coli with terminally differentiated human urothelial cells', *Infection and Immunity*, 74(1), pp. 750–757. doi: 10.1128/IAI.74.1.750-757.2006.

Smith, Y. C. *et al.* (2008) 'Hemolysin of uropathogenic Escherichia coli evokes extensive shedding of the uroepithelium and hemorrhage in bladder tissue within the first 24 hours after intraurethral inoculation of mice', *Infection and Immunity*, 76(7), pp. 2978–2990. doi: 10.1128/IAI.00075-08.

Sokurenko, E. V. *et al.* (1994) 'FimH family of type 1 fimbrial adhesins: Functional heterogeneity due to minor sequence variations among fimH genes', *Journal of Bacteriology*, 176(3), pp. 748–755. doi: 10.1128/jb.176.3.748-755.1994.

Song, J. *et al.* (2009) 'TLR4-mediated expulsion of bacteria from infected bladder epithelial cells', *Proceedings of the National Academy of Sciences of the United States of America*, 106(35), pp. 14966–14971. doi: 10.1073/pnas.0900527106.

Sood, A. *et al.* (2015) 'Incidence, admission rates, and economic burden of pediatric emergency department visits for urinary tract infection: data from the nationwide emergency department sample, 2006 to 2011', *Journal of pediatric urology*, 11(5), pp. 246-e1.

Southgate, J. *et al.* (1994) 'Normal human urothelial cells in vitro: proliferation and induction of stratification.', *Laboratory investigation; a journal of technical methods and pathology*, 71(4), pp. 583–594.

Southgate, J. (1999) 'Cytokeratin expression patterns in normal and malignant urothelium: A review of the biological and diagnostic implications', *Histology and Histopathology*, 14(2), pp. 657–664. doi: 10.14670/HH-14.657.

Spaulding, C. N. *et al.* (2017) 'Selective depletion of uropathogenic E. coli from the gut by a FimH antagonist', *Nature*. Nature Publishing Group, 546(7659), pp. 528–532.

van Spriel, A. B. (2011) 'Tetraspanins in the humoral immune response.', *Biochemical Society transactions*, 39(2), pp. 512–517. doi: 10.1042/BST0390512.

van Spriel, A. B. *et al.* (2012) 'The tetraspanin CD37 orchestrates the α(4)β(1) integrin-Akt signaling axis and supports long-lived plasma cell survival.', *Science signaling*, 5(250), p. ra82. doi: 10.1126/scisignal.2003113.

van Spriel, A. B. and Figdor, C. G. (2010) 'The role of tetraspanins in the pathogenesis of infectious diseases', *Microbes and Infection*, 12(2), pp. 106–112. doi: https://doi.org/10.1016/j.micinf.2009.11.001.

Stapleton, A. E. *et al.* (2011) 'Randomized, placebo-controlled phase 2 trial of a Lactobacillus crispatus probiotic given intravaginally for prevention of recurrent urinary tract infection', *Clinical infectious diseases*, 52(10), pp. 1212–1217.

Stickler, D. J. (2008) 'Bacterial biofilms in patients with indwelling urinary catheters', *Nature clinical practice urology*. Nature Publishing Group, 5(11), pp. 598–608.

Storm, R. J. *et al.* (2017) 'Human Adenovirus Type 37 Uses α(V)β(1) and α(3)β(1) Integrins for Infection of Human Corneal Cells.', *Journal of virology*,

91(5). doi: 10.1128/JVI.02019-16.

Sun, T. T. (2006) ‘Altered phenotype of cultured urothelial and other stratified epithelial cells: Implications for wound healing’, *American Journal of Physiology - Renal Physiology*, 291(1). doi: 10.1152/ajprenal.00035.2006.

Susa ., K. *et al.* (2021) ‘Cryo-EM structure of the B cell co-receptor CD19 bound to the tetraspanin CD81’, *Science*. American Association for the Advancement of Science, 371(6526), pp. 300–305. doi: 10.1126/science.abd9836.

Susa, K. J. *et al.* (2021) ‘Cryo-EM structure of the B cell co-receptor CD19 bound to the tetraspanin CD81.’, *Science*, 371(6526), pp. 300–305. doi: 10.1126/science.abd9836.

Tabasi, M. *et al.* (2015) ‘Phenotypic assays to determine virulence factors of uropathogenic Escherichia coli (UPEC) isolates and their correlation with antibiotic resistance pattern’, *Osong public health and research perspectives*, 6(4), pp. 261–268.

Tabasi, Mohsen *et al.* (2016) ‘Genotypic characterization of virulence factors in Escherichia coli isolated from patients with acute cystitis, pyelonephritis and asymptomatic bacteriuria’, *Journal of Clinical and Diagnostic Research*, 10(12), pp. DC01–DC07. doi: 10.7860/JCDR/2016/21379.9009.

Tabasi, M. *et al.* (2016) ‘Genotypic characterization of virulence factors in Escherichia coli isolated from patients with acute cystitis, pyelonephritis and asymptomatic bacteriuria’, *Journal of Clinical and Diagnostic Research*, 10(12), pp. DC01–DC07. doi: 10.7860/JCDR/2016/21379.9009.

Takahashi, S. *et al.* (2013) ‘A randomized clinical trial to evaluate the preventive effect of cranberry juice (UR65) for patients with recurrent urinary tract infection’, *Journal of Infection and Chemotherapy*, 19(1), pp. 112–117.

Tambyah, P. A. and Maki, D. G. (2000) ‘Catheter-associated urinary tract infection is rarely symptomatic: a prospective study of 1497 catheterized patients’, *Archives of internal medicine*. American Medical Association, 160(5), pp. 678–682.

Taur, Y. and Smith, M. A. (2007) ‘Adherence to the Infectious Diseases Society of America guidelines in the treatment of uncomplicated urinary tract infection’, *Clinical infectious diseases*, 44(6), pp. 769–774.

TerBush, A. A. *et al.* (2018) ‘A Kaposi’s Sarcoma-Associated Herpesvirus Infection Mechanism Is Independent of Integrins α3β1, αVβ3, and αVβ5.’, *Journal of virology*, 92(17). doi: 10.1128/JVI.00803-18.

Terlizzi, M. E., Gribaudo, G. and Maffei, M. E. (2017) ‘UroPathogenic Escherichia coli (UPEC) infections: Virulence factors, bladder responses, antibiotic, and non-antibiotic antimicrobial strategies’, *Frontiers in*

Microbiology, 8, p.1566. doi: 10.3389/fmicb.2017.01566.

Termini, C. M. and Gillette, J. M. (2017) 'Tetraspanins function as regulators of cellular signaling', *Frontiers in Cell and Developmental Biology*, 5(APR), pp. 1–14. doi: 10.3389/fcell.2017.00034.

Tham, T. N. *et al.* (2010) 'Tetraspanin CD81 is required for Listeria monocytogenes invasion', *Infection and Immunity*, 78(1), pp. 204–209. doi: 10.1128/IAI.00661-09.

Theodorescu, D. *et al.* (1990) 'Overexpression of normal and mutated forms of HRAS induces orthotopic bladder invasion in a human transitional cell carcinoma', *Proceedings of the National Academy of Sciences of the United States of America*, 87(22), pp. 9047–9051. doi: 10.1073/pnas.87.22.9047.

Thumbikat, P., Berry, R. E., Zhou, G., *et al.* (2009) 'Bacteria-induced uroplakin signaling mediates bladder response to infection', *PLoS Pathogens*, 5(5). doi: 10.1371/journal.ppat.1000415.

Thumbikat, P., Berry, R. E., Schaeffer, A. J., *et al.* (2009) 'Differentiation-induced uroplakin III expression promotes urothelial cell death in response to uropathogenic E. coli', *Microbes and Infection*. Elsevier Masson SAS, 11(1), pp. 57–65. doi: 10.1016/j.micinf.2008.10.008.

Tian, W. *et al.* (2015) 'Utility of uroplakin II expression as a marker of urothelial carcinoma', *Human Pathology*. Elsevier Inc., 46(1), pp. 58–64. doi: 10.1016/j.humpath.2014.09.007.

Tokuhara, T. *et al.* (2001) 'Clinical significance of CD151 gene expression in non-small cell lung cancer', *Clinical Cancer Research*, 7(12), pp. 4109–4114.

Tong, S. Y. C. *et al.* (2015) 'Staphylococcus aureus infections: epidemiology, pathophysiology, clinical manifestations, and management', *Clinical microbiology reviews*. Am Soc Microbiol, 28(3), pp. 603–661.

Tonnaer, E. L. G. M. *et al.* (2006) 'Involvement of glycosaminoglycans in the attachment of pneumococci to nasopharyngeal epithelial cells', *Microbes and Infection*, 8(2), pp. 316–322. doi: 10.1016/j.micinf.2005.06.028.

Tu, L., Sun, T.-T. and Kreibich, G. (2002) 'Specific heterodimer formation is a prerequisite for uroplakins to exit from the endoplasmic reticulum', *Molecular biology of the cell*. Am Soc Cell Biol, 13(12), pp. 4221–4230.

Tugues, S. *et al.* (2013) 'Tetraspanin CD63 promotes vascular endothelial growth factor receptor 2-β1 integrin complex formation, thereby regulating activation and downstream signaling in endothelial cells in Vitro and in Vivo', *Journal of Biological Chemistry*, 288(26), pp. 19060–19071. doi: 10.1074/jbc.M113.468199.

Turner, A. M. *et al.* (2008) 'Generation of a Functional, Differentiated Porcine Urothelial Tissue In Vitro', *European Urology*, 54(6), pp. 1423–1432. doi: 10.1016/j.eururo.2008.03.068.

Ulett, G. C. *et al.* (2013) 'Uropathogenic Escherichia coli virulence and innate immune responses during urinary tract infection', *Current Opinion in Microbiology*, 16(1), pp. 100–107. doi: 10.1016/j.mib.2013.01.005.

Umeda, R. *et al.* (2020) 'Structural insights into tetraspanin CD9 function', *Nature Communications*. Springer US, 11(1), pp. 1–7. doi: 10.1038/s41467-020-15459-7.

Valle, J. *et al.* (2008) 'UpaG, a new member of the trimeric autotransporter family of adhesins in uropathogenic Escherichia coli', *Journal of Bacteriology*, 190(12), pp. 4147–4161. doi: 10.1128/JB.00122-08.

Varley, C. L. *et al.* (2004) 'Role of PPARγ and EGFR signalling in the urothelial terminal differentiation programme', *Journal of Cell Science*, 117(10), pp. 2029–2036. doi: 10.1242/jcs.01042.

Vences-Catalán, F. *et al.* (2017) 'CD81 as a tumor target', *Biochemical Society Transactions*, 45(2), pp. 531–535. doi: 10.1042/BST20160478.

Ventress, J. K. *et al.* (2016) 'Peptides from tetraspanin CD9 are potent inhibitors of Staphylococcus aureus adherence to keratinocytes', *PLoS ONE*, 11(7), pp. 1–17. doi: 10.1371/journal.pone.0160387.

Veranič, P., Romih, R. and Jezernik, K. (2004) 'What determines differentiation of urothelial umbrella cells?', *European Journal of Cell Biology*, 83(1), pp. 27–34. doi: 10.1078/0171-9335-00351.

Višnjar, T. *et al.* (2017) 'Uroplakin traffic through the Golgi apparatus induces its fragmentation: New insights from novel in vitro models', *Scientific Reports*, 7(1), pp. 1–16. doi: 10.1038/s41598-017-13103-x.

De Vita, D. and Giordano, S. (2012) 'Effectiveness of intravesical hyaluronic acid/chondroitin sulfate in recurrent bacterial cystitis: A randomized study', *International Urogynecology Journal*, 23(12), pp. 1707–1713. doi: 10.1007/s00192-012-1794-z.

Walsh, C. and Collyns, T. (2017) 'The pathophysiology of urinary tract infections', *Surgery (United Kingdom)*, 35(6), pp. 293–298. doi: 10.1016/j.mpsur.2017.03.007.

Wand, M. E. *et al.* (2011) 'Macrophage and Galleria mellonella infection models reflect the virulence of naturally occurring isolates of B. pseudomallei, B. thailandensis and B. oklahomensis', *BMC microbiology*, 11(1), pp. 1–11.

Wang, S., Gao, D. and Chen, Y. (2017) 'The potential of organoids in urological cancer research', *Nature Reviews Urology*, 14(7), pp. 401–414. doi: 10.1038/nrurol.2017.65.

Wankel, B. *et al.* (2016) 'Sequential and compartmentalized action of Rabs, SNAREs, and MAL in the apical delivery of fusiform vesicles in urothelial umbrella cells', *Molecular biology of the cell*. Am Soc Cell Biol, 27(10), pp. 1621–1634.

Warren, J. W. (2001) ‘Catheter-associated urinary tract infections’, *International journal of antimicrobial agents*, 17(4), pp. 299–303.

Wawrysiuk, S. *et al.* (2019) ‘Prevention and treatment of uncomplicated lower urinary tract infections in the era of increasing antimicrobial resistance—non-antibiotic approaches: a systemic review’, *Archives of Gynecology and Obstetrics*, 300(4), pp. 821–828. doi: 10.1007/s00404-019-05256-z.

Weiner, L. M. *et al.* (2016) ‘Antimicrobial-resistant pathogens associated with healthcare-associated infections: summary of data reported to the National Healthcare Safety Network at the Centers for Disease Control and Prevention, 2011–2014’, *infection control & hospital epidemiology*, pp. 1288–1301.

Weiser, J. N., Ferreira, D. M. and Paton, J. C. (2018) ‘Streptococcus pneumoniae: transmission, colonization and invasion’, *Nature Reviews Microbiology*. Nature Publishing Group, 16(6), pp. 355–367.

Wellens, A. *et al.* (2008) ‘Intervening with urinary tract infectious using anti-adhesives based on the crystal structure of the FimH-oligomannose-3 complex’, *PLoS ONE*, 3(4). doi: 10.1371/journal.pone.0002040.

White, A., Lamb, P. W. and Barrett, J. C. (1998) ‘Frequent downregulation of the KAI1(CD82) metastasis suppressor protein in human cancer cell lines’, *Oncogene*, 16(24), pp. 3143–3149. doi: 10.1038/sj.onc.1201852.

Wiersinga, W. J. *et al.* (2018) ‘Melioidosis’, *Nature Reviews Disease Primers*, 4(1), p. 17107. doi: 10.1038/nrdp.2017.107.

Wilson, J. R. and Corlett, E. N. (2005) ‘Evaluation of human work’. Boca Raton, FL: Taylor & Francis. Available at: http://www.crcnetbase.com/isbn/9781420055948.

Wilson, J. W. *et al.* (2002) ‘Mechanisms of bacterial pathogenicity’, *Postgraduate Medical Journal*, 78(918), pp. 216–224. doi: 10.1136/pmj.78.918.216.

Winter, S. V., Zychlinsky, A. and Bardoel, B. W. (2016) ‘Genome-wide CRISPR screen reveals novel host factors required for Staphylococcus aureus α-hemolysin-mediated toxicity’, *Scientific reports*. Nature Publishing Group, 6(1), pp. 1–9.

Wright, K. J., Seed, P. C. and Hultgren, S. J. (2005) ‘Uropathogenic Escherichia coli flagella aid in efficient urinary tract colonization’, *Infection and Immunity*, 73(11), pp. 7657–7668. doi: 10.1128/IAI.73.11.7657-7668.2005.

Wright, K. J., Seed, P. C. and Hultgren, S. J. (2007) ‘Development of intracellular bacterial communities of uropathogenic Escherichia coli depends on type 1 pili’, *Cellular Microbiology*, 9(9), pp. 2230–2241. doi: https://doi.org/10.1111/j.1462-5822.2007.00952.x.

Wu, X.-R. *et al.* (2009) ‘Uroplakins in urothelial biology, function, and disease’, *Kidney international*, 75(11), pp. 1153–1165.

Wu, X. R. *et al.* (1990) 'Large scale purification and immunolocalization of bovine uroplakins I, II, and III. Molecular markers of urothelial differentiation', *Journal of Biological Chemistry*, 265(31), pp. 19170–19179.

Wu, X. R. *et al.* (2009) 'Uroplakins in urothelial biology, function, and disease', *Kidney International*, 75(11), pp. 1153–1165. doi: 10.1038/ki.2009.73.

Wu, X. R., Medina, J. J. and Sun, T. T. (1995) 'Selective interactions of UPIa and UPIb, two members of the transmembrane 4 superfamily, with distinct single transmembrane-domained proteins in differentiated urothelial cells', *Journal of Biological Chemistry*, 270(50), pp. 29752–29759. doi: 10.1074/jbc.270.50.29752.

Wu, X. R. and Sun, T. T. (1993) 'Molecular cloning of a 47 kDa tissue-specific and differentiation-dependent urothelial cell surface glycoprotein', *Journal of Cell Science*, 106(1), pp. 31–43.

Wu, X. R., Sun, T. T. and Medina, J. J. (1996) 'In vitro binding of type 1-fimbriated Escherichia coli to uroplakins Ia and Ib: Relation to urinary tract infections', *Proceedings of the National Academy of Sciences of the United States of America*, 93(18), pp. 9630–9635. doi: 10.1073/pnas.93.18.9630.

Xie, B., Zhou, G., Chan, S.-Y., *et al.* (2006) 'Distinct glycan structures of uroplakins Ia and Ib: structural basis for the selective binding of FimH adhesin to uroplakin Ia.', *The Journal of biological chemistry*, 281(21), pp. 14644–14653. doi: 10.1074/jbc.M600877200.

Xie, B., Zhou, G., Chan, S. Y., *et al.* (2006) 'Distinct glycan structures of uroplakins Ia and Ib: Structural basis for the selective binding of FimH adhesin to uroplakin Ia', *Journal of Biological Chemistry*, 281(21), pp. 14644–14653. doi: 10.1074/jbc.M600877200.

Yamada, M. *et al.* (2008) 'The tetraspanin CD151 regulates cell morphology and intracellular signaling on laminin-511', *The FEBS Journal*, 275(13), pp. 3335–3351. doi: https://doi.org/10.1111/j.1742-4658.2008.06481.x.

Yanez-Mo, M. *et al.* (2001) 'Tetraspanins in intercellular adhesion of polarized epithelial cells: spatial and functional relationship to integrins and cadherins', *Journal of Cell Science*, 114(3), pp. 577–587. doi: 10.1242/jcs.114.3.577.

Yang, Y. *et al.* (2020) 'Open conformation of tetraspanins shapes interaction partner networks on cell membranes', *The EMBO Journal*, 39(18), pp. 1–16. doi: 10.15252/embj.2020105246.

Yeung, L., Hickey, M. J. and Wright, M. D. (2018) 'The many and varied roles of tetraspanins in immune cell recruitment and migration', *Frontiers in Immunology*, 9(JUL). doi: 10.3389/fimmu.2018.01644.

Yoshida, T. *et al.* (2015) 'Dynamic Change in p63 Protein Expression during Implantation of Urothelial Cancer Clusters', *Neoplasia*. The Authors, 17(7), pp. 574–585. doi: 10.1016/j.neo.2015.07.004.

Yoshida, T. *et al.* (2018) 'Three-dimensional organoid culture reveals involvement of Wnt/β-catenin pathway in proliferation of bladder cancer cells', *Oncotarget*, 9(13), pp. 11060–11070. doi: 10.18632/oncotarget.24308.

Yu, J. *et al.* (1994) 'Uroplakins Ia and Ib, two major differentiation products of bladder epithelium, belong to a family of four transmembrane domain (4TM) proteins', *Journal of Cell Biology*, 125(1), pp. 171–182. doi: 10.1083/jcb.125.1.171.

Yu, Y. *et al.* (2016) 'Comparative lipidomic study of urothelial cancer models: Association with urothelial cancer cell invasiveness', *Molecular BioSystems*, 12(11), pp. 3266–3279. doi: 10.1039/c6mb00477f.

Zeng, P. *et al.* (2017) 'Tetraspanin CD151 as an emerging potential poor prognostic factor across solid tumors: A systematic review and meta-analysis', *Oncotarget*, 8(3), pp. 5592–5602. doi: 10.18632/oncotarget.13532.

Zhang, Y. H. *et al.* (2010) 'CD82 (CD82 molecule)', *Atlas of Genetics and Cytogenetics in Oncology and Haematology*. Jean-Loup Huret (Editor-in-Chief); INIST-CNRS (Publisher).

Zhou, G. *et al.* (2001) 'Uroplakin Ia is the urothelial receptor for uropathogenic FimH binding', *Journal of cell science*, 22, pp. 4095–4103. Available at: http://www.ncbi.nlm.nih.gov/pubmed/8270634.

Zhou, G. *et al.* (2012) 'MAL facilitates the incorporation of exocytic uroplakin-delivering vesicles into the apical membrane of urothelial umbrella cells', *Molecular biology of the cell*. Am Soc Cell Biol, 23(7), pp. 1354–1366.

Zimmerman, B., Kelly, B., McMillan, Brian J, *et al.* (2016) 'Crystal Structure of a Full-Length Human Tetraspanin Reveals a Cholesterol-Binding Pocket', *Cell*. 2016/10/27, 167(4), pp. 1041-1051.e11. doi: 10.1016/j.cell.2016.09.056.

Zimmerman, B., Kelly, B., McMillan, Brian J., *et al.* (2016) 'Crystal Structure of a Full-Length Human Tetraspanin Reveals a Cholesterol-Binding Pocket', *Cell*. Elsevier Inc., 167(4), pp. 1041-1051.e11. doi: 10.1016/j.cell.2016.09.056.

Zöller, M. (2006) 'Gastrointestinal Tumors: Metastasis and Tetraspanins TT - Malignome des Magen-Darm-Traktes: Metastasierung und Tetraspanine', *Z Gastroenterol*, 44(07), pp. 573–586. doi: 10.1055/s-2006-926795.

Zöller, M. (2009) 'Tetraspanins: Push and pull in suppressing and promoting metastasis', *Nature Reviews Cancer*, 9(1), pp. 40–55. doi: 10.1038/nrc2543.

Zuidscherwoude, M., Dunlock, V.-M. E., *et al.* (2017) 'Tetraspanin microdomains control localized protein kinase C signaling in B cells.', *Science signaling*, 10(478). doi: 10.1126/scisignal.aag2755.

Zuidscherwoude, M., Dunlock, V. M. E., *et al.* (2017) 'Tetraspanin microdomains control localized protein kinase C signaling in B cells', *Science Signaling*, 10(478). doi: 10.1126/scisignal.aag2755.